Proteomic Analysis of Interstitial Fluid for Novel Markers of the Cutaneous Response to Injury

Carolyn Anne Gill

School of Medicine

University of Southampton

A thesis submitted for the degree of

Doctor of Philosophy

August 2009

Abstract

The inflammatory response is critical to healing outcome after cutaneous injury. Our current understanding of the response to injury has been compiled from targeted studies on components expected to play a role. It was hypothesised that an unbiased approach to characterisation of soluble mediators within the injured tissue might identify additional components, thereby increasing our understanding of the cellular processes involved. The aim of this research was to develop and characterise a model of injury with the potential to identify novel mediators of the early response. Microdialysis was chosen as both the sampling method and the means by which the tissue was injured as probe insertion causes a single injury that can be sampled continuously without further damaging the tissue.

Early injury responses were initially characterised in terms of changes in blood flow and known markers of the inflammatory response, using Laser Doppler Imaging and a bead-based cytokine flow cytometric assay, respectively. A shotgun proteomic analysis was then undertaken to characterise of the protein content of the fluid obtained using microdialysis, dialysate. The phosphorylation status of proteins was also characterised following the implementation and optimisation of a recently reported method that uses dendrimer conjugation chemistry to capture phosphopeptides.

Blood flow and cytokine measurements in the dialysate confirmed the occurrence of a reproducible inflammatory response to the microdialysis injury. Proteomic analyses of dialysate suggests that it has a relatively simple protein composition and is dominated by highly abundant components. The identified proteins originate from both intra- and extracellular locations and play a range of roles, including regulation of coagulation, cellular

communication, and the immune response. Several are likely to undergo post-translational phosphorylation and hence their phosphorylation status was also investigated. Using the phosphopeptide capture method, potentially novel phosphorylation sites were identified in two abundant proteins, albumin and apolipoprotein L1 at positions S603 and S314, respectively.

Collectively, the data obtained in this investigation increase our knowledge of the proteins and processes involved in responses to injury, and suggest that microdialysis may be of some use for studies in this area. Further, analysis of protein phosphorylation in dialysate suggests that this is an informative approach that could shed light on extracellular signalling events that occur during the progression of the response to injury.

Contents

List of Figures

List of Tables

Declaration of Authorship

I, **Carolyn Anne Gill**, declare that this thesis and the work presented in it are my own and has been generated by me as the result of my own original research.

Proteomic Analysis of Interstitial Fluid for Novel Markers of the Cutaneous Response to Injury

I confirm that:

1. This work was done wholly or mainly while in candidature for a research degree at this University;
2. Where any part of this thesis has previously been submitted for a degree or any other qualification at this University or any other institution, this has been clearly stated;
3. Where I have consulted the published work of others, this is always clearly attributed;
4. Where I have quoted from the work of others, the source is always given. With the exception of such quotations, this thesis is entirely my own work;
5. I have acknowledged all main sources of help;
6. Where the thesis is based on work done by myself jointly with others, I have made clear exactly what was done by others and what I have contributed myself;
7. Either none of this work has been published before submission, or parts of this work have been published as:

Signed:

Dated:

Acknowledgements

Firstly, my thanks go to my supervisors, Professors Geraldine Clough and C. David O'Connor who have supported and encouraged me during this research. I would also like to thank Professor Clough for her expert assistance in inserting the microdialysis probes.

A special thank you goes to Paul Skipp for technical expertise with mass spectrometry and for every "one last idea" in getting the dendrimer conjugation up and running. Thanks also to Therese Nestor and Shanon Pead for technical assistance and to Dr Erika Parkinson for help setting up the Mascot searches and for advice on tools for data analysis. I am greatly appreciative of the help from Dr. Bernd Bodenmiller (ISMB, Zurich), for all his tips in fine-tuning the dendrimer conjugation protocol.

For clinical work, I thank the Wellcome Trust Clinical Research Facility and Dr. Christine Solomon for collection of dialysate for phosphopeptide analysis. Particular thanks goes to my volunteers for donating their proteins.

Thanks also go to all the company representatives who have given me free samples, especially Curtis Nicholson and Jane Limer (BD Biosciences) for training with the CBA Flex Set, Joseph Heinzelmann (Dendritic Nanotechnologies Inc.) for several dendrimer samples and the dendrimer schematic, and Laurence Kowarz (Roche) for protease and phosphatase inhibitors.

A special mention goes to my high school science teacher Mr Andrew Birbeck who initially sparked my interest in science and the ambition to pursue a career in research. Also to my partner, family and friends for their love and support, and for putting up with me during the lows and highs that come with research.

Finally, I would like to acknowledge the Gerald Kerkut Charitable Trust for supporting this research.

Abbreviations

α-CHCA	α-cyano-4-hydroxycinnamic acid
ACN	acetonitrile
AU	arbitrary units
BCA	bicinchoninic acid
BSA	bovine serum albumin
CBA	cytometric bead array
CPR	Centre for Proteomic Research
DHBA	dihydroxybenzoic acid
ELISA	enzyme-linked immunosorbent assay
DTT	dithiothreitol
FA	formic acid
FACS	flow-assisted cell sorting, refers to flow cytometry in the text
gi number	GenBank info number
GM-CSF	granulocyte macrophage-colony stimulating factor
GO	Gene Ontology
HPLC	high performance liquid chromatography
ICAM-1	intercellular adhesion molecule-1
IFN-γ	interferon γ
IL	interleukin
IMAC	immobilised metal ion affinity chromatography
LC	liquid chromatography
MALDI	matrix-assisted laser desorption/ionisation
MARS	Multi Affinity Removal System
MIP-1α	macrophage inflammatory protein-1α
MCP-1	monocyte chemoattractant protein-1
MS	mass spectrometry
MWCO	molecular weight/ mass cut-off
OSM	oncostatin M

PAGE	polyacrylamide gel electrophoresis
PE	phycoerythrin
PES	polyethersulphone
PICR	protein identifier cross-reference
PU	perfusion units
SDS	sodium dodecyl sulphate
SEM	standard error of the mean
TEAB	triethylammonium bicarbonate buffer
TFA	trifluroacetic acid
TNF-α	tumor necrosis factor-α
TiO_2	titanium dioxide
TOF	time of flight
VEGF	vascular endothelial growth factor

Chapter 1

Introduction

The current understanding of the responses that occur following an injury have so far failed to lead to efficient interventions in cases of inappropriate healing. It has been hypothesised that regulation of the inflammatory phase of the injury response is critical to healing outcome (Eming, Krieg & Davidson, 2007; Stramer, Mori & Martin, 2007). The skin represents an ideal organ in which the early responses, including the initiation of inflammation can be investigated in humans, *in vivo*.

1.1 Skin biology and the biology of injury

The skin is the most accessible and largest organ of the human body, accounting for approximately 15 % of the total adult body mass (Zhao *et al.*, 2008). The function of the skin is to provide a protective barrier between an organism and its environment. When this barrier is breached, the skin mounts an inflammatory response to prevent blood loss, to kill any invading microorganisms and to close any gaps in the skin barrier (Singer & Clark, 1999). This injury response involves a combination of resident and infiltrating cellular and molecular mediators from the circulation, which work together to bring about clearance of the wound and repair. It comprises four overlapping phases; haemostasis, inflammation, granulation and remodelling. The first phase, haemostasis, acts to reduce blood loss and plug breakages in the vessel walls and epidermal barrier with a rudimentary scab, the eschar. The second phase, in-

flammation, sees the recruitment of the cells necessary to clean the wound and begin production and remodelling of new tissue and hence arguably represents the most influential phase in the injury response. Incorrect regulation of the inflammatory response can lead to a persistent state of chronic, non-healing wounds where the inflammation is not resolved and tissue destruction continues, while an over-zealous resolution can lead to fibrosis and loss of function (Diegelmann & Evans, 2004). The goals of wound healing research are to improve both the speed and efficiency of wound closure and the aesthetics and functionality of the resultant scar tissue. Furthermore, lessons learned in uncovering improved wound healing in skin could lead to improved treatments for chronic inflammation or fibrosis in other tissues. It could also inform diagnostic tests to predict healing outcome in individual patients, so that appropriate treatment can be administered in time to prevent the development of such adverse effects.

The histology of the injury response and wound healing has been well characterised, but the mechanisms which drive these processes are not well understood. Despite advances in the understanding of growth factor and cytokine influences, therapies guided by this knowledge have failed to give significant or reliable improvements in wound outcome. Therefore an alternative approach is required to better characterise these mechanisms and improve on the current understanding. New analytical technologies, such as the different proteomic approaches might allow better characterisation of the optimal response to injury. In principal, they may identify key mediators in control of the signalling pathways involved in determining the outcome of an injury response. This potential is likely to be increased further through directly sampling soluble mediators within the injury, locally and specifically.

1.1.1 The skin as an immune organ

The skin is one of the body's first defences against pathogens, acting as a physical barrier to infection. Maintenance of the integrity of this barrier is essential and its structure reflects this protective role. It is composed of two main layers, the outer epidermis and the inner dermis. The hypodermis, the layer of cushioning subcutaneous fat immediately below the dermis, containing resident fibroblasts and macrophages,

is sometimes considered as a third layer of the skin (Kanitakis, 2002). The dermis and epidermis are further subdivided and are host to a number of key cell types and structures that contribute to the immune regulation that takes place following an injury, as shown in Figure 1.1.

The epidermis is divided into four layers, although a fifth, the stratum lucidum, is present only in palmoplantar skin. The basal layer is composed mainly of epidermal stem cells, which differentiate into mature keratinocytes during their movement towards the outer surface of the skin. Once they reach the stratum corneum, these cells, now known as corneocytes, are highly keratinised, anucleate and dead. From here, they are sloughed off to be replaced by cells migrating from the stratum granulosum. This cycle of replenishment ensures that the waterproof barrier is maintained and gives the skin the regenerative capacity that is so important in recovering from injury.

The dermis consists of two layers, the loose papillary dermis and the more dense reticular dermis, and is the site of the majority of the cutaneous vasculature. The papillary dermis is so called due to the finger-like projections or "papillae" formed from the connective tissue that give the skin its ridged appearance and increases the surface area for contact across the dermal-epidermal junction and therefore skin strength. It is comprised mainly of collagen types I and III, with elastin for elasticity and recoil. These fibres are packed more densely in the reticular dermis, which also contains reticulin fibres, composed of collagen and fibronectin. Combined, these fibres not only provide the flexibility required to resist injury, such as by compression, but also provide a scaffold for infiltrating cells during repair.

Several important structures and cell types reside in the dermis. Tissue macrophages are situated predominantly in the papillary layer, in order to rapidly intercept any invading pathogens. This removes the time delay that would result from the process of chemoattraction required to recruit blood monocytes and trigger their differentiation into mature macrophages. Mast cells are also resident and release vasoactive histamine in allergic reactions. Sebaceous glands are also located within the dermis and secrete sebum out onto the skin surface. This is a substance responsible for maintaining the acidity of the skin which limits microbial growth and therefore reduces the potential

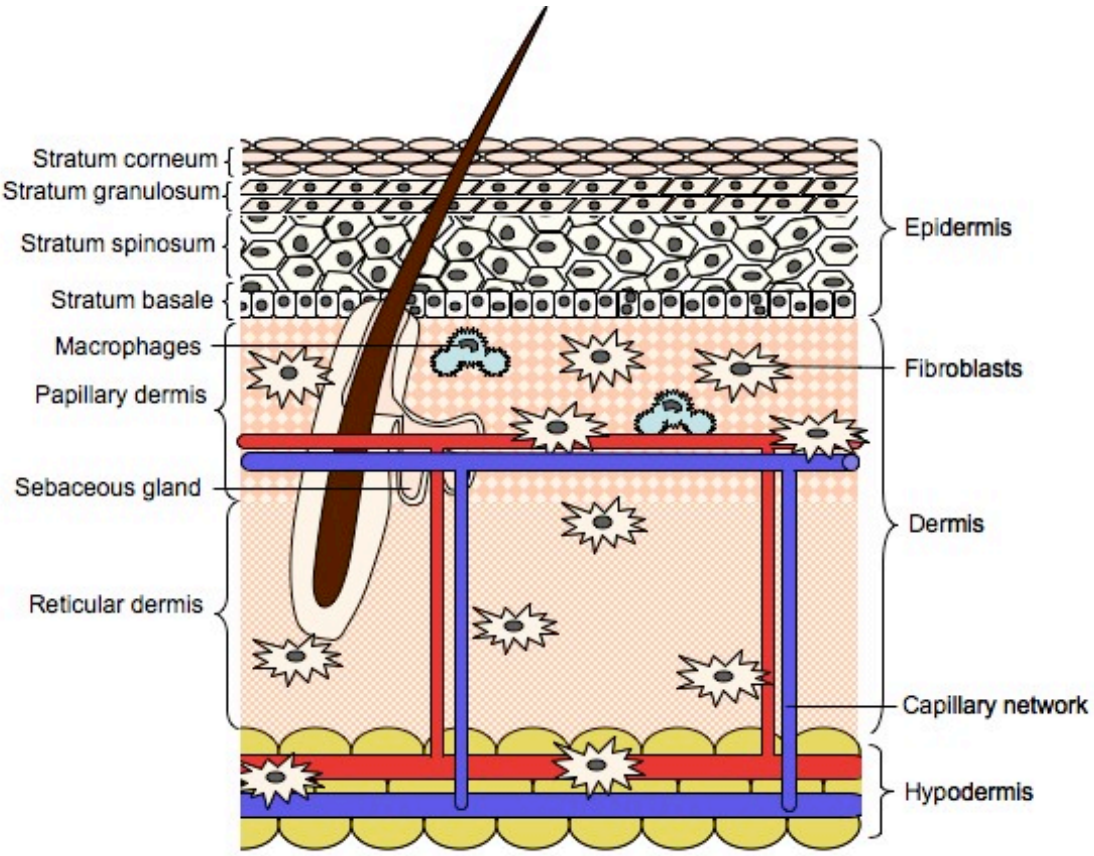

Figure 1.1: **Skin structure.** Schematic of the anatomy of human skin. The epidermis consists of predominantly keratinocytes, with melanocytes (giving pigmentation), Merkel (sensory nerve endings) and Langerhan's (specialised antigen-presenting) cells. The dermis is composed of connective tissue, predominantly collagen and elastin fibres and is interspersed with fibroblasts. The connective tissue of the papillary dermis is loose and forms papillae, finger-like projections (not shown), while that of the reticular layer is more dense (depicted as a tighter mesh). The dermis is also the site of tissue macrophages, fibroblasts, hair follicles and associated sebaceous glands, as well as the dense capillary network termed the dermal vascular plexus. The hypodermis is subcutaneous tissue predominantly composed of adipocytes (yellow ovals) and fibroblasts. Not to scale. Not all structures shown. Figure adapted from Gray (1918).

for infection in the event of injury.

Another important structure, the cutaneous vasculature, extends throughout the dermis (reviewed by Braverman, 2000). It does not reach the epidermis, which is instead supplied by diffusion from the capillaries imbedded within the dermis. This capillary network is key to the cutaneous response to injury and responsible for the visible, cardinal signs of inflammation first recorded by Celsus in the first century, AD. These signs, the redness, heat, swelling and pain are caused by increased blood flow to the damaged area and extravasation of its components into the tissue itself. This extravasation brings the cellular and molecular mediators essential to disinfecting the wound, further activating resident cells and bringing about repair. Such mediators include clotting factors to reduce blood loss and seal the wound from the external environment, proteases to degrade the extracellular matrix and macrophages to phagocytose damaged cells. This serves two purposes, to dispose of potentially damaging agents and to clear the site for the formation of new tissue. Later on, these proteases are involved in re-modelling the newly formed tissue components to form the mature scar. These cellular and molecular factors will be discussed in more detail throughout the course of this research.

Below the dermis lies a layer of adipose tissue involved in insulation and thermoregulation, nutrient storage and cushioning against impact injury. It is primarily composed of adipocytes, but also contains fibroblasts that can become adipocytes, and possibly vice versa, following acute injury (Andrade, de-Oliveira-Filho & Fernandes, 1998). However, the histological evidence for the latter process is less convincing, as the investigators were not able to observe changes in specific cells and instead had to infer whether differentiation was in the direction of adipocyte or fibroblast development from immunohistochemistry data alone. This highlights the importance of studying temporal changes in the same cells and regions of the injured tissue following such a response. Differentiation of fibroblasts into adipocytes may represent part of the re-modelling process, although it has been proposed that adipocytes are an important source of regulatory cytokines (Pachler *et al.*, 2007; summarised in Klein *et al.*, 2007).

1.1.2 Overview of the injury response and wound healing in skin

The response to injury and subsequent healing has been divided into three main overlapping stages; haemostasis and inflammation, granulation (tissue formation) and remodelling (Figure 1.2), which will now be considered.

The initial injury generally damages the vasculature, the matrix of the dermis, and cells within the epidermis - primarily keratinocytes. This damage causes activation of keratinocytes and vascular endothelial cells, among others, and the subsequent release of inflammatory mediators. Before the inflammatory response can develop, the condition of the vasculature must first be stabilised and any breaches to the endothelial layer sealed, until it can replace the missing cells.

Haemostasis is the first stage in the response to injury, its purpose is to seal and thus prevent excess blood loss from the damaged vessels, while maintaining adequate blood supply to the injured area. The process of preventing blood loss is induced by exposure of platelets to extravascular collagen, which occurs as a consequence of their movement into the tissue through those perforations in the damaged vasculature. Coagulation is initiated and fibrinogen is cleaved to give active fibrin. This in turn generates a loose matrix with fibronectin, forming the haemostatic plug that seals the gaps in the endothelium. Platelets adhere first to the fibrin matrix and then to each other to complete the seal. They are also involved in early modulation of the inflammatory response, releasing a great number of protein and lipid mediators once stimulated by aggregation. Due to their obvious importance as a source of regulatory compounds, the role of platelets in the response to injury is discussed in greater detail in Section 1.1.3.3.

Inflammatory mediators released from platelets act in synergy with those released from the damaged cells of the skin. Blood supply to the damaged tissue is increased, including a concomitant increase in vascular permeability. Recruitment of leukocytes is stimulated, to combat infection, remove necrotic tissue and promote repair. Neutrophils are the dominant leukocyte sub-type during the early inflammatory phase

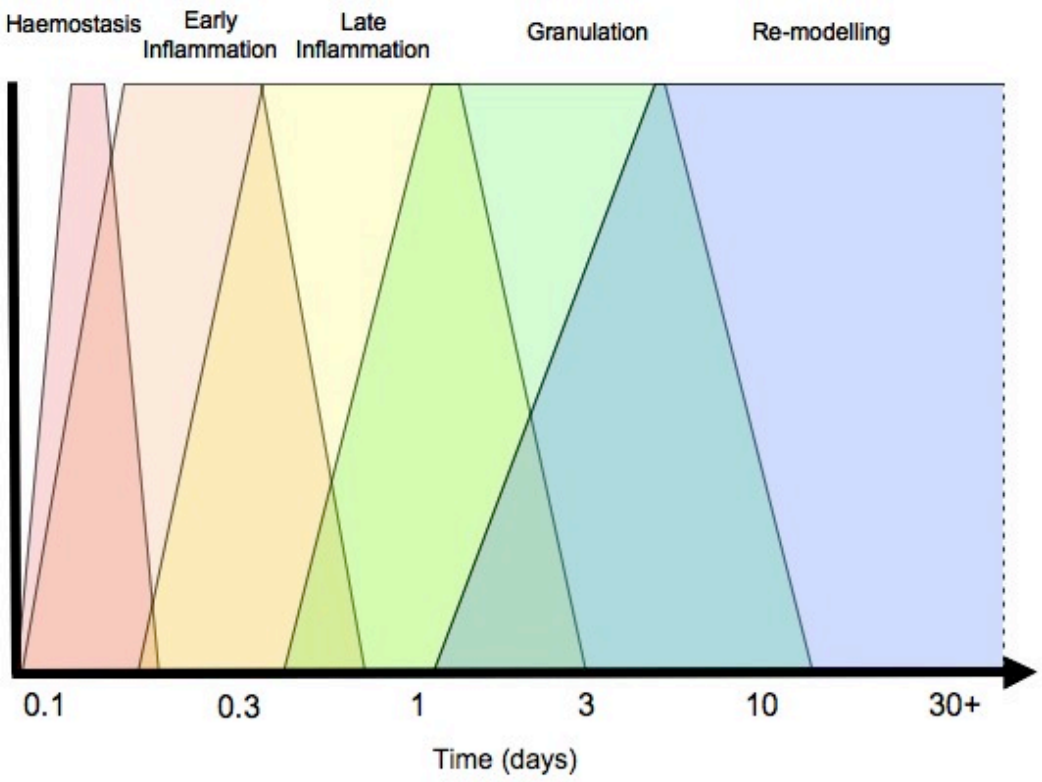

Figure 1.2: **Stages of wound healing.** Schematic of the time-course of the overlapping stages of the response to injury and subsequent wound healing. The x-axis represents the time after the injury occurs, the y-axis represents the progress of each stage. Haemostasis and inflammation are divided into three sub-stages, namely haemostasis and early and late stages of inflammation, coloured red, orange and yellow, respectively. Haemostasis typically occurs within minutes, while inflammation can take 24–48 hours, or more, to resolve. Formation of new tissue, the granulation phase, is shown in green and the remodelling of this new tissue is represented by the blue section. This remodelling may take several months to years, hence the dashed line to indicate this process continues. Figure adapted from Clark (1988).

and function to kill and phagocytose any invading pathogens as well as to begin the breakdown and removal of damaged tissue, discussed further in Section 1.1.4.1. The "respiratory burst" that releases substances, such as toxic oxygen metabolites for bacteriocidal effect, is damaging to the host and so regulation of neutrophil activity must be closely controlled. They also contribute to the chemoattraction of monocytes, immature macrophages which proliferate and mature to phagocytose apoptotic neutrophils and pathogens, and continue the debridement of the wound.

The appearance of macrophages marks the transition into the late inflammatory stage. Initially, they act to continue the amplification of inflammation, releasing pro-inflammatory mediators in response to ingestion of pathogens. Once any infection has been cleared, the phagocytosis of expired neutrophils stimulates a switch to production of anti-inflammatory mediators. This switch is critical in the resolution of the inflammatory response and the progression of repair.

In addition to their phagocytic and inflammatory functions, macrophages release growth factors, such as vascular endothelial growth factor (VEGF), basic fibroblast growth factor (bFGF), epithelial growth factor (EGF) and transforming growth factors (TGF)α and β. These stimulate the secretion of granulation tissue, including preliminary matrix components from fibroblasts and the proliferation of endothelial cells to generate new vasculature (angiogenesis). Re-epithelialisation begins at this point, with keratinocytes proliferating and migrating along the scaffold provided by the new matrix. This process displaces the eschar and exposes the replacement tissue.

Fibroblasts first secrete a loose matrix primarily composed of fibronectin and hyaluronic acid which is conducive to the cell migration and proliferation that occurs during granulation. In the remodelling phase, they switch to production of a collagen and proteoglycan matrix with a higher tensile strength, required for the mature scar. Matrix metalloproteinases play a key role in the degradation of excess fibres to leave a matrix which gives optimal organisation and tension to the new tissue.

1.1.2.1 Dysregulation of inflammation is responsible for the adverse outcomes to wound healing

The inflammatory phase of the injury response is arguably the key determinant of wound outcome (Serhan & Saveill, 2005). A weak inflammatory response risks infection of the wound, while an excessively strong response leads to delayed healing and the potential for greater scarring. Furthermore, instances of faster wound healing with less scarring occur in both foetal and oral tissues in which there is little to no inflammatory response (Lorenz & Adzick, 1993; Szpaderska, Zuckerman & DiPietro, 2003).

Inflammation is characterised by the progression of leukocyte infiltration, from predominantly neutrophils to macrophages. These cells not only act to clear the wound of debris and infection, but release pro- and anti- inflammatory mediators and take part in both the breakdown of damaged tissue and the formation of its replacement. Hence the recruitment of these cells is of direct relevance to the later stages, including matrix deposition and re-epithelialisation (Eming, Krieg & Davidson, 2007). However, it can also be damaging, in so far as neutrophil-derived proteases and reactive oxygen metabolites degrade both injured and intact tissue (Moraes, Zurawska & Downey, 2006). A continued release of pro-inflammatory components and neutrophil chemoattractants will only aggravate the situation further.

Failure to resolve the inflammatory response leads to a chronic wound status in which tissue destruction by neutrophil proteases continues. This can be a result of persistent infection causing stimulation of neutrophil activity and the associated release of cytotoxic components. It can also be a result of a breakdown in signalling, the causes of which are not yet understood (Menke *et al.*, 2007). Better characterisation of these signalling mechanisms and comparisons between normal and chronic wound environments will greatly improve treatments that promote resolution of inflammation.

The converse effect occurs when the resolution of inflammation is too rigourous and collagen production is not controlled. The deposition of collagen is important, too little results in a weak scar that may be susceptible to rupture, too much results in fibrosis. Fibrosis is defined as an excess in matrix deposition that results in alteration of the tissue architecture and associated reduction or loss of function (Wynn, 2008).

It is associated not only with disfigurement that occurs with excess scar tissue production, but also diseases such as asthma and cirrhosis of the liver. Hence, improved treatments that prevent disproportionate resolution of inflammation and regulate the growth factors that cause excessive matrix production would have significant clinical benefit.

Regulation of the first stages of the injury response, haemostasis and inflammation is clearly crucial to the wound outcome. It is therefore important to understand how these stages progress in the normal, successful response to injury.

1.1.3 Injury and Haemostasis - Setting the scene for inflammation

Injury to the skin typically causes damage to the local cells, disruption of the vasculature and subsequent extravasation of blood components. This disruption of the vasculature activates the coagulation cascade to restore haemostasis and prevent excess blood loss, and to generate a provisional fibrin matrix for the migration of leukocytes and keratinocytes during inflammation and granulation, respectively. The coagulation process is relatively well understood, so will not be discussed here. Instead, the reader is referred to the many reviews on the topic, for example, general discussions on coagulation (Hoffman & Monroe, 2007) and, more specifically, on the role of fibrin and the fibrinolysis system in wound healing (Clark, 2001; Laurens, Koolwijk & de Maat, 2006; Takada, Takada & Urano, 1994).

The response to injury also involves the intercommunication between many different cell types, both resident and from the circulatory system. It involves the activation of resident cells, such as keratinocytes and vascular endothelial cells. Platelets also provide a considerable array of inflammatory mediators. The signalling that occurs as a result of stimulation of these cell types triggers the onset of the inflammatory response. The contribution of each cell type is discussed in turn.

1.1.3.1 Keratinocyte response to damage

Keratinocytes are among the first cell types affected by penetrative injury to the skin and also one of the first to respond. They are also important later on, during granulation and re-epithelialisation. Keratinocyte activation is relatively well-described, for example, by Coulombe (1997) and Grinnell (1992). Upon injury, they release stored interleukin (IL)-1, inducing neighbouring keratinocytes to follow suit and thus amplifying the response. Release of IL-1 then induces the release of other cytokines, such as IL-6, IL-8 and granulocyte macrophage-colony stimulating factor (GM-CSF) which initiates an inflammatory response (McKenzie & Sauder, 1990). Table 1.1 shows some of the cytokines, growth factors and other components released by keratinocytes after injury and during wound healing, and some of the cell types they target.

Table 1.1: **Some examples of inflammatory mediators released by injury-activated keratinocytes**

Mediator	**Target Cells**
GM-CSF*	Neutrophils, macrophages, Langerhan's cells, T-cells
ICAM-1*	T-cells
IL-1α*	Keratinocytes, fibroblasts, T-cells, B-cells
IL-3*	Mast cells, basophils
IL-6*	Neutrophils, macrophages, keratinocytes, T- and B-cells
IL-8*	Basophils, neutrophils, T-cells
MCP-1†	Macrophages
TNF-α*	Keratinocytes, fibroblasts

IL = interleukin, GM-CSF = granulocyte macrophage-colony stimulating factor, ICAM = intracellular adhesion molecule, MCP-1, macrophage chemoattractant protein-1, TNF-α = tumour necrosis factor-alpha, *Summarised in McKenzie & Sauder (1990) †Wetzler *et al.*, 2000.

These mediators cause the up-regulation of chemotactic factors and adhesion molecules,

leading to recruitment of immune cells and the progression of the inflammatory response and resolution (Barker *et al.*, 1991; McKenzie & Sauder, 1990). Interleukin-1 is perhaps the best studied and is involved in the stimulation of over 350 genes, following injury (Yano *et al.*, 2008). Briefly, it stimulates collagenase secretion from fibroblasts to break down the existing extracellular matrix, induces expression of leukocyte chemoattractants and increases adhesion molecule expression on endothelial cells to sequester those leukocytes from the circulation. These processes will be described in greater detail in Section 1.1.4. The functions of the remaining cytokines and chemokines within the injury response and wound healing are described in several reviews (e.g. Gillitzer & Goebeler, 2001; Werner & Grose, 2003). These have a wide range of effects, but there is also a large overlap in these functions, to provide back-up mechanisms and to amplify the signals controlling inflammation.

Regulation of re-epithelialisation by keratinocytes is also under the control of cytokine and growth factor signalling. For example, interferon (IFN)-γ and tumor necrosis factor (TNF)-α are involved in the activation of peroxisome proliferator-activated receptors which stimulate keratinocyte migration to the wound edge (Tan *et al.*, 2001). GM-CSF is also released from fibroblasts, another cell type, resident within the dermis. It it involved in stimulating keratinocyte proliferation, to replace those cells lost or damaged during the injury. Keratinocytes also stimulate the production of integrins, expressed on their surface membranes, which form cell–cell and cell–matrix interactions to facilitate cell migration and adhesion in the repairing tissue (Grose *et al.*, 2002). Re-epithelialisation is not a focus of this research, but further information on the interactions of keratinocytes with fibroblasts in wound healing can be found in the several reviews (e.g. Beer *et al.*, 2000; Werner, Krieg & Smola, 2007).

Cytokines and growth factors are clearly important in regulating the recruitment and activities of both resident and infiltrating cells. However, the degree of pleiotropy and redundancy, coupled with inter-individual variability in terms of expression levels of these molecules, makes distinguishing the exact phase of injury very difficult. Alternative markers of keratinocyte activation could include anti-microbial peptides, which are also released following injury and in response to growth factor stimulation, working

to destroy invading pathogens, in concert with neutrophils (Borregaard *et al.*, 2005).

1.1.3.2 Vascular endothelial cell response to damage

Injury to the vasculature causes activation of the vascular endothelial cells forming the dermal vascular plexus. These cells play a key role in controlling the delivery of mediators to the injured site, regulation of leukocyte recruitment and in control of the extravasation of plasma proteins including immunoglobulins. Later on, in the remodelling phase, endothelial cells react to growth factors, including VEGF, to proliferate and form new vessels to supply the newly formed tissue. This latter function is part of the later, repair phase in the response to injury, so need not be discussed here.

Disruption of the endothelial cell barrier, as a result of injury, first enables the passive recruitment of leukocytes and delivery of plasma proteins to the site of injury, within the clot (Singer & Clark, 1999). Active recruitment of leukocytes to the injury site is mediated by endothelial cells, however, this will be covered in the relevant leukocyte sections below (Sections 1.1.4.1 and 1.1.4.2).

Endothelial cells are both responders and activators within the response to injury and their contribution during inflammation has been extensively reviewed (e.g. Cines *et al.*, 1998; Contran & Pober, 1990; Cook-Mills & Deem, 2005; Hack & Zeerleder, 2001; Michiels, 2003). They play an important role in the regulation of inflammatory status and are key to the recruitment of leukocytes to the site of injury. In response to cytokine stimulation, they release a range of mediators such as cytokines, prostaglandins and nitric oxide (NO). Cytokine mediators include neutrophil chemoattractants (see Section 1.1.4.1) and monocyte chemoattactant protein (MCP)-1, thus perpetuating the inflammatory response. It is interesting to note that the microvascular endothelium produces MCP-1 in response to TNF-α, but not IFN-γ, stimulation as observed in macrovascular endothelium (Goebeler *et al.*, 1997). Prostaglandins and NO are both important regulators of vascular tone, particularly of vasodilatation during very early inflammation (Goldsmith *et al.*, 1996; Williams & Peck, 1977). NO is also involved in regulation of a number of additional processes, such as modulation of adhesion molecule expression and modification of the extracellular matrix, contributing factors in control

of leukocyte recruitment (reviewed in Bruch-Gerharz, Ruzicka & Kolb-Bachofen, 1998). In synergy with prostaglandins, NO acts to reduce inflammation, inhibiting platelet aggregation and expression of adhesion molecules required for leukocyte recruitment (Kubes, Suzuki & Granger, 1991). The roles of NO and prostaglandins have been relatively well characterised and widely reviewed, so will not be discussed in further detail here.

Manipulation of vascular permeability enables regulation of the extravasation of cells and proteins from the blood into the injured tissue. If extravasation is not controlled it could lead to increased or persistent oedema and the development of a chronic wound environment. The role of endothelial junctions in the control of vascular permeability in inflammation and the injury response has recently been reviewed (Chanson *et al.*, 2005), in which several well characterised mechanisms are discussed. TNF-α stimulates a downstream signalling cascade that results in modulation of the actin cytoskeleton. The increase in permeability comes from contraction of the endothelial cells, thus creating gaps between those cells and consequently, within the endothelial barrier (Petrache *et al.*, 2003). A second important regulator of vascular permeability is VEGF, which mediates phosphorylation of vascular endothelial cadherin (VE-cadherin) and results in a reduction in adhesion between cells and a subsequent increase in permeability (Gavard & Gutkind, 2006). Similar activations occur in response to thrombin via protease activated receptors, through NF-κB signalling (Obreja *et al.*, 2006; Vogel *et al.*, 2000). Histamine, released from mast cells, causes a transient increase in permeability that lasts 5-10 minutes, beginning within seconds of release (Wu & Baldwin, 1992). This permeability increase is thought to occur by both VE-cadherin phosphorylation and calcium dependant actin modulation mechanisms, as for the previous molecules considered (van Hinsbergh & van Nieuw Amerongen, 2002). The control of vascular permeability seems to occur through a few common mechanisms, in response to a wider variety of mediators. Opportunities for manipulating these mechanisms could therefore target either components of the common downstream pathways, or the mediators and their receptors specifically, if one or more are abnormally expressed.

1.1.3.3 Platelets as an important source of mediators

Platelets are the most abundant cell type in the earliest phases of the injury response (Rožman & Bolta, 2007) and perform both haemostatic and inflammatory functions. As previously mentioned, they begin to aggregate in response to stimuli such as collagen and thrombin once the vascular endothelial barrier is breached (David *et al.*, 2003). Platelets are incorporated into the fibrin clot, derived from the cleavage of fibrinogen by thrombin, where they add to physical structure of the clot itself and act as a source of cytokines and chemotactic factors that stimulate the infiltration of leukocytes (Martin, 1997). Chemokines released from platelets and their contribution to the inflammatory status are reviewed by Gear & Camerini (2003). Briefly, factors such as "Regulated upon Activation, Normal T-cell Expressed and Secreted" (RANTES) stimulate further platelet activation, macrophage inflammatory protein-1α (MIP-1α) facilitates neutrophil recruitment, and MCP-1, monocyte recruitment. However, these chemokines are not exclusively involved in those functions mentioned. RANTES, for example, is also involved in chemoattraction of monocyte, eosinophil and lymphocytes, MIP-1α also plays a role in monocyte recruitment (reviewed in Rollins, 1997).

It is not just chemokines that are released from platelets. The alpha granules are a source of approximately 60 growth factors, adhesion proteins, anti-microbials, proteases, anti-proteases and components of the clotting and fibrinolytic systems and may represent an important source of novel mediators for therapy. For this reason, the suitability of platelets as therapeutic agents has been explored, recently reviewed by Rožman & Bolta (2007). Platelet-rich plasma, activated by addition of thrombin, forms a gel-like substance in which platelets are trapped in a fibrin mesh. This can be applied to an injury, where the trapped cells can release their granule contents and initiate healing. The advantage in this technique is that it provides multiple factors which can act in synergy with each other and thus have a stronger effect than a single factor alone. Results in diabetic patients and those with chronic ulcers have proved promising, with some studies reporting almost halving of healing time following the application of the activated platelet gel-like substance (Hom, Linzie & Huang, 2007; Mazzucco *et al.*, 2004). The main problems with this method are the variation in

platelet count between donors and the difficulty in storage without activating the cells, which reduces reliability of the treatment. However, because factors released from platelets appear to play such an important role in initiating the healing response, they may act as suitable markers of the normal response to injury. The early success of platelet gel in therapy would also suggest that the activation of platelets following injury plays a critical role in outcome and hence that the processes that occur during the early response, including inflammation, are key.

1.1.4 Inflammation and the cellular infiltrate in injury

The inflammatory component of the injury response consists of an early and late phase, as previously discussed. The early phase is characterised by the presence of neutrophils and the breaking down of existing tissue while the late phase is characterised by a dominance of macrophages, anti-inflammatory signals and the re-building of the tissue to heal the wound. Once again, the contributions of the cell types involved will be discussed in turn.

1.1.4.1 Neutrophils

Neutrophils are the second plasma-derived cell type to infiltrate the wound site, typically within only a few hours of injury. These cells are recruited early to clean up the wound by removing any invading pathogens and some of the damaged tissue as well as regulating cytokine release. Neutrophil involvement following injury involves several steps; their attraction to the site by chemokines, capture onto endothelial cells via adhesion molecules, migration between cells to reach the wound site, activation and then apoptosis once their job is complete.

The primary function of neutrophils is the debridement of the injury site, that is, removal of necrotic tissue and invading pathogens. This is achieved through the release of four types of granules - primary (azurophil), secondary (specific), tertiary (gelatinase) and secretory granules, containing plasma proteins such as albumin, immunoglobulins and transferrin. Via these granules, neutrophils release a wide range

of factors, including antimicrobials, proteases and toxic oxygen metabolites as well as numerous cytokines and chemokines (Borregaard & Cowland, 1997; Weiss, 1989). Antimicrobials and toxic oxygen metabolites form part of the armoury against any invading pathogens, aided by the phagocytic activities of the neutrophils themselves. This topic is the subject of several reviews (such as Burg & Pillinger, 2001; Levy, 1996; Witko-Sarsat *et al.*, 2000), to which the reader is referred for further details. Proteases released, such as elastase and cathepsin G also contribute to bactericidal activity and their inhibition has been shown to reduce bacterial clearance from wounds (Cole *et al.*, 2001). Their activity may also contribute to neutrophil infiltration, as targets of these enzymes include collagen, target of gelatinases, which forms part of the basement membrane through which neutrophils have to cross. Patients deficient in specific granules display reduced or absent neutrophil infiltration (Gallin, 1985; Johnston, Boxer & Berliner, 1992).

An important point to consider with these activities is the damage caused to the surrounding tissue. Indeed, in several studies of knock-out and knock-down mice, improved healing of sterile wounds has been observed where neutrophils are depleted, with relative increases of $\sim$35 % closure of wounds (Dovi, He & DiPietro, 2003). Additionally, a reduced neutrophil infiltrate is observed in oral mucosa wounds which heal more quickly than equivalent skin wounds (Szpaderska, Zuckerman & DiPietro, 2003). Collectively, this suggests that, while neutrophils are important in cleaning the injury, they are also very harmful. It would be of particular interest to study the stages leading up to recruitment of neutrophils, to identify if and how their number and activity are important contributing factors to healing outcome. Considerable progress into the understanding of neutrophil recruitment, migration and activation has been made over the past 15 years (Witko-Sarsat *et al.*, 2000).

Neutrophils are attracted to the wound by chemoattractants released from platelets and resident cells, including keratinocytes and endothelial cells. Such chemoattractants include IL-8 released from endothelial cells (Utgaard *et al.*, 1998) and Oncostatin M (OSM) (Kerfoot *et al.*, 2001), released by neutrophils themselves thereby creating a positive feedback loop (Grenier *et al.*, 1999). These attractant molecules up-regulate

expression of adhesion molecules on neutrophils that enable them to attach to selectins on the endothelial cell surface, or up-regulate the selectins themselves. The process of adhesion has been extensively reviewed (for example, by Ley *et al.*, 2007; Witko-Sarsat, 2000; Zimmerman, Prescott & McIntyre, 1992), so only key points need be discussed here. Briefly, release of chemoattractants such as IL-8 causes release of pre-stored P-selectin from Weibel-Palade bodies within endothelial cells, resulting in its translocation to the cell surface membrane. P-selectin binds to neutrophils via ligands such as P-selectin glycoprotein ligand-1 (PSGL-1) which is constitutively expressed on leukocytes (Sako *et al.*, 1993). This enables transient tethering of neutrophils to the vascular wall, a process termed "rolling", which slows them enough so that they bind to β2-integrins, forming a more stable attachment. Vessel dilatation assists neutrophil attachment as the slower flow rate gives more time for contact to occur. Firm attachment via β2-integrins may come as a result of neutrophil activation that occurs following binding between, for example, P-selectin and PSGL-1. This triggers a mitogen activated protein kinase signalling cascade that may regulate integrin specificity to enable binding to the endothelium, through an as yet unclear mechanism (Ley, 1996). The exact method by which integrins achieve firm attachment of neutrophils to the endothelium is also unclear. Hypotheses include indirect strengthening of the selectin interactions and the attachment through direct binding to other adhesion molecules, such as Intracellular Adhesion Molecule-1 (ICAM-1), the latter being the mechanism employed during T-cell recruitment (McDowall *et al.*, 1998). The attachment of neutrophils represents a bottleneck in the recruitment process, thus providing an opportunity for intervention. Characterisation of this second stage would increase the number potential targets for such an intervention, particularly as the increase in adhesion molecule expression is regulated by several different cytokines.

While such redundancy in the mechanisms bringing neutrophils to the site of injury offers an obvious evolutionary benefit, it makes identifying critical mediators for manipulation more difficult. Advances in the understanding of the regulation of neutrophil recruitment leading to an ability to manipulate this process would be of considerable clinical benefit.

1.1.4.2 Monocytes and Macrophages

Monocytes are recruited after neutrophils, usually within 24 hours after injury, reaching a maximum within 48 hours (Eming, Krieg & Davidson, 2007; Engelhardt *et al.*, 1998). They perform a number of key functions within the response to injury and represent the turning point between the pro- and anti-inflammatory stages and therefore another critical phase with regards to healing outcome. The functions performed include phagocytosis of expired neutrophils and any remaining cellular debris, presentation of antigens encountered, both amplifying, then dampening, the inflammatory response and stimulating repair through the activation of several different cell types. The role of monocytes/macrophages in the injury response and wound healing has been reviewed extensively (e.g. DiPietro, 1995; Duffield, 2003; Singer & Clark, 1999), so only a brief summary of their recruitment and functions will be given here.

Monocytes are recruited to the injured tissue following release of chemoattractant factors, such as MCP-1, IL-8, growth regulated oncogene-α and I-309, although the latter has more recently been considered to be a lymphocyte chemoattractant instead (DiPietro *et al.*, 2001; Engelhardt *et al.*, 1998; Miller & Krangel, 1992). Factors such as RANTES and MIP-1α have been shown to be important in monocyte recruitment in mice (DiPietro *et al.*, 1998). The involvement of MIP-1α in monocyte recruitment in humans is unclear. Gaga and colleagues (2008) reported increased recruitment of monocytes following injection of 10 μg of MIP-1α. However, this is a very high concentration and therefore unlikely to be representative of physiological release. Furthermore, the authors comment that in some instances, there was in fact a decrease in macrophage numbers in response to MIP-1α injection. This difference in response highlights the importance of studying the injury response in humans, as results from animal models do not always translate.

Monocytes cross the vascular endothelial barrier in a similar manner to neutrophils, first binding to ligands such as platelet/endothelial cell adhesion molecule-1 (PECAM-1) and passing between endothelial cells via endothelial cell junctions. This process has been studied and reviewed extensively, for example, by Liao *et al.* (1995) and Muller & Randolph (1999). Following their emigration from the blood to the tissue,

monocytes mature into their active macrophage form in response to local signals, such as GRO-α and MCP-1 (Gordon, 2003; Werner & Grose, 2003). Initially, they function to amplify the inflammatory response through the release of pro-inflammatory mediators such as TNF-α, IL-1β and IL-6. Later, anti-inflammatory mediators are released, including IL-10 and TGF-β, to bring about resolution of the inflammatory response. Macrophages are responsible for the production of new extracellular matrix and subsequent remodelling to provide a scaffold for replacement tissue to be built, both directly and through stimulation of other cell types (Hunt *et al.*, 1984; Leibovich & Ross, 1975). Growth factors are also released to stimulate the recruitment of fibroblasts and the migration of keratinocytes from the wound margin where they can begin the process of re-epithelialisation (Midwood, Williams & Schwarzbauer, 2004).

Macrophages have been shown to be essential to wound healing in a number of studies. One of the first to confirm their importance showed delayed wound healing in response to macrophage anti-sera (Leibovich & Ross, 1975). Mice deficient for two key modulators of macrophage recruitment and activation, MCP-1 and MIP-1α, also displayed delayed healing in terms of re-epithelialisation and vessel density (Low *et al.*, 2001). However, the differences in healing time were not significant from 10 days after injury, suggesting that a compensatory mechanism may be involved. Studies in mice deficient for neutrophils and macrophages have been shown to heal at the same rate as the wild-type equivalents (Martin *et al.*, 2003), although this may be a consequence of the absence of neutrophils and an inability to mount a "normal" inflammatory response. Without these more damaging aspects, the lack of macrophages may have less of an impact. The authors suggest that there must be a level of compensation in this situation, with platelet factors fulfilling the stimulatory functions. This model is therefore unsuitable for demonstrating the necessity of macrophages as it does not show the effect of their specific depletion or represent an otherwise "normal" system.

The majority of reports suggest that the action of macrophages is key to the correct resolution of the inflammatory response and to the initiation of repair. This is in part regulated by neutrophils, shown by studies in neutropenic mice, in which pro-inflammatory cytokine release from macrophages is not suppressed (Daley *et al.*, 2005).

This excess of pro-inflammatory factors means macrophages are often the causal factor in situations in which fibrosis occurs. This is caused by an over-production of fibroblast growth factors and by over-activity of the fibroblasts themselves (Wynn, 2008). Additionally, timely phagocytosis of neutrophils is of great importance as it prevents their necrosis and further tissue damage as a result (Vivers, Dransfield & Hart, 2002), which can lead to the development of chronic wounds. The appropriate recruitment and regulation of macrophages is therefore critical in ensuring not only stimulation of repair, but also limitation of damage.

1.1.4.3 Fibroblasts and Mast Cells

The contributions of two additional cell types - mast cells and fibroblasts - should also be noted, although they are not a focus of the present study.

Mast cells play important roles in the immediate response to injury, although their necessity for the later stages of normal wound healing is under debate (Artuc *et al.*, 1999; Egozi *et al.*, 2003; Iba *et al.*, 2004; Weller *et al.*, 2006). They comprise between 2 and 8 % of cells within the dermis, situated close to their targets and sources of stimulation, such as blood vessels which both supply exogenous signals and respond to those released by mast cells. Given their location, it is unsurprising that mast cells are one of the first cell types activated following injury. A large number of pro- and anti-inflammatory mediators are released, depending on the stage of the injury response. Of particular interest to the present study is the effect on the vasculature, as mentioned in the section on vascular endothelial cells 1.1.3.2 above.

Fibroblasts are activated in the later stages of the injury response, that is, during granulation, matrix secretion and wound contraction (Singer & Clark, 1999). They are attracted to the wound site by growth factors released by macrophages and keratinocytes, and secrete extracellular matrix components in response, particularly collagen. Following this, they undergo a maturation into myofibroblasts which are responsible for the contraction of the wound. These cells are not involved in the control of the initial response to injury and, although their correct regulation is important in preventing fibrosis, their contribution is not within the focus of this study. However,

the mechanisms leading to their recruitment is likely to be of interest earlier on. The role of fibroblasts in wound healing is the subject of a number of reviews, for example, Eckes *et al.* (2000) and Werner, Krieg & Smola (2007).

1.1.5 The need for better markers of the injury response

The pleiotropic nature of many cytokines and growth factors means these are inappropriate markers of the injury response. They are not present in distinct phases, so the presence of an individual cytokine will not necessarily be indicative of tissue status. Comparing changes in levels of a panel of such molecules would improve the accuracy of characterisation. However, the roles of these in the haemostatic, inflammatory and proliferative phases makes it very difficult to predict the cellular infiltrate, level of infection and the progression through inflammation to resolution. The suitability of cytokines as markers of the inflammatory response are considered further, in Chapter 3.

It is hypothesised that an investigation into the temporal changes in general protein content of the wound environment could lead to the identification of biomarkers for distinct stages of the injury response. To achieve this, a method to sample soluble components from the injury site is required (Sections 1.2 and 1.3), along with methods to identify unknown targets that are recovered in the sample (Section 1.4).

1.2 Methods of Studying Skin Injury

To date, the majority of investigations into skin injury have focussed on animal models and human tissue samples, both *in vitro* in terms of isolated cell populations and *in vivo*, in terms of biopsy tissue. More recently, other experiments have assessed changes in gene expression following an injurious stimulus, using cells obtained from biopsies (Bryan *et al.*, 2005), or from biological fluids such as plasma and fluid exudate from the wound surface. The transcriptional control of wound healing was reviewed recently, by Schäfer & Werner (2007). Nucleic acid samples (DNA and RNA molecules) are typically extracted from tissue or plasma samples, but proteins can also be obtained

from such body fluids. The proteins themselves, along with their modifications, should give a more accurate description of the signalling processes in operation, as previously discussed.

Proteomic technologies offer the chance of identifying novel protein mediators involved in the response to injury. However, the subset of proteins identified will be reliant on the method by which the injury is sampled. Previous studies of skin injury have focussed on the use of skin biopsy tissue from both animals and humans, in which the spatial distribution of cellular infiltrates and specific markers have been targeted and characterised. The different methods available for sampling the cutaneous response to injury will now be considered in terms of their suitability for providing a source of novel markers.

1.2.1 Tissue samples in injury research

Much of the research into the response to cutaneous injury to date has been conducted on solid tissue samples, such as skin biopsies and cell culture models. Immunohistochemistry staining of excised tissue samples have shown the location of cells, cytokines, chemokines and adhesion molecules (e.g. Engelhardt *et al.*, 1998; Juhasz *et al.*, 1993) at different timed intervals following injury. However, the removal of this tissue leaves permanent scars, which is undesirable in human studies. Futhermore, it is also not amenable to more than a few replicates or time-points per individual.

More recently, experiments have been performed using artificial skin constructs (Speikstra *et al.*, 2007), which avoids the problems of movement and availability encountered when using human volunteers, but is unlikely to be truly representative of the full systemic response. Laser capture microdissection can also been applied, to isolate specific regions of tissue for later analysis by a wide range of methods, including proteomics, to enable analysis of unknowns (Espina *et al.*, 2007). Along a similar principle, matrix-assisted laser desorption/ionisation (MALDI) imaging mass spectrometry (MS) could prove highly informative in terms of spatial analysis of protein expression in tissue sections (Stoeckli *et al.*, 2001), with temporal analysis achieved through sequential samples. Whole fresh-frozen tissue sections, individual cells or sections produced by

laser-capture microdissection are coated in an appropriate MALDI matrix and placed within a modified mass spectrometer containing a mounted camera. The camera provides a reference to the locations sampled, providing 2-D maps of protein localisation or molecular mass, with a resolution of 4 μm. However, this method requires specialist instrumentation that is not yet widely available.

Tissue samples provide a rich source of biomarkers with the potential for novel identifications, and their analysis has great potential in future studies of the injury response. However, the vast differences in concentrations of proteins and other components within these samples may complicate analysis, masking the identification of potentially key mediators. Furthermore, they do not allow for continuous sampling in an *in vivo* setting and require re-injuring the tissue to gain repeat measures. While explants and artificial skin constructs might allow for continuous sampling without re-injury, these samples are not truly representative of the full *in vivo* response.

1.2.2 Plasma and other biofluids as a source of biomarkers

The most commonly used biological fluids in biomarker discovery experiments are plasma or serum, and urine. The plasma proteome has been relatively well documented (Anderson *et al.*, 2004), but its use in injury research has been rather limited. Due to the systemic nature of serum and plasma samples, these studies tend to be of large-scale trauma or reperfusion injury instead of a localised, mechanical injury in which conditions can be controlled and manipulated to better understand the response.

The advantages of using plasma or serum samples are the extent of contact they have with every cell in the body, the ease of sampling and the abundance of established and newly developed proteomic analysis protocols. The wide reach of these samples is also to their disadvantage as a source for biomarker discovery. Proteins released from a specific population of cells will be in such low quantities relative to the common plasma proteins as to preclude their detection, a consequence of the large dynamic range of plasma. The concentrations of different proteins within plasma is thought to exceed 10 orders of magnitude, well beyond the analysis capabilities of current technology of approximately 2 – 3 in standard MS, 4 – 6 with pre-fractionation (Jacobs *et al.*, 2005).

One report, as part of the multi-centre collaborative Inflammation and the Host Response to Injury initiative (http://www.gluegrant.org/index.htm), discusses the different approaches available to reduce this sample complexity, in plasma obtained from trauma patients. In order to detect potential novel markers of the response to injury, the 12 most abundant proteins in plasma were first removed using an antibody-based depletion system, thus reducing the immediate dynamic range of protein concentrations. These proteins constitute an estimated 96 % of the total protein content and are typically found at high μ – mg/ml levels. Additional fractionations were performed to enrich for cysteinyl and glycopeptides prior to strong cation exchange chromatography, further reducing sample complexity and increasing access to the less abundant protein components (Liu *et al.*, 2006). These treatments enabled identification of many proteins involved in inflammatory reactions, including 78 cytokines and cytokine receptors. This is considerably more than the 4 out of an expected 36 found by Anderson *et al.* (2004) from 2D-gel electrophoresis-separated, Ig-depleted and low molecular weight serum fractions. However, these inflammatory markers are often constitutively expressed in plasma and may be indicative of or confounded by other disease states, as discussed in Section 1.5.2. Furthermore, these are systemic markers and as such are unlikely to provide information about the affected, local tissue environment.

Use of cerebrospinal fluid, saliva, sputum and other body fluids is increasing with demand for a more specific, localised sample, directly representative of the disease environment of interest. The applications and technical considerations of many different body fluids in proteomic analysis was recently reviewed by Hu, Loo & Wong (2006). Analysis of bronchoalveolar lavage (BAL) fluid collected from sclerotic lung was able to identify the possible involvement of several proteins in protection against inflammation (e.g. Cu-Zn superoxide dismutase, an antioxidant enzyme) and others (e.g. calumenin, a calcium-binding protein) in the progression of fibrosis (Fietta *et al.*, 2008). Similarly, cerebrospinal fluid has been analysed to determine differences between inflicted and non-inflicted traumatic brain injury in young children, which would of course have important legal applications (Gao *et al.*, 2007). Both studies highlight the importance of localised sampling in order to obtain a physiologically relevant subset of protein medi-

ators. However, with lesser known biofluids comes unexpected problems. In compiling the sputum proteome, Nicholas *et al.* (2006) had to overcome the interference of a high abundance of mucins, highly charged glycoproteins that are highly resistant to proteolysis.

Unlike the lung (BAL, sputum) or brain (cerebrospinal fluid), the skin doesn't immediately appear to have a specifically associated body fluid. Instead, the interstitial fluid that bathes all cells of the body, including those of the skin, provides a source of potential biomarkers from this organ. It is formed from plasma filtered from local capillaries due to hydrostatic pressure, and from the molecular mediators released from the local cell populations, making it a highly relevant source of protein components. The use of interstitial fluid and means of collecting it are discussed in the following section.

1.2.3 Interstitial fluid as the local alternative

The interstitial fluid space is the site of mediator exchange and communication between cells, therefore interstitial fluid itself is the most appropriate sample for investigating the signalling processes involved in the response to injury. Sampling of interstitial fluid directly enables detection of small changes in concentration of cytokines, for example, not detected in plasma samples (Pachler *et al.*, 2007). There are several methods of sampling interstitial fluid from humans *in vivo*, including fluid obtained from skin biopsy samples, suction blisters, capsules, wicks and microdialysis.

Interstitial fluid components can be obtained directly from skin biopsy and other tissue samples via gentle centrifugation (Bletsa *et al.*, 2006; Wiig, Aukland & Tenstad, 2003). Low speeds of 68-6800 $\times$ g are used, to draw off the interstitial fluid without rupturing the cells and releasing their contents. Validation studies have shown that the intracellular and plasma contamination levels are negligible (Wiig, Aukland & Tenstad, 2003). Consequently, the interstitial fluid obtained can be assumed to be identical to that *in vivo*, with an accurate representation of actual tissue protein concentrations. While this method enables efficient collection of proteins, it limits the time-course that can be studied. To study temporal changes, multiple biopsies would need to be

acquired and this still does not enable continuous sampling. While this is possible in animal studies, it is inappropriate in human studies where permanent scarring occurs and less-damaging methods, such as collection of suction blister fluid, are available.

The generation of suction blisters causes an injury response and can be used to obtain interstitial fluid. Suction blister fluid is obtained by raising blisters on the skin under negative pressure and removing fluid by aspiration with a needle. It is a very simple method that has been used extensively for characterisation of skin cytokine responses to stimuli such as ultraviolet irradiation (e.g. Kuhn *et al.*, 2006) and from skin disorders such as psoriasis (Reilly *et al.*, 2000). Studies of cutaneous wound repair utilising skin blisters tend to measure re-epithelialisation rather than the early stages of inflammation, although interstitial fluid obtained from the blisters would provide protein components for proteomics analysis. A Pubmed search for suction blister proteomics returns two studies in which several hundred protein spots were detected on 2-D electrophoresis gels from suction blister fluid obtained from both healthy and psoriatic skin (Kool *et al.*, 2007; MacDonald *et al.*, 2006). These experiments will be discussed briefly in the context of the skin proteome in Section 1.5.1 and will be covered in greater detail in Chapter 4. Unfortunately, despite these successful analyses, the suction blister method is unsuitable for continuous sampling and therefore temporal analysis of the injury response. To observe changes over time, several blisters would need to be raised and then sampled at different timed intervals, but this would still not give full flexibility of measurement.

Capsules and wicks have also been used as methods for isolating interstitial fluid components. These devices are implanted into the tissue of interest and interstitial fluid and soluble components are collected, for example, by absorption in the case of dry wicks (Wiig *et al.*, 1991). A wide range of solutes can be recovered by either method, including electrolytes and proteins such as albumin (Zurovsky, Mitchell & Hattingh, 1994) and implantation generates an injury response. To date, there have been no reports published on the proteome of interstitial fluid obtained by either method, in humans or other animals, although the ability to measure total protein concentrations would indicate the possibility exists. However, neither method is likely to be suitable

for the temporal analysis of the injury response as both suffer the same limitations of the tissue centrifugation and suction blister techniques. That is, continuous sampling of interstitial fluid cannot be performed and repeated sampling, with the associated repeated injury, would be required to obtain temporal data.

Microdialysis is an alternative method for collection of soluble components from the interstitial fluid that does allow continuous sampling. This involves the insertion of fine, porous probes which are perfused with physiological saline, mimicking a blood capillary (Ungerstedt, 1991). Soluble components from the interstitium diffuse into the probes and are collected as dialysate. The technique has the advantage that it allows continuous sampling of the interstitium without causing further damage to the tissue beyond the initial insertion injury, which is of particular benefit in the study of the early response to injury. Moreover, it enables continuous monitoring of *in vivo* processes that will be much closer to the true response than that observed for isolated tissue or cell samples treated with only a limited subset of those mediators normally available to the tissue. It was decided that microdialysis was the most appropriate method of collecting soluble bioactive mediators released from the skin after injury and this method is discussed in greater detail in the next section.

1.3 *In vivo* microdialysis for protein recovery

Microdialysis was developed in the 1960s as a method of sampling neurotransmitters from the brains of experimental animals (Bito *et al.*, 1966). Since then it has been refined and adapted for the sampling of small molecules from many other organs including skin, and more recently for the sampling of larger molecules such as proteins (Clough, 2005; Rosenbloom, Sipe & Weedn, 2005). The principles and applications of microdialysis have been extensively reviewed (e.g. Benveniste & Hüttemeier, 1990; Chaurasia *et al.*, 2007; Groth, Ortiz & Benfeldt, 2006; Shippenberg & Thompson, 1997; Stenken, 2006), so only a brief overview of the technique in the context of protein recovery is necessary here.

Microdialysis operates through the diffusion of soluble molecules from the intersti-

tial fluid space across the semi-permeable membrane of a probe continuously flushed with a suitable perfusate (Figure 1.3).

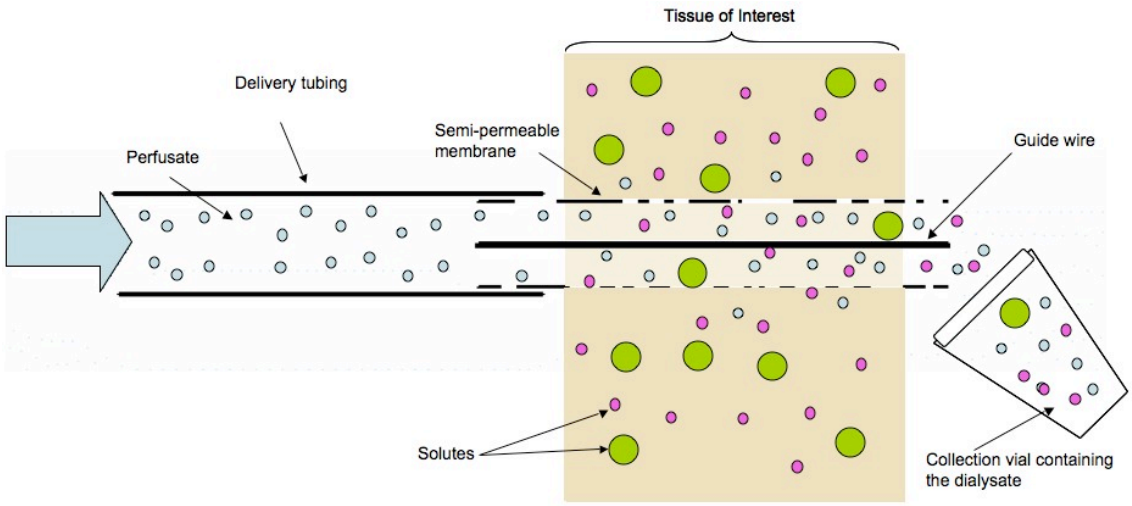

Figure 1.3: **Schematic of microdialysis.** The probe consists of a tubular semi-permeable membrane supported by internal guide wire. This is connected to delivery tubing by a water-tight seal. Perfusion of the probe with an appropriate solution, termed the "perfusate", causes solutes to diffuse into the probe, collected as dialysate. Schematic not to scale.

According to the principles of diffusion, larger molecules will travel more slowly due to greater impedance by the extracellular matrix environment. Thus, larger molecules are typically recovered at a lower efficiency than smaller ones. This is represented in Figure 1.3 by the reduced proportion of the large, green solutes in the probe and in the vial of dialysate compared to the smaller pink molecules. The continuous flow of the perfusate through the probe ensures that the concentration gradient is maintained, enabling uninterrupted sampling of a single region. This is of particular benefit during temporal experiments, especially as the collection periods can be varied to suit the sample volume requirements and time-course of the investigation. The types of molecules that are recovered can be controlled to some extent by the membrane size, that is, the molecular mass cut-off (MWCO) of the pores. Smaller MWCO membranes, for example 5 kDa, will limit recovery to small solutes and exclude most proteins. The

larger 100 or 3000 kDa membranes should theoretically allow most proteins and protein complexes to pass into the probe. However, this is rarely the case due to the reduced diffusion rates of larger molecules, discussed in greater detail in Section 1.3.1.

The 3000 kDa cut-off microdialysis probes used for recovery of larger molecules such as proteins are constructed from the membranes of renal dialysis capsules. The hollow, porous fibres are supported by an internal guide wire and fed into fine-bore polythene tubing, depicted by the black lines in Figure 1.3. This probe is connected to a syringe pump capable of delivering the perfusate, such as a physiological saline solution, at microlitre flow rates adjusted to suit the purposes of the experiment. Typical flow rates range from 0.1 μl/min for studies requiring a higher efficiency of solute recovery but low volumes of sample to 5 μl/min where larger sample volumes are required at the expense of solute recovery. The flow rate and sample volume are among the technical considerations that need to be taken into account in microdialysis experiments, discussed in the following section.

1.3.1 Technical considerations in *in vivo* microdialysis experiments

The most important considerations for protein sampling are the efficiency of microdialysis and properties that influence the types of proteins that can be recovered. The factors affecting the efficiency of solute recovery by microdialysis sampling have been extensively reviewed (e.g. Shippenberg & Thompson, 1997; Zhou & Gallo, 2005 and other reviews cited previously), but merit a brief discussion in the context of protein recovery specifically.

Microdialysis efficiency describes the relationship between the amount of a protein within the tissue and the amount that is recovered in the dialysate. It is not yet possible to determine the tissue concentration of a given protein *in vivo* from the concentration within the dialysate alone. Instead, a number of different approaches are available by which this tissue concentration can be approximated. *In vitro* experiments have shown the relative efficiency of recovery of large plasma proteins, such as human serum albu-

min, to be approximately 20 % (Winter *et al.*, 2002). However, it is inappropriate to extrapolate this to the *in vivo* environment, because the *in vitro* experiments typically dialyse proteins from a free solution. The movements of proteins in free solution are not inhibited by the presence of extracellular matrix, so there is a tendency to overestimate the *in vivo* concentration based on such experiments. Equally, the osmotic and physical pressures will be very different within the tissue, which will also influence the rate of diffusion.

In vivo methods, such as retrograde microdialysis, provide a more appropriate measure. This method calculates the percentage decrease in concentration of a solute marker between the perfusate and the collected dialysate. However, these calculations rely on the assumption that solute uptake is equivalent to the loss of solute within the perfusate. This seems unlikely given the differences in conditions between the probe lumen and the extracellular tissue space. Consequently, estimates of tissue concentration extrapolated from calibration experiments should be confirmed by other means when possible.

Despite the difficulty in determining actual *in vivo* concentration, microdialysis remains an invaluable sampling technique for its ability to recover proteins continuously and without further perturbation of the tissue. Although quantitation of tissue concentration would be of great interest, this is not always necessary. Instead, knowledge of the expected range or degree of change in concentration of a protein in dialysate can provide sufficient information about the comparative tissue status between conditions.

This continuous sampling has been used for studies over four weeks in length (Borjigin & Liu, 2008), however, there a decrease in total recovery is observed with increased time. Over the course of a dialysis experiment, the pores of the probes can become blocked, by large protein aggregates for example. *In vivo*, this is partially a result of the response to injury but in the short term, blockage occurs passively through adsorption of solutes to the membrane. Significant blocking of the larger pores was not observed until three days after implantation of the probe (Wang *et al.*, 2007). However, the extent of blockage with the smaller pores could not be determined due to limitations in the resolution of the scanning electron microscope used, so the degree of influence

remains unknown.

Experiments have shown that there is a reproducible pattern in the change in concentration of total protein recovered in dialysate over time (Clough, 2005). An initial peak in total protein recovered in dialysate is observed immediately after probe insertion. This is followed by a rapid decrease in protein concentration until it reaches a steady state after a few minutes, reflecting the reduction in protein extravasation from any damaged vasculature and also the reduction in available protein as it is removed in the dialysate. The steady-state is hypothesised to occur once the rate of removal of protein by microdialysis is balanced by rate of the replenishment from the tissue. Total protein concentration in steady-state dialysate samples from unperturbed skin and perfused at 3 μl/min is approximately 1 mg/ml (Clough, 2005), compared to skin interstitial fluid protein content estimated to be >11-30 mg/ml (Fadnes, 1975; Haaverstad, Romslo & Myhre, 1997). However, these estimates will vary depending on the animal, tissue and sampling technique used. Any change in the rate of replenishment due to biological phenomena will be reflected in a corresponding change in the amount of protein recovered in the dialysate. Hence, although the tissue concentration of any specific protein is unknown, the magnitude of change can be determined as percentage of the total protein recovered in the dialysate and thus provide important information regarding tissue status.

The effect of tissue depletion is likely to be greatest for larger proteins and consequently, their recovery is often limited, as mentioned in Section 1.3. This is simply explained by considering that the extracellular matrix exists in the form of a gel and that larger sized and higher molecular weight proteins will not be able to pass through the matrix so easily. Hence the low diffusion coefficient for large molecules and the inversely proportional relative recovery rate with size (Benveniste & Hüttemeier, 1990). A compromise between maximal recovery of large proteins and a sufficient volume of dialysate can be achieved through selection of an optimal perfusion rate. This is one of the key factors governing the amount of protein that can be recovered by microdialysis, as mentioned in the previous section. Calculations of *in vitro* protein recovery at increasing flow rates shows an exponential decrease that reaches steady state at approx-

imately 5 μl/min. Above this rate, protein recovery is not significantly compromised and may in fact be increased over longer sampling periods (Clough, 2005). However, a slower perfusion rate will enable more time for an equilibrium to develop between the probe lumen and the tissue, giving a dialysate sample that better represents the tissue concentration of individual proteins.

Finally, only those proteins which are water-soluble and freely able to diffuse within the extracellular tissue space are available for recovery by microdialysis. However, intracellular and membrane proteins or proteins within complexes bound to the extracellular matrix may be sampled following tissue disruption. Collection of lipid soluble molecules may be enhanced using different membrane or perfusate compositions (Sun & Stenken, 2003). The types of molecules that have previously been recovered using microdialysis are discussed in the following section, with particular emphasis on protein studies.

1.3.2 Types of molecules recovered by microdialysis

With the importance of microdialysis sampling in neuroscience research, a large proportion of the molecules targeted for study have been neuropeptides. A list of neuropeptides, amino acids and other small molecules, such as histamine, that have been sampled using microdialysis is given in the review by Shippenberg & Thompson (1997). Since that report, the list of proteins that have been sampled has increased as larger MWCO probes, new antibodies and new technologies have enabled recovery and detection of a wider range of large molecules (reviewed in Clough, 2005). However, these identifications are predominantly due to specific, targeted analyses and will not generate novel markers.

The past 10 years has seen an increase in popularity of a more global approach to analysis of biological fluid samples, as proteomic analyses have become more advanced and more widely available. These techniques enable identification and quantitation of unknown targets, removing the limitations to those target molecules for which suitable antibodies have not yet been generated.

Once again, neuroscience was one of the first fields to adopt such technologies

for use in conjuction with microdialysis sampling in humans. No studies combining microdialysis in animals with proteomic analysis had been published at the time of writing. Maurer *et al.* (2003; 2007) and Haskins *et al.* (2004) have been among the first groups to publish on the proteome of cerebral dialysate. In the 2003 paper, Maurer and colleagues identified 27 proteins, including 10 specific to cerebral dialysate compared to cerebrospinal fluid. Proteins identified included neuropeptide precursors, structural proteins and plasma proteins such as neurogenin, fibrinogen and creatine kinase. Thus demonstrating that this is an informative and successful approach to analysis of the local tissue environment and dialysate. The range of molecular mass and pI values for the identified proteins was between 13 – 190 kDa and 4.5 – 7.8, respectively. This is a broad range of size and a pI range similar to that of the skin (Marro, Guy & Delgado-Charro, 2001). Several classes of proteins, such as those that are insoluble or bound to insoluble structures, are excluded by microdialysis sampling for reasons covered in the previous section. However, it is likely that a large proportion of signalling molecules are able to diffuse freely through the interstitial fluid space and thus be recovered by microdialysis. Therefore, it is hypothesised that this microdialysis-injury sampling model provide a protein-rich sample from which novel markers of the injury response may be obtained. The methods by which this sample is analysed will determine the types of markers that can be identified.

1.4 Analytical approaches to characterising the injury model and identifying novel markers

Several approaches are required in characterising the inflammatory response in skin to the microdialysis model of injury. Preliminary, non-invasive measures are required, alongside measurements of existing markers, to characterise the injury model and put it into the context of the existing knowledge. Once the correlation between the sampling period and the expected progress of the response to injury have been determined, the presence of novel markers can be investigated.

1.4.1 Non-invasive quantification of the inflammatory response to skin injury

The vascular response to injury is an important measure of inflammation as it is the mechanism behind three of the cardinal signs of inflammation; calor, rubor and tumor, that is, heat, redness and oedema. The heat comes from an increased flow of blood from the body core, which is at a higher temperature than the skin circulation. This increase in blood flow to the area is visualised as the increased redness to the skin. The oedema comes from increased permeability of the capillaries to plasma and protein. It is possible to measure inflammation non-invasively, by quantifying these three properties of the inflammatory response.

1.4.1.1 Quantitation of changes in cutaneous blood flow in the response to injury

Several methods are available for the measurement of changes in cutaneous blood flow. These were reviewed by Lima & Bakker, 2005; Swain & Grant, 1989 and Vennemann, Lindken & Westerweel, 2007 and so will not be described in detail here. While skin temperature can be measured and is related to the amount of blood flow, a more appropriate and accurate measure of inflammation is the redness, that is, the amount of blood flow at the injury site.

Skin colour can be determined by colorimetric methods, as a measure for erythema (reviewed by Fullerton *et al.*, 1996). While removing the subjectivity of the human eye, these methods are better suited to studies into irritant reactions where there is a well-defined and more pronounced region of inflammation, and more direct measures of cutaneous perfusion are available.

Methods using radio-labelled tracers give a more accurate measure of skin blood flow but are invasive. Instead, a commonly used group of non-invasive methods for blood flow measurement take advantage of the Doppler frequency shift. This is the diffraction that occurs when low-power red laser light is shone onto moving objects, specifically erythrocytes within the dermal vascular plexus in this instance. The magnitude of this

diffraction is a product of the velocity of the erythrocytes, thereby giving a measure of the rate of blood flow over a given area (Vongsavan & Matthews, 1993). The two predominant forms of laser Doppler analysis are perfusion monitoring (fluximetry) and perfusion imaging, reviewed in Rajan *et al.* (2007). Both forms enable non-invasive measurements of relative quantification, but only perfusion imaging enables measurements over a two-dimensional area as opposed to the single point, continuous measurements of fluximetry. As injury affects the tissue across a three-dimensional volume as well as over time, perfusion imaging is better suited than fluximetry in this study.

1.4.1.1.1 Laser Doppler imaging to quantify blood flow Laser Doppler flowmetry was first used to measure vascular blood flow in humans during the 1970s (Stern, 1975). However, this method measures only at a single fixed point and does not take into account the local heterogeneity of blood flow in the skin. More recently, the technique has developed to enable 2-D measurements (Essex & Byrne, 1991), using a laser Doppler imager. This instrument measures blood flux within both the small, nutritive capillaries and the underlying arterioles and venules of the skin vasculature by calculating the degree of refraction of a low power laser light shone onto the skin (Basic Theory and Operating Principles of Laser Doppler Blood Flow Monitoring and Imaging (LDF & LDI), Issue 1, 2003). Figure 1.4 shows the components of the Laser Doppler Imager.

Briefly, low power (∼2 mW) laser light is shone onto the skin, via a scanning mirror that deflects the light in a raster pattern across the area of interest. On contact with the skin, the beam scatters. The majority of the light is reflected back along the same path, either from the skin surface, or from static structures within. Light that hits moving objects, predominantly erythrocytes, is refracted and returns at a different frequency. This light penetrates to a depth of between 0.6 and 1 mm below the skin surface. The returning light is detected by the photodiodes and the signal processed to produce a 2-D image of flux, the velocity of the erythrocytes as a function of their number concentration, across the scanned area. This image can then be analysed

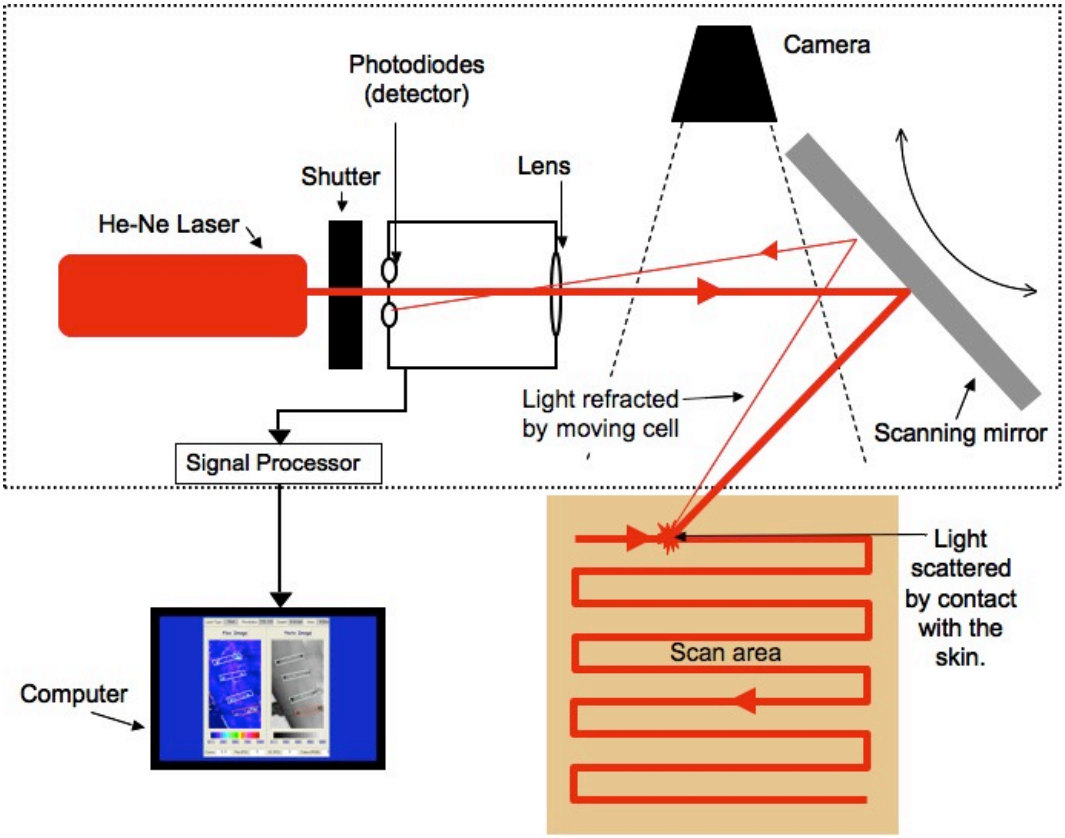

Figure 1.4: **Components of the Laser Doppler Imager**. Light from a 633 nm, Helium-Neon laser is shone onto the skin via the scanning mirror. Refracted light is detected by photodiodes and the signal processed into a 2-dimensional image. The camera takes a black and white photograph for orientation. Figure adapted from Basic Theory and Operating Principles of Laser Doppler Blood Flow Monitoring and Imaging (LDF & LDI), Issue 1, 2003.

off-line to determine mean blood flux over a given area of interest.

Laser Doppler imaging has been successfully combined with microdialysis experiments into inflammatory reactions, as it does not effect the tissue under study. It has also been used to investigate the vascular response to microdialysis probe insertion (Groth & Serup, 1998), so will provide a useful measure to show that the results obtained in the present study are comparable with the existing literature and are thus representative.

The main disadvantage of this method is the time taken to perform the 2-D scan, because the entire area of interest currently cannot be scanned simultaneously. This can be somewhat off-set in studies of the vascular response to microdialysis probe insertion by the necessary staggering of needle insertions. An experienced investigator can insert the guide needles within the same time frame as the scan, thus avoiding differences between insertion and scan time between injury sites.

The measurements of changes in cutaneous blood flow during inflammation can be complemented by measurements of capillary permeability to give a more comprehensive analysis of vascular responses in inflammation.

1.4.1.2 Quantifying vascular permeability in response to injury

During an inflammatory response, the permeability of dermal capillaries to protein increases to enable increased delivery of the necessary mediators. One common measure for quantifying vascular permeability and the associated local swelling, protein and fluid extravasation is to measure skin thickness, either using calipers, or by ultrasound methods. Changes in skin thickness in response to microdialysis probe insertion have been reported previously (Groth & Serup, 1998). Of the measures explored in that study, only skin thickness remained constant throughout the duration of the experiment, following probe insertion. While showing that the oedema is present over at least the first 2 hours after insertion, this does not describe any changes in the content of this fluid.

The permeability of capillaries to protein has previously been measured using radiolabelled tracers (Aschheim & Zweifach, 1961; Graham & Evans, 1991) or dyes such as

trypan or Evans blue that bind to proteins (Ferrero, 2004; Moitra, Sammani & Garcia, 2007 and references therein). However, if the dye molecules become free, they will lead to an over-estimate of capillary permeability. Furthermore, these methods are more invasive and not ideal for human *in vivo* studies, especially for measurement on a local scale. Instead, the safest, minimally invasive method would be to measure the recovery of markers of vascular permeability or of total protein concentration in the dialysate as a surrogate for extravasation. Total protein concentration can easily be quantified from 10-20 μl samples using commercially available assay kits. Several studies have already quantified the protein concentration in dialysate samples from microdialysis at different perfusion rates (Clough, 2005; Klede, Handwerker & Schmelz, 2003; Sauerstein *et al.*, 2000), which will enable comparison of the results obtained in the present study to the existing literature.

Several mediators involved in increasing macromolecule permeability of the endothelial barrier, including histamine and the cytokines TNF-α and VEGF were discussed previously, in Section 1.1.3.2. The recovery of histamine in dermal dialysate has been well characterised in several studies into skin allergy (e.g. Groth, Jørgensen & Serup, 1998; Petersen, Church & Skov, 1997), so will not be repeated here. TNF-α has been recovered from skin using microdialysis in several experiments which show only low levels, < 20 pg/ml for up to 8 hours after injury (Averbeck *et al.*, 2006; Clough *et al.*, 2007). Recovery of VEGF from the skin by microdialysis has not yet been reported, so quantification of this factor would provide a second measure of endothelial barrier permeability and contribute to knowledge of the cytokine profile in response to microdialysis probe insertion.

1.4.2 Measurement of existing markers of inflammation in dialysate samples

Previously, microdialysis samples have been analysed for specific targets, using a wide variety of methods such as enzyme-linked immunosorbent assays (ELISAs), radioimmunoassays (Blakeman, Wiesenfeld-Hallin & Alster, 2001), HPLC (Grabb *et*

al., 1998) and Western blotting (Planas *et al.*, 2002).

Western blotting techniques are not easily multiplexed, where more than one target is being investigated and the method is quite time consuming. Also, unless protein transfer is optimal, there may be loss of protein during blotting and therefore an underestimate of protein concentration. Radioimmunoassays have rather been replaced by the safer, more sensitive ELISA format. ELISAs are currently considered the gold-standard for quantification of individual target molecules and are increasingly being used in multiplex experiments (Clough *et al.*, 2007). However, multiplex kits are not very flexible and custom panels are expensive. Furthermore, the volume requirements for these assays are high, which limits the temporal resolution that can be achieved.

More recently, bead-based assays have been used to measure the concentration of multiple cytokines in dialysate samples of as little as 50 (Angst *et al.*, 2008) or 15 μl (Ao *et al.*, 2005). The two most widely available multiplex bead assay platforms are the Luminex system, requiring its own analysis instrumentation, and the cytometric bead array produced by BD Biosciences, which is compatible with most flow cytometer instruments.

1.4.2.1 Multiplexed cytokine analysis using the BD Biosciences cytometric bead array assay

The cytometric bead array (CBA) Flex Set consists of a master kit containing all the necessary buffers, and individual cytokine kits with the specific antibody-coated beads, detection reagents and standards. This allows the investigator to select a unique panel of targets, according to the requirements of their experiment.

The assay uses a sandwich principle, in which cytokines within the biological sample are conjugated first to an antibody coated bead and then to the phycoerythrin (PE) fluorescent detection reagent, as shown in Figure 1.5. The main advantages of this method over the alternatives are the effective number of replicates and the ability to multiplex in very low sample volumes ($\sim$ 50 – 100 μl).

Briefly, protein samples are incubated with the capture beads coated with antibodies to the target analyte(s), which bind if present. The fluorochrome(s) conjugated to

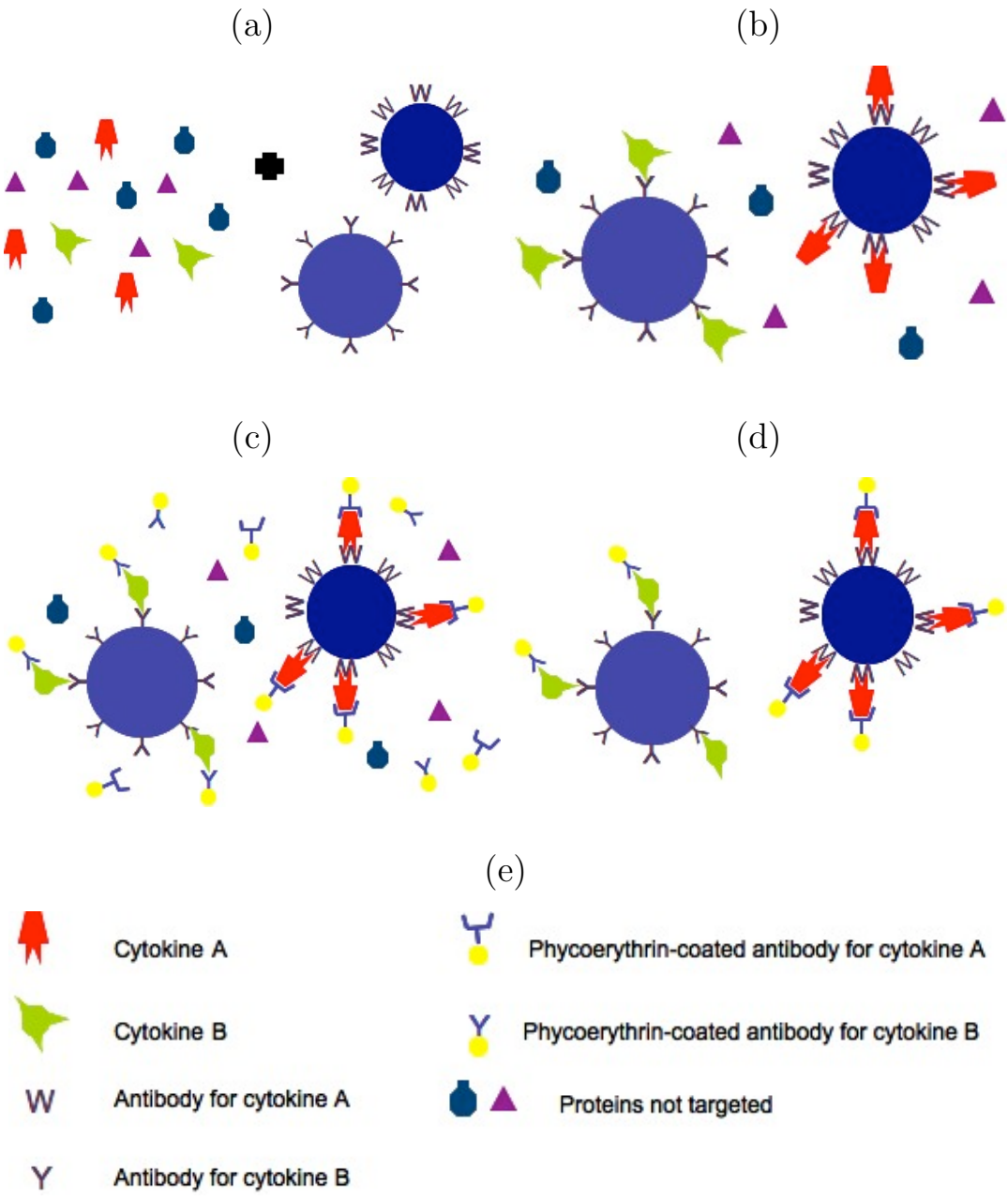

Figure 1.5: **Principle of the CBA assay.** Depiction of the main steps involved in the conjugation of cytokines from dialysate to the antibody-coated beads and detection reagent. a) The sample is incubated with the anti-body coated beads. b) Cytokines bind to the appropriate antibodies on the bead, while other molecules cannot. c) The antibody-conjugated PE detection reagent is added, binding to the corresponding cytokine. d) Unbound components are removed by a wash step. e) Key to the symbols used.

another antibody against the target analyte(s) are then added and bind to both free and bead-bound molecules. Excess capture beads and unbound fluorochromes are removed in a final wash step. Analysis is performed using flow cytometry, where the instances of the detection of each capture bead and the cumulative fluorescent intensity of the PE-detection reagent are counted for each analyte captured within the sample. Each bead is equivalent to one well in an ELISA experiment, so the CBA assay gives the equivalent of 300 replicates if the recommended settings are used (Human Soluble Protein Master Buffer Kit Instruction Manual, 2007).

Each capture bead in the Flex set is of a particular size and fluorescence. These two parameters give each bead population a characteristic profile of forward and side scatter within the flow cytometer, and therefore occupies a specific location within a two-dimensional grid. This enables up to 30 different beads to be combined into a multiplex panel, although sensitivity is reduced as the number of targets in the panel increases. There is some redundancy within the grid system, so care must be taken to ensure that bead positions are not duplicated within a multiplex panel.

Use of cytokine multiplex arrays will enable characterisation of an injury model in terms of the existing wound literature, but additional approaches are required if novel targets are to be identified.

1.4.3 Global assessment of protein content to enable the discovery of novel markers

To date, the majority of wound healing studies have used a rather piecemeal approach, investigating the roles of small groups of targets. With the development of gene microarrays, changes in RNA transcripts in response to injury have now been investigated, giving a greater view of the molecular events that occur (reviewed recently, Schäfer & Werner, 2007). However, such a global approach has been limited in terms of protein studies.

While microarrays give an important indication of the genes that are activated in a response, they cannot give any clues to the activation status of the gene products.

By studying the proteins themselves, a clearer understanding of their activation and interactions can be achieved. Furthermore, by using proteomics methods to identify the protein content of the dialysate samples from injured skin, a panel of potential markers can be determined for further investigation.

Graves & Haystead (2002) published a comprehensive review on proteomic technologies and applications in molecular biology, to which the reader is referred for a more detailed background.

1.5 Shotgun proteomics for surveying the proteome of biological fluids

Top-down or "shotgun" proteomics enables a survey of the components within a sample, the most common method being gel electrophoresis-liquid chromatography-tandem mass spectrometry (GeLC-MS/MS). This comprises an initial 1 or 2-D sodium dodecyl sulphate polyacrylamide gel electrophoresis (SDS PAGE), "Ge", separation step and subsequent band or spot excision. This is followed by in-gel digestion of proteins with a site-specific endo-protease prior to further separation by liquid chromatography (LC) and identification by tandem mass spectrometry (MS/MS). Shotgun proteomic techniques and their application to biomarker discovery and biological fluid samples is described in several review articles, including Hu, Loo & Wong (2006), McDonald & Yates (2002) and Wu & MacCoss (2002).

Two-dimensional gels are traditionally used for the identification of differentially expressed proteins, in which samples from two conditions are run on two separate gels and the differences in spot size compared. Differentially expressed protein spots can then be excised and the proteins identified. It is possible to excise all detected spots for analysis, but this risks missing proteins that are below the level of detection with the gel stain used. Instead, use of a 1-D separation provides an initial fractionation step to reduce sample complexity, without the loss of very low abundance proteins. The single gel track is divided into 20 – 30 slices of equal size which are then subjected to *in situ* digestion a site-specific protease such as trypsin. No proteins should be lost,

because the entire track is retained, as illustrated in Figure 1.6.

Digested proteins from each excised band are then fractionated further by liquid chromatography before injection into the tandem mass spectrometer, as previously described.

No studies combining microdialysis of human skin and shotgun proteomics have yet been published. However, the proteome of brain dialysate discussed in Section 1.3.2 (Maurer et al. 2003), shows that these technique can be combined successfully. While the proteome of brain dialysate will bear relatively little resemblance to that of the skin, extensive investigation is being conducted into the proteome of human plasma, from which interstitial fluid is partly derived.

One of the most comprehensive studies of the human plasma proteome to date was published in 2004 as a collaborative project combining three proteomic experiments with an extensive literature search (Anderson *et al.*, 2004). Whilst this study provided a vast amount of data, it highlighted the need for care in its interpretation. While 1175 individual components were identified between the four sources, only 46 were shared by all. A little under 20 % of proteins featured in two or more sources, although the authors inadvertently admit the literature search was not exhaustive. Indeed, pigment epithelium derived factor was included in the subset of proteins found in all three experimental datasets and not in the literature dataset, despite it being reported in plasma in 2003. Differences between experimental datasets are likely due to the different sample preparation and separation techniques, as well as inter-individual differences due to the low sample number. Knowledge of the components of plasma will inform which of those within dialysate are likely to be derived from plasma and which are more likely to have been produced locally by the injured tissue.

1.5.1 The proteome of skin

Investigations into the skin proteome using different sampling methods should inform the types of local proteins that may be recovered using microdialysis. Very few studies into the proteome of human skin *in vivo* have been published. Of those, the majority look at differential expression of proteins between healthy and diseased skin.

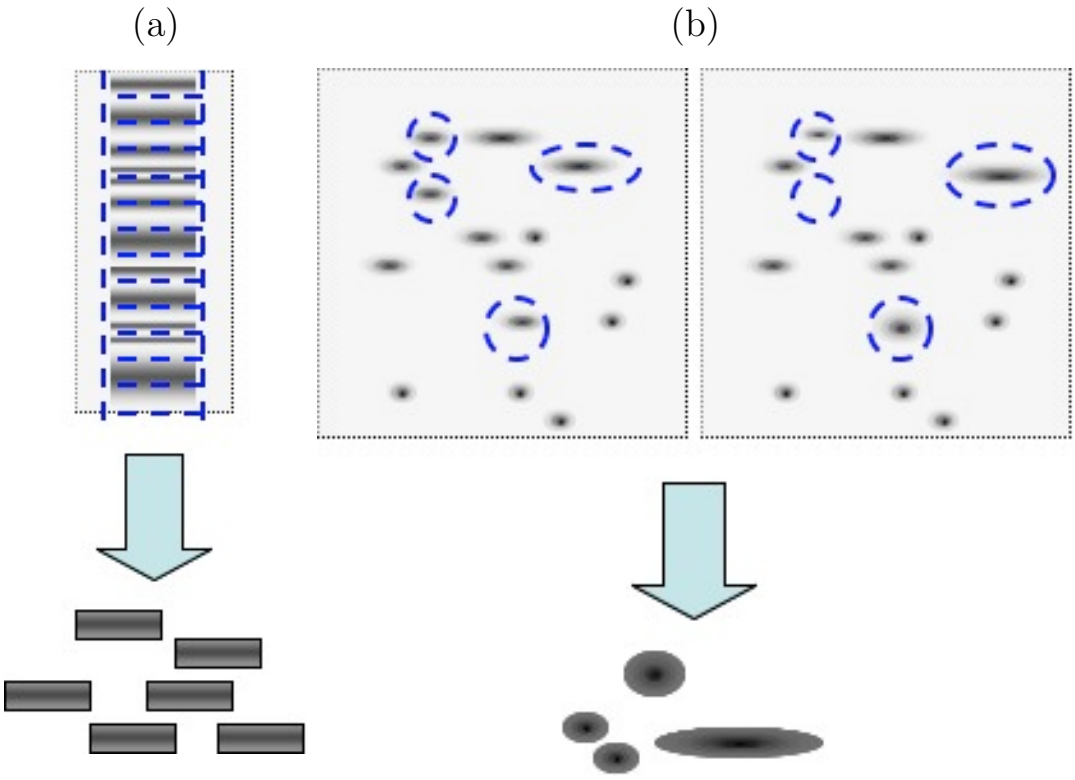

Figure 1.6: **Separation and excision of proteins from 1- and 2-D gels.** The entire track from a 1-D gel (a) is excised into equal-sized bands (blue dashed lines) which are then subjected to digestion and subsequent mass spectrometry. In contrast, detected protein spots in 2-D gels (b) are either all excised, or only those which have been differentially regulated (blue circles) - such as increased or decreased concentration (shown by changes in staining intensity, or an appearance/absence of a spot in one or other gel) or altered isoelectric point or mass (indicated by a shift in either the x- or y-axis). Proteins present below the level of detection for the chosen stain will not be visible on the gel and therefore cannot be removed and identified.

Aden *et al.* (2008) identified 23 proteins that were increased and 3 that were decreased between biopsies from healthy human skin and a fibrotic wound healing model, scleroderma lesional skin. Proteins were separated by 2-D SDS PAGE and those which demonstrated > 3-fold differences in expression between the two conditions were identified using peptide mass fingerprinting with MALDI-MS, rather than LC-MS/MS. The identified proteins included those involved in differentiation of the epidermis (keratins), motility (tropomyosin and vimentin), protein folding and protein metabolism (e.g. serum amyloid, α-1-anti-trypsin) and extracellular matrix components, such as α-collagens.

Proteomic analysis of human burn wound biopsies revealed proteins involved in acute stress, metabolic responses, inflammatory responses, cell migration and proliferation, structural proteins and those involved in the maintenance of cellular integrity (Pollins, Friedman & Nanney, 2007). These included keratins, heat shock proteins, fibrinogen and vimentin, previously identified in skin wounds. However, both this and the above-mentioned study used solid tissue samples, and so will contain a wider range of proteins, including intracellular and bound proteins that are unlikely to occur in interstitial fluid. Two studies looking at the protein content of skin blister fluid have recently been published.

Macdonald *et al.* (2006) published on the differences between normal skin and psoriatic skin in humans, using a suction blister sampling technique (n=1 in each group). A 2-D gel technique was used, in which only those spots significantly differentially expressed were subsequently identified. The proteins listed were significantly disease-associated or differentially expressed as a result of treatment with IL-1β, a pro-inflammatory cytokine. These included common plasma proteins such as complement, haptoglobin and apoliprotein. However, the authors did note a difference in the overall spot patterns compared to plasma, suggesting that there are detectable differences in the identities of proteins expressed in plasma and skin.

The following year, Kool *et al.* (2007) published on the proteome of suction blister fluid in healthy human volunteers. Although they were able to identify 401 proteins in the blister fluid, of which 202 were not found in plasma, only those that have been

reported as biomarkers or potential biomarkers were listed.

1.5.2 Considerations for biomarker discovery using proteomics.

The suction blister fluid proteome reported by Kool *et al.* (2007) used depletion of specific, highly abundant proteins to increase proteome coverage. The proteins removed included human serum albumin, estimated to comprise 40 – 50 % of the total protein content of suction blister fluid. Removal of these proteins increases the analysis capacity for less abundant components, but will reduce the overall protein concentration in a sample. In comparing the protein content in blister fluid to that in plasma, the authors report 202 proteins unique to suction blister fluid, 41 unique to plasma and 199 common to both sources. While the identification of only 240 proteins in plasma initially seems to be a dramatic underestimate, given the 1175 components identified by Anderson *et al.* (2004), each experimental source in that investigation contributed only 283 – 475 proteins once non-human proteins and redundant identifications had been removed. These differences highlight the influence of sample preparation and the analysis method chosen on the sub-set of proteins that can be identified.

Protein identities are inferred according to the matching of sequenced peptides obtained from tandem MS analyses. Complications in protein identification arise where peptide sequences are not unique to a single protein. This is particularly problematic when trying to distinguish between different isoforms of a protein. Unless a peptide containing amino acid sequences unique to a particular isoform are identified, this distinction cannot be made. Equally, where different proteins share identical regions of sequence, they may contain several identical peptides. Again, an unambiguous identification cannot be made without a unique peptide that distinguishes the true protein from the other candidates. Furthermore, there is redundancy in the protein databases, with many proteins having more than one name and associated entry. It is important that automatically-assigned identifications be manually examined to check for such instances. The problems of this inference system for protein identity assignment has been reviewed in detail (Nesvizhskii & Aebersold, 2005).

One final consideration is particularly important in terms of biomarker discovery.

It has become increasingly clear that particular groups of proteins appear on lists of differentially regulated components with surprising frequency. Petrak *et al.* (2008) conducted an investigation into reports of differentially regulated proteins, compiling a list of the most commonly identified proteins in human, rat and mouse experiments published between 2004 and 2006. Of note to this study, given the identifications in other skin proteome studies, are the inclusion of keratins and vimentin in the top 15 protein families. Analysis of post-translational modifications may shed light on whether these proteins are differentially activated in different studies.

1.6 Reversible protein phosphorylation as a crucial mechanism for regulation of protein function

Another advantage to studying proteins themselves is the ability to identify modifications and their effects. Reversible protein phosphorylation is the most common covalent modification in mammalian systems. It is involved in the control of a vast number of processes including metabolism, signal transduction, cell division, development and death, immune responses and inflammation (Berwick & Tavare, 2004).

The role of reversible protein phosphorylation in control of intracellular signalling has been investigated extensively and has been reviewed comprehensively in organisms from bacteria to humans (e.g. Hunter, 2000; Pawson & Scott, 2005; Stock, Ninfa & Stock, 1989), with over 150000 entries for "protein phosphorylation" in Pubmed. However, extracellular phosphorylation has received far less attention but is likely to be of equal importance, particularly in relation to plasma proteins and other secreted components that provide the means by which cells communicate with each other.

The role of ecto-phosphorylation by kinases on the external side of the cell surface membrane is important in control of the immune response, such as in platelet or complement activation (reviewed in Redegeld, Caldwell & Sitkovsky, 1999). The human plasma proteome has been reported to contain several extracellularly active kinases and protein phosphatases (Anderson *et al.*, 2004). This suggests that there are several sources from which regulators of phosphorylation status can infiltrate an injured tissue

and influence the function of resident proteins.

In eukaryotes, phosphorylation occurs on serine, threonine and tyrosine residues (Sickmann & Meyer, 2007), on the oxygen atom of the hydroxyl group on the amino acid side chain. The negative charge added by the phosphate group can attract positively charged amino acids within the protein, altering the conformation. This has an allosteric effect on enzyme action, for example, either activating or inhibiting the active site. Failure to correctly regulate reversible phosphorylation can lead directly to the development of diseases including alzheimers, cancer and heart disease (reviewed in Hunter, 1998, among others). Up to 5 % of the vertebrate genome is predicted to encode either protein kinases or phosphatases; enzymes that catalyse the addition or removal of a phosphate group respectively. It is hypothesised that over 30 % of all proteins can undergo phosphorylation (Schmidt, Schweikart & Andersson, 2007). However, because protein phosphorylation is a reversible, post-translational modification, it is impossible to predict accurately if, where and when a protein will be phosphorylated from the cognate DNA sequence alone. This means the protein itself must be isolated and investigated. Since many phosphoproteins are present in low numbers and only a fraction of those available phosphorylation sites are actually phosphorylated at any one time, pre-enrichment is often required. The available methods for phosphoproteome analysis, including pre-enrichment are discussed in Chapter 5, along with examples of protein phosphorylation in the regulation of the response to injury.

1.7 Aims and Objectives of the Study

To date, the sequence of events that occur following an injury and the subsequent inflammation have been partially characterised in terms of cellular infiltrate and a few key cytokines and growth factors. However, these have failed to lead to the development of suitable treatments. It would be of considerable clinical benefit to have a diagnostic test with which to predict the healing outcome for an individual patient, and in cases where aberrant responses were expected, a method by which to identify which factors were altered. The aim of this study was to explore the very early injury environment

to search for potential markers of the response to injury, particularly those that could function as targets for improved treatments.

The hypothesis tested in this work was that interstitial fluid represents an important source of mediators directly involved in the response to injury. Local sampling of mediators within the interstitial fluid space will provide a novel and relevant insight into the extracellular signalling processes that are involved in the initiation and development of the acute inflammatory response following injury.

The combination of dermal microdialysis and proteomics technologies provided a novel method of biomarker discovery, however, as they had not been used together in skin research, it was first necessary to conduct studies in healthy volunteers to validate the suitability of these methods. An improved model of injury is required, as existing methods are either not well tolerated in temporal or repeat investigations or are unsuitable for such localised sampling. It was hypothesised that through the use of global protein analyses, the temporal response to needle injury could be better characterised in terms of a greater range of mediators and therefore lead to the identification of more specific markers of the injury response.
The aims of this project were as follows:

1. To develop a model of skin injury suitable for sampling early biomarkers of the tissue response.

2. To validate the injury model using known biomarkers of the injury response.

3. To identify protein content of interstitial fluid obtained from injured skin.

4. To investigate post-translational modifications of proteins relevant to the early injury response.

The work conducted to develop and validate the model of injury is covered in Chapter 3, the protein content of dermal interstitial fluid is covered in Chapter 4 post-translational modifications are investigated in Chapter 5.

Chapter 2

Materials and Methods

This chapter presents the methods used during the course of this research. The reagents and instruments used are listed first, followed by the general methods. Specific alterations to the protocols given in this chapter are included in the appropriate results chapter.

2.1 Reagents and instrumentation

The reagents used in this study are listed in Table 2.1. Where identical reagents have been sourced from multiple companies, their use has been noted as appropriate (within the text). Water used was ultra-pure unless stated, purified using a MilliQ system (Millipore). All experiments, including incubation and centrifugation steps, were conducted in a temperature controlled environment at 22°C, unless otherwise stated.

Table 2.1: **List of the reagents used during the course of this research and the supplier from which they were obtained.**

Reagent/ Item	**Company**
Acetonitrile	Fisher Scientific
Acetyl chloride	Fluka
α-cyano-4-hydroxycinnamic Acid	Sigma
β-Casein from Bovine Milk	Sigma
Bicinchoninic Acid Assay Kit	Sigma
Biosafe Coomassie G-250 Stain	BioRad
Calibrite Beads	BD Biosciences
CBA 30-plex Bead Mixture	BD Biosciences
"cOmplete mini" EDTA-free protease inhibitors	Roche Diagonostics Limited
Cryo-Vial, 1.0 ml Ult. Security Ext Thd FS	Alpha Labs
2,5-Dihydroxybenzoic Acid	Aldrich
DTT (Dithiothretiol)	Sigma
EMLA Local Anaesthetic Cream	Astra Zeneca
FACS tubes (Polystyrene)	BD Biosciences
Fine bore polythene tubing (O.D. 1.05 mm, I.D. 0.52 mm)	Portex
Flexifuse tubing	Alaris Medical
Glu^1–fibrinopeptide B	Sigma
Human IFN-γ Flex Set (Bead E7)	BD Biosciences
Human IL-10 Flex Set (Bead B7)	BD Biosciences
Human IL-6 Flex Set (Bead A7)	BD Biosciences
Human MCP-1 Flex Set (Bead D8)	BD Biosciences
Human MIP-1α Flex Set (Bead B9)	BD Biosciences
Human OSM Flex Set (Bead D5)	BD Biosciences
Human Soluble Protein Master Buffer Kit	BD Biosciences
Human VEGF Flex Set (Bead B8)	BD Biosciences

Reagent/ Item	**Company**
Hydrochloric Acid	Fisher Scientific
Imidazole	Sigma
Iodoacetamide	Sigma
MES (2-(N-Mopholino) ethanesulfonic acid) Buffer	Sigma
Methanol (standard)	Fisher Scientific
Methanol (anhydrous)	Fisher Scientific
Multi affinity removal system column Human 6	Agilent Technologies
N-(3-Dimethylaminopropyl)-*N*'-ethylcarbodiimide	Fluka
NaCl	Fisher Scientific
NanoSep Centrifugal Device, 3 kDa MWCO	Pall Corporation
NanoSep MF Centrifugal Device, 0.2 μm	Pall Corporation
NuPAGE 4-12% Bis-Tris Gels	Invitrogen
NuPAGE MOPS SDS running buffer	Invitrogen
NuPAGE LDS sample buffer	Invitrogen
Orthophosphoric Acid (H_3PO_4)	Fisher Scientific
Paraformaldehyde	Fluka
Phosphopeptide Positive Control Set from bovine casein	Sigma
Phosphorous Pentoxide for dessicators	BDH
PhosSTOP phosphotase inhibitor cocktail	Roche Diagnostics Limited
PhosTrap Phosphopeptide Enrichment Kit	Perkin Elmer
Plasmaphoresis membrane (3000 kDa MWCO, polyethersulphone)	Asahi Medical
Precision Plus All Blue pre-stained protein standards	BioRad
ProQ Diamond Phosphoprotein Stain	Molecular Probes

Reagent/ Item	**Company**
"rAPID" Alkaline Phosphatase	Roche Applied Science
Rapigest SF surfactant	Waters
Ringer's Saline	Baxter
Sanitary Silicone Sealant	Bostik
Spin Concentrator, 4 ml, 5 kDa MWCO	Agilent Technologies
Stainless Steel Wire	Goodfellow
Starburst Dendrimer DNT-128, Generation 5.0, 1, 12-diaminododecane core	Dendritic Nanotechnologies
Sypro Ruby stain for total protein	BioRad
Tegaderm® Transparent Film Dressing - Universal	3M
Triethylammonium Bicarbonate Buffer	Sigma
Trypsin from Bovine Pancreas	Sigma
Tygon ® Autoanalysis tubing (ID. 0.015 in, OD. 0.087 in)	Cole Palmer
Ultrafree-MC Biomax Centrifugal Filter Device (5 kDa cut-off)	Millipore

The instruments used in experimentation in the present study are listed in Table 2.2.

Table 2.2: **Instrumentation used during the course of this research.**

Instrument	**Company, Location**
BD FACSCalibur™Flow Cytometer (4-colour)	BD Biosciences, Oxford, UK.
Biofuge Pico Ultra-centrifuge	Heraeus, Hanau, Germany.
CMA 100 Syringe pump	CMA, Solna, Sweden.

Instrument	**Company, Location**
Global Ultima Q-TOF Mass Spectrometer III and associated equipment (CapLC system, μHPLC pump, low volume autosampler, Streamselect μ-column switching module, nanoLockSpray)	Waters, Manchester, UK.
Laser Doppler blood flow Imager	Moor Instruments, Axminster, UK.
Sorvall LegendRT Centrifuge 120v	Thermo Fisher, San Jose, USA.
LTQ-Orbitrap Mass Spectrometer and associated Surveyor equipment	Thermo Fisher, San Jose, USA.
MALDI-TOF Mass Spectrometer	Waters, Manchester, UK.
Microtiter plate reader	Dynex Technologies Ltd., Worthing, UK.
Nano-reverse phase C_{18} PepMap analytical column (150 mm $\times$ 75 μm i.d)	Dionex, Camberley, UK.
Novex Mini-Cell and Powerease 500	Invitrogen, Carlsbad, USA.
PepMap C_{18} guard column (5 mm $\times$ 300 μm id)	Dionex, Camberley, UK.
pH Meter	Jenway, Dunmow, UK.
SpeedVac	Savant Instrumentation, Framingdale, USA.
VersaDoc Model 3000 gel imager	BioRad, Hemel Hempstead, UK.

The methods are divided into three sections covering establishment and characterisation of the model, analysis of the protein content of dialysate and optimisation of methods for the analysis of protein phosphorylation in dialysate.

2.2 Measurements of cutaneous blood flow and dialysate sample collection

Microdialysis was used both as the method of sampling and the method of injuring the skin of healthy human volunteers. The inflammation that occurred in response to the insertion injury was quantified, first by non-invasive measurements of blood flow and then by measuring the changes in concentration of specific inflammatory markers in dialysate samples.

2.2.1 Microdialysis probe construction

Microdialysis probes were constructed in-house by the insertion of a 7 cm length of straightened stainless steel guide wire into an equal length of polyethersulphone (PES) 3000 kDa MWCO plasmaphoresis membrane. This probe was then inserted for 1 cm into a 12 cm length of Tygon® tubing via a 23G hypodermic needle 1 – 2 cm length of fine bore polythene tubing inserted into the opposite end to form a connector, both were then secured with household, silicone-based sealant. Finished probes (Figure 2.1) were placed in pairs or individually in self-seal sterilisation pouches and sterilised by ethylene-oxide gas by InHealth Decontamination, Cardiff.

2.2.2 *In vivo* dialysate sample collection

Healthy human volunteers were recruited from the staff and students of the University of Southampton. Volunteers gave informed written consent and the study was conducted in the Wellcome Trust Clinical Research Facility at Southampton General Hospital under ethics granted by South West Hampshire Research Ethics Commitee (REC 346/03/t and 138/01/w). Volunteers were asked to refrain from excessive alcohol intake in the 24 hours prior to the study and from caffeine and strenuous exercise for six hours before. None of the volunteers were on any medication and all were asked not to take anti-inflammatory preparations in the week leading up to the experiment.

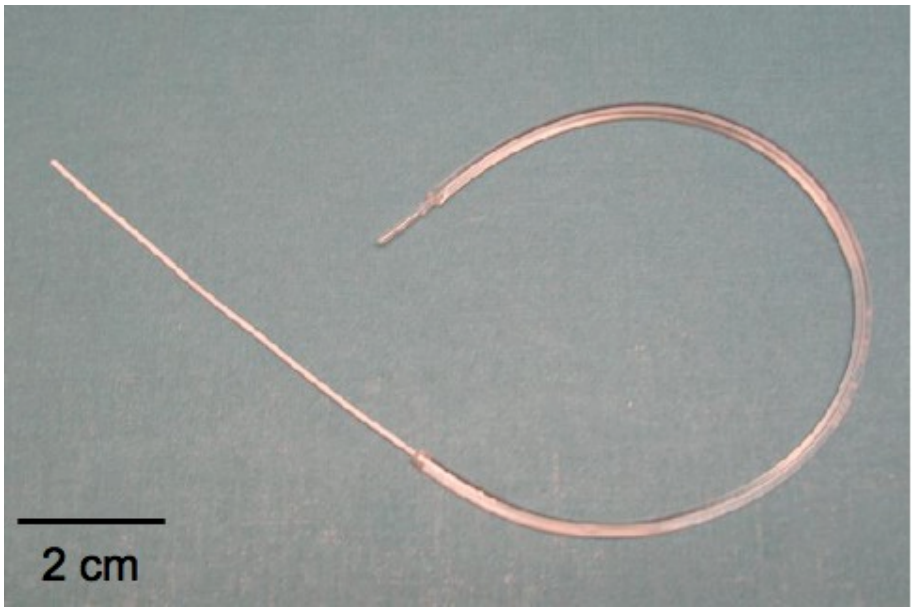

Figure 2.1: **3000 kDa MWCO Microdialysis Probe.** Photograph of a 3000 kDa MWCO microdialysis probe. All probes were approximately 17 cm in length, with 6 cm of the strengthened membrane exposed (left-hand section of the probe)

All experiments were conducted in the morning in a quiet, temperature controlled environment at 22°C.

The equipment set-up for the *in vivo* microdialysis experiments is shown in Figure 2.2.

Local anaesthetic cream (EMLA®, Astra Zeneca) was applied under occlusion (Tegaderm dressing) to a site no less than 7 cm above the fold of the wrist, 90 minutes prior to the volunteers' arrival at the clinical research facility.

On arrival, volunteers were positioned supine on a bed with the dialysis arm raised to heart level on a pillow and allowed to equilibrate. Anaesthetic was removed on arrival, 30 minutes before probe insertion, using a damp paper towel and the area was allowed to air-dry. The area of anaesthesia was checked by gently pressing the skin with a needle tip and asking the volunteer to report on any sensation.

Microdialysis probes were connected to a syringe pump (CMA 100, CMA) via flexifuse tubing secured to 1 ml syringes by 19G size hypodermic needles. Syringes were filled with Ringer's saline, the perfusate. Perfusion at 3 μl/min was started,

Figure 2.2: **Microdialysis equipment set-up.** Photograph of the lay-out of the microdialysis equipment during an experiment. The volunteer is placed on a bed, perpendicular to the syringe pump and laser doppler scanner, with the non-dominant forearm raised to heart level. Flexifuse tubing connects the syringes within the pump to the probes.

before intradermal insertion, to check patency of the probes. Probe insertion was carried out by Professor Geraldine Clough and is detailed in Figure 2.3.

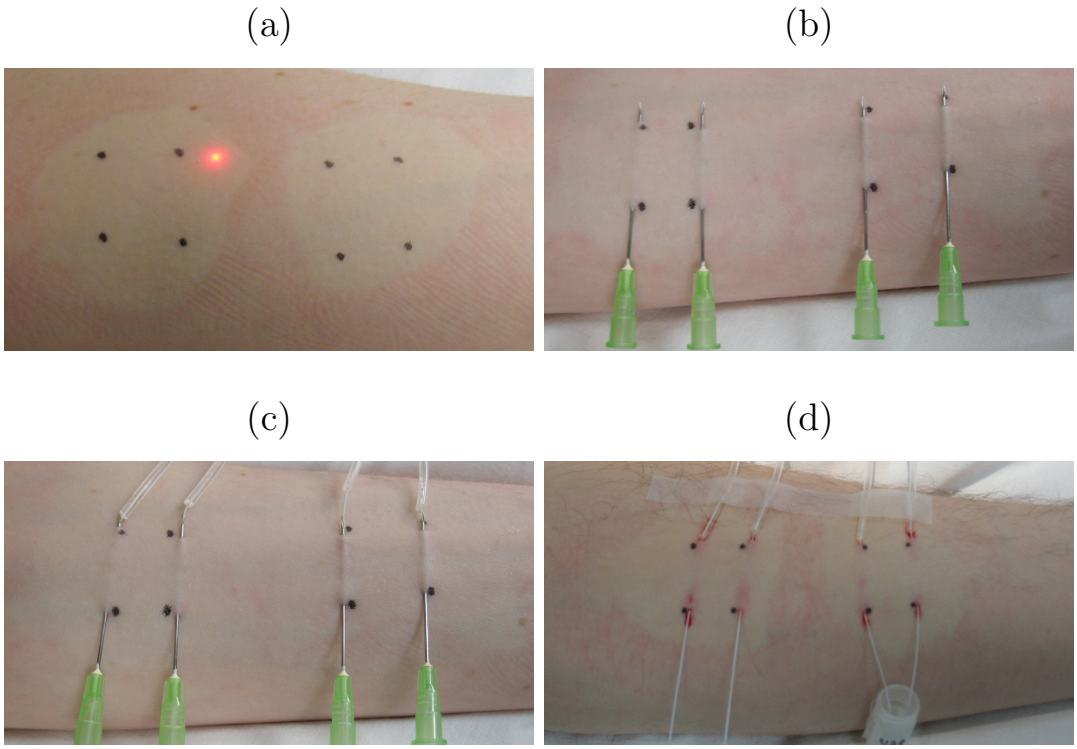

Figure 2.3: **Microdialysis probe insertion.** Photographs detailing the process of intradermal insertion of microdialysis probes. a) Anaesthetised areas with markings to indicate each pair of entry and exit points, 2 cm apart. b) Needles in place. c) Probes inserted through needles. d) Probes in place, with and without collection vials for illustration. In all photographs, the pairs of dots are 2cm apart, from top to bottom.

Briefly, the insertion sites were marked out by pairs of dots 2 cm apart, within the anaesthetised area (Figure 2.3a). Hypodermic needles (21G size) were inserted intradermally for 2 cm (b), beside the marked sites to avoid tattooing the volunteer, and the probes threaded in through the tip of the needle (c). The needles were then carefully removed, the probes trimmed with sterile scissors and cryogenic vials positioned to collect the dialysate (d). Perfusion continued during insertion and collection of the dialysate began immediately after. The dialysate collection periods are detailed in the individual results chapters, as different collection times were required for each set of

experiments. Samples were flash-frozen in liquid nitrogen immediately after collection and stored on ice until being transferred to -80°C at the end of the experiment.

2.2.3 Measurement of cutaneous blood flux by laser Doppler imaging

Changes in microvascular perfusion of the microdialysis probe insertion sites were quantified as a surrogate measure of inflammation, by laser Doppler imaging using a Laser Doppler blood flow Imager. Two-dimensional images are created by scanning a defined area, in a raster pattern.

Single 2-D scans were performed, of a 4 × 8.6 cm area over the microdialysis probes and at a resolution of 115 × 115 pixels. A baseline scan was performed before insertion of the microdialysis probes, at 5 minute intervals from 5 – 90 minutes and 120, 150 and 180 minutes post-insertion. Mean blood flux was calculated off-line within a defined region of interest using the Moor image review software (moorLDI V3.5 Research Software for Laser Doppler Blood Flow Imager, Moor Instruments). Pre-defined, regular shaped regions of interest could not be used because it was not possible to place the arm exactly perpendicular to the scanner. Instead, regions had to be manually defined for each scan. An area of 1.01 ± 0.09 cm^2 (mean ± SD) was drawn around each insertion site, as determined by the image review software, using the black and white photograph image for reference. This ensured that the probe, and therefore the injury site, was within the analysis region. Figure 2.4 shows a representative scan, with its corresponding black and white photograph showing the position of the probes for comparison, and the regions of interest over which the mean blood flux was recorded during analysis.

For each image acquired, the mean blood flux at the four injured sites was recorded and the mean of these calculated.

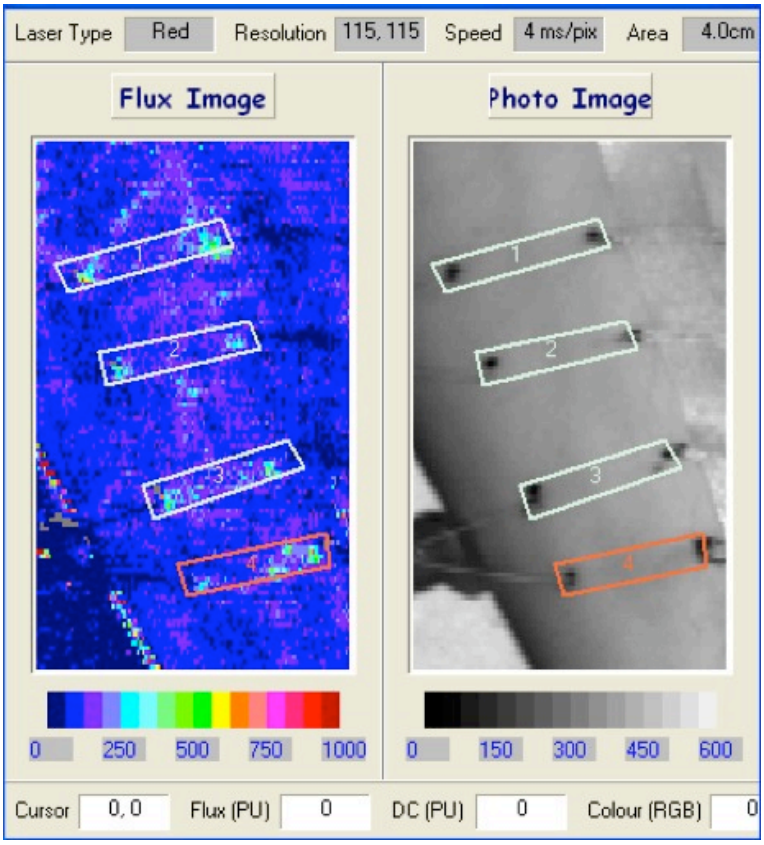

Figure 2.4: **Representative laser Doppler scan image and corresponding photograph.** The rate of blood flow is indicated by coloured pixels, corresponding to the key shown below the Flux Image (left). The photograph (right) provides a visual record of the scan area, in which the probes are visible running across the image, with the injury site marked by pairs of black dots. The numbered boxes represent the regions of interest, approximately 1 cm^2, in which mean blood flux was calculated.

2.3 BCA Assay to estimate total protein concentration in the dialysate

Protein concentration was estimated using the Bicinchoninic Acid (BCA) assay. This colourmetric assay relies on the reduction of Cu^{2+} ions by peptide bonds (and also cysteine, cystine, tryptophan and tyrosine residues), where the degree of reduction is proportional to the amount of protein present. Standards of bovine serum albumin in the appropriate buffer were prepared in 0.1 mg/ml intervals between 0 and 1 mg/ml. 20 μl of standard or sample was added per well to a flat-bottomed 96-well plate. $CuSO_4$ reagent was added to bicinchoninic acid solution at a ratio of 1:50 and 200 μl added per well to a 96-well microtiter plate, according to the manufacturer's protocol. Plates were read at 570 nm after 30 minutes using a microtiter plate reader. Protein concentrations were calculated automatically, using the associated analysis software (Dynex Revelation v 3.2).

2.4 Multiplex cytokine analysis

Cytokine analysis was conducted using a BD^{TM} CBA Flex Set, a bead-based assay for analysis using flow cytometry (FACS). The Flex Set consisted of a master buffer kit containing proprietary wash buffers, diluents and set-up beads, and individually supplied antibody-coated capture beads. Calibrite beads for instrument calibration and a 30-plex bead set for determining correct resolution were obtained separately.

The conjugation protocol, instrument set up and analysis were conducted according to the manufacturers recommended protocol for plasma samples. The alterations included to adapt the protocol for dialysate samples are discussed in the following sections.

2.4.1 Preparation of standards and samples for cytokine quantification

Lyophilised standards were transferred to a single 5 ml polystyrene FACS tube and equilibrated in 4 ml proprietary assay diluent for 15 minutes to reconstitute. Serial dilution of this top standard (2500 pg/ml) was performed to give concentrations of 2500, 1250, 625, 312.5, 156, 80, 40, 20, 10, 5 and 0 pg/ml. Dialysate samples were thawed on ice. Stock solutions of 1 × concentrated pooled capture beads and PE detection reagents were prepared by dilution with the appropriate diluents, according to the manufacturer's protocol. Fifty μl of the capture bead solution was added to 50 μl of each standard or sample mixed gently and incubated for 1 hour at room temperature. Fifty μl PE detection reagent was then added to each tube for a 2 hour incubation at room temperature, protected from light. Samples were fixed by addition of paraformaldehyde at a final concentration of 1% for 20 minutes, then centrifuged at 200 × g for 5 minutes. The supernatant was removed and the pellet re-suspended in 300 μl of wash buffer. All standards and samples were then stored at 4°C, protected from light, until analysis no more than one week later.

2.4.2 Instrument set-up for the CBA Flex Set

Instrument set-up was performed according to the manufacturer's recommended protocol. Briefly, the FACSCalibur was calibrated by following the FACSComp software wizard (BD Biosciences) using positive and negative control Calibrite bead samples. Next, the recommended template was set up using CellQuest Pro software. Five calibration samples were prepared as described in the FACS Calibur instrument set-up manual, using the set-up beads supplied in the master buffer kit. These were used to adjust the gates within the template and set compensation levels to enable all 30 of the beads within the 30-plex standard to be resolved. A test sample of the beads to be used in the multiplex was also analysed to check that those bead populations were sufficiently well resolved.

2.4.3 Data acquisition and analysis for the Flex Set

Instrument settings were checked prior to analysis, using the 30-plex standards, an aliquot of capture beads and the 2500 pg/ml standard. Analysis was conducted according to the manufacturer's protocol. Standards and samples were vortexed before analysis, to re-suspend any settled beads. A total of 300 events per analyte were aquired for each sample using CellQuest Pro software (BD Biosciences) and analysis was performed using FCAP array software (Version 1.0.1 for Mac, Soft Flow), following the analysis Wizard.

2.5 Proteomic analysis of dermal dialysate samples

Two different experiments were performed to identify proteins in dermal dialysate. The first experiment was conducted to determine the protein content of dermal dialysate. A second experiment was conducted in which specific highly abundant proteins were depleted from the dialysate samples, prior to determining protein content. This was expected to reduce the dynamic range of protein concentrations within the sample and subsequently increase the identifications of less abundant components. This second sample required additional preparation steps, described in Section 2.5.2. Subsequent steps were common to both experiments.

2.5.1 Preparation of dialysate samples for GeLC-MS/MS

Dialysate samples were centrifuged at 16060 $\times$ g for 5 minutes to remove insoluble components. Proteins in the dialysate were separated 1-D SDS PAGE, described in Section 2.5.3.

2.5.2 Depletion of abundant proteins from dialysate

The highly abundant proteins anti-trypsin, IgA, IgG, haptoglobin, serum albumin and transferrin were removed from the dialysate using an antibody-based depletion method. Dialysate samples were thawed on ice, pooled, and concentrated using a 5

kDa-MWCO spin concentrator device. The protein concentrations of the concentrated samples were then estimated by BCA assay. Depletion was performed by high performance liquid chromatography using a Multi-Affinity Removal System (MARS) column. Proprietary buffers were supplied with the column, labelled A and B.

Concentrated dialysate was diluted five-fold in Buffer A and injected via a 2 ml loop onto the MARS column. A gradient was performed with 100 % Buffer A 12 minutes, 18 minutes with 100 % Buffer B and Buffer A again for the final 15 minutes, all at a flow rate of 200 μl/min. Fractions were collected into a 96-well plate and pooled from the appropriate wells as shown (Figure 2.5).

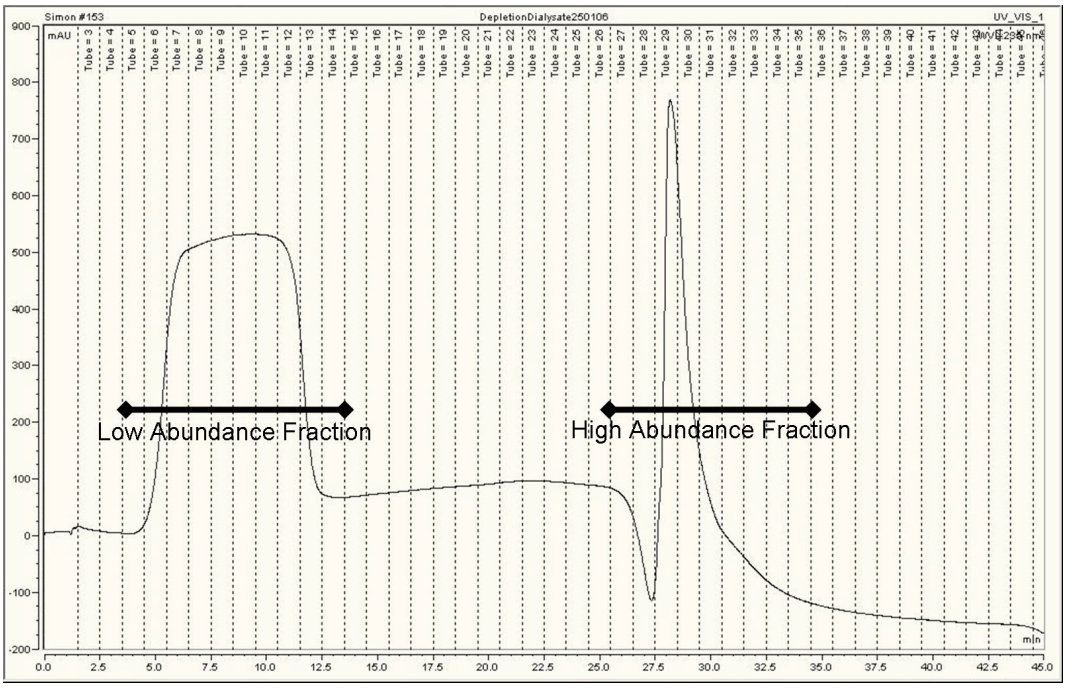

Figure 2.5: **Example of an HPLC Chromatogram from a Depletion experiment.** HPLC chromatogram showing the high and low abundance fractions obtained following depletion of high abundance proteins from dialysate. Dialysate was injected at time = 0. The highly abundant proteins anti-trypsin, Immunoglobulins A and G, haptoglobin, serum albumin and transferrin bound to the column in the presence of buffer A during the first 12 minutes, while the low abundance fraction was eluted (left-hand peak, wells 5 –14). Following the switch to buffer B, the bound, highly abundant proteins were released and eluted (right-hand peak, wells 27 – 35).

Following depletion, the high and low abundance fractions were concentrated to approximately 50 μl by lyophilisation *in vacuo* and prepared for MS analysis as described for non-depleted dialysate above.

2.5.3 One-dimensional SDS polyacrylamide gel electrophoresis

Prior to mass spectrometry preparation, proteins were separated using 1D-SDS PAGE. Samples were prepared by adding protein in solution, of known concentration as determined by BCA assay, to 1/4 volume NuPAGE LDS sample buffer and 50 mM dithiothreitol (DTT) reducing agent (final concentration), to a maximum volume of 40 μl. Samples were then heated to 70°C for 10 minutes before being added to the gel. Ten μl Precision Plus All Blue pre-stained protein standards were used as molecular mass markers (range 10 – 250 kDa, molecular masses shown on each gel image presented). Pre-cast 4-12 % Bis-Tris NuPAGE gels were placed inside the electrophoresis chamber and MOPS running buffer added, diluted in H_2O as appropriate. Protein standards (10 μl) were added to the first well and prepared dialysate samples added to subsequent wells. Electrophoresis was conducted using a pre-set protocol for NuPAGE gels, at 200 mV, for 45 minutes or until the dye-front reached the bottom of the gel. Gels were removed from their casing and rinsed in H_2O before staining with coomassie blue dye.

2.5.4 Staining of SDS PAGE gels using coomassie blue dye

Colloidal coomassie blue was used to visualise dialysate proteins in the gels to be prepared for MS analysis. Gels were incubated for one hour in ∼100 ml stain, then rinsed in water for one hour and again over night to de-stain, all with gentle rocking. Imaging was performed on a VersaDoc model 3000, using a white-light stage and PDQuest software version 7.1.0, with pre-set parameters for coomassie-stained protein gels. The transform function was used to alter the contrast of the whole gel image, to optimise band visibility. The optimised images were exported as .tiff files.

2.5.5 Digestion and liquid chromatography-tandem mass spectrometry for protein identification.

Once stained, bands were excised from the appropriate track and placed one-per-well in a 96-well microtiter plate for *in situ* digestion with trypsin. Digestion and preparation of the resulting peptides for MS analysis was conducted by Paul Skipp, according to a standard protocol (Shevchenko *et al.*, 1996). NanoLC-MS/MS analysis was also performed by Paul Skipp, as follows.

NanoLC separations were performed using a CapLC system, consisting of a μHPLC pump and low volume autosampler coupled to a Streamselect μ-column switching module. Samples, in microtiter plates stored at 10°C, were loaded via the autosampler onto a PepMap C_{18} guard column (5 mm $\times$ 300 μm id) for pre-concentration and desalting using 100 % solvent C (3 % acetonitrile (ACN) + 0.1 % formic acid (FA, in water) at a flow rate of 20 μl/min. The eluent was diverted to waste. After 6 minutes of washing, the nano-reverse phase C_{18} PepMap analytical column (150 mm $\times$ 75 μm i.d) was switched into line using the Streamselect μ-column switching module and a separation gradient was performed as detailed below. A flow rate of 200 nm/min was set for all experiments.

All data were acquired using a Q-ToF Global Ultima fitted with a nanoLockSpray source. [Glu^1]-fibrinopeptide B ([M+2H]$^{2+}$ = 785.8426) was used as the internal lock-mass calibrant for the nanoLockSpray source. For automated data directed acquisitions, a survey scan was acquired from m/z 375 to 1800 (1.0 sec scan, 0.1 sec inter-scan delay) in positive ion mode with the switching criteria for MS to MS/MS including (i) ion intensity (15 counts per second) and (ii) charge state ($^+2$, $^+3$, $^+4$). Product ion spectra were acquired from m/z 50 to 1800 at 1 scan per second until the data had been collected for 12 sec or if the ion intensity fell below a threshold of 5 counts per second before the 12 sec had elapsed. Six channels were available for product ion acquisition. The collision energy used to perform the MS/MS was automatically varied according to the mass and charge state of the eluting peptide using a collision energy profile. Instrument control and data acquisition were provided by the software, MassLynx 4.0

(Waters).

The data acquired were searched against the NCBI non-redundant human protein database using Mascot (Matrix Science) and ProteinLynx software (v. 2.05, Waters/ Micromass) to identify matching proteins. Identified proteins were characterised according to their functional and locational classifications within the Gene Ontology database (http://amigo.geneontology.org, release 2008–09–30).

2.6 Methods and optimisation for phosphoproteomic analysis

Three approaches were investigated to determine the most appropriate method with which to analyse protein phosphorylation in dialysate. A model phosphoprotein, β-casein from bovine milk, was used to optimise each method before analysis of dialysate. The first method employed a phosphoprotein-specific gel stain to analyse protein phosphorylation in whole proteins. The other two methods, titanium-dioxide affinity capture and dendrimer conjugation chemistry, were used to capture phosphorylated peptides from protein digests for mass spectrometric analysis.

2.6.1 Sample preparation and staining protocol for the Pro-Q Diamond phosphoprotein stain

For model protein samples, β-casein was reconstituted in water and serially diluted to give the required concentration. These were lyophilised *in vacuo* and resuspended in 25 μl H_2O + 5 μl LDS sample buffer. Standards were prepared by adding 4 μl Peppermint Stick phosphoprotein standards to 6 μl LDS sample buffer and heating to 95°C for 4 minutes. Standards comprised two phosphorylated proteins, β-casein and ovalbumin at 23.6 and 45 kDa respectively, and four non-phosphorylated proteins - namely lyzozyme (14.4 kDa), avidin (18 kDa) bovine serum albumin (66.2 kDa) and β-galactosidase (116.2 kDa). Gel electrophoresis was performed as previously described (Section 2.5.3).

Once removed from their casing, gels were fixed in a solution of 50 % methanol + 10 % acetic acid for 3 × 30 minute washes, then again overnight. Fixed gels were washed for 3 × 10 minutes the following morning, in H_2O, prior to a 90 minute incubation in Pro-Q Diamond phosphoprotein stain, protected from light. De-staining was performed using 20 % ACN + 5 % 1 M sodium acetate (pH 4.0) for 3 × 30 minute washes, also protected from light and rinsed 3 × 5 minutes in H_2O. Imaging was performed using the UV transilluminator function of the VersaDoc model 3000, with a 520 nm long pass filter, pre-sets for Sypro Ruby-stained protein gels and a 15 second exposure.

2.6.2 Protocol for Sypro Ruby staining for total protein

After imaging, gels stained for phosphoprotein with ProQ-Diamond stain were incubated in 500 μl Sypro Ruby stain for total protein overnight with gentle rocking, protected from light. Gels were de-stained for 3 × 30 minutes in 10 % methanol + 7 % acetic acid and rinsed three times in H_2O before imaging as for the Pro-Q Diamond stained gels.

2.6.3 Densitometry analysis of stained gels

Quantitative analysis of staining was performed using Quantity One software (Bio-Rad). Briefly, lanes were defined manually and the bands of interest selected. Regions were defined by eye using the rectangular volume tool which calculated staining intensity per mm^2 within that region, given as INT*mm^2.

2.6.4 Sample preparation for phosphopeptide analysis

Two methods were used for phosphopeptide capture and their subsequent identification using mass spectrometry. Neither titanium-dioxide affinity capture or dendrimer conjugation chemistry were established methods within the Centre for Proteome Research and the latter is a relatively new technique, so both methods required some optimisation before use with dialysate. Optimisation of these methods were conducted using increasingly complex model protein samples, followed by preliminary analyses of

dialysate samples. Sample preparation differed depending on the sample to be analysed, so each is described separately. When comparisons between the two capture methods were performed, four samples were prepared from a single digestion, that is, two sets of 10 μl for digest and methylation analysis, and the remainder divided in two for capture by each method. The second digestion including Rapigest surfactant (Section 2.6.4.3) was a later addition to the protocol and while not used in the dialysate experiment, is strongly recommended for use in future.

2.6.4.1 Control phosphopeptides

Mono and tetraphosphopeptides purified from digests of bovine β-casein were reconstituted in H_2O to give a final concentration of 0.1 mg/ml for each. This stock solution was stored at -20°C. Five μl of each phosphopeptide were pooled and lyophilised *in vacuo* to give a total of 1 μg peptide per experiment.

2.6.4.2 Model protein

A 1 mg/ml solution of β-casein in 100 mM triethylammonium bicarbonate buffer (TEAB) was prepared and 20 μg trypsin, also dissolved in 100 mM TEAB, was added for an overnight incubation at 37°C. Either 2.5 μl (100 pmoles) or 25 μl (1 nmole) were lyophilised *in vacuo* for each experiment, as specified.

2.6.4.3 Model protein mixture

One mg/ml stock solutions were prepared for each of two phosphorylated (β-casein and casein) and 3 non-phosphorylated (bovine serum albumin, cytochrome c and myoglobin) proteins. One hundred μl of each were combined and digested with 20 μg trypsin per experiment, incubating at 37°C. A second, 4 hour digestion was performed in 100 mM TEAB + 0.1 % Rapigest to ensure complete digestion.

2.6.4.4 Dialysate

Dialysate samples, collected as detailed in Section 2.2.2, were thawed on ice and pooled to give approximately 1-2 mg total protein. Removal of salts and buffer exchange

were performed simultaneously by filtering the dialysate through a 5 kDa MWCO spin concentrator. Three washes with 1 ml 100 mM TEAB were completed, keeping the dialysate proteins in a minimum of 100 μl of liquid at all times. The protein content of the desalted sample was estimated by BCA assay (Section 2.3). Next, the dialysate was reduced in 10 mM DTT, incubating for 1 hour at 56°C. Reduced cysteine residues were alkylated by the addition of 50 μl 55 mM iodoacetamide, incubating at room temperature for 30 minutes, in the dark. Trypsin was added in a 1:50 ratio and incubated at 37°C overnight to allow complete digestion. Digested dialysate samples were lyophilised *in vacuo* and stored at 4°C until required, although samples were used immediately when possible.

2.6.5 Methyl-esterification of peptides to prevent non-specific binding to acidic amino acids

Exposed carboxyl groups are known to interact non-specifically with many affinity-based phosphopeptide capture methods. Peptides were subjected to methyl-esterification, the replacement of carboxyl with methyl groups, to block any such non-specific interactions.

Dried samples of peptide were placed in a desiccator with P_2O_5 under vacuum, overnight. A methanolic HCl solution was prepared by adding acetyl chloride to anhydrous methanol in a 160 μl: 1 ml ratio, as required. Five hundred μl of this solution were added per mg of the desiccated peptides (to a minimum of 50 μl) and incubated for 2 hours at 12°C. The author wishes to acknowledge the assistance of Dr. Bernd Bodenmiller of the Institute for Molecular Systems Biology, Zurich for suggesting the use of the desiccator and anhydrous methanol for this process.

2.6.6 Phosphopeptide capture using TiO_2-affinity beads

Titanium dioxide (TiO_2)-affinity capture was performed using a Phos-Trap^{TM} kit according to the manufacturer's protocol, with some minor modifications. Briefly, methylated peptides (Section 2.6.5) were reconstituted in 10 μl H_2O + 90 μl proprietary

binding buffer and captured as follows. A stock of bead solution was prepared by adding H_2O and TiO_2 microbead solution at volumes of 190 and 10 μl times the number of samples, respectively. Two hundred μl of the bead solution were added to each 0.5 ml microcentrifuge tube, vortexing in between to keep the beads suspended evenly. After 1 minute on the magnet, the supernatant was carefully removed and the beads re-suspended in 200 μl binding buffer once removed from the magnet. This wash step was repeated twice further before each 100 μl sample was added per tube to the beads and incubated for 1 – 2 minutes before placing on the magnet for 1 minute. The supernatant containing unbound peptide was removed and reserved. The beads were then washed 3 – 5 times with 200 μl binding buffer, pooling the reserved supernatants each time. A final wash was performed using 200 μl proprietary washing buffer, and the supernatant completely removed and discarded. Captured peptides were recovered by incubating the beads in 10 μl proprietary elution buffer for 1 minute, pipetting up and down gently to mix. The supernatant was collected and prepared as appropriate (Sections 2.6.9 and 2.6.10) for analysis.

2.6.7 Phosphopeptide capture using dendrimer conjugation chemistry

The dendrimer conjugation chemistry method for phosphopeptide enrichment has been reported only once and had not been established within the Centre for Proteome Research previously. The protocol consists of four stages, namely preparation of the samples and lyophilisation of the dendrimers, conjugation of phosphorylated peptides to the dendrimer, removal of non-bound proteins and hydrolysis and recovery of phosphorylated peptides and their subsequent analysis by mass spectrometry. A series of optimisation experiments were required to improve upon early phosphopeptide enrichment results. These experiments are described in Chapter 5, while the optimised method is presented here.

2.6.7.1 Dendrimer conjugation chemistry

To maintain the necessary pH for conjugation, dendrimers were pH-adjusted prior to lyophilisation. For each reaction, 80 μl dendrimer solution (DNT-128, Dendritic Nanotechnologies) was diluted with 400 μl of 100 mM MES buffer and adjusted to pH 5.5 by titration with 1 M HCl. The pH-adjusted dendrimers, approximately 9 mg per conjugation, were then lyophilised *in vacuo* to dryness. A reaction solution of 200 mM MES, 100 mM imidazole and 100 mM EDC was prepared and adjusted to pH 5.5 in the same manner. Forty μl of this solution per reaction was added to the dried dendrimers as appropriate and vortexed to solubilise. The dendrimer-reaction solution was then transferred to the dried, methylated peptides, vortexed to mix, and incubated at room temperature overnight with strong shaking.

2.6.7.2 Removal of non-bound peptides

Centrifugal filter devices (5 kDa MWCO Ultrafree MC with polyethersulphone membrane) were pre-washed with 400 μl each of the following; 500 mM NaOH, H_2O, 10 % trifluoroacetic acid (TFA) and H_2O. Washes were performed by centrifugation at 4500 $\times$ g for approximately 20 minutes or until the liquid had completely passed through. If the pre-wash was performed the day before use, 400 μl H_2O was used as a storage solution and spun through just before the filter units were needed. The author wishes to acknowledge Dr. Bernd Bodenmiller for suggesting the inclusion of this pre-wash step also.

Following the overnight incubation, 400 μl 50 % methanol was added to the dendrimer-peptide sample, mixed, and the solution transferred to the pre-washed filter device. As for the pre-wash, centrifugation was performed at 4500 $\times$ g in 20-minute intervals, separated by brief vortexing. This was repeated until the majority of the liquid had passed through. At this point, the eluate was removed and reserved if needed. Further washes were performed as follows; 2 $\times$ 2 M NaCl in 50 % methanol, 3 $\times$ 50 % methanol, 5 $\times$ H_2O. If necessary, after the second H_2O wash, 400 μl H_2O was added and the filter device stored at 4 °C overnight with the remainder of the washes performed the next

day. A minimum of three further H_2O washes were performed to remove any polymer contaminants that may have leached from the filter unit overnight.

2.6.7.3 Hydrolysis and recovery of captured phosphopeptides

After the final H_2O wash, 300 μl 10 % TFA was added to the dendrimer-phosphopeptide conjugate mixture for a 60 minute incubation at room temperature before centrifugation to elute the released phosphopeptides. Two further washes with H_2O were performed, the eluates pooled with the TFA wash. The pooled sample was lyophilised *in vacuo*, to dryness. Samples were analysed by MALDI-TOF (Section 2.6.9) or tandem MS (Section 2.6.10). When necessary, samples were re-methylated to improve the signal-to-noise ratio where de-methylation, caused by EDC, had occurred. Re-methylated samples were cleaned using ZipTips (Section 2.6.8) prior to re-analysis.

2.6.8 Zip-Tip clean up for the removal of salts

Re-methylated samples were desalted using C18 ZipTips (Millipore), to remove any salts that could interfere with MALDI-time-of-flight (TOF) MS analysis. One ZipTip was used per sample, as follows. Tips were primed by wetting with 10 μl 100 % ACN three times and the equilibrated three times with 10 μl 0.1 % TFA. Next, lyophilised samples, reconstituted in 10 μl 0.5 % TFA (pH $<$ 3), were passed through the tip ten times by gently pipetting up and down to allow peptides to bind to the C18 material inside the tip. Salts were removed by three washes of the tip with 5 % methanol + 0.1 % TFA and the de-salted peptides were eluted in 10 μl 50 % ACN + 0.1 % TFA.

2.6.9 MALDI-TOF MS analysis of peptide samples

MALDI-TOF MS was used in the optimisation experiments, to check for the presence of peptides of known mass. MALDI target plates were cleaned in water, then methanol, and MilliQ-purified water, prior to incubation in a sonicator bath in methanol + H_3PO_4 for 10 minutes. A final rinse with methanol was performed and the plate allowed to air-dry.

For phosphorylated peptide samples, a matrix of 2 mg dihydroxybenzoic acid (DHBA) in methanol + 0.1 % H_3PO_4 was prepared. For all other samples, the matrix consisted of 2 mg α-cyanohydroxycinnamic acid (α-CHCA) in 50 % ACN + 0.1 % TFA.

Lyophilised samples were reconstituted in 10 μl H_2O and mixed in a 1:1 ratio with the matrix. De-salted samples for MALDI-TOF MS analysis were eluted in 50 % elution buffer and 50 % of the appropriate matrix. Reconstituted samples with high pH were adjusted to a pH < 6 using TFA. 1.4 μl of each sample in matrix was added per well of the cleaned MALDI target plate. Mass spectrometric analysis was performed using a MALDI-TOF instrument, with high and medium laser energy for the DHBA matrix and α-CHCA matrices, respectively. Approximately 5 minutes of scans were combined for each spectrum and the baseline subtracted. No export function exists for the spectra images, so a copy of the image was made using the print screen function of Microsoft Windows and saved as a .jpg file using Microsoft Paint.

2.6.10 Tandem mass spectrometric analysis of phosphopeptide samples

Lyophilised phosphopeptide samples were reconstituted in 10 μl 1 % FA. LC-MS/MS was conducted by Paul Skipp according to the protocol in Section 2.5.5, with the following modifications. A neutral loss scan was performed from 350 to 1800 (1 sec per scan) switching between a low collision energy (10 eV) and a high collision energy (37 eV). When a fragment exhibited a neutral loss of 98, 49 or 33.6 from singly, doubly or triply charged parent ions respectively, MS/MS was performed on the precursor ion using a collision energy profile as described above.

2.6.11 Identification of phosphorylation sites using linear trap quadropole-orbitrap MS

The LC-MS/MS system consisted of a quaternary Surveyor pump, a Surveyor autosampler and LTQ-Orbitrap equipped with a nanospray source. This work was carried out by Dr. Gary Wolfenden, at Thermo Electron (UK) Ltd.

Separation of samples was achieved using a binary gradient from 5 % buffer A (5 % ACN + 0.1 % FA) to 80 % buffer B (95 % ACN + 0.1 % FA) over 60 minutes using a C18-RP trap column for desalting and a C18-RP analytical column, prior to injection into the mass spectrometer. A survey scan (300 – 1400 m/z) was performed in the Orbitrap analyser (at R = 60000) and was followed by MS2 of the five most intense ions in both the Orbitrap and the LTQ analysers. MS3 of all ions showing a neutral loss of phosphoric acid (98 Da) from the precursor ion was also performed.

Data was processed and searched against the NCBI non-redundant human protein database using BioWorks (Thermo Fisher). All P-ser and P-thr peptides were required to show a neutral loss of phosphoric acid (98 Da) from the precursor ion, fragment ions, and/or trigger the neutral loss-dependent MS3 scan.

Chapter 3

Characterisation of the Model of the Injury Response

3.1 Introduction

The purpose of the work described in this chapter was to develop and characterise a model of injury that would provide samples for proteomic analyses that could potentially allow the identification of biomarkers that predict an individual's capacity to resolve an injury. An ideal method of injury should give a reproducible response, be minimally invasive and well tolerated by the patient, leaving minimal scarring. The use of microdialysis as the sampling technique within this study provides a method of injury in that probe insertion via a guide needle is known to cause an injury response (Ault *et al.*, 1994; Groth & Serup, 1998; Mathy *et al.*, 2003). Particular advantages of this model are that sampling occurs continuously from the moment of trauma, allowing flexible temporal analysis and causing no further injury, thus preventing any interference or modulation of inflammation by additional stimuli. Additionally, most subjects show no signs of scarring within a few weeks (Clough, personal communication). The response to needle insertion has been well characterised in terms of the vascular changes and in the release of inflammatory mediators, thus providing a basis to which the results of this study can be compared to determine the reliability and reproducibility of this model.

To characterise the inflammatory status of this model, a panel of additional cytokines was required that represented different aspects of the injury response. It was therefore appropriate to review the various pro- and anti-inflammatory cytokines, along with markers of cellular recruitment and of the vascular response, to correlate with measurements of blood flow. The pro- and anti-inflammatory cytokines needed to be known markers of the appropriate phase in response to injury and recoverable by microdialysis. IL-6 and IL-10 were chosen as these have been implicated in several processes within the inflammatory response and measured within dialysate previously (see Sections 3.1.1 and 3.1.7. Figure 3.1 shows some of the cytokines involved in regulating the response to injury and some of the effects they cause, including release of additional mediators and vascular effects.

The typical time course of the injury response would suggest that haemostasis occurs over a matter of minutes, with inflammation lasting several days. As the early response is of particular interest in the present study, only those mediators expressed during haemostasis and early inflammation would be expected. Therefore particular attention was given to markers of initial damage, such as those released from damaged keratinocytes and endothelial cells as well as activated platelets. These cells release cytokines, such as IL-1β, IL-6 that initiate the inflammatory response and IL-8 and OSM that stimulate the recruitment of neutrophils. To describe the expected cellular infiltrate, representative chemoattractants or secreted chemokines were chosen for each of the three most important cell types; platelets (MIP-1α), neutrophils (OSM) and monocytes/macrophages (MCP-1). Cytokines such as IL-8, IL-6 and IL-1 variants have been well studied, but the recovery by microdialysis of several of the other markers, including MIP-1α and OSM have not yet been reported, so it is also of general interest whether these can be measured in dialysate. The relevance of the chosen mediators as markers of the inflammatory response are briefly discussed in the following sections.

3.1.1 IL-6 as a pro-inflammatory mediator in injury

Interleukin-6 was selected because it is a pro-inflammatory cytokine and key regulator of the synthesis of acute phase proteins during inflammation (Castell *et al.*,

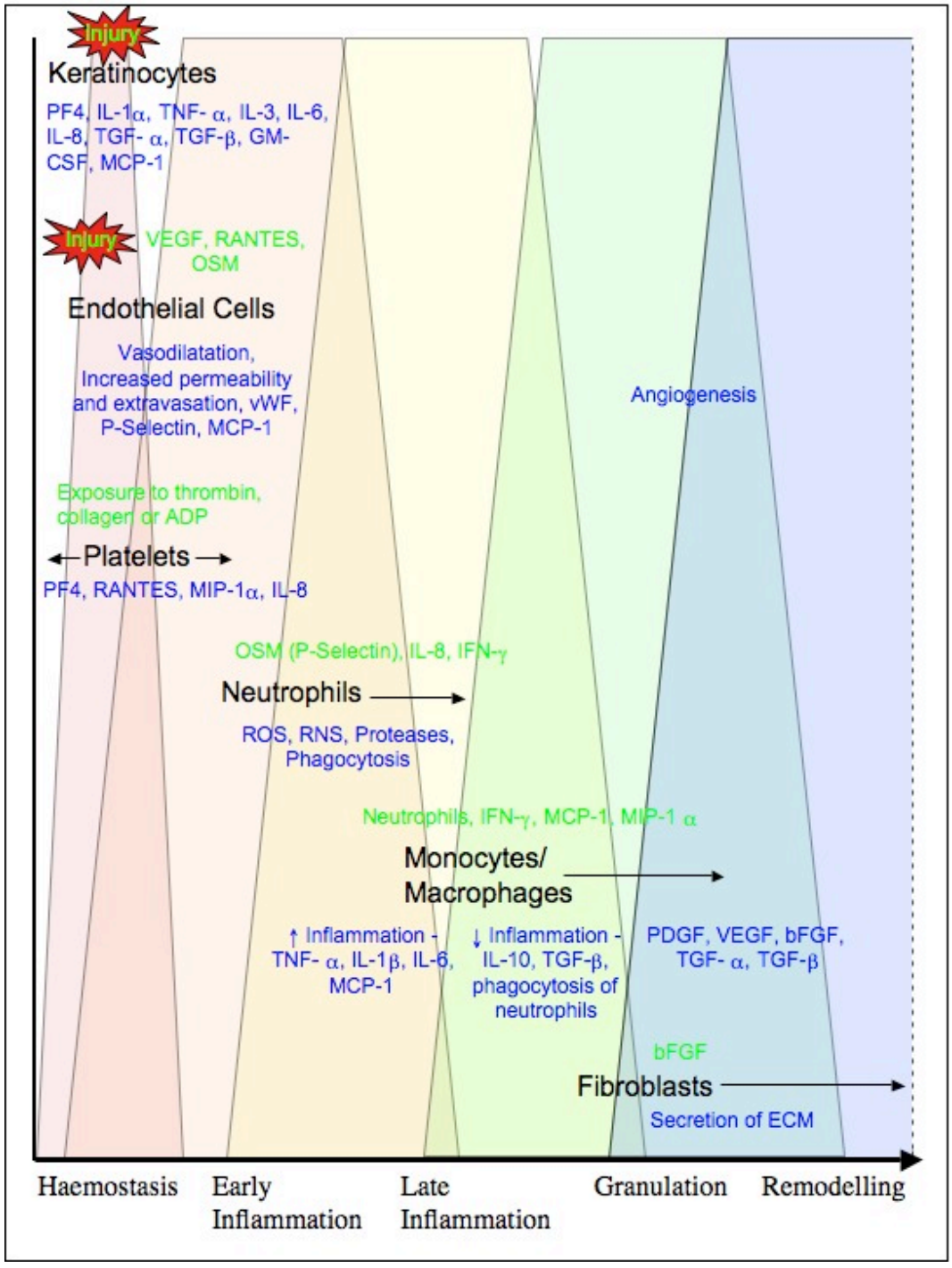

Figure 3.1: **Potential cytokine targets for characterising inflammation in the injury model.** Schematic of the different phases in the injury response, with the approximate timing of the contributions of different cell types. Stimulatory components are given in green, their effects, including mediators released, in blue.

1989; Henrich, Castell & Andus, 1990). It is hypothesised that IL-6 is involved in the progression of the inflammatory response through to its resolution by regulation of pro-inflammatory cytokine release. This progression also includes the transition from neutrophilic infiltrate to one of monocytes (Gabay, 2006). Maturation of monocytes into phagocytic macrophages eliminates not only the neutrophils, but other debris within the wound site. IL-6 is also involved in leukocyte recruitment, through stimulation of MCP-1 secretion and production of cellular adhesion molecules such as ICAM-1 (Romano *et al.*, 1997). Of particular interest is the observation that IL-6 levels are lower in wounds of the oral mucosa, a tissue that tends to heal much faster than the skin (Szpaderska, Zuckerman & DiPietro, 2003). This suggests that the control of the magnitude and/ or time-course of IL-6 expression is key in wound outcome.

3.1.2 Oncostatin M as an anti-inflammatory mediator or a chemoattractant for neutrophils?

Oncostatin M is an IL-6 family cytokine of approximately 28 kDa. Released from macrophages, T cells and keratinocytes at the wound margin (Goren *et al.*, 2006), it has been strongly implicated in the attenuation of the inflammatory response after injury. Here, it has been shown to inhibit TNF-α production and sepsis in response to common inflammatory stimuli (Wahl & Wallace, 2001) and regulate release of acute phase proteins from the liver (Richards *et al.*, 1992). The former report also describes the attenuation of inflammation by OSM in mice with induced rheumatoid arthritis. However, one study demonstrated the incompatibility between human OSM and the murine OSM receptor, casting doubt on the validity of these observations (Lindberg *et al.*, 1998).

In contrast to its reported anti-inflammatory effects, OSM has been found to modulate expression of IL-6 (Brown *et al.*, 1991). Modur *et al.* (1997) found that OSM actually induced inflammation, causing up-regulation of P-selectin and subsequent adhesion and transmigration of neutrophils. This finding has been repeated in a number of different tissues and cell types, including human dermal microvascular endothelial

cells (Kerfoot *et al.*, 2001) in which a 96 % selectivity for neutrophils was observed. This marker was of particular interest, as to the best of the author's knowledge, it had not been measured in the context of inflammation induced by mechanical injury prior to this study.

3.1.3 MCP-1 for the recruitment of monocytes

MCP-1 is produced by a variety of cell types, including keratinocytes, endothelial cells, Langerhan's cells and tissue macrophages, in response to an inflammatory stimuli (Gibran *et al.*, 1997). The primary role of MCP-1 is the chemoattraction of monocytes to areas of inflammation where they mature into macrophages, the roles of which were discussed previously, in Section 1.1.4.2. MCP-1 appears to be of particular importance in wound healing, as MCP-1 -/- mice were unable to compensate for the absence, exhibiting delayed re-epithelialisation, angiogenesis and collagen formation (Low *et al.*, 2001). Detection of MCP-1 would indicate both activation of endothelial cells and the chemoattraction of monocytes to the injury site.

3.1.4 MIP-1α as a marker of platelet degranulation and leukocyte recruitment

The function of MIP-1α in injury is less clear, in that while important in monocyte recruitment (DiPietro *et al.*, 1998), MIP-1$\alpha^{-/-}$ knock-out mice are able develop alternative, compensatory mechanisms (Low *et al.*, 2001). The level of redundancy between chemokines meaning that others can fulfil its role. Within the response to injury, MIP-1α is first released from platelets, then later from various other cell types which the initial platelet-derived burst recruits (Menten, Wuyts & Van Damme, 2002). MIP-1α would be expected early in the response to injury as it is constituitively expressed in the alpha-granules of platelets and released during their activation (Gear & Camerini, 2003, Klinger *et al.*, 1995), as well as being released later on by macrophages among other cell types. MIP-1α mRNA was detected within three hours post excisional wounding in adult mice, remaining elevated until 48 hours (Bryan *et al.*, 2005). MIP-

1α protein levels were not reported. No human microdialysis studies have looked at MIP-1α recovery, so it is of general interest whether this chemokine can be detected, as well as informative in terms of the time course of the response to injury and of platelet involvement.

3.1.5 VEGF as a regulator of vascular permeability

VEGF was first known as vascular permeability factor, although it has perhaps become better known for its role in the regulation of angiogenesis. The roles of VEGF in wound healing and regulation of vascular permeability have been reviewed extensively (e.g. Bates & Harper, 2002; Bates & Jones, 2003 and Breen, 2007) and it has numerous functions within inflammation (Angelo & Kurzrock, 2007).

VEGF acts through mediating phosphorylation of junctional proteins such as VE-cadherin, which leads to a loss of endothelial barrier integrity and thus increasing permeability (Gavard & Gutkind, 2006). This effect has been confirmed, for example, through the use of a VEGF antagonist which reduced oedema formation following ischemia/reperfusion injury within the murine brain (van Bruggen *et al.*, 1999). In the context of wounds, VEGF was detected in rat skin incisions within the earliest time point investigated (at 24 hours) and found to be secreted by neutrophils (Nogami *et al.*, 2007). Clearly, it would be of interest to know if VEGF is expressed during immediate early responses to skin injury.

3.1.6 IFN-γ in the switch to adaptive immunity and the antimicrobial response

The detection of IFN-γ would be significant as it has been reported to be involved in the switch from innate to adaptive immunity, being a key regulator of macrophage activation and subsequent antigen presentation (Schroder *et al.*, 2004). High levels of IFN-γ may indicate that this switch will occur, or the presence of pathogens that would require removal by the activated macrophages if detected later. Sources of IFN-γ include leukocytes within the systemic circulation including natural killer cells, T cells

and antigen-presenting cells as well as cells resident in the dermis, such as dendritic cells. With a local source, it could be expected to be detected early on in response to injury.

3.1.7 IL-10 as a marker of the switch from a pro- to an anti-inflammatory environment

IL-10 was selected because it is an anti-inflammatory mediator and therefore an indicator of the onset of resolution of inflammation. It is of interest due to the successes in improved wound resolution observed in animal studies in which IL-10 had been administered (de Vries, 1995). Additionally, it is resposible for the down-regulation of several pro-inflammatory cytokines, including TNF-α, IL-6 and IL-8 (Goldman, Marchant & Schandené, 1996). IL-10 has been measured in dialysate, falling from $\sim$ 150 pg/ml in samples collected 0 – 8 hours after insertion to just above 0 by the 24 – 32 hour collection (Averbeck *et al.* 2006). The measurement of IL-10 in the present study, using shorter collection periods, will improve the temporal resolution and determine whether IL-10 is released immediately after injury, or increases later on in the response.

3.1.8 Aims

The aims of this chapter were as follows:

- To develop a method of injuring the skin.
- To quantify the vascular responses to this physical trauma.
- To collect and measure known inflammatory mediators.
- To explore the time course of the injury response in this model.
- To inform future study protocols for proteomic analysis of novel markers of the injury response.

3.2 Methods

3.2.1 Volunteers

Healthy human volunteers were recruited from the students of the University of Southampton as described in Section 2.2.2. Four males and one female were recruited for the experiments discussed in this chapter, with a mean age of 25.2 ± 2.8 years.

3.2.2 Microdialysis

Microdialysis probes were constructed and sterilised as described in Section 2.2.1. Probe insertion was performed as described in Section 2.2.2. Dialysate was collected from four probes placed in the dermis of the non-dominant volar forearm and was sampled over consecutive 30 minute periods for the three hours immediately following microdialysis probe insertion (shown in Figure 3.2). These periods were chosen based on the literature, laser Doppler results from preliminary data (not shown) and those discussed in this chapter.

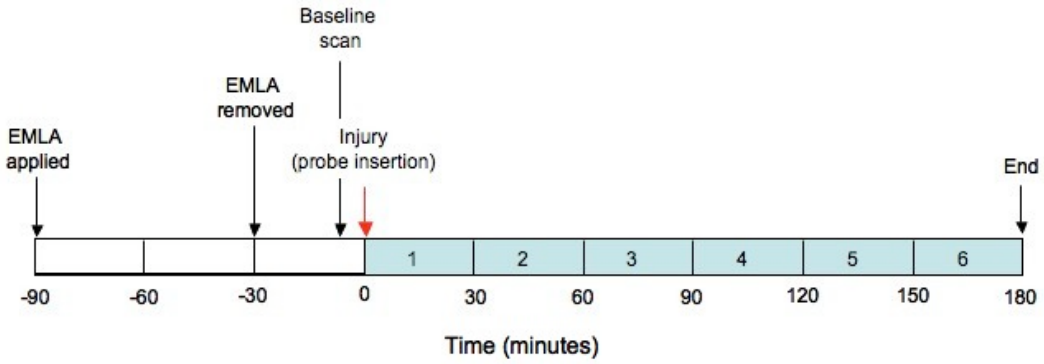

Figure 3.2: **Dialysate collection protocol for cytokine and total protein analysis.** Protocol used for the collection of dialysate for analysis of specific markers of injury. Numbered blue boxes indicate the six dialysate collection periods. Laser Doppler scans were performed before insertion to represent baseline and then every 5 minutes, starting 5 minutes after injury.

At the end of each collection, the dialysate from all four probes was pooled, divided

into aliquots, and flash-frozen in liquid nitrogen, as previously described. One 75 μl aliquot was used for the quantifying the amount of protein per ml of dialysate and a second 75 μl for quantifying the recovery of specific markers of injury.

3.2.3 Laser Doppler Imaging to measure blood flow

Laser Doppler imaging was performed to measure the rate of blood flux at the injury site, as described in Section 2.2.3. Values of mean blood flux are reported in arbitrary perfusion units (PU).

3.2.4 BCA assay for quantitation of total protein in the dialysate

The concentration of total protein per ml in each dialysate collection was estimated by BCA assay (Section 2.3). Samples were diluted with an equal volume of Ringer's saline. Bovine serum albumin (BSA) standards were prepared in Ringer's saline in 0.1 mg/ml increments from 0-1 mg/ml. A total of 20 μl of standard or sample was added per well, in duplicate, and incubated with the prepared assay reagent for 30 minutes, as per the manufacturers recommended protocol. Absorbance was read at 570 nm using a microtiter plate reader. The limits of detection were 200-1000 μg/ml. Protein concentrations were calculated against a standard curve ($r^2 \geq 0.98$) constructed by the analysis software and manually adjusted for dilution factor.

3.2.5 Multiplex cytokine analysis of markers of inflammation

The concentration of selected cytokines was measured using a CBA Flex set, an antibody-coated bead-based assay from BD Biosciences (Section 1.4.2.1). Samples were prepared according to the manufacturers recommended protocol and analysed by flow cytometry, as described in Section 2.4. Data were analysed using the FCAP Array (Soft Flow Inc.) wizard, using the manufacturers recommended settings. All standard curves gave an r^2 value of 0.98 or greater and gave a detection range of 5-2500 pg/ml for all cytokines.

3.2.6 Statistics

The significance of the difference in mean blood flux or mean cytokine concentration between different time points was determined using a Student's paired t-test. In all cases, a probability value of $P < 0.05$ was taken to be significant. All values are given in the format Mean $\pm$ standard error of the mean (SEM) unless otherwise stated. Correlations were assessed using the Pearson's Rank correlation test and repeated measures analysis of variance (ANOVA) was conducted, where appropriate. All graphs and statistical analyses were prepared and performed using GraphPad Prism software version 5.

3.3 Results

3.3.1 Assessment of the changes in blood flux induced by microdialysis probe insertion injury

Figure 3.3 shows the typical blood flux response to needle insertion, before and 15 minutes after injury as measured using laser Doppler imaging. All values are given as mean ± SEM, in perfusion units (PU).

In this example, before insertion, the mean blood flux over the four regions of interest was 66 ± 4 PU, n = 4. Fifteen minutes after needle insertion, there was a visible increase in mean blood flux in the vessels and at the insertion sites, to 373 ± 47 PU in the regions of interest. This is representative of those responses seen in the rest of the volunteer group. Figure 3.4 summarises the changes in mean blood flux over three hours after needle insertion.

Before injury, baseline mean blood flux was 78 ± 14 PU (n = 4 volunteers). After insertion, blood flux increased significantly from the baseline value, reaching a peak of 368 ± 67 PU at 10 minutes ($p = 0.013$, Student's paired t-test). It then declined over time, until 70 minutes, where blood flux was no longer significantly above baseline ($p = 0.56$, Student's paired t-test). There was no significant difference between the value for mean blood flux at 10 minutes and those other measurements taken within the first 30 minutes, as determined by Student's paired t-test ($p > 0.05$), so this period of 0 – 30 minutes after injury was defined as the peak phase. The period from 70 minutes to the end of the experiment was defined as the steady-state phase, during which time a mean blood flux of 172 ± 3 PU was maintained. The intermediary period of 30 – 70 minutes, over which the mean blood flux decreased, was defined as the decline phase. These three phases correspond to the proposed 30-minute dialysate collection periods, with the first collection covering the peak phase, the second sampling over the majority of the decline period and the four remaining collections corresponding to the time over which blood flux had reached a steady state and the early phase of the inflammatory response was underway.

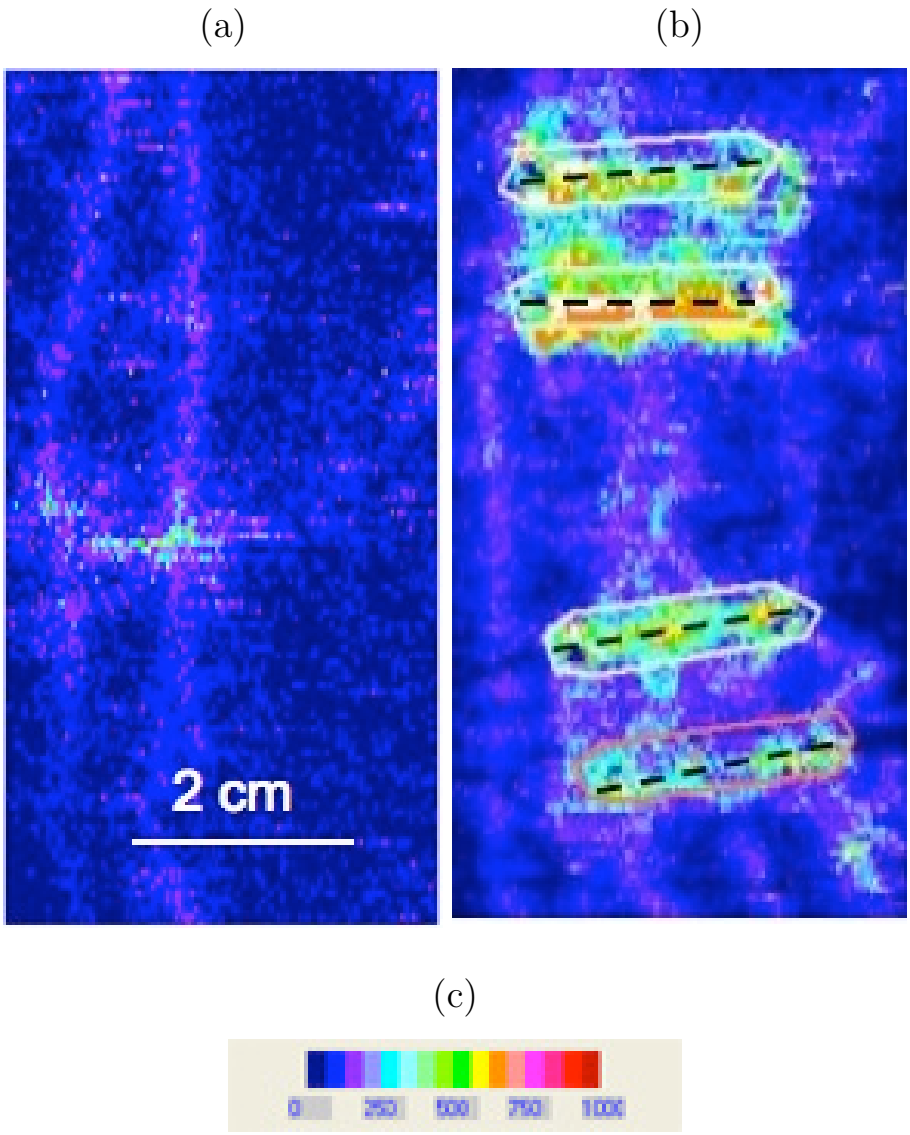

Figure 3.3: **Laser Doppler images of blood flow before and after probe insertion** Scans of the area around the injury site taken a) 5 minutes before and b) 15 minutes after probe insertion. c) Key denoting the relationship between pixel colour and blood flux in perfusion units (PU). Dashed lines indicate probe location, white boxes indicate the region of interest over which area the mean blood flux was calculated.

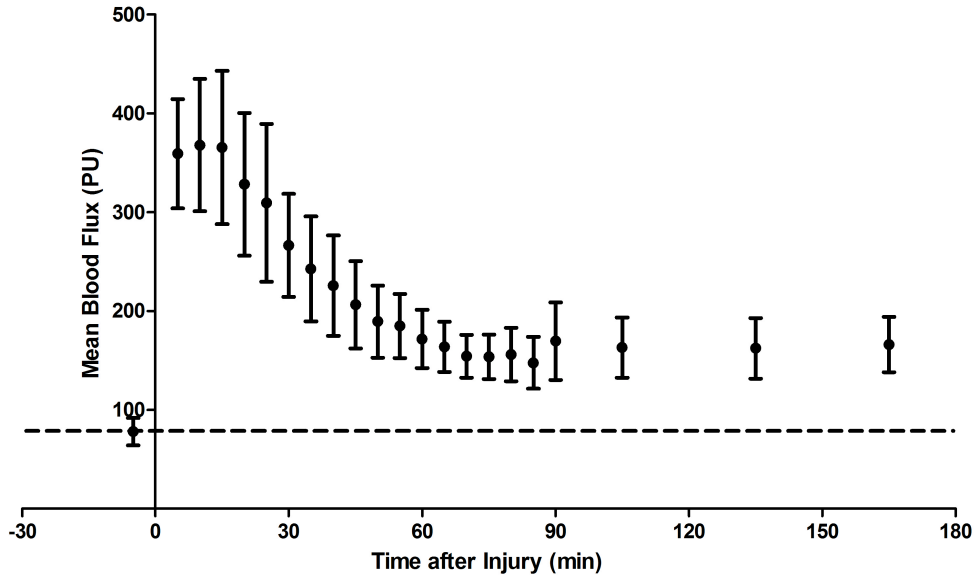

Figure 3.4: **Changes in mean blood flux over three hours following microdialysis probe insertion** Peak mean blood flux is observed within 15 minutes, followed by a decline until 65 minutes where a steady state is reached. The dashed line represents the mean value for baseline. Values are mean ± SEM, n = 4 volunteers. The first volunteer was excluded due to a change in the measurement protocol from every 30 minutes to every 5 minutes, as a result of data collected in that experiment.

3.3.2 Analysis of the changes in total protein recovery in the dialysate over time

The second step in characterising inflammation in response to injury was to assess the changes in protein concentration in the dialysate as an increase in protein extravasation should result in an increase in protein concentration within the dialysate. The mean protein concentration of each 30 minute collection is shown below in Figure 3.5.

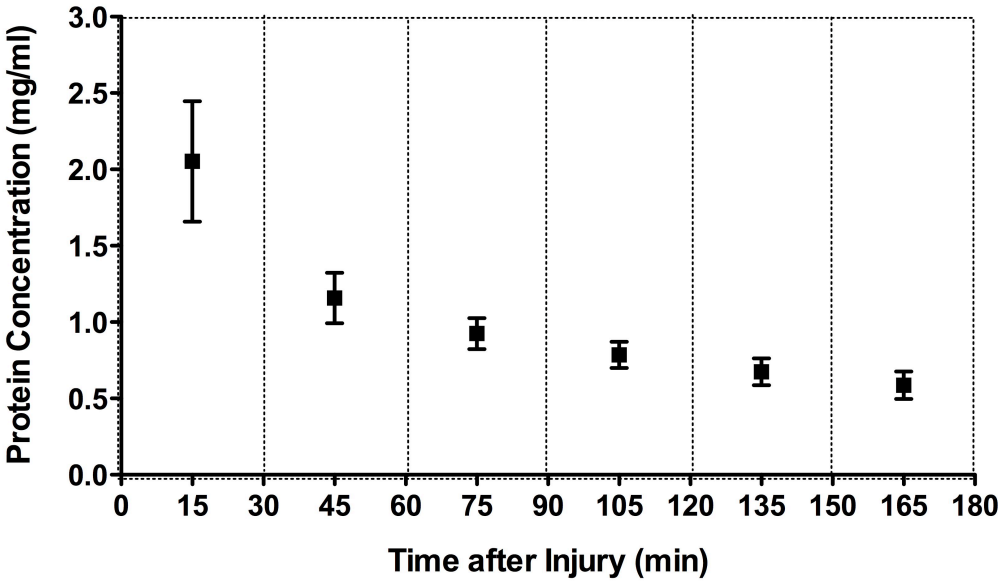

Figure 3.5: **Total protein in the dialysate over time** Total protein in the dialysate in each collection period, denoted by the boxes. Values are Mean ± SEM, n = 5.

Total protein concentration was highest in the first collection, at 2.1 ± 0.4 mg/ml and decreased over subsequent collections, to 0.59 ± 0.09 mg/ml. Only the first collection contained protein at a significantly higher concentration than the other timepoints ($p = 0.0009$, repeated measures ANOVA with Bonferroni multiple comparisons post-test). The changes in protein concentration gave a similar profile to the changes in blood flux. The relationship between these two parameters is shown in Figure 3.6. The mean blood flux for all four sites over each 30 minute collection period was compared

against the protein concentration for that collection.

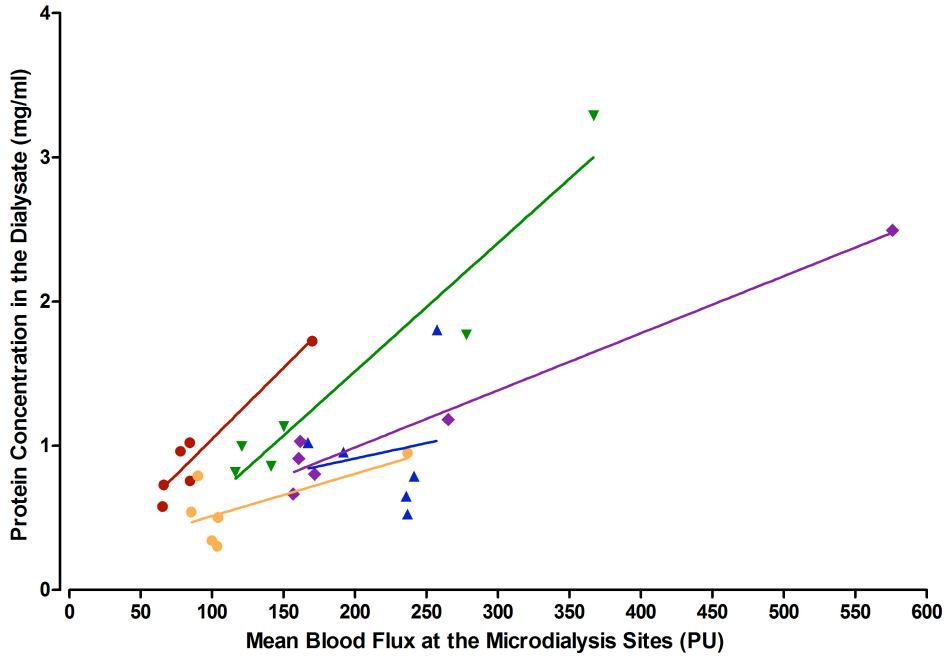

Figure 3.6: **Relationship between mean blood flux and protein concentration** Linear relationship between the mean blood flux and total protein concentration for each dialysate collection, by volunteer. Each volunteer is indicated by a different colour. Values are mean ± SEM, n = 5 volunteers. A positive correlation is observed for the dataset as a whole (Pearson r = 0.817 $p < 0.0001$, $r^2 = 0.668$). Individual correlations are as follows, in the format Pearson r value, p value and r^2 value; red = 0.96, 0.003 and 0.92, green = 0.96, 0.002 and 0.92, blue = 0.16, 0.759 and 0.03, purple = 0.98, 0.0005 and 0.97 and orange = 0.67, 0.15 and 0.44.

Overall, there was a strong correlation between the total protein concentration in the dialysate samples and the mean blood flux over the corresponding collection period (Pearson r = 0.817 $p < 0.0001$, $r^2 = 0.668$, Pearson's rank correlation). Individually, three volunteers gave very strong correlations and the remaining two had no significant correlation.

3.3.3 Analysis of changes in markers of inflammation following needle insertion injury

Four of the seven cytokines in the panel were detected in the dialysate samples. Those not detected were IL-10, IFN-γ and OSM. IL-6, MCP-1 and VEGF were recovered successfully while MIP-1α was only detected in the final collection, above the negative control of 0 pg/ml but below the lowest standard of 5 pg/ml. Figure 3.7 shows the concentration of the different markers of inflammation recovered in each dialysate collection for each volunteer.

MCP-1 (Figure 3.7a) was recovered in the first dialysate collection from two volunteers, at 9.47 $\pm$ 4.13 pg/ml (mean $\pm$ SEM). The concentration of MCP-1 in the dialysate increased steadily over time, reaching 279.23 $\pm$ 41.89 pg/ml (n = 5) by the final collection.

VEGF was detected in low concentrations in the first collection from three volunteers, at 6.11 $\pm$ 0.36 pg/ml. Recovery of VEGF was varied but gave no significant change over the duration of the experiment. The mean concentration detected ranged from 2.54 $\pm$ 1.15 pg/ml at 45 minutes post injury to 5.53 $\pm$ 2.26 pg/ml at 165 minutes, however this was not a linear increase.

IL-6 was first detected in the third collection, at 21.81 $\pm$ 16.10 pg/ml (n = 5). The concentration of IL-6 increased significantly over subsequent time points, to 195.52 $\pm$ 69.98 pg/ml (n = 5) in the final collection (p = 0.03, Student's paired t-test). The rate of increase in MCP-1 recovery was greater than that of IL-6 between the fourth and sixth collections.

MIP-1α was detected in three volunteers in the final collection at 0.97 $\pm$ 0.34 pg/ml (n = 3), above the level of the negative control.

To assess whether a greater hyperaemia or total protein concentration were correlated with an increased expression, and therefore recovery, of cytokines, area under the curve (AUC) was calculated for each dataset. No correlation was found between total cytokine concentration and either total blood flux or total protein recovered (Pearson's rank = 0.564 and 0.663, r^2= 0.318 and 0.439 and p= 0.322 and 0.223, respectively).

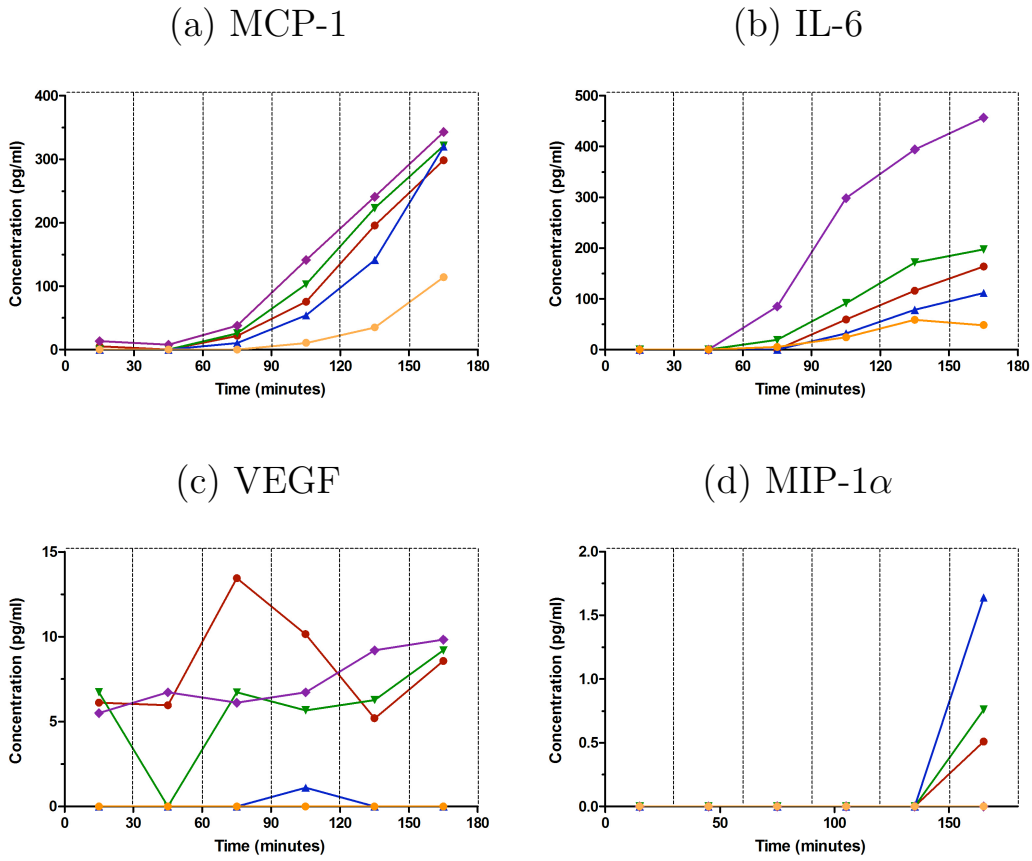

Figure 3.7: **Changes in concentration of specific cytokines in dialysate over the three hours after insertion** Concentrations of a) MCP-1 b) IL-6, C) VEGF and d) MIP-1α in the dialysate over time from probe insertion. Times represent the mid-point of the collection periods denoted by the dotted-line boxes. Data are plotted for each volunteer to show individual responses.

3.4 Discussion

The aim of the work presented in this chapter was to develope and characterise a model of injury in skin that was suitable for future proteomic studies into the response. The injury needed to be reproducible between volunteers, and to not leave lasting cosmetic damage. Characterisation of this model involved measurement of the vascular and inflammatory responses to the injury using established methodology so that the findings could be compared back to the literature as an additional measure of reproducibility. The injury caused by the insertion of microdialysis probes was chosen because it enables continuous measurement of a single injury without further the perturbation that is unavoidable with other combinations of sampling and stimuli.

3.4.1 The vascular response to microdialysis probe insertion injury

The intradermal insertion of microdialysis probes caused a significant increase in cutaneous blood flow at the insertion sites, observed in the first measurement after insertion. This increase was sustained, beginning to decline after 15 minutes. By 70 minutes after the insertion injury, blood flux had stabilised above baseline, although this was not a significant increase above baseline measurements (Student's paired t-test). The increase in blood flow within the superficial capillaries was associated with an increase in flow in the larger, deeper vessels, visible in the baseline scans as lines of raised flux.

The responses observed in the present study are supported by those reported previously (Anderson, Andersson & Wårdell, 1994 and Groth & Serup, 1998). Although the magnitude of the responses cannot be directly compared as these reports give values in volts, rather than perfusion units, the peak hyperaemia and decline to steady state occur within very similar time frames. This suggests that the response is reproducible both between volunteers and between clinical settings and that this method is appropriate for monitoring the initial vascular response to trauma. However, there are limits to the information that this technique can provide. Once steady state has been

reached, there are no further significant changes while blood flux returns to baseline levels more than 24 hours post injury (Anderson, Andersson & Wårdell, 1994). Additional methods are required to understand the mechanisms behind the increases in cutaneous blood flux and any associated processes involved in the development and progression of the inflammatory response.

3.4.2 Changes in protein recovery following microdialysis probe insertion injury

The protein concentration within the dialysate followed the a similar pattern of decline over time to the blood flux measurements, approximating steady state by the fourth collection. Protein recovery was slightly higher than previously observed in the literature, with a mean ± SEM in the first collection of 2.05 ± 0.39 mg/ml compared to published values of 0.65 and 1.2 mg/ml. This concentration fell to 0.59 ± 0.09 mg/ml in the final collection (150 – 180 minutes post-insertion), compared to 0.43-0.5 mg/ml in previous experiments (Klede, Handwerker & Schmelz, 2003; Sauerstein *et al.*, 2000). This difference is unlikely to be a result of perfusion rate, as the rate used in this study was in-between those used in the two published reports. The significance of this increased recovery is unknown and may be a result of different sensitivities in the assay methods, or of the reduced dialysis length of 1.5 cm, compared to 2 cm in the present study. The magnitude of difference in observed concentrations is low enough that this should not be cause for concern.

Changes in protein extravasation have been measured using microdialysis, particularly in the context of chemically-induced inflammation. However, it may not be suitable as a measure as an indicator of inflammatory status in injury. This is partly because the baseline protein concentration cannot yet be determined, in that sampling the interstitial fluid space currently requires breaching the skin barrier, thus causing injury. As a consequence, it is impossible to know whether the steady-state concentrations are representative of a return baseline levels or of an equilibrium between delivery and removal, by metabolism and microdialysis respectively. Furthermore, these changes

in protein recovery occur over a very rapid timescale (Clough, 2005) that corresponds to the time over which proteins can escape via damaged vessels before clotting seals gaps in the vessel wall, rather than with the progression of the inflammatory response.

Interestingly, a strong positive correlation between protein recovery and mean blood flux was observed in three volunteers. The volunteer (represented by orange data points throughout the chapter) who displayed the smallest increase in mean blood flux above baseline also gave the lowest total protein recovery, although the correlation was only very weakly positive (Pearson r = 0.67, r^2 = 0.44) and not statistically significant (p = 0.15). The mechanisms responsible for regulating protein extravasation and blood flux are not known to be related, but the association of these two parameters may be related to the magnitude of the response to an injury.

3.4.3 Cytokine release after microdialysis probe insertion injury

The third component of the characterisation was the quantification of inflammatory mediators recovered in the dialysate. Of the seven mediators analysed, four were detected. Those not detected were OSM, IFN-γ and IL-10, the anti-inflammatory mediator. Although previously measured within the first eight hours after probe insertion (Averbeck *et al.*, 2006), the absence of IL-10 within the three hour time course was unsurprising as it is more likely to be released later on, towards the end of the pro-inflammatory phase. The absence of OSM and IFN-γ was a surprising as both are implicated in the early inflammatory response. IFN-γ has been detected before in dialysate within the group, reaching between 20 and 100 pg/ml within 2 hours after probe insertion (Clough *et al.*, 2007), although was undetectable in 8 hour collections in a study by a different group (Averbeck *et al.*, 2006). When detected, the levels were highly variable between volunteers and showed no trend over time or increase in response to allergen (Clough *et al.*, 2007). It is still possible that IFN-γ is released during this period at concentrations too low to be detected in the dialysate, however, studies within mice suggest that this is not the case (Bryan *et al.*, 2005). With either

situation, however, it can be concluded that a switch to an adaptive immune response is unlikely and that IFN-γ-induced macrophage activation has not yet occurred.

The recovery profile of VEGF was unexpected, in that there was no significant differences over time and indeed no real trend, with high inter-individual variation given the low levels recovered (Figure 3.7c). These low values are consistent with the concentration of VEGF recovered by microdialysis from tumour (2.4 pg/ml) and unaffected (6.0 pg/ml) breast tissue (Garvin & Dabrosin, 2008).

Predominantly considered to be an angiogenic factor responsible for the proliferation of endothelial cells, VEGF was first implicated in the modulation of vascular permeability (Senger *et al.*, 1983). With this in mind, it was hypothesised that VEGF would be detected early on in the response to injury to enable the extravasation of cellular or molecular components from the blood and that it would correlate with protein concentration of the dialysate. No reports have yet been published in which measurements are taken of VEGF recovered from skin by microdialysis. One study on human skeletal muscle, *in vivo*, measured VEGF before and during exercise, from 60 minutes after insertion. VEGF levels remained relatively unchanged in the initial resting phases before exercise (Höffner *et al.*, 2003). This observation matches that in the present study. However, the Höffner study did not conduct any measurements in the first hour, in which the effects on vascular permeability would be expected. The absence of any clear trend in VEGF recovery suggests that another factor or combination of several mediators may responsible for the increase in vascular permeability after injury, such as histamine or neuropeptides such as bradykinin.

Recovery of MIP-1α did not occur as would have been expected for a marker of platelet activation (Figure 3.7d). Very low concentrations were detected only in the final collection (150 – 180 minutes after insertion) from three of the five volunteers, compared to the early increases that would be expected from release by activated platelets. However, this corresponds well with murine mRNA data in which expression increased from approximately three hours post-injury (Bryan *et al.*, 2005). With mRNA data however, the effect of pre-generated stores cannot be taken into account, therefore any protein released from platelets is likely to have been missed. The recov-

ery of MIP-1α only within the final collection shows that this is not a good marker for platelet recruitment, at least. Activation of platelets occurs almost immediately after injury, however the exact time course of the release of alpha granule contents, including MIP-1α after injury is as yet unclear in this situation. Additional markers would be required in future to better characterise the action of platelets and a longer time-course would be needed to characterise the recovery of MIP-1α itself within this model.

Release of OSM was predicted to occur within one hour of the initiation of an inflammatory response. Its absence in this situation would suggest that the inflammation induced by microdialysis probe insertion injury was not severe enough to require the IL-6 amplification effects or neutrophil attraction within this time frame. It is also possible that OSM was released, but not at a great enough concentration to be recovered at a concentration high enough to allow detection. OSM has not been measured before in an injury situation, however, in patients with sepsis, OSM has been measured at concentrations of around 45 nM, with levels being low or undetectable in healthy subjects (Guillet *et al.*, 1995).

Alternatively, the diffusion rate of OSM may be too low or the molecule itself incompatible with the microdialysis membrane. OSM has a theoretical pI of 10.7, similar to that of MCP-1 (10.5), so an incompatibility of molecular charge status between the protein and the microdialysis membrane is unlikely to be responsible for the absence of OSM in the dialysate. The time-course of OSM expression following mechanical injury has also not yet been reported, however polymorphonuclear neutrophils stimulated with bacterial lipopolysaccharide and GM-CSF can produce OSM within one hour (Grenier *et al*, 1999) suggesting that it is released rapidly. OSM was detected within four hours in the equivalent control populations, therefore, if it is released in response to injury, it may be not be released until after the three hour time course studied. Early detection of OSM in situations of sepsis and LPS-induced inflammation suggest a role in anti-bacterial effects consistent with neutrophil chemoattraction, but the results of the present study indicate it is unlikely to be involved very early on in injury.

The macrophage chemoattractant, MCP-1, was observed during the first three hours after injury. For two of the volunteers, MCP-1 was detected in the very first collection, albeit at low concentrations. Only one volunteer had detectable levels in the second collection. This would suggest that this is the result of early, low level release rather than a constitutive expression. Although this could also be a result of expression below the concentration required for sufficient recovery to enable detection. Recovery of MCP-1 greatly increased from the third collection (60-90 minutes post injury) onwards.

MCP-1 has been recovered previously using microdialysis, in human abdominal tissue (Riese *et al.*, 2003), but the collection period in relation to insertion is unclear. Baseline levels, that is without additional stimuli, were recorded in the range of 2-6000 pg/ml between 60 and 320 minutes post-insertion (Murdolo *et al.*, 2007). These values were adjusted concentrations, to represent interstitial fluid concentration based on measurements of relative recovery of approximately 20 %, so the actual levels measured in the dialysate will be lower (approximately 400-1200 pg/ml). Similar levels were observed in dialysate obtained from mice within one hour of LPS administration, un-stimulated values were reported within the low pg/ml range (Ao *et al.*, 2005). Most volunteers displayed concentrations around 300 pg/ml within the final collection, slightly lower than the values obtained in dialysate from abdominal tissue but still comparable. The recovery profile obtained in this study matches that seen in previous experiments, in which the concentration in response to an inflammatory stimulus continues to increase over the three hour time frame examined, and beyond (Ao *et al.*, 2005). This is somewhat surprising, as macrophages are generally not recruited until after neutrophils. However, the exact time that blood-derived monocytes first enter the wound is unknown, further than within the first 24 hours (DiPietro, 1995). An increase in expression this early on suggests that MCP-1 may be involved in other processes during the earlier stages of the inflammatory response. It is a known stimulator of cytokine production in monocytes (Jiang *et al.*, 1992), however, this would be expected even later than the initial chemoattraction. Given the multi-functionality of many cytokines and chemokines, it is probable that MCP-1 fulfils other roles in the early inflammatory response yet to be determined. It is known to be released from

keratinocytes (Wetzler *et al.*, 2000) and endothelial cells (Gerritsen & Bloor, 1993) after injury, and a recent review highlights a possible role in modulation of vascular permeability (Wallez & Huber, 2008).

IL-6 was recovered in the third dialysate collection, 60 – 90 minutes after injury. The concentration of IL-6 in the dialysate continued to increase over subsequent collections. This was very similar to the time course reported by Sjögren, Svensson & Anderson (2002). In all but one volunteer, IL-6 was first detected at less than 50 pg/ml, increasing to between 50 – 200 pg/ml by three hours. One volunteer showed considerably higher release, reaching 456 pg/ml. The concentrations in this study are higher than those reported by Sjögren and colleagues (10 – 70 pg/ml and one volunteer above the highest standard of 100 pg/ml). The differences in concentration between the two investigations is particularly surprising, given the lower perfusion rate (1 μl/min) used. This could be a result of the dilutions performed in order to obtain enough volume for the assay or, from the dilution that occurs as a result of the reduced volume loss associated with the push-pull microdialysis method used. This method removes the dialysate under a pressure equal to that of the perfusate inflow, reducing the loss of the perfusate to the tissue surrounding the probe. Alternatively, it could be an consequence of improved detection methods and sensitivity since the experiments were conducted. The difference is unlikely to be due to the different microdialysis sampling methods (push-pull versus the push-only method used in the present study) as little difference is seen for *in vivo* recovery of Il-6 reported by Sjögren and colleagues. The concentrations of IL-6 seen by Clough *et al.* (2007) were obtained from undiluted samples and are closer to those observed in this study, reaching a mean of 137 pg/ml by 4.5 hours post insertion. The increased perfusion rate of 5 μl/min may account for the slightly lower levels and later time of increase compared to those seen in the present study. IL-6 is not constitutively expressed in normal skin (Sugawara *et al.*, 2001), so the detection of IL-6 is significant because it confirms that an inflammatory response has been initiated. As previously discussed, IL-6 is a key mediator within inflammation with many regulatory roles, so it would be of particular interest to see how its expression correlates with downstream targets.

No correlations were found between cytokine concentration and either measure of the vascular response to injury, suggesting that the regulation of these parameters are not closely related (data not shown).

The multiplex cytokine assay worked well with the dialysate samples, both in terms of volume requirements and sensitivity. In some cases, the dialysis efficiency may not have been high enough for recovery of a sufficient concentration of cytokine to enable detection. However, it is not possible to determine whether this is the case, or if no cytokine was released within the tissue. As explained in Chapter 1, while *ex vivo* experiments can give an estimate of dialysis efficiency, these are unreliable estimates as *in vitro* dialysis conditions are very different compared to the *in vivo* environment. In the present study, the aim was to obtain an overview of the injury environment and therefore a more comprehensive characterisation. The exact tissue concentration is not necessarily required as the amount recovered should be equally representative between volunteers. As long as the recovery is reasonably reproducible, it would still be possible to differentiate between a normal and an abnormal response on the basis of cytokine levels relative to each other, and of the time-course by which they are observed in the dialysate. Figure 3.8 shows those of the panel of cytokines which were detected in the dialysate, in relation to the cell types either activated or stimulated in the injury model.

The inflammatory profile obtained from the measures that were detected in the present study is indicative of the activation of keratinocytes and endothelial cells following injury. This suggests that the three-hour time-course is sampling the early pro-inflammatory environment just prior to the recruitment of neutrophils, in which the signals for leukocyte recruitment are being generated. However, the number of processes in which these cytokines are involved span four of the five stages of the injury response. These results highlight the need for more specific markers of injury to better characterise the response and for more accurate targets for therapeutic intervention.

3.4.4 Summary

The microdialysis probe insertion method of injury generated a reproducible inflammatory response. This response was consistent with the very early stages of inflammation and measurements of existing markers of inflammation were consistent with those reported in the literature. While there are some limitations within the sampling technique, these are far outweighed by the advantages of localised, continuous collection without causing further injury. The vascular responses, protein recovery and cytokine profiles obtained were similar to those predicted. However, the involvement of each mediator in more than one process within the inflammatory response highlights the problems of using such multifunctional molecules, both as markers of inflammation and targets for therapy. It is clear that alternative approaches are required. This work has shown that a sufficient amount of protein-rich fluid can be obtained from the injury environment using microdialysis, from which novel mediators of the injury response may be identified. The next chapter describes the analysis of the protein content of this fluid.

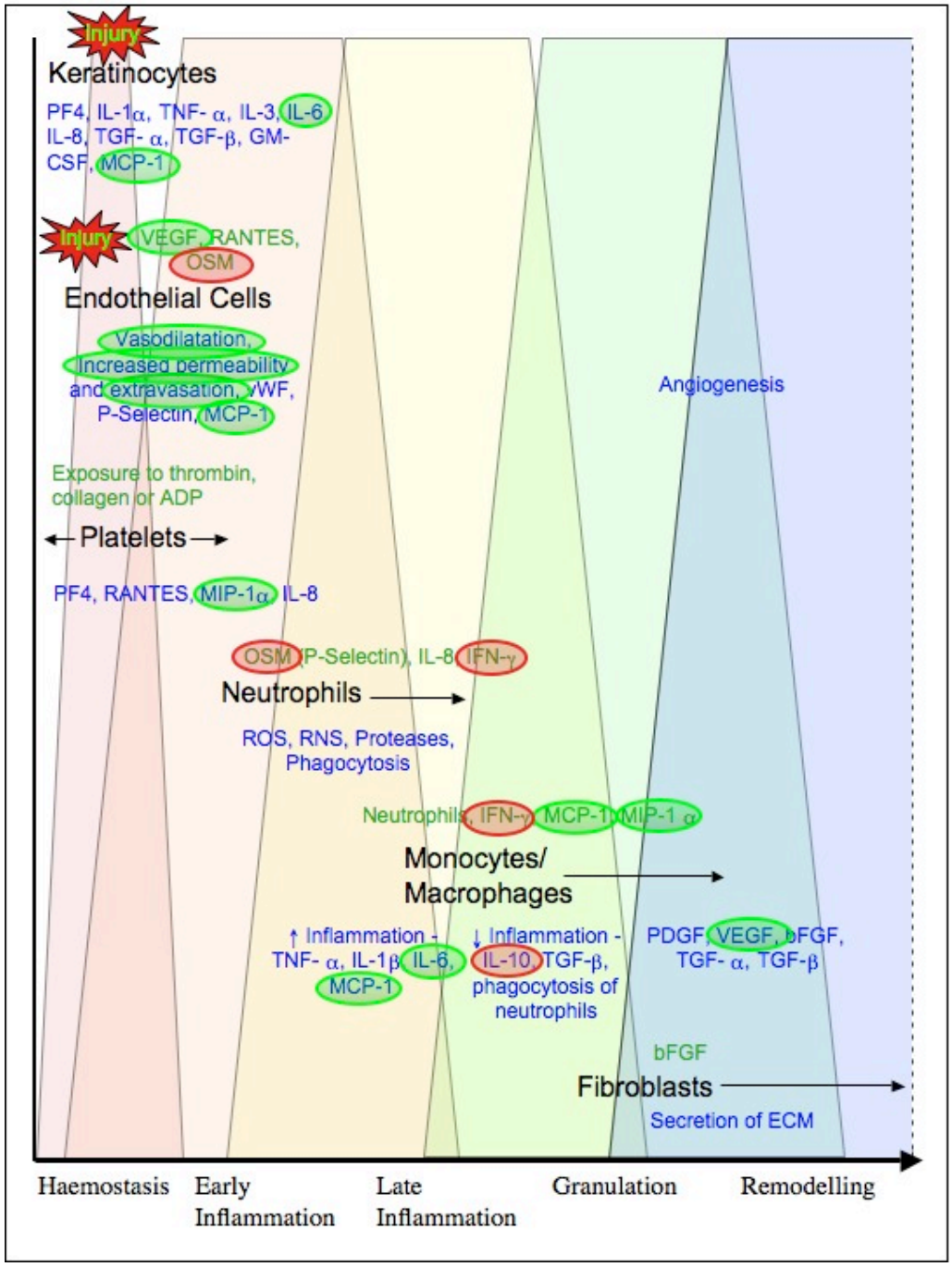

Figure 3.8: **Overview of the results of the characterisation study in the context of injury signalling** The measures of inflammation detected (green) are placed in the context of the signalling overview. Those not detected (red) are also shown. The x-axis shows the chronology of the stages of the injury response. Cell types are listed from top to bottom in order of expected involvement, although keratinocytes and endothelial cells are stimulated simultaneously by the injury itself.

Chapter 4

Proteomic Profiling of Dermal Dialysate

4.1 Introduction

Recent research (reviewed in Chapter 1) and the data presented in Chapter 3 have shown that measurements of cytokines and growth factors are insufficient for characterising responses to injury and to treatment of fibrosis or non-healing wounds. It is therefore clear that alternative markers are required to give a more comprehensive understanding of the cutaneous response to injury.

It was hypothesised that the combination of a localised sampling technique and a more global approach to characterisation of the wound environment would lead to the identification of novel markers of the injury response. At the time of this study, the proteome of human dermal dialysate had not been determined, so the first step was to characterise the protein profile that could be obtained. A baseline survey was conducted using dialysate samples obtained 30 – 150 minutes after injury, after the initial peak protein in concentration observed over the first 30 minutes, as shown in Chapter 3. This survey was conducted using a shotgun proteomics approach, discussed in Section 1.5, to enable identification of potentially unknown components.

Characterisation of the injury model in Chapter 3 indicated that the three hour time course chosen covers the activation of resident cell types and of platelets recruited

to the site of injury. It would be expected that the predominant proteins detected would be representative of the acute phase and of cell damage. Several studies into the proteome of the skin have been conducted, as discussed in Section 1.5.1. Although the proteome obtained will depend on the sampling method, it is likely that there would be considerable overlap in protein profiles. Two studies (Kool *et al.*, 2007; Macdonald *et al.*, 2006) reporting on the associations of proteins identified in human suction blister fluid to various disease states do not list any proteins in common, although different complement factors are present in both datasets. The seeming absence of shared proteins is likely due to only those proteins of interest to the particular study being listed and not the entire dataset obtained. Full listings are not available in supplementary data, so this cannot be confirmed. Several acute phase response proteins were identified between the two papers, including ceruloplasmin, apolipoprotein, orosomucoid and haptoglobin related proteins, which would be expected to increase following injury and hence could be expected in dermal dialysate.

No proteomic analysis of human dermal dialysate samples had been reported to date, although the combination of microdialysis with proteomics has been applied to neuroscience research. Analysis of dialysate obtained following microdialysis within the human brain identified 27 proteins. Of these, the majority were acute phase proteins, with considerable overlap with those seen in the suction blister skin studies (Maurer *et al.*, 2003). Ten proteins were apparently specific to brain dialysate, as they had not been previously identified in cerebrospinal fluid. This suggests that locally produced components can be detected using these techniques, over and above those systemically produced components. The total amount of protein in samples used in determining the cerebral dialysate proteome was between 0.08 and 0.40 mg/ml, compared to the total protein concentration of 0.59 – 2.1 mg/ml in dermal dialysate samples measured in Chapter 3. This suggests that there will be sufficient protein in the dermal dialysate for proteome analysis.

4.1.1 Specific protein depletion to improve proteome coverage

One concern with the global profiling approach is the abundance of several plasma proteins, particularly immunoglobulins and serum albumin. With the limited capacity of the mass spectrometer, these proteins may reduce the detection of less abundant components. This proves particularly problematic with profiling of plasma/serum, derived from multiple sources. It is unknown whether this is likely to be a problem in profiling the proteome of dialysate from skin. However, given that serum albumin is estimated to comprise approximately 70 % of the total protein in cerebral and dermal dialysate (Winter *et. al.*, 2002), it is likely to.

Two approaches are employed to improve detection of lower abundance proteins; the removal of the higher abundance proteins, or fractionation of the sample to reduce complexity. Depletion appears to be the most common method of reducing the effect of high abundance proteins with fractionation sometimes used as a secondary step. Fractionation can either occur in the form of a gel-based methods, such as 1- or 2-D–SDS PAGE, or through use of liquid chromatography (Faca *et al.*, 2007).

Depletion has previously been conducted using dye-affinity (Ahmed *et al.*, 2003) and immuno-affinity (Cho *et al.*, 2005) methods. In the former study, a dye-based depletion method followed by 2-D-gel fractionation was used. Dyes such as Cibacron Blue used in the Affi-Gel Blue system have a high affinity for serum albumin and are hypothesised to bind via ionic interactions to a dinucleotide-binding or similar domain, enabling removal of the protein from complex biological samples (Leatherbarrow & Dean, 1980). This method is not entirely specific for serum albumin, but can be used to remove one of the most more highly abundant proteins from serum or plasma samples. The resulting lower-abundance fraction contained approximately 96 - 99 % less total protein, with a corresponding 86 - 126 % change in the number of protein spots identified, compared to untreated serum.

More recently, antibody-based depletion methods have been developed and display a greater specificity for the target proteins. A comparison of the dye- and immuno-affinity methods confirmed that a multiaffinity removal column using polyclonal antibodies to the six most abundant proteins in plasma to be the most efficient method

for depletion (Echan *et al.*, 2005). Accordingly, a Multiple Affinity Removal System (MARS) column supplied by Agilent was used in the present study. Echan and colleagues also stress the need to reduce non-specific loss of proteins, particularly those bound to the highly abundant proteins that are removed. It was therefore necessary to analyse the protein content of both depleted and non-depleted dermal dialysate samples.

4.1.2 Aims

The aim of the research presented in this chapter was to use proteomic analysis to identify the proteins contained in dermal dialysate from injured skin. This research was not strictly hypothesis-driven, however it had the potential to generate hypotheses once the types of proteins present in such samples had been identified.

Specific objectives were as follows:

- To determine whether proteomics technologies were appropriate for the identifying novel proteins within dermal dialysate.
- To determine the effect of depletion of specific highly abundant proteins on the detection of less abundant components.
- To place the identified proteins in the context of the response to injury through comparison with reports of injury research in both skin and other tissues.

4.2 Materials and Methods

4.2.1 Collection of dermal dialysate for proteome profiling

Dermal dialysate was collected as described in Section 2.2.2, using probes produced as described in Section 2.2.1. Dialysate for the non-depleted analysis was collected from one healthy male volunteer (aged 34 years) and for the depletion study, from two healthy male volunteers (mean age = 32.5 ± 6 years). Briefly, four probes were inserted into the dermis of the non-dominant volar forearm, no less than 7 cm from the fold of the wrist, as shown in Figure 2.3. Following insertion, probes were perfused with Ringer's saline solution for 30 minutes to enable the initial insertion trauma to settle. This settling period was added to reduce the amount of albumin and haemoglobin, known to be higher within the first 5 minutes after insertion (Clough, 2005). The purpose of these profiling experiments was to determine the protein content of dermal dialysate samples, including proteins that may serve as markers of the injury response. Due to the predicted >70 % loss off total protein following depletion of highly abundant components, a larger volume of dialysate was required to determine the protein content of depleted dialysate. The timing of the study is illustrated in Figure 4.1.

Figure 4.1: **Dialysate collection protocol for proteomic profiling of depleted dialysate.** Shaded boxes indicate the collection periods. Dialysate for the non-depleted sample was collected only during the first collection period, while the depleted sample was collected from both.

At the end of each one-hour collection period, samples were flash-frozen in liquid

nitrogen and stored on ice until they could be transferred to -80°C, on completion of the experiment. Protease inhibitors were not used in this experiment as they contain protein components that may influence the proteome obtained.

4.2.2 Preparation of dermal dialysate and estimation of protein concentration

For the depletion experiment, dialysate samples were thawed on ice and pooled to give a total 1.8 ml. This was concentrated to 250 μl using a 5 kDa MWCO spin concentrator and enabled a reduction in the salt content of the sample. Following this, the protein concentration of the concentrated dialysate was estimated by BCA assay (Section 2.3). The concentrated sample was taken for depletion, described in the next section. Dialysate for the initial proteome analysis without depletion was thawed on ice, but sample concentration prior to separation by 1-D SDS PAGE was not required.

4.2.3 Depletion of the six most abundant proteins in plasma

Depletion was conducted as described in Section 2.5.2. This generated a low abundance fraction containing the proteins that did not bind to the column, and a high abundance fraction containing those proteins that bound to the column and that were eluted once the low abundance fraction had been collected. The protein content was estimated for the low abundance fraction. However, the protein concentration of the high abundance fraction could not be determined due to the interference of urea in the elution buffer. The two fractions were concentrated by lyophilisation to 50 μl, 30 μl (approximately 95 μg total protein in the low abundance fraction) was taken from each for separation by 1-D SDS PAGE.

4.2.4 Protein separation by 1-D SDS PAGE

The non-depleted dialysate and concentrated high and low abundance dialysate fractions (30 μl) were prepared for SDS PAGE by heating at 70°C for 10 minutes in

25 % sample buffer and 1 % sample reducing agent. 1-D SDS PAGE was conducted as described in Section 2.5.3, following the protocol for staining with colloidal coomassie.

4.2.5 Shotgun proteomics analysis

For both the non-depleted and low abundance depleted samples, the gel lanes of interest were excised and cut into approximately 20 even slices. Protein digestion and mass spectrometry were conducted as described in Section 2.5.

4.2.6 Characterisation of identified proteins using the AmiGO database classification

The genInfo (gi) number for each protein in turn was cross-referenced using the Protein Identifier Cross-Reference service (PICR) (http://www.ebi.ac.uk/Tools/picr/search.do) to determine the Uniprot ID. Input parameters were limited to *Homo sapiens* and returning only active mappings. The databases used were SwissProt and TrEMBL. In cases where the gi number produced no results, accession numbers were obtained from the NCBI protein database (http://www.ncbi.nlm.nih.gov/sites/entrez?db=protein) and this number used instead. This Uniprot ID was then used to search the Gene Ontology (GO) database, found at http://amigo.geneontology.org/cgi-bin/amigo/go.cgi. Cellular component and biological process terms were collated and terms at Tree Level Three were determined. Where a protein gave more than one third-level term, all were collected and all groups reported. Specific functions in the response to injury, focusing on mechanical injury, were determined through literature searches for the protein name and "injury" or "wound healing", using PubMed (http://www.ncbi.nlm.nih.gov/PubMed/). Where more than 200 results were found, the search was limited further by specifying "human" and then "skin".

4.3 Results

4.3.1 Proteome analysis of dermal dialysate

The total amount of protein in the non-depleted dialysate was estimated at 1.9 mg/ml by BCA assay. Figure 4.2 shows the 1-D SDS PAGE profile of the separated dialysate proteins.

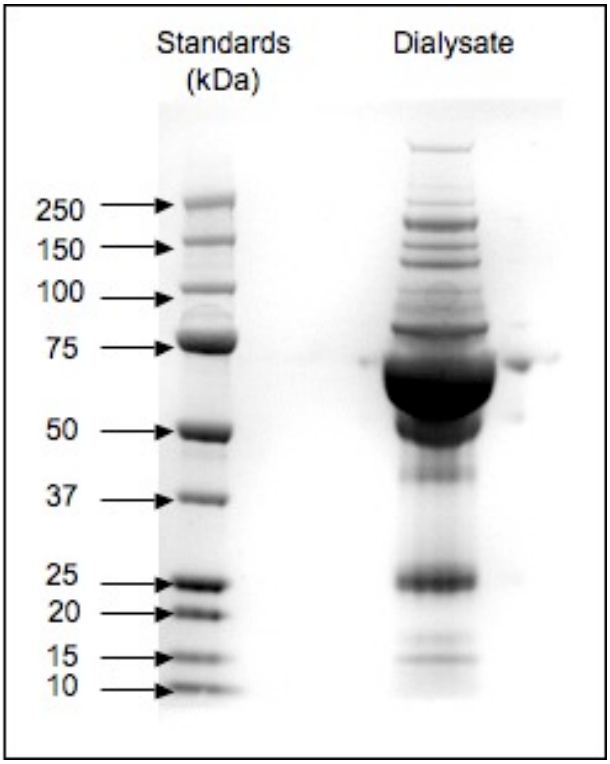

Figure 4.2: **One-dimensional SDS PAGE of dermal dialysate.** The figure shows the profile of proteins contained in 30 μl dialysate, collected 30 – 90 minutes after injury, from a single volunteer.

Several distinct bands were detected on the gel, although the profile is dominated by a large smear at $\sim$ 50-75 kDa, most likely corresponding to human serum albumin. The remainder of the track contains clearly distinguished bands ranging from $\sim$ 15 kDa to $>$ 250 kDa. Six proteins were unambiguously identified within the dialysate and are listed in Table 4.1. Full information, including the specific peptides identified,

is provided in Appendix One.

Table 4.1: **Proteins identified in non-depleted dermal dialysate collected 30 – 90 minutes after injury**

gi	**Uniprot ID**	**Protein Name**	**Mass (Da)**	**pI**	**Coverage (%)**	**Peptides**
4502027	P02768	Albumin	71317	5.92	39.1	21
66932947	P01023	α-2-Macroglobulin	164614	6.00	5.9	6
4557485	P00450	Ceruloplasmin	122983	5.44	2.3	2
4557385	P01024	Complement Component 3	188585	6.02	6.0	7
11321561	P02790	Hemopexin	52385	6.55	14.5	4
4557871	P02787	Transferrin	79280	6.81	26.2	11

The proteins identified fell within a mass range of 52 - 189 kDa, showing that relatively large proteins could be recovered by microdialysis at high enough concentrations to enable analysis by proteomic technologies. No proteins corresponding to the extremes of the mass range observed in the gel were identified. The most abundant protein identified was human serum albumin, with 21 different peptides identified over 87 scans and a coverage of 39.1 % of the total protein sequence. Transferrin was the second most abundant protein, with 11 peptides matched to give a 26.2 % coverage. Ceruloplasmin was the least abundant in the sample, with two peptides matched and a 2.3 % coverage of the whole protein. Figure 4.3 shows the cellular component, that is, the physical structure or compartment, with which each protein is associated.

As expected, all six of the proteins were associated with the extracellular region and are known to be highly abundant in plasma. Three proteins were also associated with intracellular components. The biological processes performed by the dialysate proteins are shown in Figure 4.4. Inexplicably, one protein, transferrin, did not have

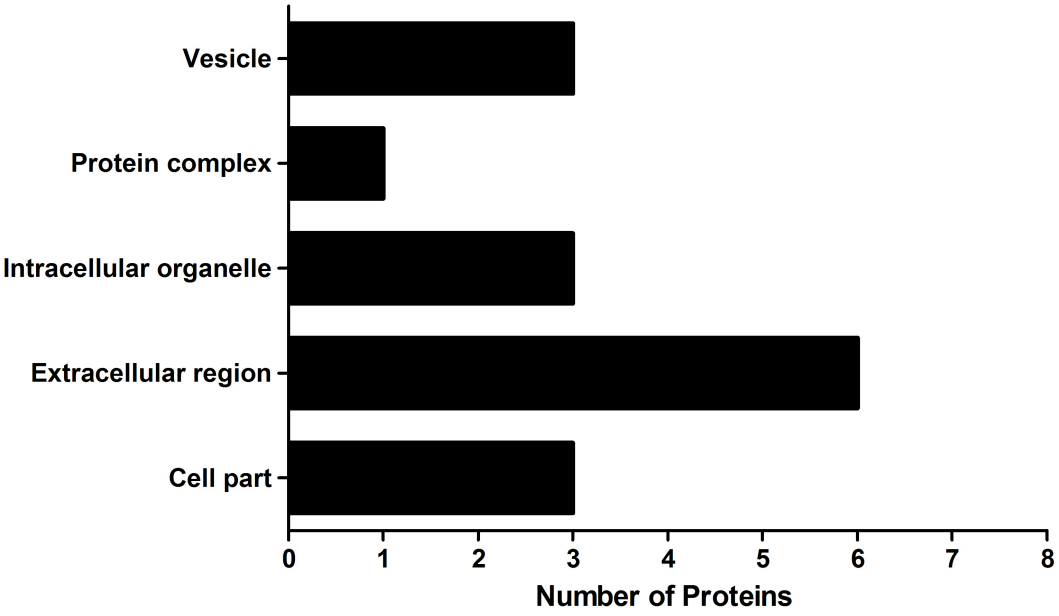

Figure 4.3: **Cellular component of the proteins in non-depleted dermal dialysate.** The bar graph shows a summary of the different cellular components from which the proteins identified in the non-depleted dialysate sample (collected 30 – 90 minutes after injury from a single volunteer) are associated. Each protein may be active within more than one component, in which case, all associated components were included. Components correspond to Gene Ontology tree level 3 terms and are grouped to avoid repetition of very similar terms, e.g. membrane-bound organelle and intracellular organelle.

any functional terms associated with its human form. Where a protein had more than one association, each category was included.

The reported generalised functions of the identified proteins include cellular communication, coagulation, immune response, and the responses to stimulus, to stress and cell death, indicating a link to the processes that occur in response to injury. Four classes of biological processes were associated with three or more proteins, including two terms for general regulation and two in the response to stress or an external stimulus. The remaining terms were associated with only one or two different proteins each.

While there were no associated terms for human transferrin, the entry for rat transferrin includes terms such as involvement in acute phase response and homeostasis. It is also known to be involved in the injury response.

4.3.2 Depletion of highly abundant plasma proteins to increase protein detection in proteomic profiling of dermal dialysate

The protein concentration in the concentrated dialysate was estimated to be 4.7 mg/ml by BCA assay, equivalent to 1.7 mg as a starting amount. The concentration of the low abundance fraction was estimated to be 160 μg/ml, giving a total of $\sim$250 μg for SDS PAGE. Figure 4.5 shows the 1-D gel profiles of the low and high abundance fractions of dialysate obtained after depletion of the six most abundant proteins in plasma; albumin, anti-trypsin, haptoglobin, IgA, IgG and transferrin.

There was a significant difference in profile between the high and low abundance fractions, with the large smear observed in the non-depleted sample (Figure 4.2) only present in the high abundance fraction. In place of this smear, the low abundance fraction contained discrete bands, showing that, as expected, the high abundance proteins were indeed masking other proteins. This was confirmed by the identification of a total of 29 proteins in the depleted sample (Table 4.2), a 4.8-fold increase on the number identified in the non-depleted sample. Full details, including peptide sequence

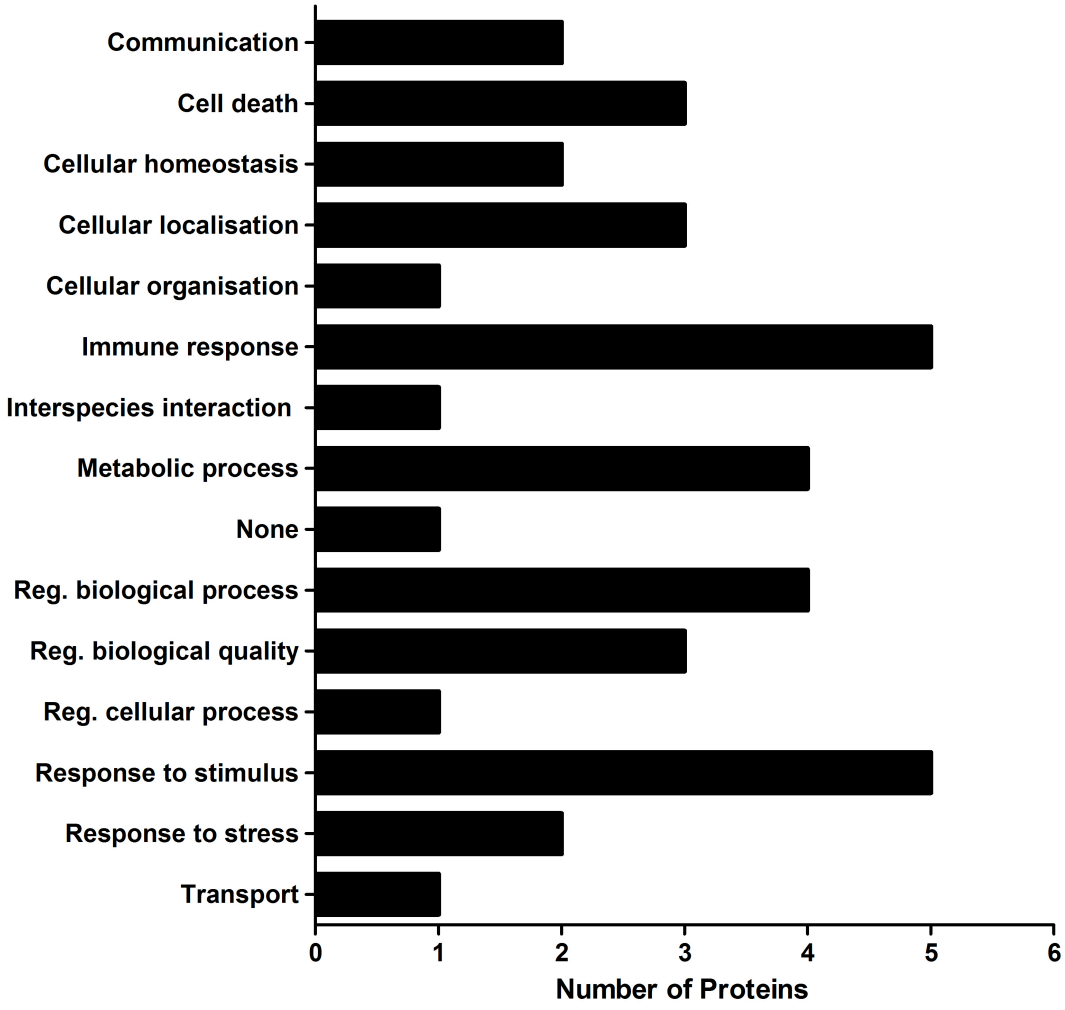

Figure 4.4: **Biological processes performed by the proteins in dermal dialysate.** The bar graph shows the different biological processes for the proteins identified in non-depleted dialysate (collected 30 – 90 minutes after injury from a single volunteer), according to the Gene Ontology classification. Processes correspond to level 3 terms within the Gene Ontology classification, with similar terms e.g. regulation of the response to stimulus and response to external stimulus grouped appropriately. Regulation is abbreviated to "Reg." for aesthetic purposes.

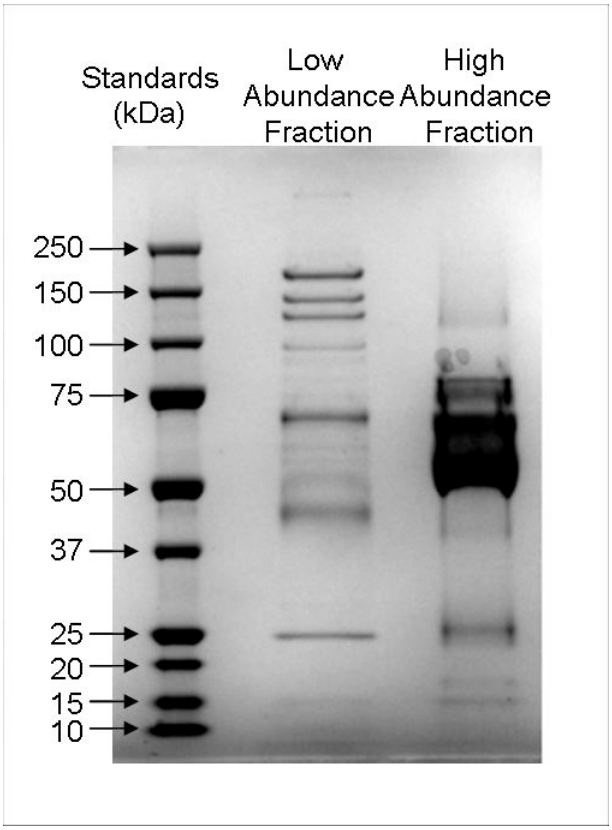

Figure 4.5: **One-dimensional SDS PAGE of Depleted Dialysate.** Gel image showing the two fractions obtained from depletion of dialysate, collected 30 – 150 minutes after injury and pooled from 2 volunteers. Lane 1 shows pre-stained standards, lane 3 shows the low abundance fraction (unbound proteins) and lane 5 shows the high abundance protein fraction (albumin, anti-trypsin, haptoglobin, IgA, IgG and transferrin).

information is provided in Appendix Two.

Of these 29 proteins, four were previously identified in the non-depleted dialysate; α-2-Macroglobulin, Ceruloplasmin, Complement Component 3 and Hemopexin. All protein identifications were made on the basis of two or more different peptides and only four proteins had less than 10 % protein coverage. In this sample, the mass range of identified proteins was 16 - 189 kDa, a greater range than non-depleted sample. A large proportion of the proteins (46 %) were within the 50 - 75 kDa range previously dominated by the highly abundant proteins. The pI range was 4.93 - 8.34, a similar range to that observed for proteins in the non-depleted sample.

The associated cellular components of each of the proteins identified in the depleted sample were determined using the same Gene Ontology database classifications as for the non-depleted sample and are shown in Figure 4.6.

As expected, the majority of the proteins identified (62 %) were active within the extracellular region. An identical proportion had intracellular activities, including some exclusively, such as the keratins. Five proteins had no cellular component associated, although the two of those are known to act within the intracellular component and the remainder have been identified in plasma.

The biological processes performed by the 29 proteins identified in the depleted dialysate sample, according to the gene ontology classifications, are shown in Figure 4.7.

Unsurprisingly, a greater variety of biological processes were represented by the proteins identified in the depleted sample compared to the non-depleted sample. All those terms associated with proteins identified in the non-depleted sample were represented in the depleted sample, along with 12 more. Processes potentially key to the injury response that were included in this second, depleted sample include cell adhesion, proliferation, gene expression, secretion and tissue remodelling. The most common associated function categories were general regulation of biological processes and also of the response to stress and external stimuli, as for the non-depleted sample. Metabolic processes were also highly represented, with 10 proteins associated. Three proteins did not have any biological process terms of level 3 or higher associated with

Table 4.2: **Proteins identified in depleted dermal dialysate.**

gi	**Uniprot ID**	**Protein Name**	**Mass (Da)**	**pI**	**Coverage (%)**	**Peptides**
21071030	Q68CK0	α-1B-Glycoprotein	54790	5.56	29.5	9
4502067	P02760	α-1-Microglobulin	39888	5.95	15.9	4
66932947	P01023	α-2-Macroglobulin	164614	6.00	44.4	44
4557287	P01019	Angiotensinogen	53406	5.87	13.4	5
4757756	P07355	Annexin A2	38808	7.57	10.9	3
4557327	P02647	Apolipoprotein A-1	30759	5.56	47.9	17
4557321	P02749	Apolipoprotein H	39598	8.34	17.1	4
4504349	P68871	β-globin	16102	6.75	68.7	8
4502517	P00915	Carbonic Anhydrase 1	28909	6.59	23.0	4
4557485	P00450	Ceruloplasmin	122983	5.44	30.0	23
73858568	P05155	Component 1 inhibitor	55347	6.09	14.4	6
4557385	P01024	Complement Component 3	188585	6.02	19.1	7
67782358	P00751	Complement Factor B	86847	6.67	24.3	12
11321561	P02790	Hemopexin	52385	6.55	40.3	15
4504579	P05156	I Factor (complement)	68120	7.72	3.3	2
17318569	P04264	Keratin 1	66198	8.16	33.1	15
47132620	P35908	Keratin 2a	65678	8.07	13.5	8
17318574	P19013	Keratin 4	57649	6.25	4.3	2
4504919	P05787	Keratin 8	53671	5.52	5.0	2
55956899	P35527	Keratin 9	62255	5.14	21.8	11
9257232	P02763	Orosomucoid 1	23725	4.93	40.8	7
4505529	P19652	Orosomucoid 2	23873	5.03	32.8	7
4505881	P00747	Plasminogen	93247	7.04	10.0	5
4506355	P20742	Pregnancy zone protein	165215	5.97	7.4	7
50659080	P01011	SERPIN A3	47792	5.33	17.3	5
4502261	P01008	SERPIN C1	53025	6.32	27.6	12
39725934	P36955	SERPIN F1	46454	5.97	14.8	6
4507725	P02766	Transthyretin	15991	5.52	49	5
32483410	P02774	Vitamin D-binding protein	54480	5.32	38	15

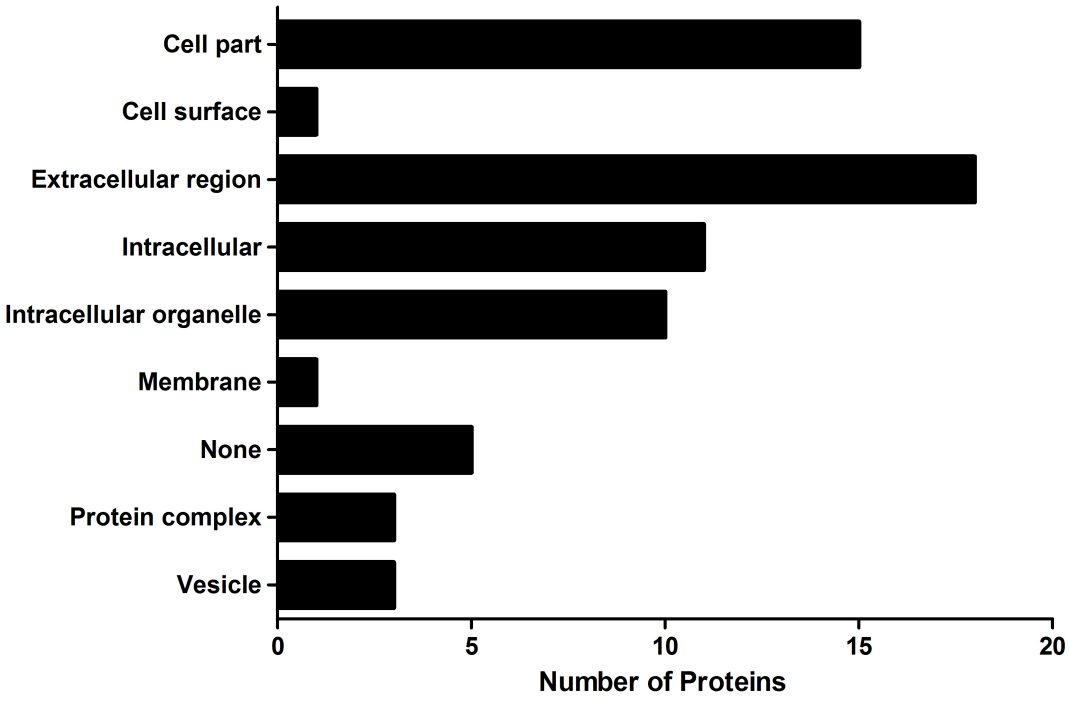

Figure 4.6: **Cellular origins of the proteins identified in depleted dialysate** Bar graph showing the different cellular components from which the proteins identified in the depleted dialysate sample (collected 30 – 120 minutes after injury and pooled from 2 volunteers) originate. Each protein may be derived from more than one component, in which case, all components were included. Components correspond to tree level 3 terms within the Gene Ontology classification.

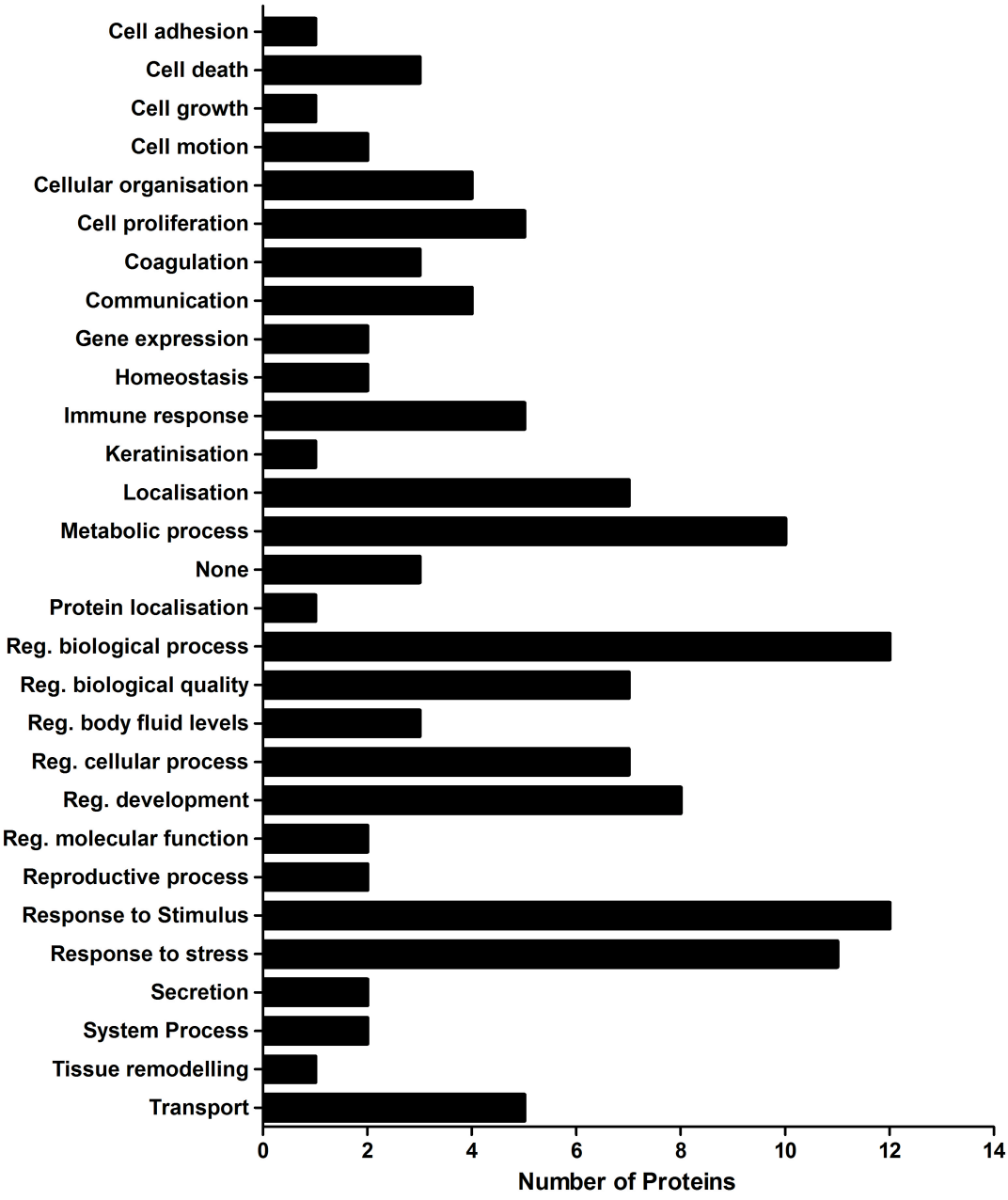

Figure 4.7: **Biological processes performed by the proteins identified in depleted dialysate.** Bar graph showing the different biological processes in which the proteins identified in dialysate (collected 30 – 150 minutes after injury from 2 volunteers) are involved, according to the Gene Ontology classification. Each protein may perform more than process, in which case, all level 3 process terms were included.

the human form; α-1B-glycoprotein, Annexin A2 and complement I factor. The function of α-1B-glycoprotein is unclear, but Annexin A2 and I factor are known to be involved in regulation of the plasmin and complement cascades respectively.

4.4 Discussion

The aims of the research presented in this chapter were to assess the suitability of the combination of microdialysis and proteomics for biomarker discovery, to catalogue the protein content of dermal dialysate from healthy human volunteers and to fit those proteins into the context of the early response to injury. Finally, any candidate proteins for further study were to be highlighted. The identification of proteins from non-depleted dialysate was severely impeded by the abundance of a few proteins. Therefore, the additional aim of investigating the effect of depletion on protein identification was also addressed. Removal of these highly abundant proteins was very efficient, with none of the six proteins identified in the depleted sample. This depletion dramatically increased the total number of proteins identified in the dermal dialysate samples. A total of 31 proteins were identified in the two experiments, from both the intra- and extracellular compartments and involved in a variety of biological processes relevant to the response to injury.

Although it would be possible to review the relevance of the identified proteins by intensive reading of the scientific literature, this becomes difficult when more than a few are under consideration. Furthermore, it is easy to miss trends when using this approach. For this reason, further analysis exploited the Gene Ontology, in which keywords from a controlled scientific vocabulary were used to cluster protein features, including their associated functional categories. The GO approach is useful for spotting broad trends and circumvents the time-consuming literature searches for obtaining insights into protein function. However, results must be interpreted with care, as the system remains rather subjective and the vocabulary is not yet complete.

4.4.1 The effect of depletion on protein identification

None of the six proteins specifically removed by the antibody-based depletion column were detected, showing that this is a very effective method of depletion. Interestingly, several keratins have been identified which may have been derived from the skin itself, demonstrating the advantages of a localised sampling method.

Depletion of the six most abundant plasma proteins from dermal dialysate increased the number of proteins identified from 6 to 31, a 5–fold increase. This 5–fold increase in the number of proteins identified is double that observed following depletion of serum by Ahmed *et al.* (2003) using dye-based methods and three times the increase in protein identifications of 1.6-fold observed by Björhall, Miliotis and Davidsson (2005), using a MARS column. This indicates that the highly abundant proteins were impeding identification of less abundant components in the non-depleted sample.

The starting amount of 1.7 mg total protein was sufficient for proteomic analysis following the removal of the six most abundant proteins in plasma. However, the total protein concentrations of 0.5 – 1 mg/ml observed in the later 30 minute collections in the previous chapter (Chapter 3) would not be enough for this analysis. Therefore a different method would be required to assess changes in protein content between these timed collections.

4.4.2 Involvement of identified proteins in the response to injury

The GO associations obtained from the identified proteins were consistent with several of these proteins being part of the acute response to injury. The biological process terms associated with the identified proteins give some initial clues as to the functions of these proteins. The most commonly associated terms were those involved in regulation of biological processes and the responses to stress and external stimuli. Also relevant were the associations with the immune response, coagulation, homeostasis and tissue remodelling, required to maintain or restore the integrity of the tissue. Proteins associated with these GO terms included α-1-microglobulin, apoliprotein H, ceruloplasmin, complement factors, hemopexin, keratin 1 and plasminogen. In terms of cellular component, proteins were derived equally from both the intra- and extracellular compartments.

The detection of exclusively intracellular proteins is most likely to be a consequence of damage causing cells to release their contents, while the proteins derived from either

both or solely extracellular sources may be released or recruited as part of the response to injury. One example is annexin A2 which, intracellularly, is translocated from the cytoplasm to the cell membrane following mechanical injury and takes part in the activation of plasmin, leading to monocyte recruitment (Falcone *et al.*, 2001; Patchell *et al.*, 2007). Soluble, extracellular, annexin A2 in plasma causes macrophage activation and subsequent cytokine release (Swisher, Khatri & Feldman, 2007). It is possible that the exclusively intracellular proteins play a role in the injury response to injury, such as members of the keratin family which are known to be involved in repair later in the response (reviewed in DePianto & Coulombe, 2004).

Two proteins, angiotensin and keratin 2a, were associated with cell growth and proliferation processes, such as those that occur during repair. This is consistent with reports that angiotensin is involved in regulation of VEGF (Williams *et al.*, 1995). This indicates that it may be involved in regulation of the repair and replacement of the damaged vasculature. Angiotensinogen had the greatest number of biological process terms associated (44), so would be expected to perform further functions in the response to injury. Several forms of angiotensin exist, released from cleavage of angiotensinogen by neutrophil serine proteases and subsequent processing with angiotensin-converting enzyme (ACE) (Ramaha & Patson, 2002; Santos, Campagnole-Santos & Andrade, 2000). These proteins perform a range of functions, predominantly vasoactive effects, and have been reported to play an important role in wound healing through modulation of cell proliferation, differentiation and control of blood pressure and therefore tissue perfusion. The discovery of several of the necessary components of the renin-angiotensin system in cutaneous wounds suggests that angiotensin plays a vital part in the response to injury.

Many of the other proteins identified in the dermal dialysate samples have been associated with the response to injury. Table 4.3 summarises some of these roles, where functions have been reported in the literature.

Table 4.3: **Proteins identified in dermal dialysate and their function within the response to injury.**

Protein Name	**Function within the response to Injury**
α 1B-glycoprotein	None known
α-1-microglobulin/ bikunin precursor	Heme scavenger during inflammation, thought to reduce oxidative stress (Allhorn *et al.*, 2003).
α-2-macroglobulin	Down-regulates acute inflammation through binding of growth factors and cytokines with differential affinity depending on it's oxidation status (Wu *et al.*, 1998).
albumin	Increased at the injury site in response to IL-1α as part of the acute phase reaction, although this is more likely to be a result of infiltration of plasma to the damaged area (Perl *et al.*, 2003).
angiotensinogen	Increases the expression of plasminogen activator inhibitor-1 (PAI-1), an inhibitor of the conversion of plasminogen to plasmin (Vaughan, 2001). Also involved in regulation of VEGF, as has been reported for renal injury (Sataranatarajan *et al.*, 2008).
annexin A2	Recruitment to the cell surface is increased following mechanical injury (Patchell *et al.*, 2007) where it acts as a co-factor for plasminogen and tissue plasminogen activator (Ling *et al.*, 2004).
apolipoprotein A-I	May play an important role in regulating neutrophil function during the acute phase of inflammation (Blackburn *et al.*, 1991).
apolipoprotein H	Inhibitor of platelet-von Willebrand factor (vWF) interactions, preventing platelet agglutination (Hulstein *et al.*, 2007).

Protein Name	**Function within the response to Injury**
β-globin	None reported, although released iron from heme may result in oxidative stress (Balla *et al.*, 1993).
carbonic anhydrase I	None Known
ceruloplasmin	May regulate the stress-induced release of IL-1α (Mandinov *et al.*, 2003). Also functions to oxidise Fe^{2+} to Fe^{3+}, the form which can bind to transferrin (Patel *et al.*, 2002).
complement component 1 inhibitor	Regulates all three complement pathways and can inhibit endothelial cell-leukocyte adhesion (Cai & Davis, 2003).
complement component 3	Activation of the complement cascade requires cleavage of complement 3, a proinflammatory mediator responsible for enhancing vascular permeability among other functions (Sriramarao & DiScipio, 1998).
complement factor B	Catalytic component of the C3 convertase enzyme complex involved in activation of the alternative complement pathway (Le, Abbenante & Fairlie, 2007).
hemopexin	Synthesis is increased in response to increased IL-6 levels in injured peripheral nerves (Madore *et al.*, 1999; Camborieux *et al.*, 2000).
I factor	Inhibits the formation of the C3 convertase enzyme complex (Timár *et al.*, 2007).
keratin 1	Part of a multi-protein receptor complex that binds kininogen, leading to bradykinin activation, plasmin activation and subsequent vasodilation (Shariat-Madar, Mahdi & Schmaier, 2002).
keratin 2a	None Known
keratin 4	None Known

Protein Name	**Function within the response to Injury**
keratin 8	May act as a cell-surface receptor for plasminogen and tissue plasminogen activator (Kralovich *et al.*, 1998).
keratin 9	None Known
orosomucoid 1 & 2	Hypothesised to have a range of anti-inflammatory effects including maintenance of capillary integrity and inhibition of neutrophil migration, prostaglandin E_2 generation and platelet aggregation (Matsumoto *et al.*, 2007).
plasminogen	Plasma protease involved in controlled degradation of the extracellular matrix during the remodelling phase of wound repair (Shäfer *et al.*, 1994).
pregnancy zone protein	Functions as a proteinase inhibitor, including against proteins of the fibrinolytic system (Takada, Takada & Urano, 1994).
SERPIN A3 (α_1-antichymotrypsin)	Specifically inhibits superoxide formation by neutrophils and up-regulates IL-6 expression (Kilpatrick *et al.*, 1991).
SERPIN C1 (antithrombin)	Major anti-coagulant factor that regulates thrombin among other factors (Roemisch *et al.*, 2002) and may stimulate release of prostacyclin with the potential to inhibit release of reactive oxygen species and proteases from neutrophils (Okajima & Uchiba, 1998).
SERPIN F1 (pigment epithelium-derived factor)	Displays anti-angiogenic and anti-inflammatory functions including inhibition of macrophage proliferation (Zamiri *et al.*, 2006) and reduction of VEGF-induced vascular permeability and proinflammatory cytokines such as MCP-1, TNF-α and ICAM-1 (Zhang *et al.*, 2006).
Transferrin	Involved in iron ion homeostasis including its transport, reducing oxidative damage (Yeoh-Ellerton & Stacey, 2003).

Protein Name	**Function within the response to Injury**
transthyretin	None Known
vitamin D-binding protein	Responsible for actin clearance after injury, reducing the occurence of disseminated intravascular coagulation (Meier *et al.*, 2006).

The majority of the proteins identified in the dialysate samples have known roles in the response to injury. A significant proportion of the proteins identified are classed as "acute phase reactants", reflecting the considerable change in plasma concentration following the onset of inflammation. Albumin, transferrin and transthyretin are negative acute phase reactants, that is they are reduced in plasma concentration during inflammation. Alpha-1-antitrypsin, α-1-antichymotrypsin, α-2-macroglobulin, plasminogen, complement factors and ceruloplasmin are positive acute phase proteins and are thus increased during inflammation. Proteins such as α-2-macroglobulin, albumin, hemopexin and the orosomucoids are involved in regulation of, or are regulated by, cytokines. These proteins were associated with response to stimulus and to stress GO terms. They are known to be involved in the systemic response to injury and infection with their effects including the modulation of cell responses and mediator release (reviewed in Ceciliani, Giordano & Spagnolo, 2002; Suffredini *et al.*, 1999). Alpha-2-macroglobulin is one of the better characterised acute phase components and is known to function as an anti-protease and as a cytokine-binding protein (Borth, 1992; Borth & Luger, 1989).

A significant proportion of the proteins identified in the dermal dialysate samples are involved in the regulation of plasmin, a key protease in the breakdown phase of remodelling. These include plasminogen, the precursor to plasmin itself, along with keratins 1 and 8 hypothesised to be involved in a complex that forms the site of activation. This is in part regulated by plasmin activator inhibitor 1, in turn under the control of angiotensin. Annexin A2 is also part of a complex that facilitates activation of plasmin, as discussed previously.

Several of the identified proteins are reported to have roles in the detoxification

of heme released from infiltrating globin, such as the β-globin detected in this study. Ceruloplasmin oxidises iron from the form in which it is most commonly bound to hemoglobin in the absence of oxygen, to the form in which it can bind to transferrin, another protein identified here, to be removed (Osaki, Johnson & Frieden, 1966). This process is well documented, particularly in response to damage to the central nervous system (Patel *et al.*, 2002; Rathore *et al.*, 2008). Alpha-1-microglobulin also acts as a heme scavanger, further reducing potential iron-induced oxidant damage (Table 4.3).

The proteins identified in dialysate within this study are put into the context of the injury model in Figure 4.8, where functions in injury are known.

All proteins with known functions in the response to injury map onto the overview diagram, with only the iron-detoxification processes unrelated to markers previously given on the schematic. The identification of these proteins within dialysate after injury is consistent with the cytokine data from Chapter 3, however the protein data give a much clearer view of the processes involved and which pathways may be activated.

4.4.3 The suitability of combining microdialysis and shotgun proteomics technologies

This is the first report of the proteome of dermal dialysate and as such, it is not possible to compare these data to those of previous studies. The best comparison would be between proteomic studies of other skin samples, such as skin biopsies or suction blister experiments, or of microdialysis in other human tissues. Compared to proteomic studies of alternative skin samples, the number of proteins identified in dermal dialysate was very low; 31 compared to 401 in suction blister fluid (Kool *et al.*, 2007), although that study reported only 240 proteins in plasma samples analysed in parallel. This is one fifth of the identifications made in the human plasma proteome study (Anderson *et al.*, 2004), so both numbers may be an underestimate.

The relatively low number of protein identifications in the dialysate sample is most likely a consequence of the sampling technique. The proteome of cerebral microdialysate contained 27 proteins, including three different forms of both tubulin and

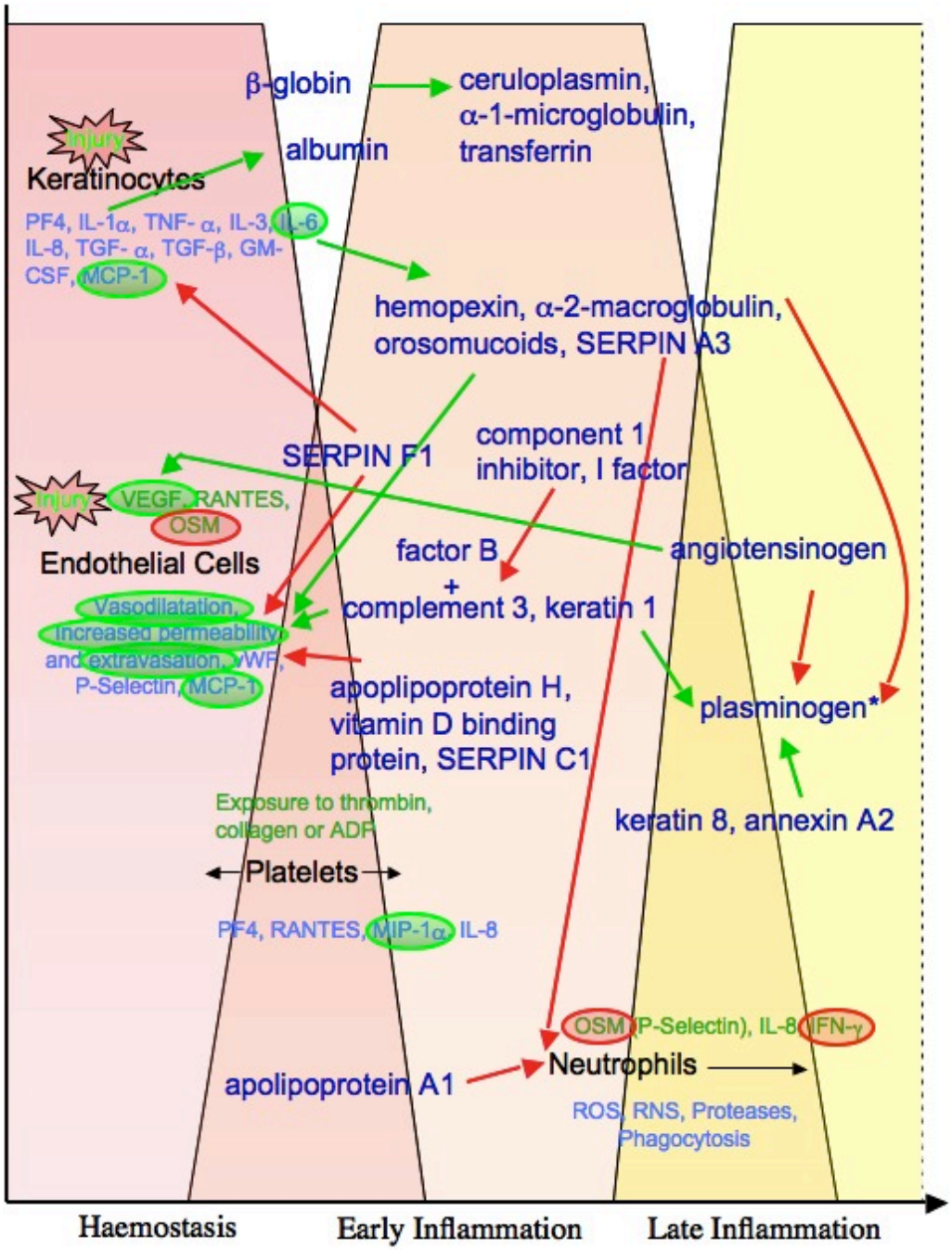

Figure 4.8: **Overview of the involvement of proteins identified in dialysate in the injury response.** Proteins identified within dialysate in this study are given in dark blue. Inhibitory interactions are shown by red arrows, activating interactions are shown with green arrows. Factors characterised in the previous chapter (Chapter 3) are shown circled, in green if detected and red if not. * Plasminogen is involved in stimulation of cytokine expression from macrophages and in control of the fibrinolytic system, along with pregnancy zone protein, not pictured.

haptoglobin proteins (Maurer *et al.*, 2003), slightly fewer than detected in dermal dialysate. The number may be limited by the method sampling, or of separation, as proteins were resolved on 2-D gels and only proteins detected by the presence of stained spots were removed for analysis, a problem from which the present study did not suffer. In addition, no depletion methods were employed to remove albumin. While this cerebral dialysate proteome shares many components with dermal dialysate (35 %, Table 4.4) that indicate a common response to probe insertion may occur, it is not representative of the skin.

Table 4.4: **Proteins common to both dermal and cerebral dialysate**

Protein Name	**Dermal Dialysate (Uniprot ID)**	**Cerebral Dialysate (Uniprot ID)**
α-1B-glycoprotein	Q68CK0	P04217
α-1-microglobulin	P02760	P02760
albumin	P02768	P02768
apolipoprotein A-1	P02647	P02647
β-globin	P68871	P02023
complement component 3	P01024	P01024
plasminogen	P00747	P00747
serpin A3	P01011	P01011
transthyretin	P02766	P02766
transferrin	P02787	P02787
vitamin D binding protein	P02774	P02774

No proteins common to the human skin proteome study of Kool *et al.* (2007) were found, presumably due to only an incomplete list being reported. Of the few proteins

reported as identified in Macdonald *et al.* (2006), four are shared with dermal dialysate; apolipoprotein A1, ceruloplasmin, complement factor B and vitamin D binding protein. It is likely that there are many more common proteins, but without access to the full list of identifications, this cannot be confirmed.

Kool *et al.* (2007) used a different method of categorising proteins to that used in the present study, although they still exploited the Gene Ontology terminology. The Gene Ontology strategy, reviewed recently by Dimmer *et al.* (2008), was established in 1998 (Ashburner *et al.*, 2000) to provide a standardised classification system for gene and protein annotation. It enables clearer comparisons between different datasets and experiments conducted in unrelated laboratories. AmiGO is one of the primary search and browse tools provided by The Gene Ontology Consortium and is updated frequently, thus representing the most straight-forward method for determining GO associations for the dialysate dataset. Tools such as DAVID used by Kool *et al.* enable more automated annotation. However, these are primarily intended for gene expression or microrray analysis and are more appropriate for large datasets for which manual searching is not practical. The advantage of manual searching being the researcher's direct input, allowing associations to be made that may not be made by a computer. The majority of GO terms associated with the proteins identified in dialysate were relevant to the injury response and the method by which it was created, showing this to be an appropriate classification system.

Several skin-specific proteins were identified in this study, namely keratin variants, which suggest that this is a suitable method for analysis of the local tissue environment. However, care should be taken when confirming identification of keratins in proteomics, particularly in studies of the skin. It is not possible to determine whether keratins are derived from the sample or from contamination during processing and depletion will only increase the detection of contaminants. Precautions were taken to minimise contamination, e.g. the use of filtered air in the Centre for Proteome Research (CPR). Furthermore, keratin contamination within the CPR has not been a problem previously and the direct involvement of two of the six identified keratins in the response to injury suggests that these are likely to be genuine identifications from the dialysate sample

itself. Proteome profiling of murine skin revealed several different keratins (Huang *et al.*, 2003), while profiling of other murine organs did not identify any (Cutillas & Vanhaesebroeck, 2007). This was rather surprising as keratins are within the top 15 protein families identified in proteomic profiling experiments, with keratin 8 the tenth most commonly identified protein in differential expression experiments (Petrak *et al.*, 2008). Apolipoprotein A1 is frequently identified in rodent experiments, but is not one of the top 10 proteins identified in human profiling studies. Annexins are also very common, highlighting the fact that protein identifications should be examined in context before additional or novel functions are attributed.

While the combination of microdialysis and proteomics appears to be compatible, the proteins identified represent only a small fraction of the total protein complement of the response to injury. This was to be expected, given the experimental conditions, such as solubility and diffusion rate, imposed by the microdialysis sampling method. Depletion of the most highly abundant proteins significantly increased the number of less abundant proteins identified but the dynamic range of concentrations remains too large for comprehensive characterisation. For example, no cytokines were detected in the proteome study, despite their measurement in samples from equivalent time points after injury. This is likely to be a result of sub-optimal sensitivity in terms of the mass spectrometer and its analysis capacity for complex samples, although this will improve as the technology becomes more sophisticated and more mature.

4.4.4 Summary

This is the first report combining dermal microdialysis and proteomics with depletion of highly abundant proteins. Depletion enabled a 5–fold increase in the number of proteins identified in dermal dialysate. A starting concentration of 1.7 mg, obtained from 1.8 ml dialysate, was sufficient for this analysis. However, this is a very large volume and is not practical for the higher resolution analysis required in investigating 30-minute timed samples as 12 probes would be required to collect that amount within the specified time period. For temporal analysis of protein content, a different method with lower volume requirements is needed.

The majority of proteins identified within dermal dialysate appear to be abundant plasma proteins. However, this does not mean that they cannot play an important role in the early response to injury. Rather than investigating the changes in concentration of these proteins, it may be of greater benefit to characterise reversible post-translational modifications, such as protein phosphorylation. To date, however, such studies have been restricted by technological limitations which need to be overcome if comprehensive information on this aspect of the response to tissue injury is to be obtained.

Chapter 5

Optimisation of phosphopeptide capture methods for analysis of protein phosphorylation in dermal dialysates

5.1 Introduction

The importance of the reversible phosphorylation of proteins in the regulation of many intracellular processes is well known and well studied. However, its role in regulation of extracellular processes has received considerably less attention. The discovery of many extracellular protein kinases, e.g. in plasma and from cells such as platelets has lead to an understanding that proteins can be modified within the tissue space, thereby potentially altering their function after release, as discussed in Chapter 1. Although no kinases or phosphatases were identified in dermal dialysate (Chapter 4), more than one-half of those proteins identified have been reported to contain phosphorylation sites, as discussed in the following section.

5.1.1 Identification of proteins that may undergo post-translational modification due to regulation or response to injury

Sixteen of the proteins identified in dermal dialysate samples (Chapter 4) have reported phosphorylation sites (Table 5.1). Some of these have known regulatory functions related to responses to injury.

Many phosphorylation sites within these proteins have been identified by global profiling studies. While the functions of the majority of these phosphorylation events remain unknown, some have been assigned a role in specific cellular processes. For example, complement component 3 is phosphorylated following the local decrease in pH that occurs after an injury (Forsberg *et al.*, 1989). This phosphorylation prevents the inhibitory cleavage of C3 by complement factors H and I (Ekdahl & Nilsson, 1995) indicating that the complement cascade is actively maintained.

Differential phosphorylation of serpin f1 (pigment epithelium derived factor), involved in VEGF regulation, switches the protein between its anti-angiogenic and neurotrophic roles. Phosphorylation on the S24 and S114 residues causes a conformational change that prevents phosphorylation of S227 and preserves the anti-angiogenic, anti-neurotrophic form. Phosphorylation of all three of these sites yields a stronger anti-angiogenic form (Maik-Rachline & Seger, 2006).

Annexin A2 is also of interest as it has been directly implicated in the response to injury. Phosphorylation of S25 is involved in regulation of the cell cycle, molecular associations and in the intracellular location of the protein.

5.1.2 Methods for investigating the phosphoproteome

There are several methods for analysing phosphoproteins, ranging from radio-isotope labelling of metabolically active cells and western blotting with phospho-specific antibodies, to the use of immobilised metal affinity (IMAC) and other chromatographic techniques to isolate phosphoproteins and phosphopeptides. Most of these methods employ mass spectrometry to identify phosphoproteins of interest. For recent reviews

Table 5.1: **Published phosphorylation sites for proteins identified in the dermal dialysate samples**

Protein	**Reported* Phosphorylation Sites**
α-1-microglobulin	T198
α-2-macroglobulin	Y497, Y695, Y708
albumin	S82, Y108, Y162, Y164, Y365, Y377, Y394
annexin A2	T2, S11, S17, T18, Y23, S25, Y29, Y74, Y108, T122, S126, Y187, Y198, Y234, Y237, Y274, Y315, Y316, Y317
apolipoprotein A1	S201‡
β-globin	Y35, S44, Y130, Y145
ceruloplasmin	S204, T674, Y784, Y787
complement 3	Y489, S742
keratin 1	S20, Y374, S501, T506, Y565
keratin 4	Y329, Y344
keratin 8	S9, S21, S22, S24, Y25, S27, S34, S35, S36, S37, S39, S43, S74, Y204, S240, S243, S251, S253, S258, Y267, S274, Y282, S330, S400, S410, S424, Y427, T431, S432, S436, Y437, S438, S441, S442, S445, S451, S475, S477, S478
keratin 9	Y485
plasminogen	S597
pregnancy zone protein	Y700, Y701
SERPIN f1	S24, S114, T226, S227
transferrin	Y536, Y666

* As listed at www.phosphosite.org, October 2008, unless otherwise stated. ‡ Beg *et al.*, (1989). S = serine, T = threonine and Y = tyrosine phosphorylated.

on current methods for analysis of the phosphoproteome, see Delom & Chevet, (2006), Paradela & Albar, (2008), Raggiaschi, Gotta & Terstappen, (2005) and Schmidt, Schweikart & Andersson, (2006). Of particular interest in these reviews are the more recent methods in which phosphopeptides are linked to molecules that can be readily isolated from a sample solution. These methods impart increased specificity due to the direct interactions with the phosphate group. Two key strategies in this respect are the use of biotinylation and phosphoramidate chemistry. The biotinylation technique replaces phosphate groups with a biotin tag, thereby allowing phospho-serine, -tyrosine or -threonine-containing peptides to be isolated on an immobilised avidin support (Oda, Nagasu & Chait, 2001). However, there are a high proportion of side-reactions as cysteine residues can also bind the biotin tag if efficient blocking steps are not carried out. Furthermore, the removal of the phosphate groups that occurs during the process makes the identification of the site of phosphorylation difficult to confirm. The presence of the biotin tag indicates the site of modification, but it is difficult to determine whether the site is a true phosphorylation site or uncovered due to non-specific reactions with the biotin tag.

Of direct relevance to this study is the phosphoramidate chemistry scheme developed by Tao *et al.*, (2005). This method involves covalent binding of phosphopeptides to the amine groups of a synthetic polyamine dendrimer via the formation of phosphoramidate bonds and is discussed in greater detail in Section 5.1.4.

To investigate changes in the phosphoproteome of the interstitium as sampled by microdialysis, the method of analysis must obviously be sufficiently sensitive to recognise the fraction of proteins that are phosphorylated within it. Radio-isotope labelling is not applicable to dialysate, as the sample is not metabolically active. Gel-based methods, such as a western blotting in conjugation with phospho-specific antibodies, are also unsuitable. While sensitive enough to detect femtomolar levels of phosphorylated proteins, the antibodies have varying specificity, as they are raised against specific epitopes and may not recognise phosphorylation at sites where the amino acid sequence differs. Antibodies against the rarest form of phosphorylation, phospho-tyrosine, are considered most effective. The more common phospho-serine and phospho-threonine

forms are less immunogenic, so efficient antibodies are harder to generate (Kauffman, Bailey & Fussenegger, 2001). In addition to the limitations posed by the antibodies, western blotting itself may not be ideally suited to comprehensive phosphoproteome analysis. Even in two dimensions, it is difficult to resolve every protein clearly in a gel and, as noted in the previous chapter, highly abundant proteins frequently obscure less abundant components. Moreover, proteins transferred to a membrane will be limited to those within the pI range of the 2-D gel and not all proteins will be transferred equally during blotting, preventing accurate qualitative analysis. Finally, removal of the antibodies requires harsh chemical conditions that may disrupt phosphorylation, complicating later analyses to identify the phosphoprotein and the phosphorylated residue(s). An alternative approach would be to stain the gel directly with a reversible phospho-specific dye. While this has improved sensitivity and specificity, it suffers similar limitations to western blotting with regards to protein separation and is biased towards multiply phosphorylated and highly abundant proteins. This method could prove useful as a simple "first look" to determine whether a sample contains phosphorylated proteins, in conjunction with another method with which to identify those proteins. It would also provide a good comparison with the proteome data from Chapter 4, as identical separation techniques, that is 1-D SDS PAGE, would be used.

The low abundance of the phosphorylated form of many proteins hinders their identification within complex samples. Furthermore, the acidic nature of the phosphate group means that phosphorylated proteins have a higher affinity for certain metal and plastic surfaces and may be lost by adsorption. This, along with low ionisation efficiency, makes mass spectrometric analysis of phosphorylated proteins and peptides difficult. Immunoprecipitation with anti-phosphoprotein antibodies has been used to enrich for phosphorylated proteins in a small number of studies (Gronborg *et al.*, 2002). However, as discussed above, the limitations of epitope recognition make this an unsuitable technique. Methods taking advantage of the affinity for metals have proven more successful in reducing sample complexity.

Affinity chromatography methods have been extensively employed and are currently the most popular methods of enriching for phosphorylated proteins. These

methods take advantage of the shift in pI resulting from the addition of the acidic phosphate group as it increases protein affinity for positively charged moieties. Schmidt, Schweikart & Andersson, (2006) recently published a comprehensive review of chromatographic methods in phosphoproteome analysis, in which the principle and examples were discussed. Andersson & Porath, (1986) first observed that phosphopeptides displayed an affinity for metal ions, particularly Fe(III). Using immobilised Fe^{3+} ions on a chromatographic support, they were able to fractionate hen egg-derived ovalbumin into three differentially phosphorylated fractions by elution with solvents at varying pH and phosphate concentrations. While non-specific binding and the narrow pH range of operation still limit the IMAC technique, improvements are published on a regular basis. For example, dioxides of both titanium and zirconium have recently emerged as better alternatives.

5.1.3 Titanium dioxide affinity chromatography for capture of phosphopeptides

The use of TiO_2 for isolation of phosphopeptides from complex mixtures was first reported in 2004 (Pinkse *et al.*, 2004). Two main formats have been used, namely chromatography columns and coated magnetic beads. The chromatography column format is advantageous in that it enables online MS analysis. However, the initial set-up is complex, requiring specialist equipment, and the experiment itself is time-consuming in terms of machine use. In contrast, TiO_2-coated magnetic beads are commercially available and allow phosphopeptide isolation within 30 minutes or less. The captured sample can then be processed as appropriate for analysis or further preparation.

This method is more specific than IMAC, reportedly giving a phosphopeptide recovery of >90 % (Klemm *et al.*, 2006) compared to 70 – 90 % for IMAC (Dubrovska & Souchelnytskyi, 2005). Specificity has been increased to 100 % in low-complexity samples, through the addition of 200 mg/ml dihydroxybenzoic acid (DHBA) to peptide samples, prior to separation (Larsen *et al.*, 2005). This level of specificity is unlikely in more complex samples and the high affinity of TiO_2 for phosphopeptides may prove a

problem when eluting multiply phosphorylated peptides, accounting for the low level of their detection in other studies (Thingholm *et al.*, 2008).

5.1.4 Dendrimer-conjugation chemistry

A new method for phosphopeptide capture was recently reported by Tao *et al.* (2005). The dendrimer conjugation chemistry method involves the covalent and reversible binding of the phosphate group to the amine group on a synthetic branched compound (dendrimer) that functions as a soluble polymer support. Peptide samples containing both phosphorylated and non-phosphorylated peptides are mixed with the dendrimers, in the presence of imidazole and carbodiimide catalysts at pH 5.5. Under these conditions, the dendrimers conjugate with the phosphate groups on phosphopeptides in the sample. Non-bound peptides can then be removed in a simple washing step. Phosphorylated peptides are subsequently removed from the dendrimer by hydrolysis and can be analysed by mass spectrometry to identify the parent protein and the site of phosphorylation. Figure 5.1 shows the structure of the polyamidoamine (PAMAM) dendrimer molecule used for phosphopeptide capture in the present study.

The dendrimer molecule is highly branched, with the long 12-carbon chains making the separation between amine groups great enough to enable more than one phosphopeptide to bind per dendrimer. The many amine groups exposed are available to bind covalently to the phosphate groups of serine, threonine or tyrosine-containing phosphopeptides. The chemistry of the conjugation reaction between the dendrimer and the phosphate group of a phosphopeptide is detailed in Figure 5.2.

Under acidic conditions, the carbon of the carbodiimide (EDC) performs an electrophilic attack on the oxygen atom (O^-) within the phosphate group. This complex is extremely unstable and is replaced by the imidazole in a substitution reaction. A second substitution reaction occurs as the imidazole is replaced by the dendrimer. Hydrolysis with TFA releases the phosphopeptides for analysis.

The benefit of this phosphoramidate chemistry method over other derivatisation techniques is that it enables retention of the phosphate group, allowing the phospho-

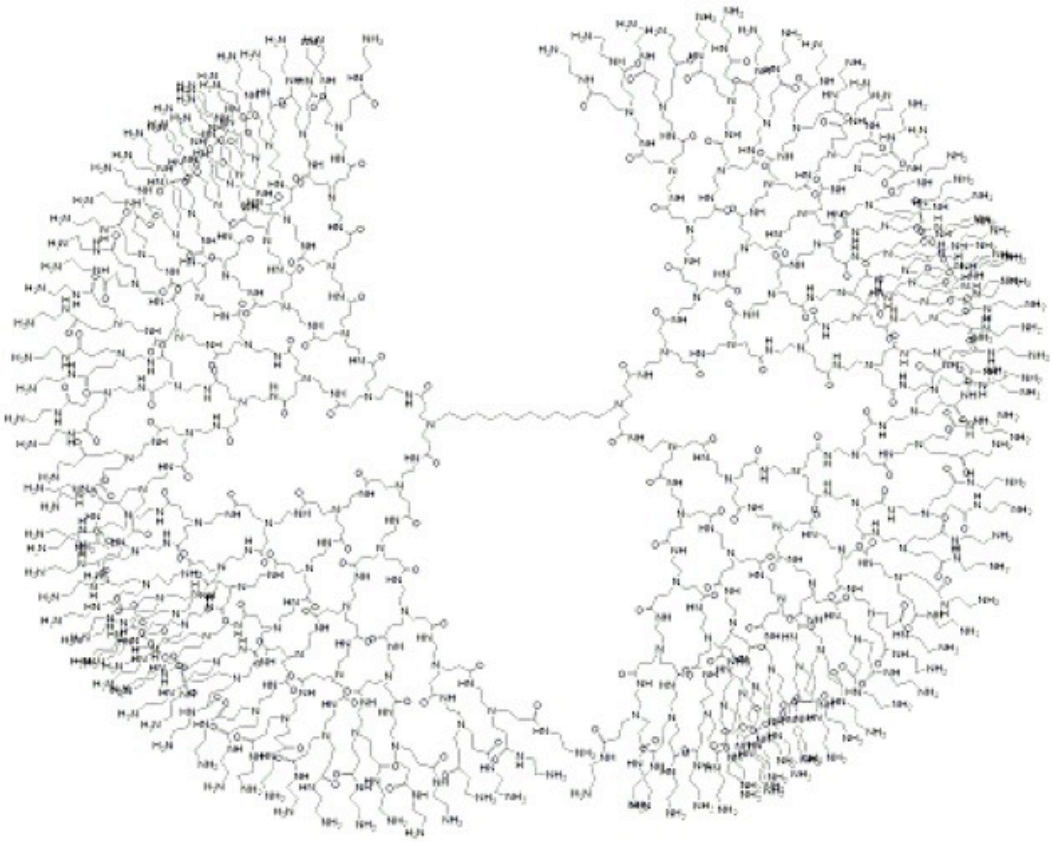

Figure 5.1: **Schematic of a dendrimer molecule.** Generation 5.0 1, 12-diaminododecane core PAMAM dendrimer with terminal amine groups exposed. Image created by Joseph Heinzelmann of Dendritic Nanotechnologies.

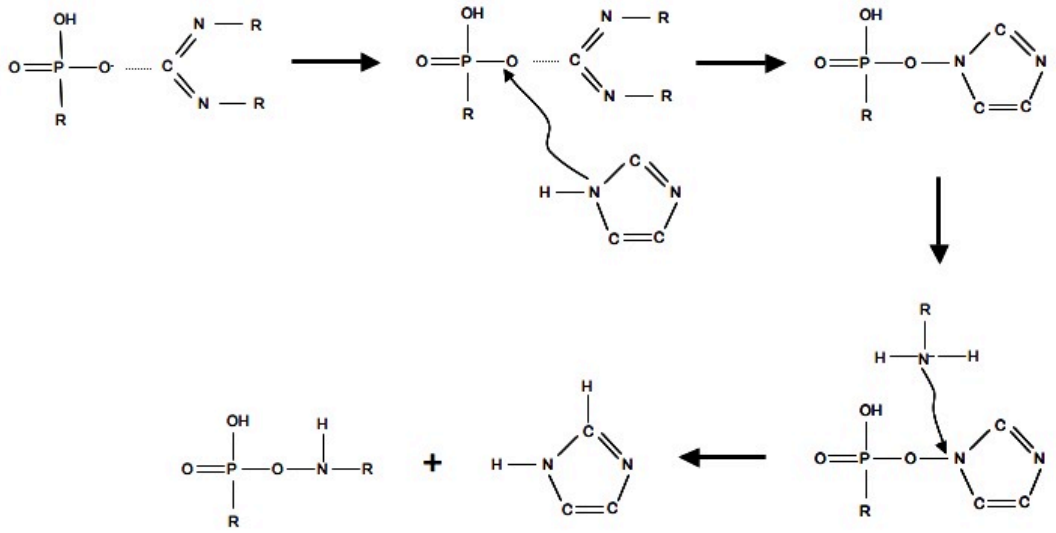

Figure 5.2: **Schematic of the chemistry of the conjugation between dendrimer and phosphopeptides.** The phosphate group on a phosphopeptide (R-PO_3H) undergoes electrophilic attack (represented by the horizontal dotted line) by the EDC catalyst (R_2CN_2), subsequently replaced by imidazole ($C_3H_2N_2$). A final substitution occurs when the amine group of the dendrimer (RNH_2) displaces the imidazole, binding to the phosphopeptide via the phosphate group.

rylation site to be identified (Bodenmiller *et al.*, 2007). As this is a relatively new method, it was not well established and required considerable optimisation before use with dialysate samples. The low complexity of dialysate compared to cell lysate samples would suggest that prior immunoprecipitation may not be required. This may facilitate the detection of unknown phosphorylation sites as the components that can be detected will not be limited to those proteins that are recognised by existing antibodies. Finally, the approach should avoid problems with the elution of multiply phosphorylated peptides reported for TiO_2, as peptides are eluted by hydrolysis rather than relying on affinity changes.

5.1.5 Specific objectives

The aim of the research described in this chapter was to investigate post-translational modifications of those proteins identified in dermal dialysate and their relevance to the injury response. Specific objectives were as follows:

- To evaluate the suitability of existing methods for protein phosphorylation analysis.
- To optimise methods of phosphopeptide isolation and enrichment for use with dialysate samples.
- To identify phosphorylated proteins in dermal dialysate obtained from injured skin.

5.2 Materials and Methods

Three methods were employed for phosphoproteome analysis of dermal dialysate. The first method used a dye specific for phosphorylation which could be used to stain phosphorylated proteins within a 1-D SDS PAGE gel. Two further methods were required, an affinity-based method using TiO_2-coated microbeads and a chemical derivatisation method using dendrimers as a soluble support.

5.2.1 Samples used in optimisation studies

Evaluation of the phosphoprotein gel stain was performed using bovine β-casein, a model phosphoprotein. This is method is described in the relevant section (Section 5.2.2). Initial optimisation of the TiO_2 and dendrimer methods was performed using tryptic digests of β-casein, containing a singly phosphorylated peptide of 2062 Da (mono-phosphopeptide), a quadruply phosphorylated peptide of 3122 Da (tetra-phosphopeptide) and other, non-phosphorylated peptides. The full sequence along with sites for trypsin cleavage is given in Figure 5.3 below.

MK||VLILACLVALALAR||ELEELNVPGEIVESLSSSEESITR||INK||K||
IEK||FQSEEQQQTEDELQDK||IHPFAQTQSLVYPFPGPIPNSLPQNI
PPLTQTPVVVPPFLQPEVMGVSK||VK||EAMAPK||HK||EMPFPK||Y
PVEPFTESQSLTLTDVENLHLPLPLLQSWMHQPHQPLPPTVMFPP
QSVLSLSQSK||VLPVPQK||AVPYPQR||DMPIQAFLLYQEPVLGPV
R||GPFPIIV

Figure 5.3: **Amino acid sequence of bovine β-casein.** Single-letter code amino acid sequence of bovine β-casein, UNIPROT ID P02666. Vertical lines (green) represent expected trypsin cleavage sites, red text indicates phosphorylated amino acids.

Table 5.2 lists the peptides resulting from a theoretical digest of β-casein that are within the range of 750-3500 Da. One missed cleavage was allowed in case of incomplete digestion.

Initial experiments also used 0.5 μg each of the purified mono- and tetra- phosphopeptides. For later optimisations, the starting amounts of β-casein digest was 2.5 μg

Table 5.2: **List of Peptides obtained from a theoretical digest of β-casein**

Peptide Sequence	**Predicted peptide mass† (Da)**	**Predicted methylated mass (Da)**
E^{M}LE^{M}E^{M}LNVPGE^{M}IVE^{M}S^{P}LS^{P}S^{P}E^{M}E^{M} SITRINK^{M}(17–43)	**3321.4**	**3433.4**
AVPYPQRD^{M}MPIQAFLLYQE^{M}PVLGPVR^{M} (192–217)	2997.6	3039.6
D^{M}MPIQAFLLYQE^{M}PVLGPVRGPFPIIV^{M} (199–224)	2909.6	2951.6
RE^{M}LE^{M}E^{M}LNVPGE^{M}IVE^{M}S^{P}LS^{P}S^{P}E^{M} E^{M}SITR^{M}(16–40)	**3122.3**	**3234.3**
E^{M}LE^{M}E^{M}LNVPGE^{M}IVE^{M}S^{P}LS^{P}S^{P}E^{M}E^{M} SITR^{M}(17–40)	**2966.2**	**3078.2**
IE^{M}KFQS^{P}E^{M}E^{M}QQQTE^{M}D^{M}E^{M}LQD^{M}K^{M} (45–63)	**2432.1**	**2544.1**
D^{M}MPIQAFLLYQE^{M}PVLGPVR^{M}(199–217)	2186.2	2228.2
FQS^{P}E^{M}E^{M}QQQTE^{M}D^{M}E^{M}LQD^{M}K^{M} (48–63)	**2061.9**	**2159.9**
VLPVPQKAVPYPQR^{M} (185–198)	1591.9	1605.9
VLILACLVALALAR^{M} (3–16)	1438.9	1452.9
HKE^{M}MPFPK^{M} (121–128)	1013.5	1041.5
E^{M}AMAPKHK^{M} (115–122)	911.4	939.4
VKE^{M}AMAPK^{M} (113–120)	830.5	844.5

^{P} Phosphorylated residue, ^{M} Residue available for methylation, † Mass includes phosphorylation where appropriate. Bold text highlights the phosphopeptides. Digest conditions were; untreated cysteines, monoisotopic mass ($[M+H]^{+}$), maximum 1 missed cleavage, only peptides larger than 750 Da included. Peptides over 3500 were excluded. Numbers in brackets indicate the position of that peptide in the sequence.

(100 pmoles). The data presented in this chapter were obtained from β-casein digests unless stated otherwise.

Further optimisation was made using a more complex sample, namely a tryptic digest of five proteins; bovine β-casein, casein and serum albumin, and equine cytochrome C and myoglobin. The expected peptides were determined by theoretical digestion using the PeptideMass tool (http://ca.expasy.org/tools/peptide-mass.html). Sites of phosphorylation were determined according to the respective entry on www.phosphosite .org. Protein accession numbers were entered into the NCBI protein database http://ww w.ncbi.nlm.nih.gov/sites/entrez?db=protein to obtain the protein sequence. The protein sequence was entered into the PeptideMass tool and peptide treatment variables were selected. Peptide masses were set to $[M+H]^+$ and monoisotopic values. Cysteines were untreated, one missed cleavage was allowed and the option for peptide size to be displayed was set to >750 Da. The phosphopeptides expected from this mixture, their parent protein name and accession number are listed in Table 5.3.

Once optimisation using model samples were completed, preliminary analyses of protein phosphorylation in dialysate were conducted to confirm that phosphorylated peptides could be captured.

Dialysate samples used were obtained during the first 30 minutes after injury and were pooled from two volunteers. Samples were collected as detailed in Section 2.2.2, according to the protocol depicted in Figure 5.4.

The protein content of these optimisation samples was estimated by BCA assay. The samples for dendrimer and TiO_2-affinity capture contained 872 μg and 780 μg total protein, respectively. Highly abundant proteins were not removed, because phosphopeptides from these proteins were also of interest. Samples from the first 30 minutes after insertion were used due to their higher protein concentration. Phosphatase inhibitors were not used in these preliminary studies. Dialysate samples were desalted, reduced, alkylated and digested as described in Section 2.6.4.4.

Table 5.3: **Phosphopeptides expected in the 5–protein mix**

Phosphopeptide Sequence	**Predicted peptide mass† (Da)**	**Predicted modified peptide‡ mass (Da)**
Casein α-S1 subunit (P02662)		
QME^{M}AE^{M}SIS^{P}S^{P}S^{P}E^{M}E^{M}IVPNS^{P}VE^{M}QKHIQK^{M}	2827.4	3231.4
VNE^{M}LSKD^{M}IGS^{P}E^{M}S^{P}TE^{M}D^{M}QAME^{M}D^{M}IK^{M}	2438.1	2790.1
QME^{M}AE^{M}SIS^{P}S^{P}S^{P}E^{M}E^{M}IVPNS^{P}VE^{M}QK^{M}	2321.1	2725.1
VPQLE^{M}IVPNS^{P}AE^{M}E^{M}RLHSMK^{M}	2177.1	2313.1
YKVPQLE^{M}IVPNS^{P}AE^{M}E^{M}R^{M}	1872.0	2008.0
D^{M}IGS^{P}E^{M}^{P}STE^{M}D^{M}QAME^{M}D^{M}IK^{M}	1767.8	2025.8
VPQLE^{M}IVPNS^{P}AE^{M}E^{M}R^{M}	1580.8	1761.8
Casein α-S2 subunit (P02663)		
NANE^{M}E^{M}E^{M}YSIGS^{P}S^{P}S^{P}E^{M}E^{M}S^{P}AE^{M}VATE^{M}E^{M}VK^{M}	2688.2	3134.2
NTME^{M}HVS^{P}S^{P}S^{P}E^{M}E^{M}S^{P}IISQE^{M}TYKQE^{M}K^{M}	2684.2	3088.2
NAVPITPTLNRE^{M}QLS^{P}T^{P}SE^{M}E^{M}NSK^{M}	2428.2	2644.2
NTME^{M}HVS^{P}S^{P}S^{P}E^{M}E^{M}S^{P}IISQE^{M}TYK^{M}	2299.0	2689.0
KTVD^{M}ME^{M}S^{P}TE^{M}VFTK^{M}	1514.7	1650.7
TVD^{M}ME^{M}S^{P}TE^{M}VFTKK^{M}	1514.7	1650.7
TVD^{M}ME^{M}S^{P}TE^{M}VFTK^{M}	1386.6	1522.6
E^{M}QLS^{P}TS^{P}E^{M}E^{M}NSKK^{M}	1379.7	1595.7
E^{M}QLS^{P}TS^{P}E^{M}E^{M}NSK^{M}	1251.6	1467.6
Casein β subunit (β-casein) (P02666)		
RE^{M}LE^{M}E^{M}LNVPGE^{M}IVE^{M}S^{P}LS^{P}S^{P}S^{P}E^{M}E^{M}SITR^{M}	2803.5	3235.5
E^{M}LE^{M}E^{M}LNVPGE^{M}IVE^{M}S^{P}LS^{P}S^{P}S^{P}E^{M}E^{M}SITR^{M}	2647.3	3079.3
IE^{M}KFQS^{P}E^{M}E^{M}QQQTE^{M}D^{M}E^{M}LQD^{M}K^{M}	2352.1	2544.1
FQS^{P}E^{M}E^{M}QQQTE^{M}D^{M}E^{M}LQD^{M}K^{M}	1981.9	2159.9

^{P} Phosphorylated, ^{M} Methylated, † Unmodified mass. ‡ Assumes full methylation and phosphorylation. Theoretical digest conditions; untreated cysteines, monoisotopic mass ($[M+H]^{+}$), maximum 1 missed cleavage, peptides > 750 Da included. Peptides over 3500 and under 1000 Da excluded.

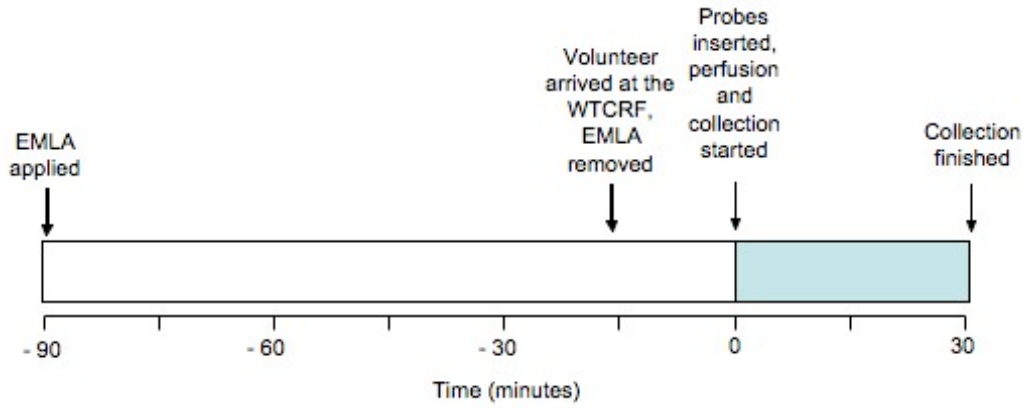

Figure 5.4: **Dialysate collection protocol for phosphopeptide enrichment optimisation.** The figure shows the timescale of the microdialysis experiment used to collect dialysate for the optimisation of phosphopeptide capture. Samples were collected over 30 minutes immediately after probe insertion. Pooled dialysate from two different volunteers was used for each experiment in this study.

5.2.2 Detection of phosphorylation using ProQ Diamond phosphoprotein stain

The sample preparation, electrophoresis, staining procedures and analysis are described in full in Sections 2.5.3, 2.6.1 and 2.6.2. Briefly, lyophilised β-casein was solubilised in 25 μl H_2O + 5 μl LDS sample buffer to give samples of the following total protein amounts: 40, 20, 10, 5, 2.5, 1.25, 0.63, 0.31 and 0.15 μg. One-dimensional SDS PAGE was performed and the resulting gel stained first with ProQ Diamond phosphoprotein stain and secondly with Sypro Ruby total protein stain. Following image capture (Section 2.5.3), the staining intensity was measured by densitometry analysis using Quantity One software as previously described (Section 2.6.3). The mean intensity for each β-casein band was plotted against concentration, using GraphPad Prism software (GraphPad Software).

5.2.3 Titanium dioxide affinity for capture of phosphopeptides

Samples were prepared and methylated as described in Section 2.6.4. Initial experiments used 0.5 μg each of the purified mono- and tetra-phosphopeptides. Starting amounts of β-casein digest were 2.5 μg (100 pmoles) unless stated. Captures were performed as detailed in Section 2.6.6.

The limits of detection were investigated by attempting to capture phosphopeptides from a doubling dilution series (40, 20, 10, 5, 2.5, 1.25, 0.63, 0.31, 0.15 and 0.08 μg). To compare the TiO_2 and dendrimer methods, a digest containing 5 μg of each protein was prepared by incubation with 1.5 μg of trypsin at 37°C overnight. A second 4 hour digestion was performed with the addition of 0.1 % RapiGest and 1 μg trypsin. Half of this digest, equivalent to 100 pmoles β-casein, was taken for TiO_2 affinity capture and the other half for dendrimer conjugation capture.

5.2.4 Optimisations of phosphopeptide capture by dendrimer conjugation chemistry

Initial experiments following the protocol published by Tao *et al.* (2005) were unsuccessful (data not shown). It was therefore necessary to conduct a series of optimisation experiments to enable the efficient and specific capture of phosphorylated peptides from complex mixtures. Table 5.4 summarises the differences between the original conjugation protocol and the final optimised method developed during the course of the project. The methods used during optimisation are described over the remainder of this section and the results obtained form a significant proportion of this chapter.

Table 5.4: **Changes made to the original dendrimer protocol***

Protocol Stage	**Published method**	**Optimised method**
Digestion of protein sample	Digestion using 1 μg trypsin.	Digestion improved with use of 0.1 % RapiGest SF surfactant (Waters) and trypsin in 1:20 ratio with total protein.
Methylation of peptides	Peptides reconstituted in 75 μl methanolic HCl (100 μl acetyl chloride + 500 μl anhydrous methanol). Incubated at 12 °C for 90 minutes.	Peptides reconstituted in methanolic HCl prepared by the addition of 160 μl acetyl chloride to 1 ml pre-cooled anhydrous methanol at a ratio of 500 μl per mg protein, to a minimum of 100 μl. Incubated at 12 °C for 2 hours.
Conjugation of phosphopeptides to the dendrimer	Reaction solution containing 50 mM EDC, 100 mM imidazole, 200 mM MES buffer and 9 mg dendrimer (Sigma). Forty μl reaction solution added to dried peptides and incubated for 10 hours.	Reaction solution containing 100 mM EDC, 100 mM imidazole and 200 mM MES buffer all adjusted to pH 5.5, and 9 mg of pH-adjusted dendrimer (Dendritic Nanotechnologies). Forty μl reaction solution added to dried peptides and incubated for 16 hours.
Removal of non-bound peptides	Several washes with 3 M NaCl in 30 % methanol in water	Sequence of 1 × 50 % methanol, 2 × 2 M NaCl in 50 % methanol, 3 × 50 % methanol and 5 × water.
Recovery of phosphopeptides	10 % TFA for 30 minutes, washed through with 30 % methanol.	10 % TFA for 60 minutes, washed through with water.
MALDI Analysis	Matrix unspecified	Improved matrix using dihydroxybenzoic acid and orthophosphoric acid.

* Original published method is that found in Tao *et al.* (2005).

The methods used to achieve these optimisations are described below. The optimised methods are reported in Sections 2.6.4 – 2.6.10.

5.2.4.1 Methylation to prevent non-specific binding

Peptides were methylated to block non-specific binding due to the carboxyl groups of acidic amino acid residues. Initially, a methanolic HCl solution was prepared from 160 μl acetyl chloride added dropwise to 1 ml methanol pre-cooled to -20°C. Peptides were incubated with 75 μl of this solution for 90 minutes at 12°C. It was subsequently discovered that although there was full methylation of the peptides prior to capture, some methyl groups were lost during capture. This resulted in multiple peaks for each peptide, due to different methylation variants. The method was therefore improved through the use of anhydrous methanol and a two hour incubation with 500 μl methanolic HCl per 1 mg peptide, to a minimum of 100 μl. Dried peptides were desiccated overnight in the presence of P_2O_5 prior to methylation.

5.2.4.2 Optimisation of the conjugation stage

The first experiments using the original conjugation protocol were unsuccessful. One explanation was that addition of the dendrimer caused an adverse change in pH – when the dried dendrimers were added to the reaction solution of approximately pH 6, the overall pH increased. This problem was solved by independently adjusting the pH of the dendrimers prior to lyophilisation. Three hundred and fifty μl of 100 mM MES buffer solution was added to 80 μl dendrimer, as supplied in methanol and the pH adjusted to 5.5 by titration with 1 M HCl before lyophilisation *in vacuo*. The reaction solution (200 mM MES, 100 mM EDC and 100 mM imidazole) was adjusted to pH 5.5, again by titration with 1 M HCl and added to the dried, pH-adjusted dendrimers. This solution in turn was added to dried, methylated peptides and incubated at room temperature for 16 hours with strong shaking.

5.2.4.3 Reduction of co-purifying contaminants

Early experiments indicated that the captured phosphopeptides were contaminated with polymers that had leached from the filter membrane. Accordingly, alternative filters were tested to determine whether different membrane compositions released fewer contaminants and different solvent conditions were investigated to see if it was possible to reduce polymer solubilisation.

The original 5 kDa MWCO Ultrafree MC polyethersulphone (PES) filter was compared against a 3 kDa MWCO NanoSep filter with Omega, modified PES membrane and a NanoSep with BioInert modified nylon membrane (kindly donated by VWR International). Regenerated cellulose membranes were not tested as these had been found to be inappropriate in earlier stages of the optimisation (data not shown). Filters were subjected to the original wash procedure of 1 × 50 % methanol, 4 × 2 M NaCl in 50 % methanol and 4 × 50 % methanol, followed by 60 minutes incubation with 10 % TFA and two further washes with 50 % methanol. The final filtrate, combining the TFA wash and subsequent methanol washes, was lyophilised and analysed by MALDI-TOF MS (Section 2.6.9).

A panel of different solvents were prepared (Table 5.5) to determine which would cause the least polymer contamination.

Table 5.5: **Different solvents tested for their effect on leaching of polymer contaminants from the filter membrane**

20 % ethanol	40 % ethanol
60 % ethanol	10 % acetonitrile
20 % acetonitrile	10 % methanol
50 % methanol	water

Filters were washed 6 times with 400 μl solvent, incubated for one hour with 10 % TFA and washed twice further with solvent. Washes were performed by centrifugation

at 5000 × g for 15 minutes or until all the liquid had passed through. The TFA and subsequent washes were combined to form the final filtrate equivalent to the eluted phosphopeptide sample. Each wash filtrate was lyophilised and analysed for polymer content by MALDI-TOF MS (Section 2.6.9). The five most commonly found peaks were determined manually and the intensity of those peaks recorded for each of the final filtrates obtained from each solvent.

A pre-wash step was also added in which filters were washed prior to use, to remove any loose polymer. Washes were performed using 400 μl of 500 mM NaOH, water, 10 % TFA and water again. Centrifugation was at 5000 × g for 15 minutes or until all the liquid had passed through. Cleaned filters were stored at 4 °C with 400 μl water overnight, or used immediately. This step was added at the suggestion of Dr. Bernd Bodenmiller.

5.2.4.4 Investigation into the effect of different matrix compositions

Phosphorylation is an acidic modification, making phosphorylated peptides harder to ionise when using a positive ion analysis mode. Additionally, phosphopeptides have a high affinity for metal and so can bind to the MALDI target plate, further reducing ionisation efficiency.

To improve the ionisation of these negatively charged peptides, two modifications were made. First, the target plates were washed with orthophosphoric acid (H_3PO_4) in methanol to block potential phosphate binding sites on the plate. Secondly, an alternate matrix was used to improve phosphopeptide ionisation. DHBA is known to improve capture of phosphopeptides in TiO_2 chromatography systems (Larsen *et al.*, 2005), but was shown to be unnecessary in IMAC (Imanishi, Kochin & Eriksson, 2007). It has also been used as a matrix for phosphopeptide analysis by MALDI MS in a limited number of studies (Kjellström & Jensen, 2004). It was hypothesised that together with orthophosphoric acid, DHBA could enhance the detection of phosphopeptides in positive ion mode. Three DHBA-based matrix solutions were prepared as detailed in Table 5.6 and the effect on signal intensity of the two purified phosphopeptides determined.

Table 5.6: **Different solvents tested for their effect on leaching of polymer contaminants from the filter membrane**

Matrix 1	2 mg α-cyano-4-hydroxycinnamic acid + 1 ml 50 % acetonitrile + 0.2 % TFA
Matrix 2	2 mg dihydroxybenzoic acid + 1 ml 100 % methanol + 1 % H_3PO_4
Matrix 3	2 mg dihydroxybenzoic acid + 1 ml 50 % methanol + 1 % H_3PO_4
Matrix 4	2 mg dihydroxybenzoic acid + 1 ml 50 % acetonitrile + 1 % H_3PO_4

One μl of each phosphopeptide was mixed in a 1:1 ratio with each matrix and 1.4 μl per sample spotted onto separate wells of a cleaned MALDI plate for analysis by MALDI-TOF MS. High laser energy was required for the DHBA-based matrix preparations.

5.2.4.5 Remethylation of captured samples to improve detection of phosphopeptides

The recovered peptides consistently displayed a reduction in methylation status following dendrimer conjugation, later attributed to the presence of EDC. This increased the complexity of the sample, as several methylation variants were detected for each peptide, and reduced the signal intensities of individual peaks of interest. With a biological sample, this additional variation would complicate LC-MS/MS analysis, giving a higher incidence of false-positive identifications. Accordingly, an additional methylation step was added after the capture stage to replace any methyl groups lost during conjugation. Captured peptide samples were lyophilised, dessicated and methylated as described in Section 2.6.5.

5.2.4.6 Mass spectrometry for identifying the captured phosphopeptides

Three different types of mass spectrometry were used to analyse the captured phosphopeptides, namely matrix-assisted laser desorption/ionisation-time of flight (MALDI-

TOF), liquid chromatography-tandem mass spectrometry (LC-MS/MS) using a quadropole-time of flight instrument, and tandem mass spectrometry with an ion trap for ion selection and fragmentation, using an LTQ Orbitrap XL (linear trap quadropole-orbitrap) instrument. Details of these are given in Sections 2.6.9, 2.6.10 and 2.6.11. Estimates of relative abundance for the MALDI-TOF MS experiments were measured in arbitrary units (AU), based on the intensity of the tallest peak, given on each spectrum.

5.3 Results

5.3.1 Use of a phosphoprotein-specific gel stain to quantify protein phosphorylation

Initially, a phospho-specific gel stain was used to analyse post-translational protein phosphorylation in dialysate. Figure 5.5 shows the intensity of staining obtained from different concentrations of a known phosphorylated protein, β-casein.

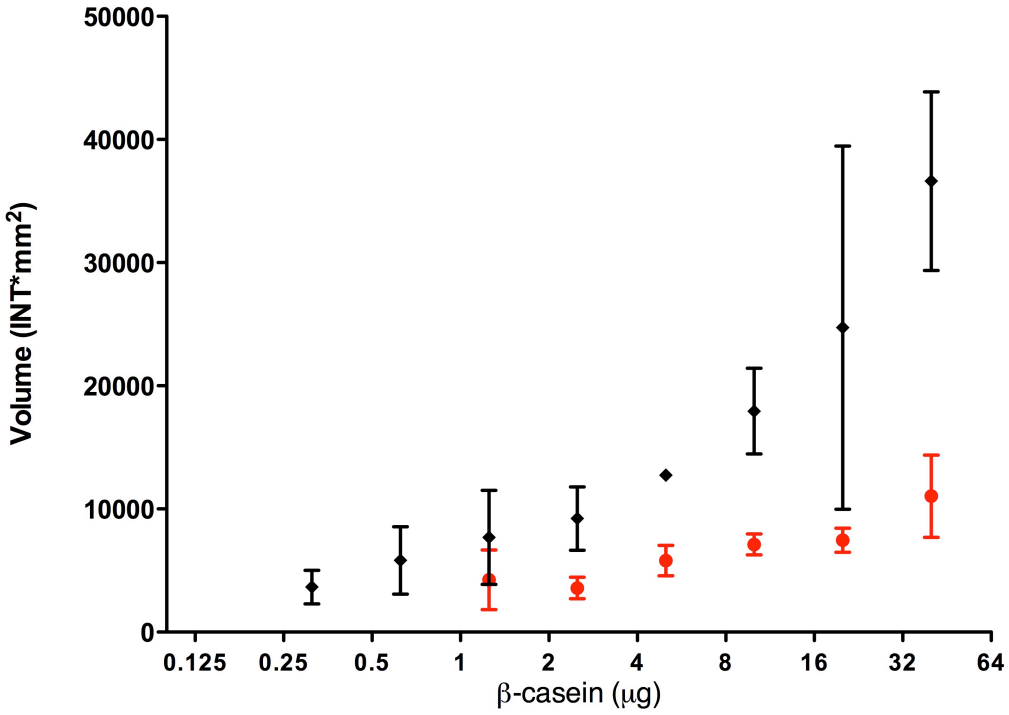

Figure 5.5: **Limits of detection of phosphorylated proteins by phosphoprotein and total protein stains.** The staining intensity of the ProQ Diamond phosphoprotein stain (red) and Sypro Ruby total protein stain (black) for different concentrations (40, 20, 10, 5, 2.5, 1.25, 0.63, 0.3 and 0.15 μg) of the phosphorylated protein β-casein (n = 2).

The lowest concentration of β-casein detected with the stain for total protein was 0.31 μg whereas the phosphoprotein stain detected β-casein at 1.25 μg and higher. Staining intensity with ProQ Diamond was variable, especially with large amounts of protein and demonstrated very little linear relationship between the amount of phos-

phorylated protein and staining intensity. Staining with Sypro Ruby was also variable but the staining intensity was more proportional to the protein concentration. In summary, the phospho-specific stain had limited sensitivity and relatively poor quantification for large concentrations of a known phosphorylated protein. Furthermore, the stain would not enrich for phosphorylated proteins and additional methods would be required. It was therefore decided that it was not sensible to pursue this staining approach.

5.3.2 Phosphopeptide enrichment using titanium-dioxide (TiO_2) beads

A trypsin digest of the model phosphorylated protein β-casein should produce two phosphopeptides: a singly phosphoryated peptide at *m/z* 2160 $[M+H]^+$ and a quadruply phosphorylated peptide at *m/z* 3236 $[M+H]^+$ when both are fully methylated.

The ability of TiO_2-coated beads to capture and enrich these phosphopeptides was therefore investigated. Figure 5.6 shows a representative MALDI-TOF MS spectrum of the β-casein peptides captured by the TiO_2 beads.

The two β-casein phosphopeptides were detected (seen as *m/z* 2160 and 3237 $[M+H]^+$), but the spectrum was dominated by larger peaks at *m/z* 1595, 2042 and 2707 $[M+H]^+$. No matches were found for *m/z* 2042 and 2707 $[M+H]^+$. The peak at *m/z* 1595 $[M+H]^+$ corresponds to the mass of an α s2 casein peptide, $E^MQLS^PTS^PE^ME^MNSKK^M$, although its identification could not be confirmed by LC-MS/MS. This is a contaminant and part of the parent protein from which β-casein is derived. The peak at *m/z* 1553 $[M+H]^+$ matches the mass of a methylation variant of that at *m/z* 1595 $[M+H]^+$, as the difference is equivalent to the loss of three of the four methyl groups. Additionally, peaks at *m/z* 2707 and 2696 $[M+H]^+$ correspond to predicted mass of the peptide $VNE^MLSKD^MIGS^PE^MS^PTE^MD^MQAME^MD^MIK^M$ from α-S1-casein, minus one phosphate group and both one phosphate and one methyl group, respectively. No potential match could be determined for *m/z* 2042 $[M+H]^+$. LC-MS/MS analysis (data not shown) was only able to identify the mono-phosphopeptide from β-casein.

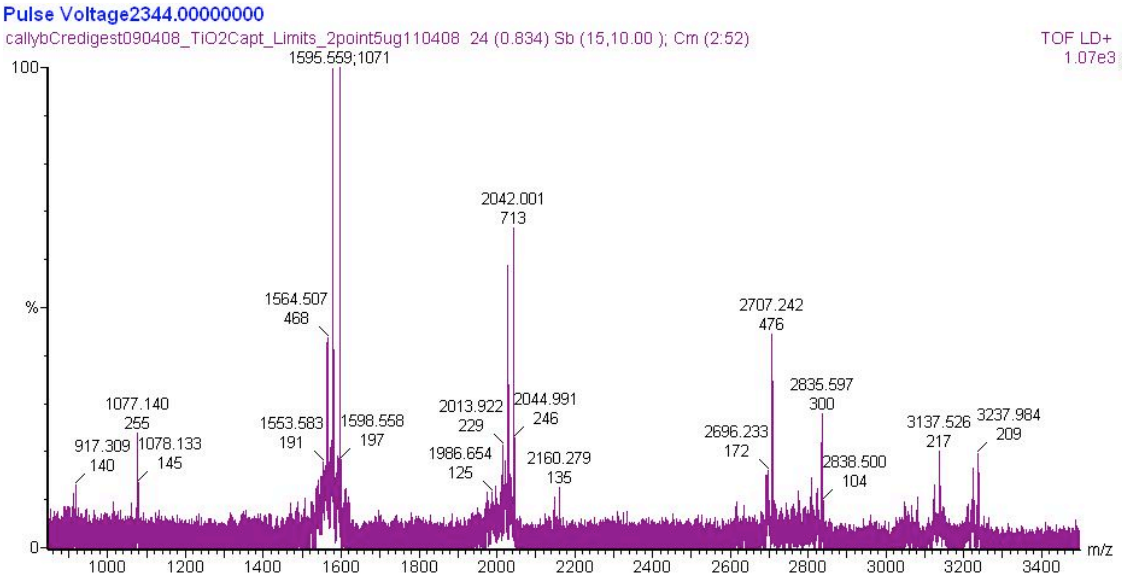

Figure 5.6: **Peptides captured from 100 pmoles β-casein by TiO_2 beads.** Known peptides captured include those at m/z 1595 – α s2 casein, 2160 – mono-phosphopeptide β-casein, 3137 – α s1 casein, 3235 – tetra-phosphopeptide β-casein. Peptides at m/z 2042, 2707 and 2835 $[M+H]^+$ did not correspond to any predicted phosphopeptides.

Experiments to determine the minimum detection limit were successful for the lowest amount of β-casein, 80 ng (data not shown). This confirmed that the TiO_2 bead capture is a sensitive method, but the detection of the other unidentified peaks shows that it is not necessarily specific. While this method would reduce sample complexity and enrich for phosphorylated peptides, there remains a need for a more specific method.

5.3.3 Optimisation of phosphopeptide capture and enrichment by dendrimer conjugation chemistry

Figure 5.7 shows a representative spectrum obtained from the initial successful capture of phosphopeptides from a tryptic digest of β-casein using dendrimer conjugation chemistry.

While successful, these captures were not optimal. Firstly, the mono-phosphopeptide

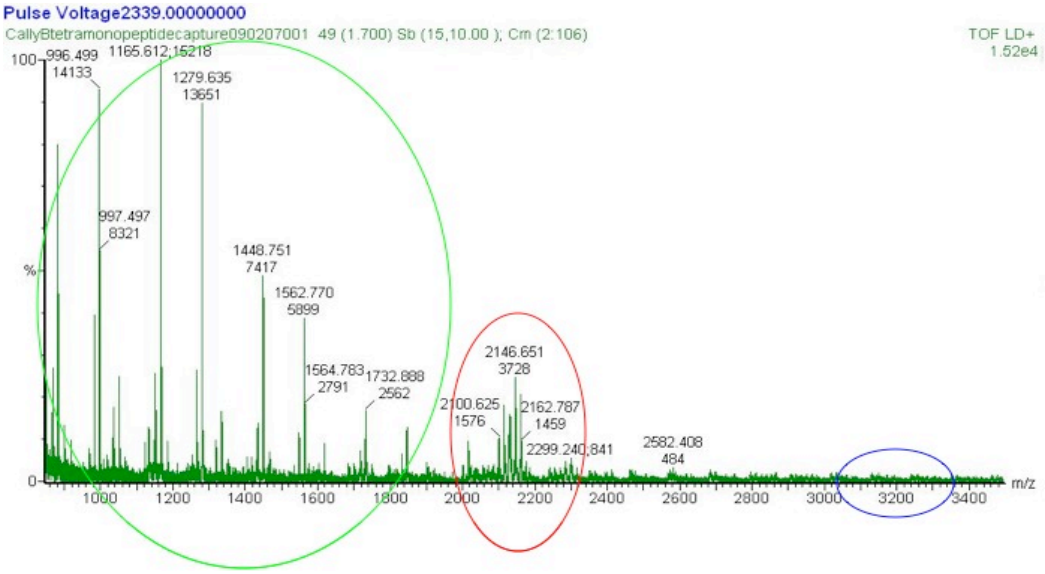

Figure 5.7: **Example of a spectrum obtained from early attempts at phosphopeptide capture using dendrimer conjugation chemistry.** Peptides captured from 100 pmoles of a tryptic digest of β-casein. The mono-phosphopeptide peak with sub-optimal methylation is circled in red, the tetra-phosphopeptide peak was absent (circled in blue) and the contamination is circled in green.

peak (red circle in the Figure) was split between several methylation variants where there was sub-optimal, or loss of, methylation. Secondly, the tetra-phosphopeptide was not detected (blue circle), possibly due to inefficient ionsation during MS analysis. Finally, and most notably, there was considerable contamination (green circle) obscuring identification of true peptides. The captured mono-phosphopeptide peak was 25 % the height of the tallest contaminant peak. The regularity of the m/z values of the contaminants strongly suggested that the problem was due to polymer leaching, e.g. from the filter membrane.

5.3.3.1 Optimisation of the filtration stages to reduce polymer contamination in the captured sample

With the discovery that polymer contaminants were derived from the membrane of the filter device, an alternative was required. Three membrane compositions were

compared; the original PES membrane, modified PES "Omega" and a modified nylon "Bioinert" membrane. Several other filter constructs had been deemed unsuitable in earlier optimisation steps. Figure 5.8 shows the amount of contamination obtained from each filter type.

The Omega membrane released the most contaminants (Figure 5.8b) whereas the Bioinert membrane (Figure 5.8c) gave the fewest. The remaining contaminants in the latter were highly abundant compared to those generated by the Omega membrane (5710 AU compared to 1350 AU) but were still half that of the tallest peak obtained from the original Ultrafree membrane (10500 AU). Unfortunately, the Bioinert membrane was later found to be incompatible with the dendrimer and hence could not be used.

The original Ultrafree MC filter with the standard polyethersulphone membrane (Figure 5.8a) was the best compromise, despite the high abundance of the contaminant peaks. However, an alternative method of reducing contamination was still required. Therefore, the effect of different solvents on the membrane was assessed to determine whether polymer leaching could be reduced by using different wash solutions. Table 5.7 shows the intensity of contaminants detected in the final filtrate obtained from each solvent.

Two solvents exhibited the highest contamination giving the highest intensity for two of the most common peaks each, 10 % methanol and 60 % ethanol. Water alone gave the least contamination with four of the five most common peaks not detected. The one contaminant peak detected was at the lowest intensity for that peak. Twenty percent acetonitrile appeared to cause the least leaching of polymer. However, it caused leaching of a large number of less common contaminants not included in the table. Of the remaining solvents, 50 % methanol gave the least contamination. This was the solvent originally used and none of the other solvents presented a better alternative, apart from water alone. As an organic solvent was required, it was decided that a two-step wash procedure was necessary. The combination of 50 % methanol followed by water enabled optimal removal of non-bound peptides and reduced polymer contamination.

Contamination was further reduced by a pre-wash protocol added at the suggestion

(a)

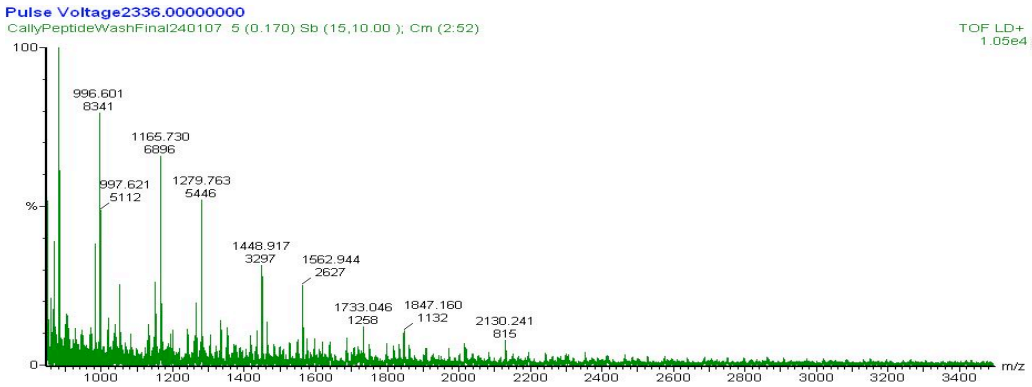

(b)

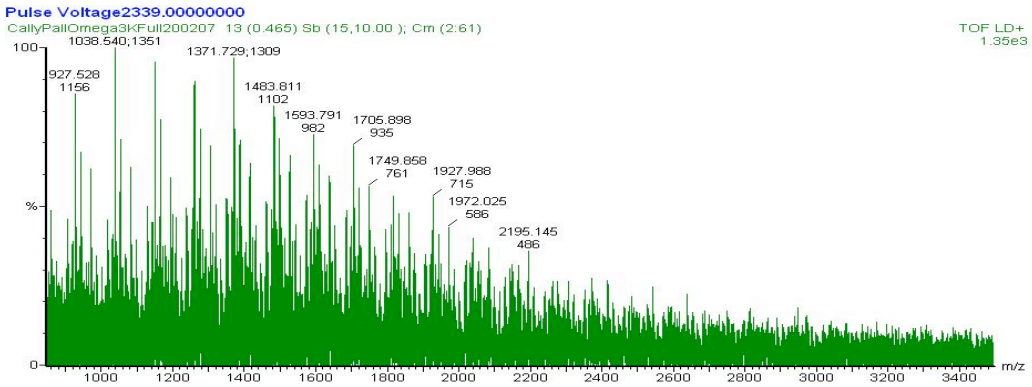

(c)

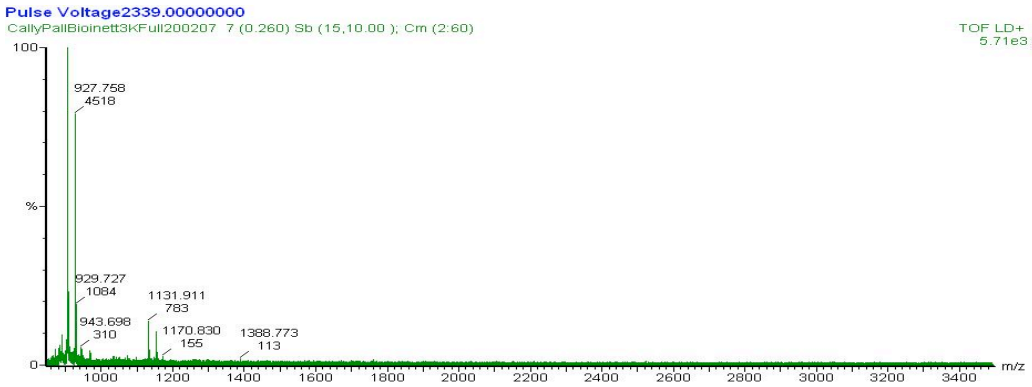

Figure 5.8: **Comparison of contamination from different types of filter membrane.** Contaminant peaks contained in the final wash filtrate (10 % TFA and 2 × 50 % methanol, equivalent to eluted phosphopeptide samples) were analysed by MALDI-TOF MS. Samples were generated using the following wash sequence (5 × 2 M NaCl, 5 × 50 % methanol) through a) Ultrafree MC filter with polyethersulphone membrane, b) NanoSep with Omega modified polyethersulphone membrane and c) NanoSep with Bioinert modified nylon membrane.

Table 5.7: **Polymer peak intensities under different solvent conditions**

	Signal Intensity of Contaminant Peak* (AU)				
Solvent	996 Da	1165 Da	1279 Da	1733 Da	2016 Da
10 % acetonitrile	2230	2360	3220	795	302
20 % acetonitrile	246	443	321	138	131
20 % ethanol	2710	3880	**3720**†	995	503
40 % ethanol	3160	4760	2430	606	410
60 % ethanol	2510	3000	2800	**1550**	**984**
10 % methanol	**5450**	**6480**	1980	nd‡	nd
50 % methanol	1040	1350	1120	748	394
H_2O	nd	nd	119	nd	nd

* Peak values given as m/z $[M+H]^+$, † Bold type indicates the highest value in each column, ‡ indicates where the peak was not detected under those conditions.

of Dr. Bernd Bodenmiller of the Institute for Molecular Systems Biology, Zurich. Filters were washed with NaOH, TFA and water as described previously (Sections 2.6.7.2 and 5.2.4.3). Figure 5.9 shows the reduced contamination achieved.

The most dominant peak is that of the captured mono-phosphopeptide, with contaminants at 20 % or lower compared to the size of the mono-phosphopeptide peak. This was a significant improvement on the 400 % observed in the initial capture protocol (Figure 5.7).

5.3.3.2 Optimisation of MALDI-TOF MS analysis conditions to improve detection of phosphopeptides

Table 5.8 shows the signal intensity obtained for the mono- and tetra- phosphopeptides analysed using different matrix compositions for MALDI-TOF MS.

The tetra-phosphopeptide was not detected with the α-CHCA matrix and mono-phosphopeptide detection was poor compared to the alternatives. In contrast, all three

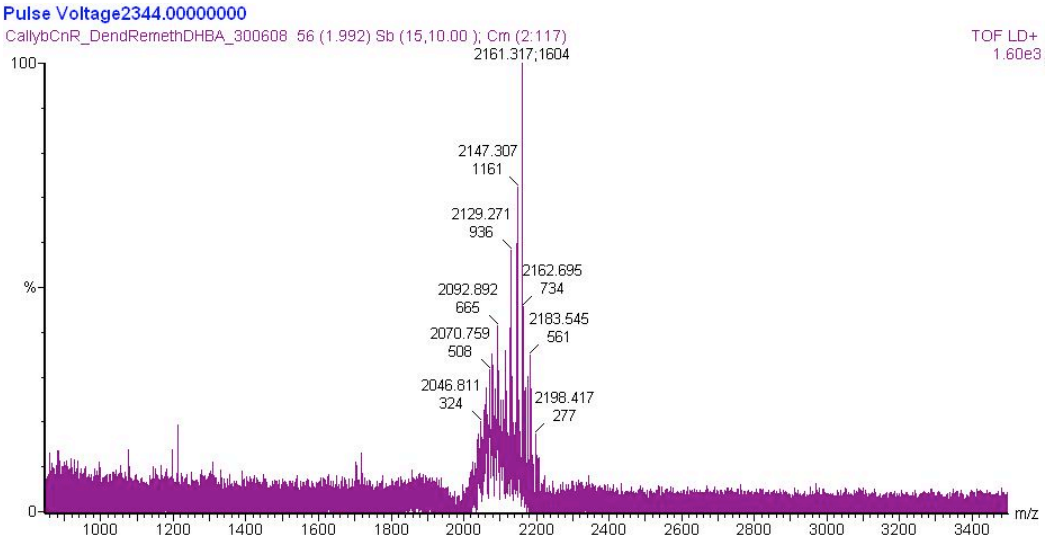

Figure 5.9: **Reduced polymer contamination with optimised wash protocols.** Dendrimer capture of methylated mono-phosphopeptide (main peak cluster) from 100 pmoles β-casein digest. Contaminant peaks (left) fall below 20 % of the highest peak.

DHBA-based matrix preparations enabled the detection of the tetra-phosphopeptide. Matrix 2 gave the highest signal intensity for the mono-phosphopeptide (13200 AU) while matrix 4 gave the highest signal intensity for the tetra-phosphopeptide (3520 AU). Matrix 2 was chosen as the best preparation to use as it gave the greatest increase (6.8–fold) in detection of the mono-phosphopeptide and performed better in subsequent tests (data not shown).

5.3.3.3 Re-methylation of captured samples to improve signal intensity and reduce unnecessary sample complexity

Re-methylation of lyophilised samples after phosphopeptide capture increased the signal intensity of the fully methylated form of the mono-phosphopeptide (Figure 5.10).

The captured mono-phosphopeptide was detected in eight methylation variants (Figure 5.10a). The most predominant peak was the 4 × methylated mono-phosphopeptide at m/z 2117 $[M+H]^+$ with an intensity of 904 AU. Remethylating the captured sample reduced the profile to one large and two small peaks, representing the fully methylated (m/z 2159 $[M+H]^+$) and the 6 and 5 × methylated (m/z 2145 and 2131

(a)

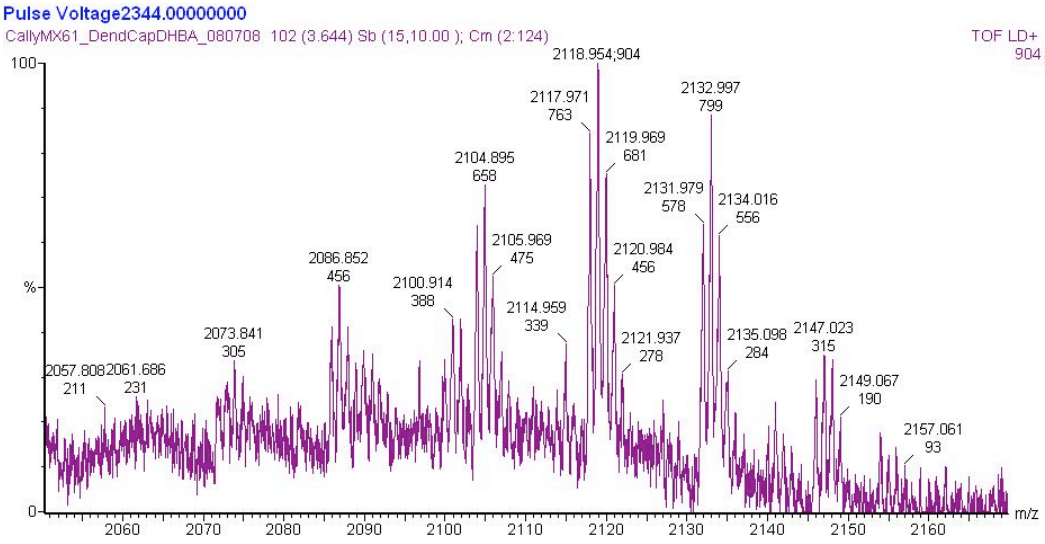

(b)

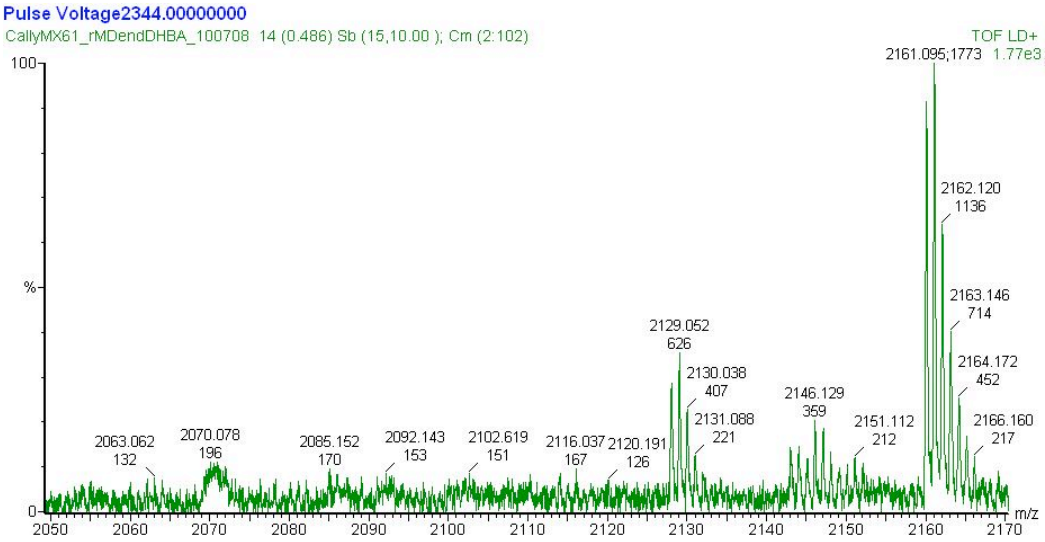

Figure 5.10: **The effect of re-methylation on sample complexity.** a) Profile of mono-phosphopeptide captured by dendrimer conjugation from 100 pmoles β-casein. Methylation variants observed were 6, 5, 4, 3, 2, 1 and 0 $\times$ methylated (m/z 2145, 2131, 2117, 2103, 2089, 2075 and 2061 $[M+H]^+$, respectively) b) Dendrimer-captured mono-phosphopeptide from β-casein, after re-methylation to improve signal intensity and reduce complexity. The fully (7 $\times$) methylated form was predominant (m/z 2159 $[M+H]^+$). Small peaks were present for the 6 and 5 $\times$ methylated forms.

Table 5.8: **Signal intensities of the mono- and tetra- phosphopeptide peaks for each matrix**

	Signal Intensity (AU)	
Matrix	Mono-phosphopeptide	Tetra-phosphopeptide
Matrix 1	1950	not detected
Matrix 2	**13200**†	2730
Matrix 3	4570	2110
Matrix 4	8090	**3520**

† Bold text indicates the highest values in each column. Matrix 1 = α-CHCA in 50 % ACN + 0.2 % TFA. Matrix 2 = DHBA in methanol + 1 % H_3PO_4. Matrix 3 = DHBA in 50 % methanol + 1 % H_3PO_4. Matrix 4 = DHBA in 50 % ACN + 1 % H_3PO_4.

$[M+H]^+$, respectively) forms. The predominant peak in the remethylated sample, the fully methylated variant, was double the intensity of that observed prior to remethylation, at 1770 AU. Analysis of the limits of detection, as conducted for the TiO_2 bead method, showed that dendrimer conjugation could also capture the mono-phosphopeptide from the lowest concentration investigated, 80 ng.

5.3.3.4 Identification of phosphopeptides from β-casein captured using dendrimer conjugation and LC-MS/MS

Figure 5.11 shows the tandem mass spectrometry data obtained for the mono-phosphopeptide identified from capture using the dendrimer method.

The spectrum in Figure 5.11a shows the loss of phosphoric acid from b and y ions, equivalent to 98 Da. Figure 5.11b shows the ions detected in this experiment, indicated in red. This fragmentation data confirms the peptide sequence and the identification of the known phosphorylation site on the serine residue, for example on the b_3 ion at 345.16.

(a)

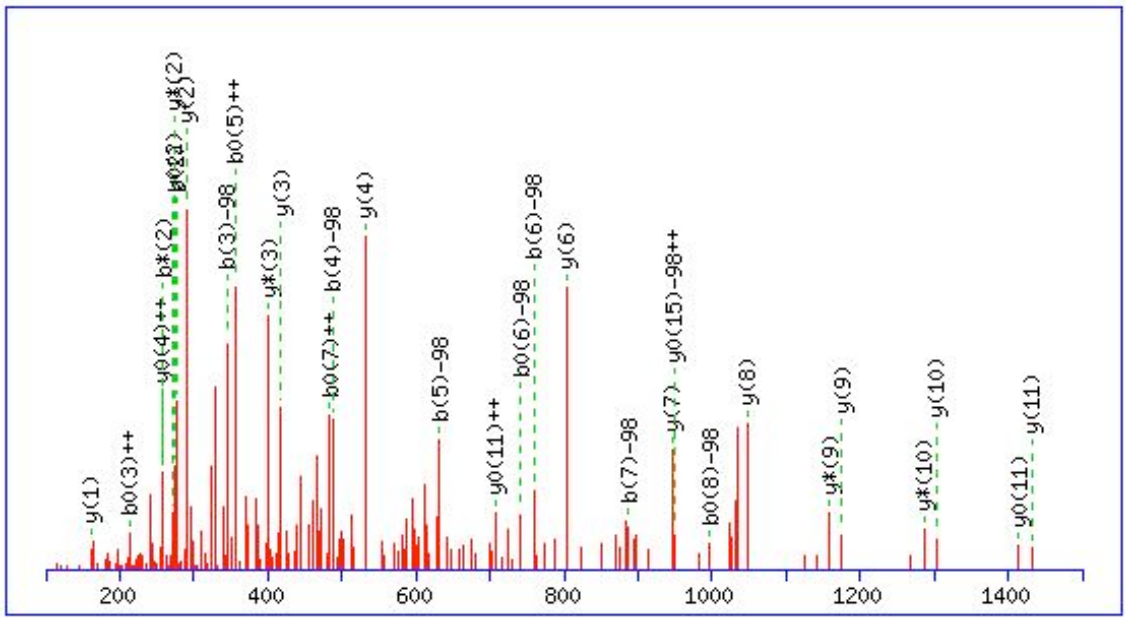

(b)

#	b	b^{++}	b*	b*$^{++}$	b^{0}	b^{0++}	Seq.	y	y^{++}	y*	y*$^{++}$	y^{0}	y^{0++}	#
1	148.08	74.54					F							16
2	276.13	138.57	259.11	130.06			Q	1914.89	957.95	1897.87	949.44	1896.88	948.94	15
3	345.16	173.08	328.13	164.57	327.15	164.08	S	1786.83	893.92	1769.81	885.41	1768.82	884.92	14
4	488.21	244.61	471.19	236.10	470.20	235.61	E	1717.81	859.41	1700.79	850.90	1699.80	850.40	13
5	631.27	316.14	614.25	307.63	613.26	307.13	E	1574.75	787.88	1557.73	779.37	1556.74	778.88	12
6	759.33	380.17	742.30	371.66	741.32	371.16	Q	1431.70	716.35	1414.67	707.84	1413.69	707.35	11
7	887.39	444.20	870.36	435.69	869.38	435.19	Q	1303.64	652.32	1286.61	643.81	1285.63	643.32	10
8	1015.45	508.23	998.42	499.71	997.44	499.22	Q	1175.58	588.29	1158.55	579.78	1157.57	579.29	9
9	1116.50	558.75	1099.47	550.24	1098.49	549.75	T	1047.52	524.26	1030.49	515.75	1029.51	515.26	8
10	1259.55	630.28	1242.53	621.77	1241.54	621.28	E	946.47	473.74	929.45	465.23	928.46	464.73	7
11	1388.60	694.80	1371.57	686.29	1370.59	685.80	D	803.41	402.21	786.39	393.70	785.40	393.21	6
12	1531.65	766.33	1514.63	757.82	1513.64	757.33	E	674.37	337.69	657.35	329.18	656.36	328.68	5
13	1644.74	822.87	1627.71	814.36	1626.73	813.87	L	531.31	266.16	514.29	257.65	513.30	257.16	4
14	1772.80	886.90	1755.77	878.39	1754.79	877.90	Q	418.23	209.62	401.20	201.11	400.22	200.61	3
15	1901.84	951.42	1884.81	942.91	1883.83	942.42	D	290.17	145.59	273.14	137.08	272.16	136.58	2
16							K	161.13	81.07	144.10	72.55			1

Figure 5.11: **Peptide results for the mono-phosphopeptide identified by LC-MS/MS following dendrimer capture from 1 nmole β-casein digest.** a) LC-MS/MS spectrum showing the loss of phosphoric acid (98 Da) from both b and y ion series b) Table of results showing the peptide sequence determined. Red text indicates ions matched in this experiment.

5.3.4 Comparison of phosphopeptide capture by the optimised TiO_2 bead and dendrimer conjugation chemistry methods

The two optimised phosphopeptide capture methods were compared directly using a common starting sample. Figure 5.12 shows the peptide profiles obtained following MALDI-TOF MS analysis of the captured samples.

The two phosphopeptides from β-casein were captured by both methods. The mono-phosphopeptide was most prominent in the TiO_2–captured sample, with an intensity of 2940 AU. In the dendrimer capture, the mono-phosphopeptide was only 30 % of the tallest peak, but was detected with an approximate intensity of 5900 AU. This was double the intensity of the mono-phosphopeptide in the TiO_2–captured sample. The tetra-phosphopeptide was detected in its fully methylated (*m/z* 3235 $[M+H]^+$) form in the TiO_2–captured sample. The peak at *m/z* 3122 $[M+H]^+$ observed in both captures corresponds to the *m/z* value of the unmethylated form of the tetra-phosphopeptide.

The largest peak detected in the dendrimer capture, at *m/z* 1634 $[M+H]^+$ did not correspond to any of the expected phosphopeptides. It most likely represents either $KTVD^MME^MS^PTE^MVFTK^M$ or $TVD^MME^MS^PTE^MVFTKK^M$ from α-S2-casein, minus one methyl group.

LC-MS/MS analysis identified only the mono-phosphopeptide from β-casein, producing spectra similar to that shown in Figure 5.11.

5.3.5 Orbitrap analysis of phosphopeptides captured from β-casein using dendrimer-conjugation

It was possible that the type of mass spectrometer used also had an influence on the type of phosphopeptide detected from the captured sample. Table 5.9 shows the peptides identified from a dendrimer capture of 100 pmoles β-casein using an LTQ linear ion trap-orbitrap (LTQ-orbitrap) mass spectrometer to avoid the bias against

(a)

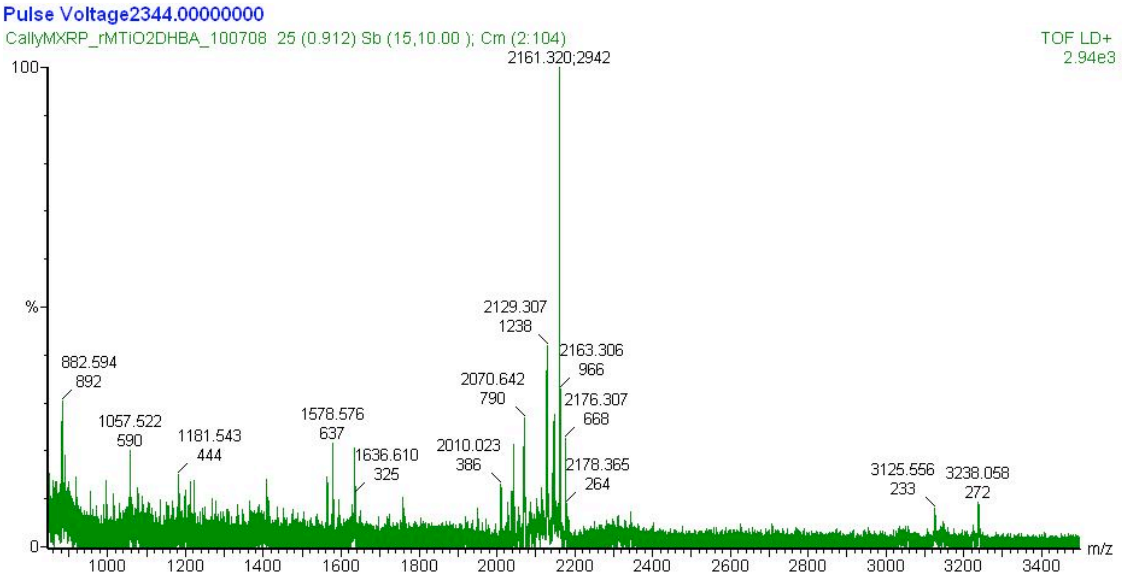

(b)

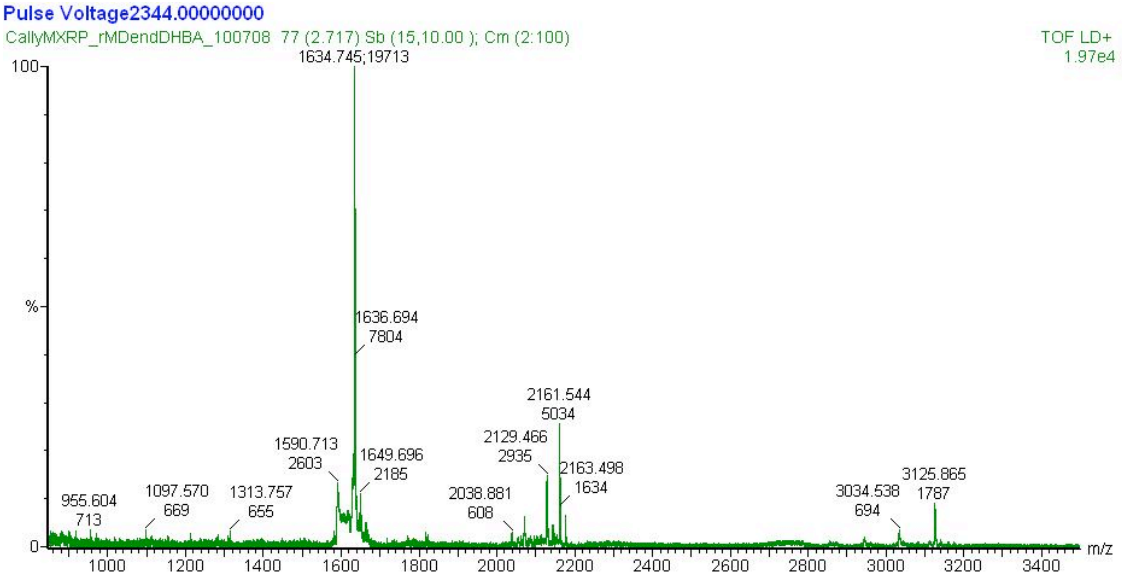

Figure 5.12: **Comparison of phosphopeptide captures by TiO_2 and dendrimer methods.** MALDI-TOF MS spectra showing the phosphopeptides captured from a tryptic digest of the 5-protein mix by a) TiO_2 and b) dendrimer methods. The β-casein mono– (m/z 2161 $[M+H]^+$) and tetra-phosphopeptides are present with the tetra– in both fully methylated and unmethylated forms (m/z 3122 and 3235 $[M+H]^+$ respectively). Captures were from a common sample containing 25 μg total protein, 5 μg of each peptide, giving 100 pmoles β-casein available per capture.

multiply phosphorylated peptides experienced with LC-MS/MS (this work was carried out by Dr. Gary Wolfenden, at Thermo Electron (UK) Ltd.).

Table 5.9: **Peptides identified from a dendrimer capture of β-casein by Orbitrap analysis**

Peptide	**Mass (Da)**	**Charge**
β-casein		
K. FQS^{P}E^{M}E^{M}QQQTE^{M}D^{M}E^{M}LQD^{M}K^{M}	2159.9377	3
K. FQS^{P}E^{M}E^{M}QQQTE^{M}D^{M}E^{M}LQD^{M}K^{M}	2159.9377	2
K. FQSE^{M}E^{M}QQQTE^{M}D^{M}E^{M}LQD^{M}K^{M}	2061.9614	2
K.IE^{M}KFQS^{P}E^{M}E^{M}QQQTE^{M}D^{M}E^{M}LQD^{M}K^{M}	2544.1749	3
α-S2-casein		
R.E^{M}QLS^{P}TS^{P}E^{M}E^{M}NSK^{M}	1467.5650	2
K.TVDME^{M}S^{P}TE^{M}VFTKK^{M}	1650.7695	2
K.TVDME^{M}STE^{M}VFTKK^{M}	1552.7931	2

Sequences in single letter amino acid code. ^{M} = methylated residue, ^{P} = phosphorylated residue.

The mono-phosphopeptide from β-casein was detected in several forms. The fully digested peptide was detected in both phosphorylated and unphosphorylated forms and the phosphorylated form in both doubly and triply charged variants. One peptide was the result of an incomplete digest (2544.1749 Da) and is the fully methylated, phosphorylated, triply charged form. Two different peptides were detected from α-casein. This is a contaminant derived from casein, the parent protein to both β and α-casein. A singly phosphorylated peptide of 1650.7695 Da and a doubly phosphorylated peptide of 1467.5650 Da were detected. From these data, it can be concluded that use of more advanced mass spectrometry techniques significantly improves the number and type of captured phosphopeptides that can be detected.

5.3.6 Identification of phosphorylated proteins in dialysate

A preliminary analysis was conducted to determine whether phosphorylated peptides could be captured from dialysate. Figure 5.13 shows a representative MALDI-TOF MS profile obtained from 1 mg methylated trypsin-digests of dialysate collected during the first 30 minutes after injury.

The MALDI-TOF MS profiles of peptides from methylated dialysate were dominated by a peak at *m/z* 1927 $[M+H]^+$. The abundance of this peptide and other peaks, at *m/z* 1495, 1665, 1728 $[M+H]^+$ have suppressed the detection of less abundant components. In Figure 5.13b, there are more higher molecular mass peptides such as those at *m/z* 2356, 2656 and 2864 $[M+H]^+$. Those lower molecular mass peaks shared with the first sample (Figure 5.13a) are less abundant, but still present.

Figure 5.14 shows the peptide profiles of dialysate captured by the two phosphopeptide enrichment methods.

The peak at *m/z* 1927 $[M+H]^+$ which dominated the methylated dialysate spectrum was not present in either captured sample. Many more peaks were detected in the captured samples, demonstrating the suppressive effects of the abundant ions seen in the methylated spectra, prior to capture. Peaks detected from both capture methods include those at *m/z* 955, 1028, 1177, 1571, 1653, 1667, 2655, 2669 and 2683 $[M+H]^+$. The latter three are likely to be methylation variants of the same peptide as they are each 14 Da apart.

No peptides were identified using electrospray ionisation (ESI) LC-MS/MS on the Q-TOF Global Ultima, so the phosphopeptides captured by dendrimer conjugation from a second sample of dialysate were identified using an LTQ-orbitrap mass spectrometer. Table 5.10 lists those peptides in which potentially novel phosphorylation sites were identified.

Three phosphopeptides were confirmed in dialysate, one from an albumin variant, at S277, and two from apolipoprotein L1 at S311 and S314. MS^3 data provided confirmatory information for the apolipoprotein L1 phosphorylation site identifications (Figure 5.15 and Table 5.11).

MS^2 analysis shows the position of the *y* ion terminating in a phosphorylated serine.

(a)

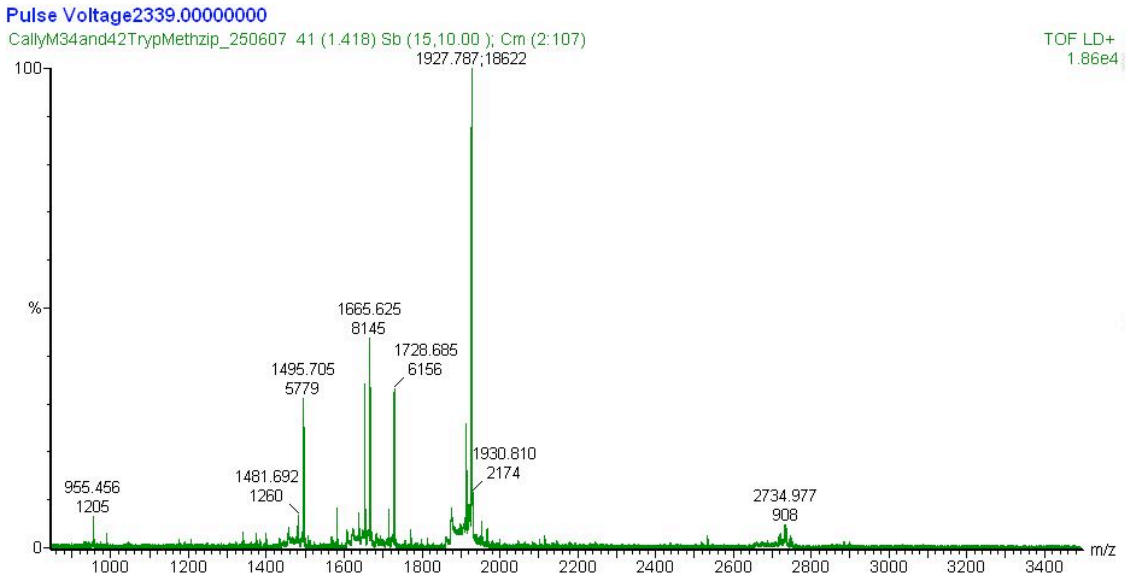

(b)

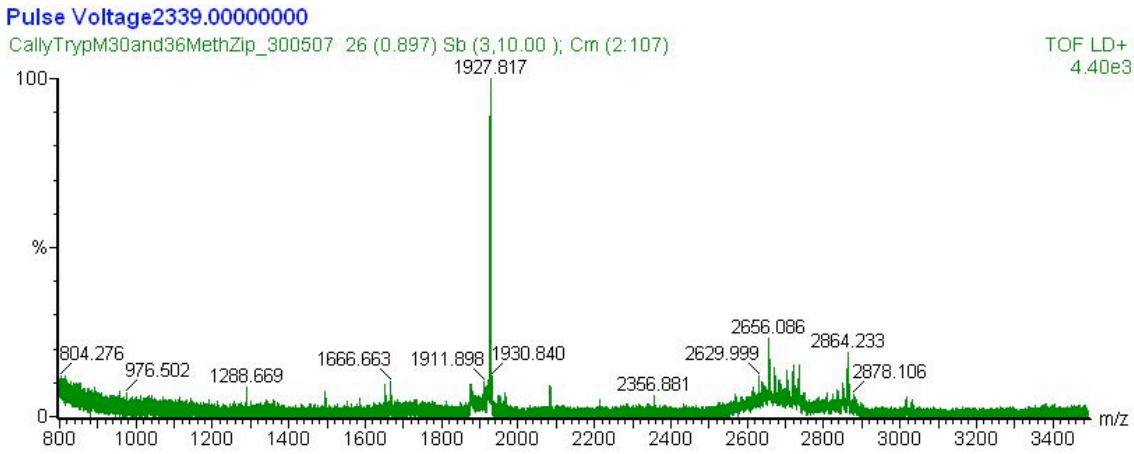

Figure 5.13: **MALDI-TOF MS profile of methylated peptides from dialysate.** Methylated peptides derived from a tryptic digest of dialysate pooled from two volunteers prior to a) TiO_2 and b) dendrimer capture. The starting concentrations were $\sim$ 800 μg total protein.

(a)

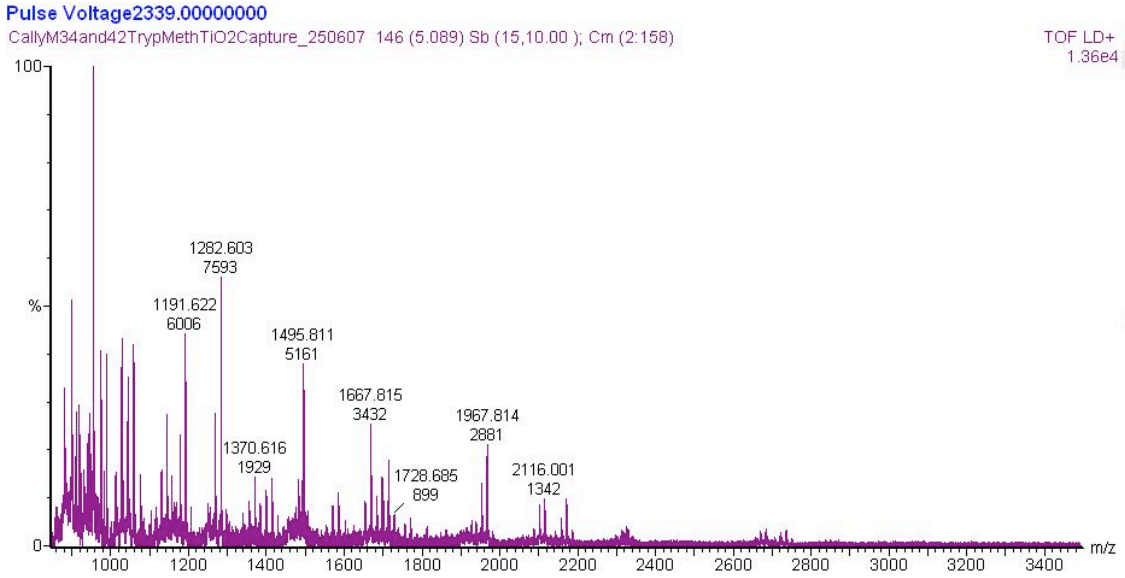

(b)

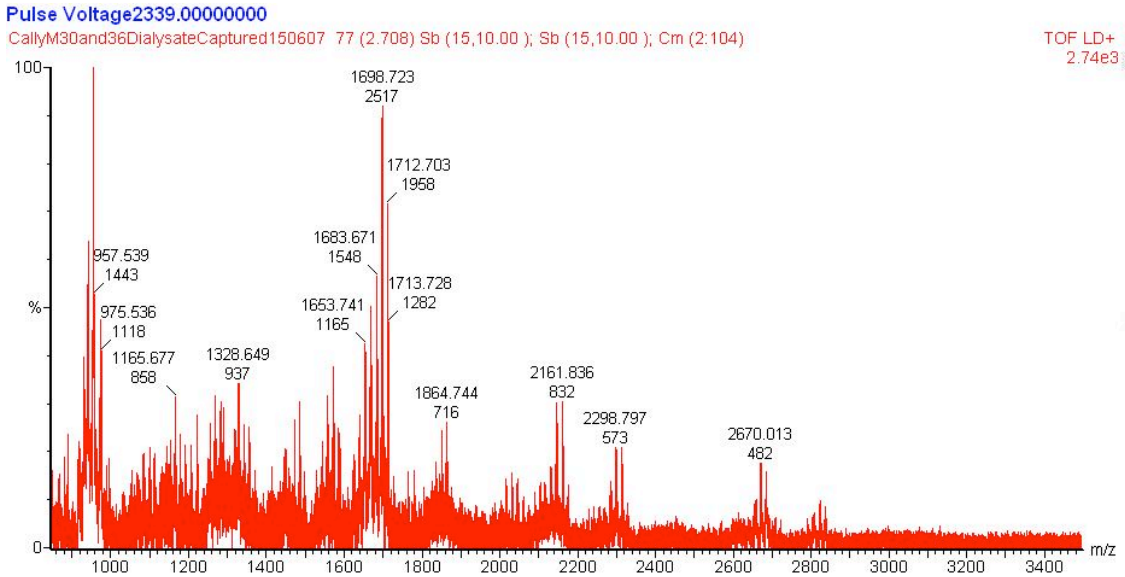

Figure 5.14: **MALDI-TOF MS profiles of peptides captured from dialysate by TiO_2 and dendrimer methods.** Peptides captured from methylated trypsin digest of dialysate samples, shown in Figure 5.13, by a) TiO_2 beads and b) dendrimer conjugation.

(a)

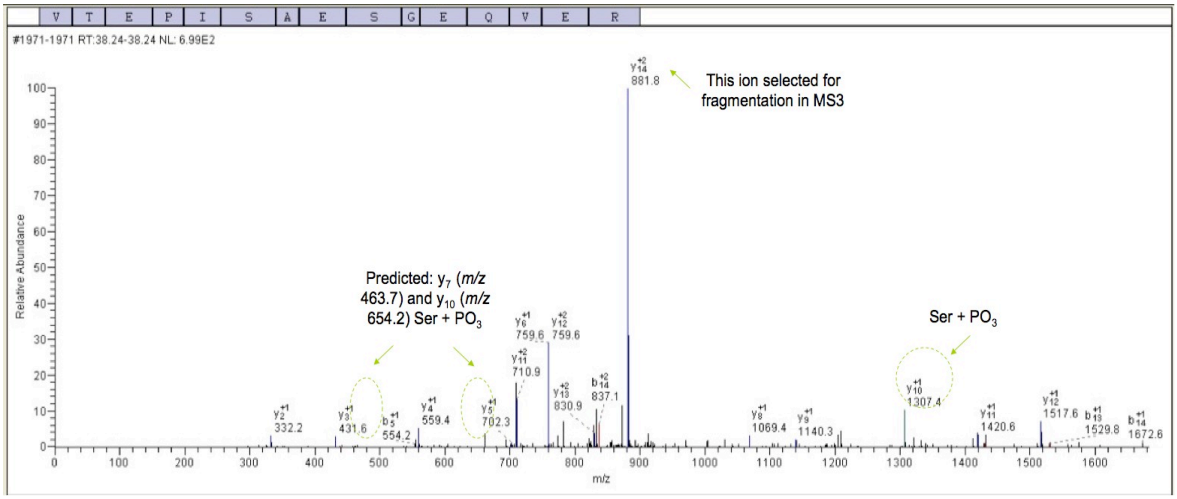

(b)

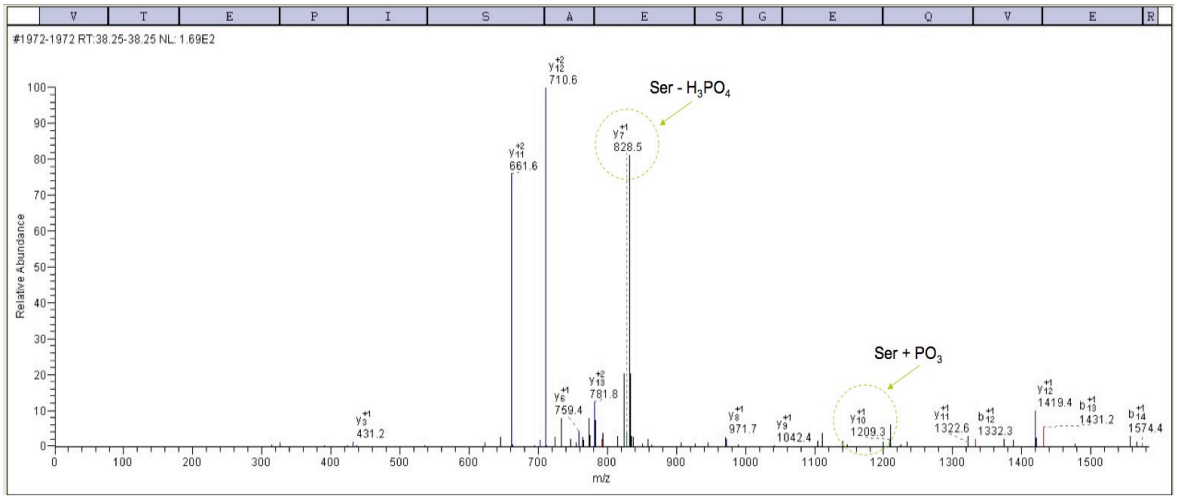

Figure 5.15: **LTQ-orbitrap mass spectra showing fragmentation of the phosphorylated apolipoprotein L1 peptide.** Mass spectrum showing the y and b ion series obtained from fragmentation of the apolipoprotein L1 phosphopeptide, in (a) MS^2 and (b) MS^3. The MS^2 data shows the predicted position of peaks for y ions with terminal phosphorylated serine residues. MS^3 confirms the presence of the y_7 and y_{10} ions, the former having lost phosphoric acid (98 Da) and the latter retaining its phosphate (see Table 5.11).

Table 5.10: **Phosphopeptides identified from a dendrimer capture of dermal dialysate by Orbitrap analysis containing novel phosphorylation sites**

Peptide	**Mass (Da)**	**Charge**
Apolipoprotein L1		
R.VTE^{M}PIS^{P}AE^{M}S^{P}GE^{M}QVE^{M}R^{M}.V (306 – 320)	1860.8028	2
R.VTE^{M}PIS^{P}AE^{M}SGE^{M}QVE^{M}R^{M}.V(306 – 320)	1762.8265	2
Serum Albumin		
K.LVAAS^{P}QAALGL^{M} (273 – 283)	1027.6146	2

Sequences in single letter amino acid code. ^{M} = methylated residue, ^{P} = phosphorylated residue. Data obtained from a demonstration experiment so may not be the full list of identifications.

Fragmentation of the y_{14} ion at m/z 881.8 $[M+2H]^{2+}$ in MS^3 showed evidence of two phosphorylated serine residues. The difference of 167 Da between the y_{10} and y_9 fragment ions corresponds to the loss of a phosphorylated serine. In contrast, the difference of 69 Da between the y_8 and y_7 fragment ions corresponds to the loss of a serine residue that had previously lost phosphoric acid (98 Da), for example, during MS^2 fragmentation.

The phosphopeptide identified from the albumin variant also corresponds to the full sequence of human serum albumin. This entire variant sequence was found to comprise residues 333 – 609, placing the phosphorylation site at S603. The albumin phosphorylation site is not listed within the corresponding entry on www.phosphosite.org, and hence represents a novel phosphorylation site. Phosphorylation at S311 of apolipoprotein L1 has previously been confirmed, while the site at S314 has not (Mancone *et al.*, 2007). This is a second novel phosphorylation site detected in dermal dialysate.

The 3-D structure of apolipoprotein L1 has not yet been solved, so it is not possible to show the location of the phosphorylation site. However, such data is available for the albumin peptide. Figure 5.16 shows the location of the novel phosphorylation site

Table 5.11: **Ion series obtained from MS^2 and MS^3 analysis of captured dialysate proteins using an LTQ-orbitrap mass spectrometer**

MS^2					MS^3				
†	***b* ion** (m/z)	**End Residue**	***y* ion** m/z			***b* ion** (m/z)	**End Residue**	***y* ion** m/z	
1	50.5415	V	—	15	1	100.757	V	—	15
2	101.0653	T	881.3708	14	2	201.1234	T	1663.7580	14
3	172.5944	E^M	830.8470	13	3	344.1816	E^M	1562.7103	13
4	221.1208	P	759.3179	12	4	441.2344	P	1419.6521	12
5	277.6629	I	710.7915	11	5	554.3184	I	1322.5993	11
6	361.1620	S^P	654.2494	10	6	721.3168	S^P	1209.5153	10
7	396.6806	A	570.7503	9	7	792.3539	A	1042.5169	9
8	468.2097	E^M	535.2317	8	8	935.4121	E^M	971.4798	8
9	551.7089	S^P	463.7026	7	9	1004.4342	S^P	828.4216	7
10	580.2196	G	380.2034	6	10	1061.4556	G	759.3995	6
11	651.7487	E^M	351.6927	5	11	1204.5139	E^M	702.3781	5
12	715.7780	Q	280.1636	4	12	1332.5725	Q	559.3198	4
13	765.3122	V	216.1343	3	13	1431.6409	V	431.2613	3
14	836.8414	E^M	166.6001	2	14	1574.6991	E^M	332.1928	2
15	—	R^M	95.0709	1	15	—	R^M	189.1346	1

† = Residue number, ^{P} = potentially phosphorylated residue, ^{M} = methylated residue. Blue text indicates confirmed *y* ions, red text indicates confirmed *b* ions, green text indicates loss of 98 Da corresponding to phosphoric acid.

within the 3-D structure of the serum albumin.

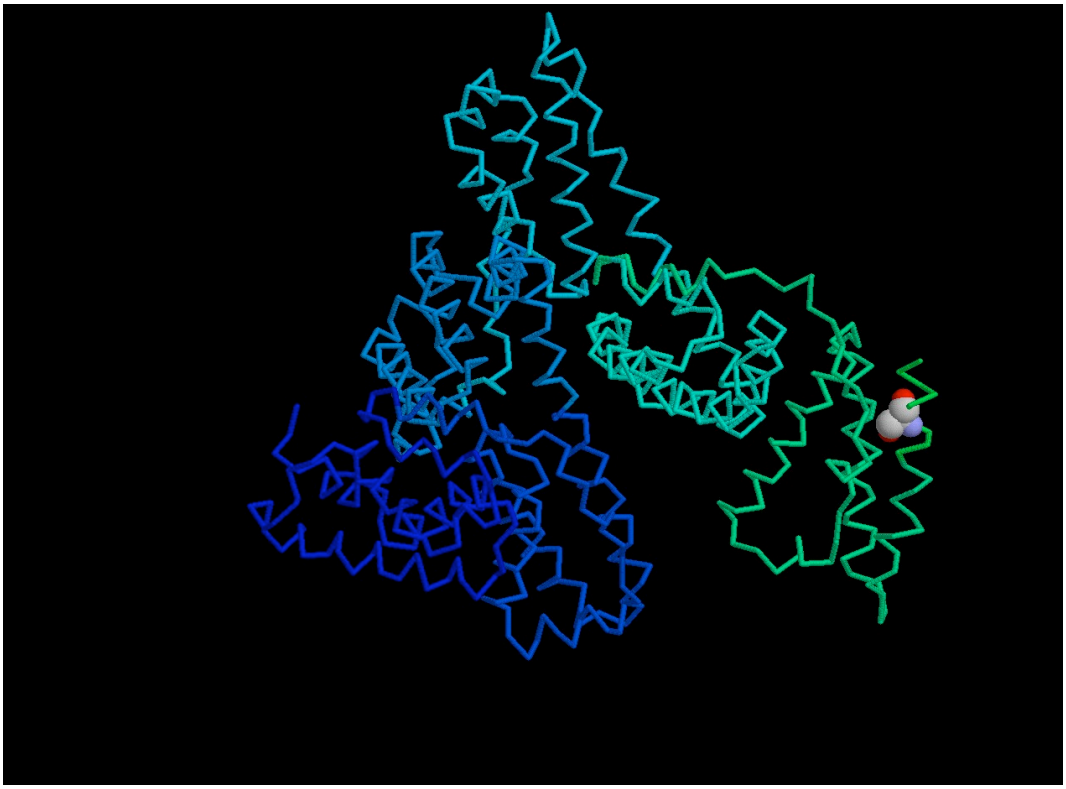

Figure 5.16: **Three-dimensional structure of human serum albumin protein showing the novel phosphorylation site.** The image shows the carbon backbone of the protein, coloured from dark blue at the N' terminus through to green at the C' terminus. The serine found to be phosphorylated in the present study, S603, is shown in a ball structure near the C' terminus. Image generated using Rasmol.

The figure shows the 3-D structure of serum albumin, with the binding-site indicated by the cleft between the two sides of the molecule. The newly-identified phosphorylation site, serine 603, is shown in a ball format, close to the C' terminus on the outside of the molecule. The significance of the location of this phosphorylation site will be considered in Section 5.4.5.

5.4 Discussion

Reversible protein phosphorylation is a key regulatory process that to date has primarily focused on studies within cells, as opposed to the extracellular environment. This chapter describes studies to compare three methods for the identification of phosphorylated proteins; it also describes the first attempts to study protein phosphorylation in dermal dialysate samples. One method for studying protein phosphorylation was found to be unsuitable, while the remaining two were found to be complementary. Using these two methods to enrich for phosphopeptides within dermal dialysate samples, two novel phosphorylation sites were detected.

5.4.1 Use of ProQ Diamond staining for phosphoprotein detection

The results of the phosphoprotein staining experiments were rather disappointing, but not unexpected. There was a 32–fold difference between the highest and lowest protein concentrations detected (1.25 – 40 μg), but only a $\sim$3–fold difference in staining intensity with ProQ Diamond across that range. This is in contrast to the $\sim$5 – fold difference in staining intensity with Sypro Ruby with equivalent concentrations. The minimum detection limit of 1.25 μg phosphoprotein with ProQ Diamond is high in biological terms and was unlikely to be encountered in dialysate samples.

The very low intensity values obtained for ProQ Diamond staining compared to measurements of total protein by Sypro Ruby are unlikely to be due to loss of phosphorylation. Mass spectrometric analysis of a sample of β-casein from the same batch indicated that the protein is found almost exclusively in its phosphorylated form from this source. The non-phosphorylated form is easier to ionise and hence is likely to be easier to detect than the phosphorylated form. Therefore, partial phosphorylation of the β-casein is unlikely to explain the discrepancy between the amount of protein detected by ProQ Diamond and Sypro Ruby. The low staining efficiency could be a consequence of the differing accessibility of the phosphate group. However, within the gel, the protein is unlikely to be folded such that the phosphate group is obscured from

a molecule as small as a dye.

Several reviews, including that by Delom & Chevet (2006), have concluded that in-gel phosphoprotein stains such as ProQ Diamond are not sensitive enough for comprehensive phosphoproteome analysis. Furthermore, recent reports suggest that the stain may not be absolutely specific for phosphoproteins, for example El-Khatib, Good & Muench, (2007), Gorg, Weiss & Dunn, (2004) and Murray *et al.*, (2004). Taken with the results from this study, it appeared that more efficient methods were required.

5.4.2 Phosphopeptide enrichment by TiO_2-affinity capture

Phosphopeptide enrichment using the TiO_2-affinity method was a significant improvement on the use of a phosphoprotein stain for detection of β-casein phosphorylation. This method was able to detect phosphopeptides from the lowest concentration tested, 80 ng, confirming it to be more sensitive. At face value, however, it did not appear to be very specific, with several unexpected and unidentified peaks dominating the spectrum. Peptide sequence data could not be obtained using MALDI-TOF MS, but potential matches could be manually assigned to almost all of these peptides when methylation variants were considered. Significantly, the peak at m/z 2042 $[M+H]^+$ could not be assigned to any variants of any of the expected phosphopeptides or non-phosphorylated peptides. While it is possible that the unidentified components represent novel phosphopeptides, it is equally possible that they are not phosphorylated. The existance of methylation variants supports the points raised by Larsen *et al.* (2005) regarding the complexity introduced by incomplete methylation.

Overall, four different potential phosphopeptides were identified out of 20 possible matches, if the contaminant proteins are included. In comparison, Larsen *et al.* (2005) found 9 different phosphopeptide variants from a list of 23 potential sequences, with an additional 9 peptides that were not thought to be phosphorylated. In the present study, the mono- and tetra- phosphopeptides from β-casein were present as expected, although at surprisingly low abundance. The other two were potential matches for phosphopeptides from α-S1 and S2-casein, contaminants derived from the purification process. Four peaks could not be assigned, one large and three small in intensity.

The detection of contaminants derived from the parent protein suggests that this method is very sensitive. However, the detection of equal numbers of unidentifiable peptides compared to known phosphopeptides also indicates that it may not be very specific. The TiO_2 technique is discussed further, in comparison to the dendrimer method and with regards to LC-MS/MS analysis in Section 5.4.4.

5.4.3 Optimisation of dendrimer conjugation chemistry for phosphopeptide enrichment

Initial experiments to capture purified phosphopeptides using the original, published dendrimer conjugation chemistry method were unsuccessful. Through a series of optimisation experiments, the method has been improved and successfully applied to both purified phosphopeptides and more complex samples containing a mixture of several proteins, as well as for the preliminary analysis of biological samples.

Two early optimisation steps to reduce the amount of dendrimer lost through the filter unit were not presented in the results section, but merit a brief consideration here. Lyophilisation of the first wash filtrate revealed dendrimer (Sigma) present in the wash-through. The filter unit's molecular weight cut-off value of 5 kDa reflects the average, rather than the maximum size of molecule that can pass through. It can generally be expected that molecules up to three times this value can cross the membrane. However, the mass of the dendrimer compound should have been 29 kDa, which meant they should not have been able to pass through. Several different filter units were tested, with the same result. One-dimensional SDS PAGE revealed that the dendrimer had degraded and was present in two forms, including a band at 15 kDa which could potentially pass through the filter. As an alternative source, Dendritic Nanotechnologies, the original manufacturer, were able to supply the dendrimers direct. These were a great improvement, with little to no dendrimer found in the wash-through.

One of the most significant problems with the published method was that it produced highly abundant contaminant peaks within the low m/z range of the MALDI-TOF MS spectra of captured peptides. The regular spacing of these peaks suggested

that they might be polymers and their appearance solely in the captured samples suggested that the source was most likely to be the filter unit or the dendrimer. Further studies confirmed this hypothesis and showed that alternative filter units gave worse results. Although alternative solvent combinations were not exhaustively tested, further experimentation is likely to only give slight improvements. The combination of the methanol and water solvent wash scheme and incorporation of a pre-wash step gave a satisfactory resolution to this problem.

Use of the DHBA-based matrix improved the detection of the mono-phosphopeptide and enabled detection of the tetra-phosphopeptide by MALDI-TOF MS. The reasons for this improvement are unknown, highlighting the present lack of knowledge about suitable matrix preparations and an inability to rationally predict behaviour of such compounds. Recently, Jaskolla *et al.* (2008) attained a significantly improved sensitivity and peptide recovery through use of a modified α-cyanocinnamic acid matrix. Sequence coverage of bovine serum albumin was increased from 4 % with the α-cyano-4-hydroxycinnamic acid matrix to 48 % with the 4-chloro-α-cyanocinnamic acid matrix. The authors suggest that the lower proton affinity of the latter preparation improve the ionisation of basic peptides. It is possible that the low coverage of phosphopeptides captured from β-casein and the five-protein mix is a consequence of sub-optimal matrix conditions. These observations suggest that further work to optimise matrices for peptide and phosphopeptide analyses are likely to prove worthwhile.

The final problem with the initial dendrimer method was the loss of methylation after the conjugation reaction. Re-methylation of captured samples reduced the complexity of the mass spectra and hence increased the signal intensity of the fully methylated peptides by approximately 2–fold. The loss of methylation can be explained by reports that the carbodiimide component can hydrolyse the methyl esters (Guo, Galan & Tao, 2007). This loss of methylation is important, as the carboxyl groups may become available for non-specific binding. It was not, however, limited to the dendrimer technique – loss of methylation was also observed in the TiO_2-captured samples. That re-methylation improves this situation suggests that this is an actual loss of methyl groups, not a bias towards peptides without full methylation. Methylation neutralises

the charge associated with the carboxyl groups, which should also improve ionisation. However, the additional lyophilisation steps that are necessary to the re-methylation process lead to loss of peptide by adsorption. Consequently, this step is only recommended for cases where the fully methylated peptide is not dominant or where there is clear spreading of the signal over peaks differing by units of 14 Da.

It appears that the optimised dendrimer method has improved on the original method (Tao *et al.*, 2005), in terms of reduced contaminants and detection of the tetra-phosphopeptide shown in the comparison with TiO_2. However, as highlighted by the differences in results obtained from different mass spectrometers, it is not appropriate to compare the results directly. The different analysis conditions and machine used will have influenced the spectra obtained. Instead, the type of mass spectrometer employed is a more appropriate consideration. The use of MALDI-TOF-MS provided a simple method of confirming that known peptides were being captured. Once variables were introduced, including even the methylated peptides from β-casein or the five-protein mix discussed in the next section, peak assignment became more ambiguous and further analysis to confirm the peptide identity and phosphorylation site or sites was required. Liquid chromatography coupled with tandem mass spectrometry on a Q-TOF instrument identified only the mono-phosphopeptide in both samples of β-casein alone, or in the five-protein mix. The use of an LTQ-orbitrap system significantly increased the number of phosphopeptides identified in the captured sample. This was most likely due to the improved ionisation methods, additional MS dimensions and the dynamic exclusion technique that prevents re-analysis of abundant peaks in the same MS/MS scan. These factors mean that the LTQ-orbitrap is currently the most efficient method for analysis of protein phosphorylation of those examined.

5.4.4 Assessment of the comparison of TiO_2 and dendrimer captures

The dendrimer method clearly benefits from less non-specific binding and less contamination than the TiO_2-affinity method, with only expected phosphopeptides or

their methylation variants detected. It also appears to be more efficient as recovery of the mono-phosphopeptide from β-casein was approximately 2.3–fold higher for the dendrimer method; ≈5900 AU compared to ≈2940 AU with TiO_2. Very few of the different expected phosphopeptides were detected in either capture. This may be a result of there being twice the concentration of peptides from the β subunit of casein, as it was included as both a subunit of whole casein and in the purified form. However, this explanation seems unlikely given that the largest peak in the dendrimer-captured profile corresponds to a methylation variant of an α-S2-casein phosphopeptide.

The TiO_2–affinity method did capture the fully methylated form of the tetra-phosphopeptide from β-casein and hence may be more effective at capturing multiply phosphorylated proteins. This observed difference between the capture profiles from the two methods may be a chance occurence, that is, a consequence of the low ionisation efficiency of multiply phosphorylated peptides in particular. The capture of multiply phosphorylated peptides was not improved by LC-MS/MS analysis, which also biases against such peptides, due to the ionisation process favouring positive ions. Only the mono-phosphopeptide from β-casein was detected from both capture samples by this analysis. Unfortunately, it was not possible to analyse these samples using the LTQ-orbitrap mass spectrometer, which potentially would have been useful given the additional identifications made from the dendrimer-captured β-casein sample (Table 5.9). The results obtained from both MALDI-TOF and LC-MS/MS analyses suggest that both capture methods should be used to gain a more comprehensive coverage of the phosphoproteome.

Bodenmiller *et al.* (2007) published a comparison between TiO_2 affinity, phosphoramidate chemistry and IMAC for phosphopeptide capture. The phosphoramidate chemistry that was used was a variation on the dendrimer technique used by Tao *et al.* (2005), in which cystamine was used in place of the dendrimer. Assessment of the reproducibility showed phosphoramidate chemistry to be slightly more reproducible (96.2 % internal similarity, compared to 95.7 % for TiO_2 and 93.9 % for IMAC) in terms of retention and intensity. It also displayed the highest overlapping of features; 80 %, compared to 76, 74 and 85 % for TiO_2, IMAC and the starting sample respec-

tively. Importantly, overlap between the three methods was relatively low at ∼35 %. This difference could not be accounted for by inclusion of non-phosphorylated peptides isolated by non-specific binding, suggesting that a combination of methods is required for comprehensive phosphoproteome analysis.

5.4.5 Preliminary analyses of protein phosphorylation in dermal dialysate samples

Analysis of protein phosphorylation in dermal dialysate revealed two novel phosphorylation sites; S314 in apolipoprotein L1 and S603 in serum albumin. Dialysate samples obtained during the first 30 minutes after injury were digested, methylated and subjected to phosphopeptide enrichment by either TiO_2-affinity or dendrimer capture. The captured samples were analysed by MALDI-TOF MS to determine whether there were peptides present. Identification of phosphopeptides captured from dialysate using the dendrimer conjugation method was performed using LTQ-orbitrap mass spectrometry.

The two pooled dialysate samples produced similar digest profiles. The same dominant peaks were observed in each sample, but at different relative intensities. This appears to suggest that the profiles of peptides in the digests are consistent between volunteers. However, due to the high abundance of albumin, these profiles are likely to show predominantly albumin peptides and hence appear very similar. The other components will be at a lower abundance and therefore suppressed by the higher abundance components. This should not have presented a problem with the captures, as only those peptides that are phosphorylated should bind.

A theoretical digest of human serum albumin shows that at least three of the dominant peptides could be derived from albumin. Those at *m/z* 1495, 1665 and 1927 $[M+H]^+$ correspond to the mass of the fully methylated forms of $RHPD^MYSVVLLLR^M$ (residues 361 – 372), $KVPQVSTPTLVE^MVSR^M$ (438 – 452) and $RHPYFYAPE^M$ $LLFFAK^M$ or $HPYFYAPE^M$ $LLFFAKR^M$ (169 – 183/ 170 –184), respectively. Neither are known to be phosphorylated.

The number of peaks in the captured dialysate spectra was increased compared to

before capture, for both methods. None of those peaks dominant in the methylated dialysate spectra prior to capture were present in the captured samples. The peak at *m/z* 1667 $[M+H]^+$ could either have been revealed by the removal of the one at *m/z* 1665 $[M+H]^+$, or could be the same peptide shifted slightly due to day-to-day machine variation.

The profiles of the captured samples contained many more peaks than observed in the methylated digests before enrichment. They shared several features, as listed previously, but showed more differences than similarities. This could be the result of several factors. First, the two different capture methods will have different specificities and differing abilities to access phosphorylation sites (see Bodenmiller *et al.*, 2007). Secondly, these captures were not from a common starting sample and although the starting profiles contained very similar components, it is likely that the less abundant components differed slightly. Finally, the samples were analysed on different days. Day-to-day variability in the MALDI-TOF MS instrumentation means that there is the possibility of slight differences (<2 Da) in the *m/z* values of a peptide on different days, depending on the calibration.

It is not possible, from the MALDI spectra, to be certain that all the peptides captured were actually phosphorylated. A common method of confirming phosphorylation status is to treat the sample with a phosphatase enzyme to remove the phosphate group prior to re-analysis, looking for the corresponding loss of 80 Da (phosphate) or 98 Da (phosphoric acid). Experiments to dephosphorylate the captured samples had mixed success (data not shown). The main problem was the loss of signal caused by the additional processing and lyophilisation steps on an already small amount of sample. However, further work in this area together with LTQ-orbitrap analysis would help assign the unknown peaks.

Analysis of dendrimer-captured dermal dialysate samples using LTQ-orbitrap enabled identification of potentially novel phosphorylation sites in both serum albumin and apolipoprotein L1. Unfortunately, due to the analysis using the LTQ-orbitrap instrument being part of a demonstration, only select data were obtained. It is therefore not known whether additional phosphopeptides or any of the other albumin phospho-

rylation sites were detected. None of the phosphorylation sites listed in Table 5.1 were detected. This is most likely a consequence of the relative abundance of serum albumin and the very small sample sizes used. However, the samples used were selected for their high protein content, including serum albumin which was known to contain phosphorylation sites. Another factor which is likely to have contributed to the low number of phosphopeptides was that phosphatase inhibitors were not used in this preliminary study. Their use in future experiments could increase the number of phosphopeptides captured.

The novel phosphorylation sites identified in this study could represent modifications that occur specifically within the skin, or in response to injury. However, as novel identifications, their functions and related kinases are not yet known. Apolipoprotein L1 has previously been classed as a potential biomarker for fibrosis, due its reduced expression in serum samples from liver cirrhosis patients, compared to healthy controls (Gangadharan *et al.*, 2007). Within the last few months, it has emerged as an inducer of cell death, itself induced by cytokines IFN-γ and TNF-α (Zhaorigetu *et al.*, 2008). However, the function of the phosphorylation is unknown, and the absence of a solved 3-D structure makes it difficult to predict any potential functions. The location of S603 of serum albumin on the external face of the molecule suggests that it is unlikely to be involved in regulation of protein binding from within the binding site itself. It could alter protein binding through allosteric interactions. The identification of novel phosphorylation sites in plasma proteins sampled from a non-plasma source makes it tempting to speculate that these proteins are phosphorylated within the skin in response to injury. Further work is needed to better characterise these and other phosphorylation sites from proteins identified in dermal dialysate, as well as potential interaction partners, to determine the significance of these findings.

5.4.6 Summary

The aim of the research presented in this chapter was to investigate post-translational modifications, specifically protein phosphorylation, in dermal dialysate collected during the response to injury. To achieve this, three leading methods of phosphorylation

analysis were evaluated, in-gel staining, TiO_2-affinity chromatography and a chemical derivatisation method, dendrimer conjugation chemistry. The phosphoprotein gel stain was found to be unsuitable, but the remaining two methods were complimentary, once optimised. Optimisation of the dendrimer conjugation chemistry method gave improved specificity over the TiO_2 bead method, although it has not been confirmed whether the tetra-phosphopeptide could be captured using this technique. The LTQ-orbitrap mass spectrometry system was found to be the most effective method for phosphopeptide characterisation, giving the highest number of phosphopeptides identified. Preliminary analysis of protein phosphorylation in dermal dialysate samples was successful and two potentially novel phosphorylation sites were discovered. The identification of these novel phosphorylation sites provides scope for further investigation to determine whether these modifications serve a purpose specific to the cutaneous response to injury.

Chapter 6

General Discussion

It is becoming increasingly clear that the inflammatory phase of the injury response is critical to healing outcome. The mediators that control the progression of the inflammatory response have been partially characterised, such as cytokines and growth factors, but this has failed to lead to satisfactory therapeutic interventions.

The current understanding of the response to injury has been developed incrementally by studying specific markers that are predicted to identify a current stage in the progression of the response, or to have an involvement in the regulation. The present research tested the hypothesis that a more global approach to the characterisation of soluble components present within the wound environment, using shotgun proteomics, could potentially identify novel biomarkers of the injury response.

Existing injury models can provide protein-containing fluids for analysis, but are limited in that one injury gives only one sample for analysis. Instead, a model was required in which the same injury could be sampled more than once in order to study the progression of the inflammatory response over time. Therefore, one of the primary aims of this research was to develop and characterise a model of skin injury from which unknown components could be sampled continuously, and catalogued in order to identify potentially novel markers of the injury response. The microdialysis injury model was chosen for its ability to combine injury and sampling, as well as its applicability to other tissues. With this method, it was possible to sample the injured tissue continuously without causing additional trauma, which could potential modify

the response.

Characterisation of the microdialysis injury model using known markers of inflammation fulfilled the second aim of this thesis, showing that it produced a response comparable to existing models and that a protein-rich fluid could be obtained. Dermal microdialysis and proteomics had not been combined previously, so it was first necessary to determine the types of proteins contained within dialysate. Thus, the third aim of this research was to catalogue the proteins that could be identified using these techniques. The proteins identified were predominantly abundant plasma proteins with roles in different aspects of the response to injury and inflammation. Further characterisation was achieved by investigating post-translational protein phosphorylation, the final aim, in which potentially novel phosphorylation sites were discovered.

6.1 Is microdialysis probe insertion an appropriate model of injury?

Much of the research into the response to injury and subsequent wound healing has been conducted in animals. While this provides an important insight into conserved responses, there still remain subtle differences between model animals, and human patients. It is therefore beneficial to develop models of studying injury responses in human volunteers. Existing models, such as the incisions and skin biopsies used in animal experiments, have seen limited use in human studies. Several disadvantages for each model, e.g. discontinuous sample, has prompted a search for an alternative. The first aim of this project was to develop and characterise a model of injury in skin that would provide a protein-rich fluid, representative of the interstitium, for analysis.

Microdialysis was chosen as the method by which solutes from the interstitium could be sampled continuously, for reasons detailed in Chapter 1. This also provided the means of injuring the skin and removed the potential for additional damage associated with isolating the injured tissue for analysis, as with incisional and excisional wound models. The main advantages of the microdialysis injury model over existing methods is that it generates a reproducible trauma whilst incorporating a sampling

method that is both local and minimally invasive. This method also enables a flexibility in the time-course that can be sampled, to balance protein requirements with temporal resolution. Furthermore, the injury caused by the probe insertion process is relatively small and most volunteers heal without visible scarring (Clough, personal communication; personal observation), an advantage in human studies where cosmetic outcome is of importance.

The three hour time course was chosen for the present study because it was known that cytokines were recovered in dialysate samples within this time, thus indicating that the inflammatory response was underway. This meant that haemostasis and the initiation of the inflammatory response, and therefore potential markers of these processes, would be sampled. The temporal flexibility of microdialysis sampling means that this time course could be extended or altered in future experiments, either to follow the progression of the response further, or to increase the temporal resolution. Changing temporal resolution will have no impact on the tissue, but the injury response is likely to have an impact on the recovery of solutes over time. This is initially due to blockage of the pores of the probe by larger solutes or complexes. Over the following days, the tissue remodels itself and further blocks pores with new connective tissue (Wang *et al.*, 2007).

The vascular response to the injury was very similar to that seen in previous microdialysis experiments (Anderson, Andersson & Wärdell, 1994 and Groth & Serup, 1998), although data on the vascular response to other incision models are unavailable. Therefore, it was more informative to consider the content of the dialysate samples to determine whether microdialysis is an appropriate model of injury.

6.2 Is dialysate an appropriate source of potential biomarkers of the response to injury?

Physically, the injury caused by microdialysis probe insertion is similar to an incision, because no tissue is removed. The difference between the microdialysis insertion model and incisional wounds is that the insertion of the guide needle primarily damages

the dermis. The epidermis is only damaged at the entrance and exit sites, compared to a typical incision which bisects the epidermis across the full length of the wound. This may reduce the number of damaged keratinocytes, and therefore the release of stored cytokines necessary for initiating the injury response. The concentration of IL-6 measured in the present study was comparable to levels found in murine incisional wound studies (Bryan *et al.*, 2005) and other human microdialysis studies (Angst *et al.*, 2008; Clough *et al.*, 2007), but higher than in excisional wounds in human suction blister and skin biopsy controls (Deerman *et al.*, 2004; Van Der Laan, de Leij & ten Duis, 2001).

Analysis of the cytokine content of dialysate showed that there was an inflammatory response to microdialysis probe insertion (Chapter 3). However, cytokines are not the only mediators involved, and cannot give a complete picture of the processes that occur. A survey of the protein content of dialysate was performed to give a broader characterisation of the components that may be active within the injury environment. The shotgun proteomic analysis of dermal dialysate conducted as part of this research shows that it contained many proteins relevant to the processes that occur as part of the injury response, both extra- and intracellular in origin, as discussed in Chapter 4.

Considerably fewer proteins were identified in the dermal dialysate, even after depletion of highly abundant proteins. Since the same shotgun approach and instrumentation have yielded many more components in other biofluids, the difference in the number of proteins identified is likely due to the differences in the protein content of the sample, and the types of proteins recovered by each approach. Also, the generation of blisters causes greater stress on the tissue and hence an increased leakage of plasma proteins that contaminate the interstitial fluid (Kool *et al.*, 2007). Their collection in the blister fluid is not inhibited by diffusion into a probe, as is the case with microdialysis. The number of proteins found in dermal dialysate was comparable to the number found in cerebral dialysate (Maurer *et al.*, 2003). The 14 % increase in dermal dialysate identifications may be due to the use of 1-D SDS-PAGE as a primary separation technique in the present study, rather than 2-D gel electrophoresis used in the brain study, which may bias against insoluble proteins or those that exist below the sensitivity level

of the staining. However, the latter is unlikely to have been a major problem, given that the sensitivity of the silver stain used is within the nanogram range (Blum, Beier & Gross, 1987). It is most likely that this difference is a function of either the mass spectrometry used or the protein content of the different tissues analysed.

Despite the apparent simplicity of dermal dialysate proteome the list is unlikely to be comprehensive. This is shown by the detection of cytokines in the present study when using antibody detection methods (Chapter 3), but not when using mass spectrometry.

Additional work with dermal dialysate conducted within the Centre for Proteome Research has used a gel-free method for identification of proteins, known as iTRAQ (Applied Biosystems). With this approach, more than 60 additional proteins were identified, without using depletion (Parkinson, personal communication). Many are variants of proteins found in the present study; for example, two additional apolipoproteins and seven further keratins. This increase is also due, in part, to the larger sample number and differences in the processing and analysis, including the omission of the depletion and gel stages, and the different mass spectrometry experiments performed. The experiments showed the presence of further relevant proteins including fibrinogen and vitronectin, involved in promoting coagulation, and kininogen-1, a precursor to bradykinin, also known to have a variety of effects in inflammation, including modulation of vascular permeability. Also identified were some of the highly abundant proteins specifically depleted in the present study, including serum albumin, transferrin and several immunoglobulin variants.

While the protein content of the dialysate samples (Chapter 4) was compiled from only two experiments, the overlap between this and the iTRAQ study shows that the proteome collated in the present study is representative of the types of proteins found in the wider population. Furthermore, the iTRAQ analysis was able to quantify changes in recovery of the identified proteins in dialysate collected in sequential samples. Quantitative data were available for one-third of the proteins, showing 1 – 2-fold changes in the amounts recovered for each (Parkinson, personal communication).

Now that some of the components of interstitial fluid are known, more sensitive

quantification methods, e.g. ELISAs or Western blotting, could be used to follow changes in the concentration of a protein recovered in dialysate samples from consecutive time-periods. However, such methods require specific antibodies and multiple experiments, which can prove very time consuming. Recent developments in proteomic methods provide an interesting alternative. Multiple reaction monitoring (MRM, also known in the singular as selected reaction monitoring, SRM) enables the absolute quantitation of large numbers of proteins using mass spectrometry (Anderson & Hunter, 2006). A similar approach has been used previously in microdialysis-mass spectrometry studies, for the measurement of metabolites, such as the neurotransmitter acetylcholine (Fu *et al.*, 2008), but has not yet been used for quantifying peptides recovered in dialysate.

The MRM technique involves defining the m/z value of a target peptide and corresponding fragment ion, which the mass spectrometer is able to detect and quantify between samples. Peptide specificity is ensured by the combination of a first-dimension MS (MS1) step which selects the target peptide and a second, MS2, step which selects for the particular compoment that is characteristic of the fragmentation spectrum. Peptide selection lists for targets are compiled either from *in silico* prediction programs, or using known peptides from proteome profiling experiments, such as those performed in the present study. The presence of highly abundant proteins does not seem to be detrimental to the detection of lower abundance components, with proteins at concentrations as low as 0.67 μg/ml (Anderson & Hunter, 2006) identified without depletion. However, fractionation or immunodepletion of the sample prior to analysis would enable greater access to the dynamic range of protein concentrations.

Quantifying changes in protein recovery will show whether any proteins are significantly up- or down-regulated over the course of the response to injury and from this, an importance to the progression of inflammation can be inferred. However, a change in concentration is not the only determinant of a role. In fact, changes in post-translational modifications are more likely to be indicative of protein activation or function within a response. Examples of the proteins found in dermal dialysate that are known to be differentially phosphorylated in response to injury were given

in Section 5.1.1. None of these were reported in the preliminary investigation into phosphorylation in dialysate, most likely due to the limited dataset that could be reported, but also to the presence of relatively abundant albumin and apolipoprotein phosphopeptides obscuring further identifications. However, the two potentially novel sites suggest that the analysis of post-translation modifications in proteins recovered in dialysate will provide novel insights into protein function and signalling during the injury response.

Collectively, these data suggest that microdialysis has the potential to recover relevant, novel markers of the injury response, provided the analysis techniques used are sensitive enough to detect relatively low abundance components. Thus, it is likely to be a useful tool in furthering our understanding of the signalling processes that occur following injury.

6.3 What new insights into the injury response have been gained?

This research originally set out to find novel markers of the response to injury using cutaneous microdialysis and shotgun proteomics. However, it was first necessary to explore the suitability of this combination of technologies for the recovery and identification of proteins relevant to the injury response.

Data from this study expanded on previous characterisations of the response to microdialysis probe insertion, in terms of the vascular response, proteins recovered, and the time-course over which they were collected. It measured the recovery of a panel of cytokines, both those which have previously been reported in human dermal dialysate (IL-6, IL-10, IFN-γ), and those which have not (MCP-1, MIP-1α, OSM, VEGF). Furthermore, the use of 30-minute collection periods enabled a greater temporal resolution than previously reported. This gives a clearer understanding of the order in which the different cytokines are released and diffuse into the probe in large enough quantities to be detected, shedding light on the activation of the resident and infiltrating cells. However, there is a limit to the information that can be gained from characterising

cytokine responses, as these are not the only mediators active during this time.

By investigating the different types of proteins that can be recovered from the injury environment, a broader characterisation of the processes involved has been achieved. While none of the proteins identified within the dermal dialysate samples were particularly surprising, or obvious candidates for novel markers, these data show that microdialysis samples relevant interstitial fluid components from the tissue. It also brings together the wider injury literature by linking together a range of processes, such as iron metabolism, which may not be immediately associated with the response to injury. Thus the research conducted during the present study represents a base for further, targeted investigations into the expression of these proteins over the course of the response to an injury in both healthy and diseased skin. From those studies, it should become possible to select appropriate biomarker candidates.

The types of proteins identified were mostly highly abundant plasma proteins, reflecting both the infiltration of plasma into the wound and also the limits of detection that are experienced with shotgun proteomics using GeLC-MS/MS. Different proteomic analysis techniques are certain to expand on the dermal dialysate proteome presented in this study, providing additional scope for potential targets.

Quantitative analysis of the changes in protein concentration between timed dialysate samples has been performed, as part of another project within the CPR. Furthermore, because the proteins identified in the present study were predominantly highly abundant plasma proteins, it is unlikely that the concentrations will change significantly within the study period while vascular permeability to protein remains elevated. This permeability is maximal by three days after an injury and remains elevated until approximately seven days (Brown *et al.*, 1992), much longer than the study period.

Instead, the present study took an alternative, complementary approach to improve the characterisation of this proteome - namely, the analysis of protein phosphorylation. This area of the research was perhaps the most fruitful in terms of novel information, identifying potentially novel phosphorylation sites in two common plasma proteins. These data suggest that future investigations into the post-translational modifications of proteins involved in the response to injury will be highly informative. While the

functions of these novel phosphorylation sites are as yet unknown, their discovery in proteins collected from the interstitial fluid space rather than directly from the vascular compartment leads to the speculation that these modifications could be location- or response- specific. Further experiments to characterise protein phosphorylation in larger or depleted dermal dialysate samples could potentially lead to the identification of further novel phosphorylation sites in a greater number of proteins. Additionally, it could define more precisely the roles of phosphorylated residues known to have a regulatory function within the injury response, such as serpin F1 and others mentioned in Section 5.1.1.

6.4 Is the microdialysis probe insertion model appropriate for the study of inflammation in other tissues or disease states?

The insertion of microdialysis probes causes an inflammatory response in the target tissue, making it an ideal method by which to study injury without the complications of additional stimuli. Microdialysis is certainly compatible for sampling interstitial fluid components from tissues other than skin, including muscle and adipose tissue (Rosdahl *et al.*, 1993), liver (Yang *et al.*, 1995) and the eye (Wei *et al.*, 2006). It has also been used to sample solutes from tumour micro-environments (Garvin & Dabrosin, 2008) and several skin diseases including psoriasis (Krogstad *et al.*, 1997) and cold urticaria (Nuutinen, Harvima & Ackermann, 2007). However, very few microdialysis experiments in these tissues have looked at the recovery of a panel of inflammatory mediators and none have used shotgun proteomics to characterise the response to insertion.

Taken at face value, the dermal dialysate proteome appears very similar to that reported for cerebral dialysate (Maurer *et al.*, 2003), which would suggest that this cutaneous injury model is appropriate for studying injury in other tissues. However, the proteomic studies primarily identified relatively highly abundant proteins released

from plasma as a result of vascular damage. This means that the proteomic profile will appear very similar, regardless of the tissue studied. Further research is required to determine whether these highly abundant proteins are suitable markers of the response to injury in skin and other tissues. This is more likely to be determined by changes in their modifications, rather than their concentration. Studies comparing healthy and diseased skin, such as psoriatic lesions, could potentially complement these observations by identifying proteins that are differentially modified or regulated.

Together, the data from the present study show that the microdialysis probe insertion injury model generates a sufficient degree of inflammation and provides relevant proteins for further study. However, while the inflammatory response generated by probe insertion is of benefit to the present study and others investigating the injury response, it is a concern for studies into the effects of additional stimuli over and above the initial wounding. Understanding of the injury response to trauma is of particular importance when it is considered that investigators frequently cite that one hour was allowed for the trauma to subside before samples were collected (e.g. Flannery *et al.*, 2007). However, the present study, and indeed several others, show that this is only the beginning of the response to injury and the associated inflammation.

Many investigations into inflammation have been conducted in which microdialysis has been used to sample the response to an experimental stimulus (e.g. Iversen *et al.*, 2003; Schmelz *et al.*, 1997; Toriyabe *et al.*, 2004). While these studies compare the test conditions to an unstimulated control to measure the effect over and above this injury response, its influence on the experimentally-induced inflammation is often overlooked even when the effect of cell damage is of particular interest (Fairweather *et al.*, 2004). Longer-term experiments have shown that the inflammatory response to probe insertion alone lasts for at least 24 hours (Averbeck *et al.*, 2006) and it is unclear whether a secondary stimulus receives a dampened or enhanced response as a result. It is also plausible that the removal of mediators into the dialysate attenuates the response, although further research is required to confirm or refute this hypothesis.

In conclusion, microdialysis gives the means by which to injure and subsequently explore the response to tissue damage in a variety of organs, through the recovery

of relevant solutes. While the shotgun proteomics technique used was not sensitive enough to identify any skin-specific markers, the analysis of protein phosphorylation and detection of potentially novel modification sites is likely to be highly informative and should shed light on cellular processes both in health and in disease.

Appendix One:

Non-depleted Dialysate Data

gi no.	Protein Name	Prot Score	Prot Matches	emPAI	Unique Pep	Exp. *m/z*	Exp. Mr	Calc. Mr	Peptide Sequence
4502027	albumin	2084	87	1.82	21	464.20	926.38	926.49	YLYEIAR
						480.73	959.45	959.56	FQNALLVR
						507.28	1012.54	1012.59	LVAASQAALGL
						509.27	1016.52	1016.53	SLHTLFGDK
						575.29	1148.57	1148.61	LVNEVTEFAK
						613.81	1225.61	1225.60	FKDLGEENFK
						656.34	1310.66	1310.73	HPDYSVVLLLR
						671.83	1341.65	1341.63	AVMDDFAAFVEK
						734.34	1466.67	1466.84	RHPDYSVVLLLR
						756.40	1510.79	1510.84	VPQVSTPTLVEVSR
						820.32	1638.63	1638.78	DVFLGMFLYEYAR
						547.30	1638.88	1638.93	KVPQVSTPTLVEVSR
						829.35	1656.68	1656.75	QNCELFEQLGEYK
						871.97	1741.92	1741.89	HPYFYAPELLFFAK
						949.87	1897.72	1897.99	RHPYFYAPELLFFAK
						955.92	1909.82	1909.92	RPCFSALEVDETYVPK
						1022.93	2043.85	2044.09	VFDEFKPLVEEPQNLIK
						830.71	2489.10	2489.28	ALVLIAFAQYLQQCPFED-HVK
						845.39	2533.14	2533.20	MPCAEDYLSVVLNQLCVL-HEK

gi no.	Protein Name	Prot Score	Prot Matches	emPAI	Unique Pep	Exp. *m/z*	Exp. Mr	Calc. Mr	Peptide Sequence
						897.33	2688.96	2689.30	RMPCAEDYLSVVLNQLCV-LHEK
						997.43	2989.28	2989.33	SHCIAEVENDEMPADLPS-LAADFVESK
4557871	transferrin	622	21	0.28	11	637.35	1272.68	1272.65	HSTIFENLANK
						677.83	1353.65	1353.62	DYELLCLDGTR
						708.38	1414.74	1414.71	SVIPSDGPSVACVK
						747.84	1493.67	1493.72	MYLGYEYVTAIR
						789.34	1576.66	1576.65	FDEFFSEGCAPGSK
						797.43	1592.84	1592.80	TAGWNIPMGLLYNK
						815.39	1628.76	1628.81	EDPQTFYYAVAVVK
						627.95	1880.84	1880.87	ADRDQYELLCLDNTR
						1036.36	2070.71	2070.92	SDNCEDTPEAGYFAVAVVK
						1095.89	2189.76	2190.00	IMNGEADAMSLDGGFVYI-AGK
						1318.76	3953.26	3953.01	AIAANEADAVTLDAGLVY-DAYLAPNNLKPVVAEFYGSK
4557385	complement component 3	105	8	0.05	7	701.39	1400.77	1400.83	SSLSVPYVIVPLK
						829.38	1656.75	1656.76	AGDFLEANYMNLQR
						851.86	1701.70	1701.79	VFLDCCNYITELR
						895.46	1788.90	1788.86	DICEEQVNSLPGSITK
						908.94	1815.87	1815.88	SNLDEDIIAEENIVSR

gi no.	Protein Name	Prot Score	Prot Matches	emPAI	Unique Pep	Exp. m/z	Exp. Mr	Calc. Mr	Peptide Sequence
						1137.07	2272.12	2272.09	VQLSNDFDEYIMAIEQTIK
						1052.43	3154.27	3154.38	YRGDQDATMSILDISMMT-GFAPDTDDLK
11321561	hemopexin	84	7	0.06	4	571.29	1140.57	1140.58	GGYTLVSGYPK
						610.78	1219.54	1219.60	NFPSPVDAAFR
						788.77	2363.29	2363.16	LLQDEFPGIPSPLDAAVE-CHR
						833.39	2497.15	2497.23	EVGTPHGIILDSVDAAFI-CPGSSR
4557485	ceruloplasmin	81	2	0.05	2	686.34	1370.67	1370.76	GAYPLSIEPIGVR
						760.34	1518.68	1518.74	ALYLQYTDETFR
66932947	alpha-2-macroglobulin	53	7	0.04	6	509.79	1017.57	1017.59	ATVLNYLPK
						632.87	1263.73	1263.66	LSFYYLIMAK
						857.43	1712.85	1712.83	SSSNEEVMFLTVQVK
						923.02	1844.02	1844.03	LLIYAVLPTGDVIGDSAK
						942.53	1883.05	1883.04	VSVQLEASPAFLAVPVEK
						1030.95	2059.89	2060.04	AFQPFFVELTMPYSVIR

gi = genBank identification number, Prot. Score = A value for reliability of identification, involving a correction to reduce the influence of low-scoring peptides, Prot. Matches = total number of peptides matched for this protein, emPAI = exponentially modified protein abundance index, Unique Pep. = the number of different peptides matched, Exp. m/z = measured m/z value, Exp. Mr = measured relative molecular mass of the peptide, Calc. Mr = theoretical relative molecular mass of the peptide.

Appendix Two:

Depleted Dialysate Data

gi no.	Protein Name	Prot Score	Prot Matches	emPAI	Uni. Pep.	Exp. *m/z*	Exp. Mr	Calc. Mr	Peptide Sequence	No. Pept. Matches
66932947	alpha-2-macroglobulin	1805	190	1.24	42	509.8	1017.58	1017.59	ATVLNYLPK	3
						542.81	1083.6	1083.61	GHFSISIPVK	6
						552.29	1102.56	1102.6	SSGSLLNNAIK	9
						558.79	1115.57	1115.6	QTVSWAVTPK	7
						567.78	1133.54	1133.58	SASNMAIVDVK	7
						605.79	1209.57	1209.64	LPPNVVEESAR	6
						613.25	1224.48	1224.54	YDVENCLANK	2
						624.80	1247.67	1247.66	LSFYYLIMAK	7
						628.29	1254.57	1254.64	AIGYLNTGYQR	4
						630.26	1258.51	1258.57	VGFYESDVMGR	4
						636.81	1271.60	1271.67	VTAAPQSVCALR	3
						669.79	1337.57	1337.64	NALFCLESAWK	5
						697.81	1393.60	1393.67	NEDSLVFVQTDK	7
						709.78	1417.54	1417.59	HYDGSYSTFGER	6
						478.26	1431.75	1431.82	MVSGFIPLKPTVK	6
						724.81	1447.60	1447.64	DMYSFLEDMGLK	4
						746.37	1490.72	1490.79	NQGNTWLTAFVLK	5
						756.34	1510.67	1510.76	AAQVTIQSSGTFSSK	5
						515.92	1544.74	1544.79	LVHVEEPHTFETVR	7
						777.86	1553.70	1553.78	VTGEGCVYLQTSLK	5
						783.38	1564.75	1564.82	ALLAYAFALAGNQDK	7
						802.90	1603.78	1603.84	IAQWQSFQLEGGLK	9

gi no.	Protein Name	Prot Score	Prot Matches	emPAI	Uni. Pep.	Exp. *m/z*	Exp. Mr	Calc. Mr	Peptide Sequence	No. Pept. Matches
						836.92	1671.83	1671.85	TEHPFTVEEFVLPK	14
						849.40	1696.79	1696.83	SSSNEEVMFLTVQVK	8
						890.48	1778.94	1779.00	DTVIKPLLVEPEGLEK	18
						922.99	1843.96	1844.03	LLIYAVLPTGDVIGDSAK	9
						924.93	1847.84	1847.87	QFSFPLSSEPFQGSYK	7
						942.50	1882.98	1883.04	VSVQLEASPAFLAVPVEK	4
						633.94	1898.80	1898.87	FSGQLNSHGCFYQQVK	8
						636.70	1907.07	1907.10	KDTVIKPLLVEPEGLEK	6
						1023.01	2044.01	2044.05	AFQPFFVELTMPYSVIR	8
						1031.03	2060.04	2060.09	LLLQQVSLPELPGEYSMK	5
						691.98	2072.9	2072.92	MCPQLQQYEMHGPEGLR	7
						704.02	2109.03	2109.07	LHTEAQIQEEGTVVELTG-R	11
						713.00	2135.99	2136.05	HNVYINGITYTPVSSTNEK-	5
						796.36	2386.07	2386.19	QQNAQGGFSSTQDTVVA-LHALSK	10
						825.73	2474.18	2474.22	SLFTDLEAENDVLHCVAF-AVPK	7
						1274.56	2547.11	2547.08	VYDYYETDEFAIAEYNAP-CSK	2

gi no.	Protein Name	Prot Score	Prot Matches	emPAI	Uni. Pep.	Exp. *m/z*	Exp. Mr	Calc. Mr	Peptide Sequence	No. Pept. Matches
						937.47	2809.38	2809.44	VVSMDENFHPLNELIPLV-YIQDPK	13
						973.15	2916.44	2916.52	AVDQSVLLMKPDAELSAS-SVYNLLPEK	29
						1055.15	3162.43	3162.56	YNILPEKEEFPFALGVQT-LPQTCDEPK	7
						1231.60	4922.37	4922.42	APVGHFYEPQAPSAEVE-MTSYVLLAYLTAQPAPT-SEDLTSATNIVK	8
17318569	keratin 1	897	104	0.7	15	487.24	972.46	972.52	IEISELNR	4
						571.26	1140.51	1140.51	DYQELMNTK	4
						590.27	1178.52	1178.59	YEELQITAGR	5
						633.29	1264.57	1264.63	TNAENEFVTIK	8
						639.34	1276.66	1276.70	LALDLEIATYR	6
						650.72	1299.42	1299.52	NMQDMVEDYR	4
						651.83	1301.64	1301.71	SLDLDSIIAEVK	7
						679.32	1356.62	1356.69	LNDLEDALQQAK	11
						692.31	1382.61	1382.68	SLNNQFASFIDK	7
						738.34	1474.67	1474.74	WELLQQVDTSTR	8
						738.35	1474.68	1474.78	FLEQQNQVLQTK	4
						829.37	1656.73	1656.79	SGGGFSSGSAGIINYQR	5
						858.89	1715.77	1715.84	QISNLQQSISDAEQR	6

gi no.	Protein Name	Prot Score	Prot Matches	emPAI	Uni. Pep.	Exp. *m/z*	Exp. Mr	Calc. Mr	Peptide Sequence	No. Pept. Matches
						883.31	1764.62	1764.73	FSSCGGGGGSFGAGGGF-GSR	2
						665.29	1992.85	1992.97	THNLEPYFESFINNLR	5
						861.00	2579.98	2580.15	MSGECAPNVSVSVSTSHT-TISGGGSR	5
4557485	ceruloplasmin	593	50	0.41	22	587.77	1173.52	1173.54	MYYSAVDPTK	4
						613.27	1224.53	1224.51	DDEEFIESNK	2
						686.38	1370.74	1370.76	GAYPLSIEPIGVR	7
						716.31	1430.61	1430.63	QSEDSTFYLGER	4
						735.41	1468.81	1468.83	DIASGLIGPLIICK	10
						735.85	1469.69	1469.72	EVGPTNADPVCLAK	9
						760.36	1518.70	1518.74	ALYLQYTDETFR	7
						788.41	1574.81	1574.85	DLYSGLIGPLIVCR	5
						794.36	1586.71	1586.73	RQSEDSTFYLGER	12
						820.38	1638.75	1638.78	AGLQAFFQVQECNK	5
						824.41	1646.81	1646.83	KALYLQYTDETFR	7
						724.32	2169.94	2170.07	LISVDTEHSNIYLQNGPDR	8
						751.29	2250.86	2250.90	MHSMNGFMYGNQPGLT-MCK	6
						564.78	2255.10	2255.15	KAEEEHLGILGPQLHADV-GDK	6

gi no.	Protein Name	Prot Score	Prot Matches	emPAI	Uni. Pep.	Exp. *m/z*	Exp. Mr	Calc. Mr	Peptide Sequence	No. Pept. Matches
						767.05	2298.12	2298.16	KLISVDTEHSNIYLQNGPD-R	20
						788.38	2362.13	2362.16	MYYSAVDPTKDIFTGLIGP-MK	7
						800.03	2397.06	2397.09	HYYIGIIETTWDYASDHG-EK	10
						825.31	2472.91	2473.06	MFTTAPDQVDKEDEDFQ-ESNK	5
						829.76	2486.25	2486.28	GPEEEHLGILGPVIWAEV-GDTIR	4
						835.70	2504.08	2504.12	SGAGTEDSACIPWAYYST-VDQVK	9
						844.41	2530.21	2530.24	SVPPSASHVAPTETFTTYEW+TVPK	11
						895.74	2684.21	2684.25	GVYSSDVFDIFPGTYQTLE-MFPR	4
4557321	apolipoprotein A-I	538	46	2.09	17	516.24	1030.47	1030.51	LSPLGEEMR	3
						615.83	1229.65	1229.70	QGLLPVLESFK	8
						618.32	1234.63	1234.68	DLATVYVDVLK	9
						626.78	1251.54	1251.61	VQPYLDDFQK	4
						642.26	1282.57	1282.57	WQEEMELYR	8

gi no.	Protein Name	Prot Score	Prot Matches	emPAI	Uni. Pep.	Exp. *m/z*	Exp. Mr	Calc. Mr	Peptide Sequence	No. Pept. Matches
						651.30	1300.59	1300.64	THLAPYSDELR	8
						651.84	1301.67	1301.64	LSPLGEEMRDR	3
						690.83	1379.64	1379.71	VQPYLDDFQKK	3
						693.83	1385.64	1385.71	VSFLSALEEYTK	7
						700.80	1399.59	1399.66	DYVSQFEGSALGK	10
						731.90	1461.78	1461.84	VKDLATVYVDVLK	6
						757.88	1513.74	1513.80	VSFLSALEEYTKK	4
						806.85	1611.69	1611.78	LLDNWDSVTSTFSK	5
						825.89	1649.76	1649.86	DLATVYVDVLKDSGR	2
						605.93	1814.76	1814.84	DSGRDYVSQFEGSALGK	10
						966.93	1931.85	1931.93	EQLGPVTQEFWDNLEK	10
						734.68	2201.01	2201.11	LREQLGPVTQEFWDNLE-K	19
11321561	hemopexin	432	65	0.84	16	487.26	972.51	972.54	LWWLDLK	5
						509.25	1016.49	1016.53	VWVYPPEK	4
						565.29	1128.56	1128.64	RLWWLDLK	2
						571.27	1140.52	1140.58	GGYTLVSGYPK	8
						579.71	1157.41	1157.46	DYFMPCPGR	7
						610.78	1219.54	1219.60	NFPSPVDAAFR	5
						634.81	1267.61	1267.67	FDPVRGEVPPR	4
						702.80	1403.59	1403.66	SWPAVGNCSSALR	5
						742.83	1483.64	1483.68	EWFWDLATGTMK	5

gi no.	Protein Name	Prot Score	Prot Matches	emPAI	Uni. Pep.	Exp. *m/z*	Exp. Mr	Calc. Mr	Peptide Sequence	No. Pept. Matches
						748.30	1494.59	1494.67	YYCFQGNQFLR	10
						750.81	1499.60	1499.68	EWFWDLATGTMK	6
						856.85	1711.68	1711.76	GECQAEGVLFFQGDR	10
						868.41	1734.80	1734.87	ALPQPQNVTSLLGCTH	6
						613.27	1836.79	1836.88	SGAQATWTELPWPHEK	6
						788.67	2362.99	2363.16	LLQDEFPGIPSPLDAAVEC-HR	3
						833.36	2497.07	2497.23	EVGTPHGIILDSVDAAFIC-PGSSR	5
9257232	orosomucoid 1	372	51	1.2	7	497.75	993.48	993.51	TEDTIFLR	6
						556.72	1111.43	1111.52	SDVVYTDWK	5
						580.77	1159.52	1159.58	WFYIASAFR	5
						723.31	1444.60	1444.65	TYMLAFDVNDEK	4
						854.90	1707.78	1707.85	NWGLSVYADKPETTK	5
						871.86	1741.70	1741.80	EQLGEFYEALDCLR	4
						584.96	1751.87	1751.95	YVGGQEHFAHLLILR	6
4557385	complement component 3	332	47	0.23	24	417.25	832.49	832.48	LPYSVVR	4
						443.76	885.50	885.52	ISLPESLK	4
						512.76	1023.50	1023.51	FISLGEACK	6
						542.28	1082.54	1082.55	GYTQQLAFR	6
						546.82	1091.62	1091.62	NTLIIYLDK	6
						633.77	1265.52	1265.61	NTMILEICTR	3

gi no.	Protein Name	Prot Score	Prot Matches	emPAI	Uni. Pep.	Exp. *m/z*	Exp. Mr	Calc. Mr	Peptide Sequence	No. Pept. Matches
						650.77	1299.52	1299.58	ACEPGVDYVYK	4
						668.36	1334.71	1334.72	APSTWLTAYVVK	7
						685.85	1369.68	1369.72	TIYTPGSTVLYR	5
						701.39	1400.76	1400.83	SSLSVPYVIVPLK	5
						735.85	1469.69	1469.77	IPIEDGSGEVVLSR	5
						491.23	1470.67	1470.74	AAVYHHFISDGVR	6
						813.93	1625.84	1625.87	RIPIEDGSGEVVLSR	6
						820.43	1638.84	1638.87	TVMVNIENPEGIPVK	8
						829.38	1656.75	1656.76	AGDFLEANYMNLQR	7
						834.34	1666.68	1666.73	VYAYYNLEESCTR	4
						851.89	1701.78	1701.79	VFLDCCNYITELR	10
						908.90	1815.79	1815.88	SNLDEDIIAEENIVSR	5
						624.67	1871.00	1871.03	TELRPGETLNVNFLLR	5
						631.00	1889.98	1890.07	LSINTHPSQKPLSITVR	3
						686.03	2055.07	2055.09	VRVELLHNPAFCSLATTK	10
						777.37	2329.10	2329.13	SEFPESWLWNVEDLKEPP-K	11
						865.42	2593.24	2593.30	TMQALPYSTVGNSNNYL-HLSVLR	7
						919.09	2754.25	2754.28	EGVQKEDIPPADLSDQVP-DTESETR	23
32483410	vitamin D-binding	314	31	0.7	15	458.22	914.43	914.45	YTFELSR	4

gi no.	Protein Name	Prot Score	Prot Matches	emPAI	Uni. Pep.	Exp. m/z	Exp. Mr	Calc. Mr	Peptide Sequence	No. Pept. Matches
	protein					578.28	1154.54	1154.62	LPDATPTELAK	6
						585.81	1169.61	1169.64	THLPEVFLSK	5
						627.83	1253.65	1253.71	HLSLLTTLSNR	4
						442.90	1325.68	1325.75	RTHLPEVFLSK	8
						677.87	1353.72	1353.75	AKLPDATPTELAK	6
						765.37	1528.72	1528.78	EDFTSLSLVLYSR	3
						783.89	1565.76	1565.81	FPSGTFEQVSQLVK	8
						847.92	1693.83	1693.90	KFPSGTFEQVSQLVK	14
						1046.89	2091.76	2091.82	SLGECCDVEDSTTCFNAK	10
						755.62	2263.83	2263.93	SCESNSPFPVHPGTAECCT-K	9
						776.71	2327.10	2327.18	EFSHLGKEDFTSLSLVLYSR	3
						789.42	2365.24	2365.26	VPTADLEDVLPLAEDITNI-LSK	10
						790.99	2369.95	2370.04	SYLSMVGSCCTSASPTVCF-LK	4
						903.04	2706.09	2706.20	HQPQEFPTYVEPTNDEICE-AFR	13
67782358	complement factor B	284	17	0.3	12	578.32	1154.62	1154.62	EELLPAQDIK	5
						621.85	1241.69	1241.70	VKDISEVVTPR	5
						638.29	1274.57	1274.65	YGLVTYATYPK	3
						653.83	1305.65	1305.65	EKLQDEDLGFL	6

gi no.	Protein Name	Prot Score	Prot Matches	emPAI	Uni. Pep.	Exp. *m/z*	Exp. Mr	Calc. Mr	Peptide Sequence	No. Pept. Matches
						754.84	1507.67	1507.68	VSEADSSNADWVTK	5
						921.97	1841.92	1841.91	EAGIPEFYDYDVALIK	7
						957.88	1913.75	1913.84	FLCTGGVSPYADPNTCR	4
						708.35	2122.01	2122.03	YGQTIRPICLPCTEGTTR	18
						761.01	2280.01	2280.03	AIHCPRPHDFENGEYWPR	9
						813.42	2437.23	2437.25	LPPTTTCQQQKEELLPAQ-DIK	9
						884.74	2651.19	2651.19	WSGQTAICDNGAGYCSN-PGIPIGTR	22
						939.12	2814.34	2814.37	LLQEGQALEYVCPSGFYP-YPVQTR	6
4557287	angiotensinogen	227	10	0.35	5	542.24	1082.46	1082.52	FMQAVTGWK	8
						649.32	1296.63	1296.71	DPTFIPAPIQAK	8
						719.32	1436.63	1436.70	SLDFTELDVAAEK	8
						757.35	1512.69	1512.76	AAMVGMLANFLGFR	6
						861.98	1721.95	1722.02	VLSALQAVQGLLVAQGR	5
55956899	keratin 9	197	24	0.29	11	530.76	1059.5	1059.56	TLLDIDNTR	3
						579.29	1156.56	1156.58	QGVDADINGLR	5
						603.79	1205.57	1205.60	QVLDNLTMEK	3
						654.33	1306.65	1306.67	IKFEMEQNLR	5
						658.33	1314.64	1314.68	DQIVDLTVGNNK	8
						793.84	1585.67	1585.76	VQALEEANNDLENK	5

gi no.	Protein Name	Prot Score	Prot Matches	emPAI	Uni. Pep.	Exp. *m/z*	Exp. Mr	Calc. Mr	Peptide Sequence	No. Pept. Matches
						623.29	1866.86	1866.91	TLNDMRQEYEQLIAK	8
						1101.99	2201.97	2202.01	SDLEMQYETLQEELMAL-K	11
						777.68	2330.02	2330.10	SDLEMQYETLQEELMALK-K	11
						837.35	2509.03	2509.12	EIETYHNLLEGGQEDFESS-GAGK	13
						968.12	2901.33	2901.40	NYSPYYNTIDDLKDQIVD-LTVGNNK	10
4505529	orosomucoid 2	184	32	0.93	7	497.75	993.48	993.51	TEDTIFLR	6
						572.73	1143.44	1143.49	SDVMYTDWK	7
						580.77	1159.52	1159.58	WFYIASAFR	5
						617.82	1233.63	1233.70	EHVAHLLFLR	6
						636.79	1271.56	1271.59	SDVMYTDWKK	3
						709.80	1417.59	1417.64	TLMFGSYLDDEK	5
						1056.95	2111.89	2111.97	EQLGEFYEALDCLCIPR	7
47132620	keratin 2a	169	38	0.1	8	487.24	972.46	972.52	IEISELNR	4
						519.24	1036.47	1036.52	YLDGLTAER	3
						597.28	1192.55	1192.61	YEELQVTVGR	5
						604.78	1207.55	1207.61	TAAENDFVTLK	3
						665.29	1328.56	1328.63	NVQDAIADAEQR	2
						665.32	1328.63	1328.72	NLDLDSIIAEVK	4

gi no.	Protein Name	Prot Score	Prot Matches	emPAI	Uni. Pep.	Exp. *m/z*	Exp. Mr	Calc. Mr	Peptide Sequence	No. Pept. Matches
						730.87	1459.72	1459.79	VDLLNQEIEFLK	2
						738.35	1474.68	1474.78	FLEQQNQVLQTK	4
4502261	SERPIN C1	155	20	0.2	11	606.3	1210.58	1210.63	FRIEDGFSLK	6
						655.27	1308.53	1308.6	DDLYVSDAFHK	7
						670.80	1339.59	1339.66	TSDQIHFFFAK	9
						695.35	1388.69	1388.75	EVPLNTIIFMGR	5
						713.29	1424.56	1424.63	DIPMNPMCIYR	3
						715.86	1429.71	1429.78	VAEGTQVLELPFK	10
						510.23	1527.66	1527.74	FATTFYQHLADSK	5
						834.93	1667.84	1667.92	GDDITMVLILPKPEK	5
						875.80	1749.58	1749.66	ADGESCSASMMYQEGK	9
						924.91	1847.81	1847.90	EQLQDMGLVDLFSPEK	12
						774.89	3095.54	3095.68	VAEGTQVLELPFKGDDIT-MVLILPKPEK	5
4506355	pregnancy-zone protein	138	24	0.12	7	509.8	1017.58	1017.59	ATVLNYLPK	3
						552.29	1102.56	1102.60	SSGSLLNNAIK	9
						716.89	1431.76	1431.82	MVSGFIPLKPTVK	6
						746.37	1490.72	1490.79	NQGNTWLTAFVLK	5
						992.02	1982.03	1982.03	GVIVRSGTHTLPVESGDM-K	2
						1023.01	2044.01	2044.05	AFQPFFVELTMPYSVIR	8

gi no.	Protein Name	Prot Score	Prot Matches	emPAI	Uni. Pep.	Exp. *m/z*	Exp. Mr	Calc. Mr	Peptide Sequence	No. Pept. Matches
						978.49	2932.45	2932.58	AVDQSVLLMKPEAELSVS-SVYNLLTVK	7
4507725	transthyretin	132	10	0.78	5	683.85	1365.69	1365.75	GSPAINVAVHVFR	9
						697.78	1393.56	1393.62	AADDTWEPFASGK	9
						761.84	1521.67	1521.71	KAADDTWEPFASGK	3
						817.70	2450.07	2450.20	ALGISPFHEHAEVVFTAN-DSGPR	12
						819.02	2454.03	2454.14	TSESGELHGLTTEEEFVEGI-YK	12
4502517	carbonic anhy-drase I	93	5	0.24	4	593.83	1185.64	1185.68	ADGLAVIGVLMK	9
						538.24	1611.69	1611.78	YSAELHVAHWNSAK	5
						871.93	1741.84	1741.90	LYPIANGNNQSPVDIK	6
						643.65	1927.92	1928.00	HDTSLKPISVSYNPATAK	9
4504349	beta globin	76	11	0.77	8	637.83	1273.64	1273.72	LLVVYPWTQR	4
						657.81	1313.61	1313.66	VNVDEVGGEALGR	7
						689.83	1377.65	1377.69	EFTPPVQAAYQK	9
						725.38	1448.75	1448.79	VVAGVANALAHKYH	7
						835.42	1668.83	1668.88	VLGAFSDGLAHLDNLK	5
						592.99	1775.95	1775.99	LLGNVLVCVLAHHFGK	5
						599.98	1796.92	1796.98	KVLGAFSDGLAHLDNLK	4

gi no.	Protein Name	Prot Score	Prot Matches	emPAI	Uni. Pep.	Exp. *m/z*	Exp. Mr	Calc. Mr	Peptide Sequence	No. Pept. Matches
						1037.95	2073.89	2073.94	FFESFGDLSTPDAVMGN-PK	8
50659080	SERPIN A3	66	8	0.07	5	531.27	1060.52	1060.58	EIGELYLPK	4
						608.34	1214.67	1214.72	ITLLSALVETR	9
						711.32	1420.62	1420.68	DEELSCTVVELK	7
						954.45	1906.88	1906.95	AVLDVFEEGTEASAATAV-K	5
						673.54	2690.12	2690.36	FNRPFLMIIVPTDTQNIFF-MSK	4
21071030	alpha 1B-glycoprotein	58	10	0.12	9	563.3	562.29	562.26	EGETK	2
						435.77	869.53	869.52	LLELTGPK	6
						544.79	1087.56	1087.58	ATWSGAVLAGR	5
						632.81	1263.60	1263.65	SGLSTGWTQLSK	2
						575.32	1722.94	1722.95	LELHVDGPPPRPQLR	6
						938.49	1874.97	1874.99	VTLTCVAPLSGVDFQLR	8
						716.67	2147.00	2147.04	IFFHLNAVALGDGGHYTC-R	8
						766.05	2295.14	2295.18	TPGAAANLELIFVGPQHA-GNYR	9
						1330.98	3989.91	3989.86	LHDNQNGWSGDSAPV-ELILSDETLPAPEFSPE-PESGR	3

gi no.	Protein Name	Prot Score	Prot Matches	emPAI	Uni. Pep.	Exp. m/z	Exp. Mr	Calc. Mr	Peptide Sequence	No. Pept. Matches
73858568	complement component 1 inhibitor	49	10	0.12	6	435.23	868.44	868.43	FPVFMGR	4
						558.80	1115.59	1115.58	LLDSLPSDTR	6
						632.82	1263.63	1263.67	TNLESILSYPK	3
						780.39	1558.77	1558.85	KYPVAHFIDQTLK	4
						797.39	1592.76	1592.78	LEDMEQALSPSVFK	7
						913.99	1825.96	1825.97	GVTSVSQIFHSPDLAIR	4
4557327	apolipoprotein H	45	8	0.17	4	552.75	1103.49	1103.54	EHSSLAFWK	9
						751.86	1501.71	1501.77	VCPFAGILENGAVR	4
						886.94	1771.87	1771.97	FICPLTGLWPINTLK	5
						795.97	2384.90	2384.99	ATFGCHDGYSLDGPEEIE-CTK	18
17318574	keratin 4	44	5	0.06	2	639.34	1276.66	1276.7	LALDIEIATYR	6
						679.32	1356.62	1356.72	NLDLDSIIAEVR	8
4504919	keratin 8	44	7	0.06	2	639.34	1276.66	1276.7	LALDIEIATYR	6
						738.36	1474.71	1474.69	LESGMQNMSIHTK	5
39725934	SERPIN F1	44	7	0.07	6	607.8	1213.59	1213.66	ELLDTVTAPQK	4
						625.81	1249.61	1249.66	DTDTGALLFIGK	4
						692.32	1382.63	1382.67	LQSLFDSPDFSK	5
						758.83	1515.65	1515.67	TSLEDFYLDEER	4
						780.37	1558.72	1558.78	LAAAVSNFGYDLYR	8
						822.85	1643.69	1643.77	KTSLEDFYLDEER	4
4502067	alpha-1	36	7	0.08	4	607.31	1212.61	1212.66	TVAACNLPIVR	7

gi no.	Protein Name	Prot Score	Prot Matches	emPAI	Uni. Pep.	Exp. *m/z*	Exp. Mr	Calc. Mr	Peptide Sequence	No. Pept. Matches
	-microglobulin					793.85	1585.69	1585.86	APQLRETLLQDFR	2
						854.86	1707.70	1707.74	EYCGVPGDGDEELLR	3
						960.44	1918.86	1918.95	GECVPGEQEPEPILIPR	6
4504579	I factor	35	2	0.05	2	579.77	1157.52	1157.52	SFPTYCQQK	2
	(complement)					596.80	1191.58	1191.63	VFSLQWGEVK	6
4757756	annexin A2	34	3	0.09	3	711.33	1420.64	1420.69	SLYYYIQQDTK	7
						730.83	1459.64	1459.67	SYSPYDMLESIR	6
						771.90	1541.78	1541.84	GVDEVTIVNILTNR	6
4505881	plasminogen	32	7	0.04	5	570.81	1139.6	1139.62	EAQLPVIENK	4
						619.34	1236.67	1236.63	FVTWIEGVMR	2
						688.31	2061.92	2061.92	NPDADKGPWCFTTDPSV-R	9
						709.33	2124.96	2124.96	ATTVTGTPCQDWAAQEP-HR	8
						896.40	2686.18	2686.19	TMSGLECQAWDSQSPHA-HGYIPSK	6

No. Pept. Matches = the number of times each unique peptide was identified. All other heading abbreviations are as defined for Appendix One.

References

Aden, N., Shiwen, X., Aden, D., Black, C., Nuttall, A., Denton, CP., Leask, A., Abraham, D. and Stratton, R. (2008) "Proteomic analysis of scleroderma lesional skin reveals activated wound healing phenotype of epidermal cell layer." *Rheumatology (Oxford)*, **47** (12) 1754 – 1760.

Ahmed, N., Barker, N., Oliva, K., Garfin, D., Talmadge, K., Georgiou, H., Quinn, M. and Rice, G. (2003) "An approach to remove albumin for the proteomic analysis of low abundance biomarkers in human serum." *Proteomics*, **3** (10) 1980 – 1987.

Allhorn, M., Lundqvist, K., Schmidtchen, A. and Åkerström, B. (2003) "Heme- Scavenging Role of α_1-Microglobulin in Chronic Ulcers." *J. Invest. Dermatol.*, **121** (3) 640 – 646.

Anderson, C., Andersson, T. and Wårdell, K. (1994) "Changes in Skin Circulation After Insertion of a Microdialysis Probe Visualized by Laser Doppler Perfusion Imaging." *J. Invest. Dermatol.*, **102** (5) 807 – 811.

Anderson, NL., Polanski, M., Pieper, R., Gatlin, T., Tirumalai, RS., Conrads, TP., Veenstra, TD., Adkins, JN., Pounds, JG., Fagan, R. and Lobley, A. (2004) "The human plasma proteome: a nonredundant list developed by a combination of four separate sources." *Mol. Cell. Proteomics*, **3** (4) 311 – 326.

Anderson, L. and Hunter, CL. (2006) "Quantitative mass spectrometric multiple reac-

tion monitoring assays for major plasma proteins." *Mol. Cell Proteomics*, **5** (4) 573 – 588.

Andersson, L. and Porath, J. (1986) "Isolation of phosphoproteins by immobilized metal (Fe^{3+}) affinity chromatography." *Anal. Biochem.*, **154** (1) 250 – 254.

Andrade, ZA., de-Oliveira-Filho, J. and Fernandes, ALM. (1998) "Interrelationship between adipocytes and fibroblasts during acute damage to the subcutaneous adipose tissue of rats: an ultrastuctural study." *Braz. J. Med. Biol. Res.*, **31** (5) 659 – 664.

Angelo, LS. and Kurzrock, R. (2007) "Vascular Endothelial Growth Factor and Its Relationship to Inflammatory Mediators." *Clin. Cancer Res.*, **13** (10) 2825 – 2830.

Angst, MS., Clark, JD., Carvalho, B., Tingle, M., Schmelz, M. and Yeomans, DC. (2008) "Cytokine profile in human skin in response to experimental inflammation, noxious stimulation, and administration of a COX-inhibitor: a microdialysis study." *Pain*, **139** (1) 15 – 27.

Ao, X., Rotundo, RF., Loegering, DJ. and Stenken, JA. (2005) "In vivo microdialysis sampling of cytokines produced in mice given bacterial lipopolysaccharide." *J. Microbiol. Meth.*, **62** (3) 327 – 336.

Artuc, M., Hermes, B., Steckelings, UM., Grützkau, A. and Henz, BM. (1999) "Mast cells and their mediators in cutaneous wound healing - active participants or innocent bystanders?" *Exp. Dermatol.*, **8** (1) 1 – 16.

Aschheim, E. and Zweifach, BW. (1961) "Kinetics of Blood Protein Leakage in Inflammation." *Circ. Res.*, **9** 349 – 357.

Ashburner, M., Ball, CA., Blake, JA., Botstein, D., Butler, H., Cherry, JM., Davis,

AP., Dolinski, K., Dwight, SS., Eppig, JT., Harris, MA., Hill, DP., Issel-Tarver, L., Kasarskis, A., Lewis, S., Matese, JC., Richardson, JE., Ringwald, M., Rubin, GM. and Sherlock, G. (2000) "Gene Ontology: tool for the unification of biology." *Nat. Genet.*, **25** (1) 25 – 29.

Ault, JM., Riley, CM., Meltzer, NM. and Lunte, CE. (1994) "Dermal microdialysis sampling *in vivo*." *Pharm. Res.*, **11** (11) 1631 – 1639.

Averbeck, M., Beilharz, S., Bauer, M., Gebhardt, C., Hartmann, A., Hochleitner, K., Kauer, F., Voith, U., Simon, JC. and Termeer, C. (2006) "*In situ* profiling and quantification of cytokines released during ultraviolet B-induced inflammation by combining dermal microdialysis and protein microarrays." *Exp. Dermatol.*, **15** (6) 447 – 454.

Balla, J., Jacob, HS., Balla, G., Nath, K., Eaton, JW. and Vercellotti, GM. (1993) "Endothelial-cell heme uptake from heme proteins: induction of sensitization and desensitization to oxidant damage." *Proc. Natl. Acad. Sci. USA*, **90** (20) 9285 – 9289.

Barker, JNWN., Mitra, RS., Griffiths, CEM., Dixit, VM. and Nickoloff, BJ. (1991) "Keratinocytes as initiators of inflammation." *Lancet*, **337** 211 – 14.

Basic Theory and Operating Principles of Laser Doppler Blood Flow Monitoring and Imaging (LDF & LDI), Issue 1 (2003) *Moor Instruments*. Available from: http://www.moor.co.uk/products/laserdoppler/imaging

Bates, DO. and Harper, SJ. (2002) "Regulation of vascular permeability by vascular endothelial growth factors." *Vascul. Pharmacol.*, **39** (4 – 5) 225 – 237.

Bates, DO. and Jones, RO. (2003) "The role of vascular endothelial growth factor in wound healing." *Int. J. Low. Extrem. Wounds*, **2** (2) 107 – 120.

Beer, HD., Gassmann, MG., Munz, B., Steiling, H., Engelhardt, F., Bleuel, K. and Werner, S. (2000) "Expression and Function of Keratinocyte Growth Factor and Activin in Skin Morphogenesis and Cutaneous Wound Repair." *J. Investig. Dermatol. Symp. Proc.*, **5** (1) 34 – 39.

Beg, ZH., Stonik, JA., Hoeg, JM., Demosky, SJ Jr., Fairwell, T. and Brewer, HH Jr. (1989) "Human Apolipoprotein A-I." *J. Biol. Chem.*, **264** (12) 6913 – 6921.

Benveniste, H. and Hüttemeier, PC. (1990) "Microdialysis - Theory and Application." *Prog. Neurobiol.*, **35** (3) 195 – 215.

Berwick, DC. and Tavare, JM. (2004) "Identifying protein kinase substrates: hunting for the organ-grinder's monkey." *Trends Biochem. Sci.*, **29** (5) 227 – 232.

Bito, L., Davson, H., Levin, EM., Murray, M. and Snider, N. (1966) "The concentration of free amino acids and other electrolytes in cerebrospinal fluid *in vivo* dialysate of brain blood plasma of the dog." *J. Neurochem.*, **13** (11) 1057 – 1067.

Björhall, K., Miliotis, T. and Davidsson, P. (2005) "Comparison of different depletion strategies for improved resolution in proteomic analysis of human serum samples." *Proteomics*, **5** (1) 307 – 317.

Blackburn Jr, WD., Dohlman, JG., Venkatachalapathi, YV., Pillion, DJ., Koopman, WJ., Segrest, JP. and Anantharamaiah, GM. (1991) "Apolipoprotein A-I decreases neutrophil degranulation and superoxide production." *J. Lipid Res.*, **32** (12) 1911 – 1918.

Blakeman, HK., Wiesenfeld-Hallin, Z. and Alster, P. (2001) "Microdialysis of galanin in rat spinal cord: *in vitro* and *in vivo* studies." *Exp Brain Res.*, **139** (3) 354 – 358.

Bletsa, A., Berggreen, E., Fristad, I., Tenstad, O. and Wiig, H. (2006) "Cytokine signalling in rat pulp interstitial fluid and transcapillary fluid exchange during lipopolysaccharide induced acute inflammation." *J. Physiol.*, **573** (1) 225 – 236.

Blum, H., Beier, H. and Gross, HJ. (1987) "Improved silver staining of plant proteins, RNA and DNA in polyacrylamide gels." *Electrophoresis*, **8** (2) 93 – 99.

Bodenmiller, B., Mueller, LN., Mueller, M., Domon, B. and Aebersold, R. (2007) "Reproducible isolation of distinct, overlapping segments of the phosphoproteome." *Nat. Methods*, **4** (3) 231 – 237.

Borjigin, J. and Liu, T. (2008) "Application of long-term microdialysis in circadian rhythm research." *Pharmacol. Biochem. Behav.*, **90** (2) 148 – 155.

Borregaard, N. and Cowland, JB. (1997) "Granules of the Human Neutrophilic Polymorphonuclear Leukocyte." *Blood*, **89** (10) 3503 – 3521.

Borregaard, N., Theilgaard-Mönch, K., Cowland, JB., Ståhle, M. and Sørensen, OE. (2005) "Neutrophils and Keratinocytes in Innate Immunity." *J. Leukoc. Biol.*, **77** (4) 439 – 443.

Borth, W. (1992) "α_2-macroglobulin, as multifunctional binding protein with targeting characteristics." *FASEB J.*, **6** (15) 3345 – 3353.

Borth, W. and Luger, TA. (1989) "Identification of α_2-macroglobulin as a cytokine binding plasma protein. Binding of interleukin-1β to "F" α_2-macroglobulin." *J. Biol. Chem.*, **264** (10) 5818 – 5825.

Braverman, IM. (2000) "The cutaneous microcirculation." *J. Invest. Dermatol.*, **5**

(1) 3 – 9.

Breen, EC. (2007) "VEGF in Biological Control." *J. Cell. Biochem.*, **102** (6) 1358 – 1367.

Brown, LF., Yeo, KT., Berse, B., Yeo, TK., Senger, DR., Dvorak, HF. and van de Water, L. (1992) "Expression of vascular permeability factor (vascular endothelial growth factor) by epidermal keratinocytes during wound healing." *J. Exp. Med.*, **176** (5) 1375 – 1379.

Brown, TJ., Rowe, JM., Liu, J. and Shoyab, M. (1991) "Regulation of IL-6 expression by oncostatin M." *J. Immunol.*, **147** (7) 2175 – 2180.

Bruch-Gerharz, D., Ruzicka, T. and Kolb-Bachofen, V. (1998) "Nitric Oxide in Human Skin: Current Status and Future Prospects." *J. Invest. Dermatol.*, **110** (1) 1 – 7.

Bryan, D., Walker, KB., Ferguson, M. and Thorpe, R. (2005) " Cytokine gene expression in a murine wound healing model." *Cytokine*, **31** (6) 429 – 438.

Burg, ND. and Pillinger, MH. (2001) "The Neutrophil: Function and Regulation in Innate and Humoral Immunity." *Clin. Immunol.*, **99** (1) 7 – 17.

Cai, S. and Davis, AE. (2003) "Complement Regulatory Protein C1 Inhibitor Binds to Selectins and Interferes with Endothelial-Leukocyte Adhesion." *J. Immunol.*, **171** (9) 4786 – 4791.

Camborieux, L., Julia, V., Pipy, B. and Swerts, JP. (2000) "Respective roles of inflammation and axonal breakdown in the regulation of peripheral nerve hemopexin: an analysis in rats and in C57BL/Wlds mice." *J. Neuroimmunol.*, **107** (1) 29 – 41.

Castell, JV., Gómez-Lechón, MJ., David, M., Andus, T., Geiger, T., Trullenque, R., Fabra, R. and Heinrich, PC. (1989) "Interleukin-6 is the major regulator of acute phase protein synthesis in adult human hepatocytes." *FEBS lett.*, **242** (2) 237 – 239.

Ceciliani, F., Giordano, A. and Spagnolo, V. (2002) "The systemic reaction during inflammation: the acute-phase proteins." *Protein Pept. Lett.*, **9** (3) 211 – 223.

Chanson, M., Derouette, JP., Roth, I., Foglia, B., Scerri, I., Dudez, T. and Kwak, BR. (2005) "Gap junctional communication in tissue inflammation and repair." *Biochim. Biophys. Acta*, **1711** (2) 197 – 207.

Chaurasia, CS., Müller, M., Bashaw, ED., Benfeldt, E., Bolinder, J., Bullock, R., Bungay, PM., DeLange, ECM., Derendorf, H., Elmquist, WF., Hammarlund-Udenaes, M., Joukhadar, C., Kellogg Jr, DL., Lunte, CE., Nordstrom, CH., Rollema, H, Sawchuk, RJ., Cheung, BWY., Shah, VP., Stahle, L., Ungerstedt, U., Welty, DF. and Yeo, H. (2007) "AAPS-FDA Workshop White Paper: Microdialysis Principles, Application, and Regulatory Pespectives Report From the Joint AAPS-FDA Workshop, November 4-5, 2005, Nashville, TN." *AAPS J.*, **9** (1) E48 – E59.

Cho, SY., Lee, EY., Lee, JS., Kim, HY., Park, JM., Kwon, MS., Park, YK., Lee, HJ., Kang, MJ., Kim, JY., Yoo, JS., Park, SJ., Cho, JW., Kim, HS. and Paik, YK. (2005) "Efficient prefractionation of low-abundance proteins in human plasma and construction of a two-dimensional map." *Proteomics*, **5** (13) 3386 – 3396.

Cines, DB., Pollak, ES., Buck, CA., Loscalzo, J., Zimmerman, GA., McEver, RP., Pober, JS., Wick, TM., Konkle, BA., Schwartz, BS., Barnathan, ES., McCrae, KR., Hug, BA., Schmidt, AM. and Stern, DM. (1998) "Endothelial Cells in Physiology and in the Pathophysiology of Vascular Disorders." *Blood*, **91** (10) 3257 – 3561.

Clark, RAF (1988) "Overview and General Considerations of Wound Repair." in

Clark, RAF and Henson, PM. *The Molecular and Cellular Biology of wound repair.*, Plenum Press, New York. pp. 4.

Clark, RA. (2001) "Fibrin and wound healing." *Ann. N. Y. Acad. Sci.*, **936** 355 – 367.

Clough, GF. (2005) "Microdialysis of Large Molecules." *AAPS J.*, **7** (3) E686 – E692.

Clough, GF., Jackson, CL., Lee, JJP., Jamal, SC. and Church, MK. (2007) "What Can Microdialysis Tell Us About the Temporal and Spatial Generation of Cytokines in Allergen-Induced Responses in Human Skin *In Vivo*." *J. Invest. Dermatol.*, **127** (12) 2799 – 2806.

Cole, AM., Shi, J., Ceccarelli, A., Kim, YH., Park, A. and Ganz, T. (2001) "Inhibition of neutrophil elastase prevents cathelicidin activation and impairs clearance of bacteria from wounds." *Blood*, **97** (1) 297 – 304.

Contran, RS. and Pober, JS. (1990) "Cytokine-Endothelial Interactions in Inflammation, Immunity and Vascular Injury." *J. Am. Soc. Nephrol.*, **1** (3) 225 – 235.

Cook-Mills, JM. and Deem, TL. (2005) "Active participation of endothelial cells in inflammation." *J. Leukoc. Biol.*, **77** (4) 487 – 495.

Coulombe, PA. (1997) "Towards a Molecular Definition of Keratinocyte Activation after Acute Injury to Stratified Epithelia." *Biochem. Biophys. Res. Commun.*, **236** (2) 231 – 238.

Cutillas, PR. and Vanhaesebroeck, B. (2007) "Quantitative profile of five murine core proteomes using label-free functional proteomics." *Mol. Cell Proteomics*, **6** (9) 1560 – 1573.

Daley, JM., Reichner, JS., Mahoney, EJ., Manfield, L., Henry, WL. Jr., Mastrofrancesco, B. and Albina, JE. (2005) "Modulation of Macrophage Phenotype by Soluble Product(s) Released from Neutrophils." *J. Immunol.*, **174** (4) 2265 – 2272.

Deerman, RJ., Bhushan, M., Cumberbatch, M., Kimber, I. and Griffiths, CEM. (2004) "Measurement of cytokine expression and Langerhans cell migration in human skin following suction blister formation." *Exp. Dermatol.*, **13** (7) 452 – 460.

Delom, F. and Chevet, E. (2006) "Phosphoprotein analysis: from proteins to proteomes." *Proteome Sci.*, **4** (1) 15 – 26.

DePianto, D. and Coulombe, PA. (2004) "Intermediate filaments and tissue repair." *Exp. Cell Res.*, **301** (1) 68 – 76.

de Vries, JE. (1995) "Immunosuppressive and Anti-inflammatory Properties of IL-10." *Ann. Med.*, **27** (5) 537 – 541.

Diegelmann, RF. and Evans, MC. (2004) "Wound healing: an overview of acute, fibrotic and delayed healing." *Front. Biosci.*, **9** 283 – 289.

Dimmer, EC., Huntley, RP., Barrell, DG., Binns, D., Draghici, S., Camon, EG., Hubank, M., Talmud, PJ., Apweiler, R. and Lovering, RC. (2008) "The Gene Ontology — Providing a Functional Role in Proteomic Studies." DOI 10.1002/pmic.200800002

DiPietro, LA. (1995) "Wound Healing: The role of the macrophage and other immune cells." *Shock*, **4** (4) 233 – 240.

DiPietro, LA., Burdick, M., Low, EQ., Kunkel, SL. and Strieter, RM. (1998) "MIP-1alpha as a critical macrophage chemoattractant in murine wound repair." *J. Clin. Invest.*, **101** (8) 1693 – 1698.

DiPietro, LA., Reintjes, MG., Low, QE., Levi, B. and Gamelli, RL. (2001) "Modulation of macrophage recruitment into wounds by monocyte chemoattractant protein-1." *Wound Repair Regen.*, **9** (1) 28 – 33.

Dovi, JV., He, LK. and DiPietro, LA. (2003) "Accelerated wound closure in neutrophil-depleted mice." *J. Leukoc. Biol.*, **73** (4) 448 – 455.

Dubrovska, A. and Souchelnytskyi, S. (2005) "Efficient enrichment of intact phosphorylated proteins by modified immobilized metalaffinity chromatography." *Proteomics*, **5** (18) 4678 – 4683.

Duffield, JS. (2003) "The inflammatory macrophage: a story of Jekyll and Hyde." *Clin. Sci. (Lond.)*, **104** (1) 27 – 38.

Echan, LA., Tang, HY., Ali-Khan, N., Lee, K. and Speicher, DW. (2005) "Depletion of multiple high abundance proteins improves protein profiling capacities of human serum and plasma." *Proteomics*, **5** (13) 3292 – 3303.

Eckes, B., Zigrino, P., Kessler, D., Holtkötter, O., Shephard, P., Mauch, C. and Krieg, T. (2000) "Fibroblast-matrix interactions in wound healing and fibrosis." *Matrix Biol.*, **19** (4) 325 – 332.

Egozi, EL., Ferreira, AM., Burns, AL., Gamelli, RL. and DiPietro, LA. (2003) "Mast cells modulate the inflammatory but not the proliferative response in healing wounds." *Wound Rep. Reg.*, **11** (1) 46 – 54.

Ekdahl, KN. and Nilsson, B. (1995) "Phosphorylation of complement component C3 and C3 fragments by a human platelet protein kinase. Inhibition of factor I-mediated cleavage of C3b." *J. Immunol.*, **154** (12) 6502 – 6510.

El-Khatib, RT., Good, AG. and Muench, DG. (2007) "Analysis of the *Arabidopsis* cell suspension in response to short-term low temperature and abscisic acid treatment." *Physiol. Plantarum*, **129** (4) 687 – 697.

Eming, SA., Krieg, T. and Davidson, JM. (2007) "Inflammation in Wound Repair: Molecular and Cellular Mechanisms." *J. Invest. Dermatol.*, **127** (3) 514 – 525.

Engelhardt, E., Toksoy, A., Goebeler, M., Debus, S., Bröcker, EB. and Gillitzer, R. (1998) "Chemokines IL-8, GROα, MCP-1, IP-10, and Mig Are Sequentially and Differentially Expressed During Phase-Specific Infiltration of Leukocytes in Human Wound Healing." *Am. J. Pathol.*, **153** (6) 1849 – 1860.

Espina, V., Heiby, M., Pierobon, M. and Liotta, L. (2007) "Laser capture microdissection technology." *Expert Rev. Mol. Diagn.*, **7** (5) 647 – 657.

Essex, TJ. and Byrne, PO. (1991) "A laser Doppler scanner for imaging blood flow in skin." *J. Biomed. Eng.*, **13** (3) 189 – 94.

Faca, V., Pitteri, SJ., Newcomb, L., Glukhova, V., Phanstiel, D., Krasnoselsky, A., Zhang, Q., Struthers, J., Wang, H., Eng, J,. Fitzgibbon, M., McIntosh, M. and Hanash, S. (2007) "Contribution of protein fractionation to depth of analysis of the serum and plasma proteomes." *J. Proteome Res.*, **6** (9) 3558 – 3565.

Fadnes, HO. (1975) "Protein Concentration and Hydrostatic Pressure in Subcutaneous Tissue of Rats in Hypoproteinemia." *Scand. J. Clin. Lab. Invest.*, **35** (5) 441 – 446.

Fairweather, I., McGlone, F., Reilly, D. and Rukwied, R. (2004) "Controlled dermal cell damage as human in vivo model for localised pain and inflammation." *Inflamm. Res.*, **53** (3) 118 – 123.

Falcone, DJ., Borth, W., Khan, KMF. and Hajjar, KA. (2001) "Plasminogen-mediated matrix invasion and degradation by macrophages is dependent on surface expression of annexin II." *Blood*, **97** (3) 777 – 784.

Ferrero, ME. (2004) "In vivo vascular leakage assay." *Methods Mol. Med.*, **98** 191 – 198.

Fietta, AM., Bardoni, AM., Salvini, R., Passadore, I., Morosini, M., Cavagna, L., Codullo, V., Pozzi, E., Meloni, F. and Montecucco, C. (2008) "Analysis of bronchoalveolar lavage fluid proteome from systemic sclerosis patients with or without functional, clinical and radiological signs of lung fibrosis." *Arthritis Res. Ther.*, **8** (6) R160.

Flannery, T., McConnell, RS., McQuaid, S., McGregor, G., Mirakhur, M., Martin, L., Scott, C., Burden, R., Walker, B., McGoohan, C. and Johnston, PG. (2007) "Detection of cathepsin S cysteine protease in human brain tumour microdialysates *in vivo*." *Br. J. Neurosurg.*, **21** (2) 204 – 209.

Forsberg, PO., Martin, SC., Nilsson, UR. and Engstrom, L. (1989) "*In Vitro* Phosphorylation of Human Complement Factor C3 by Protein Kinase A and Protein Kinase C." *J. Biol. Chem.*, **265** (5) 2941 – 2946.

Fu, B., Gao, X., Zhang, SP., Cai, Z. and Shen, J. (2008) "Quantification of acetylcholine in microdialysate of subcutaneous tissue by hydrophilic interaction chromatography/tandem mass spectrometry." *Rapid Commun. Mass Spectrom.*, **22** (10) 1497 – 1502.

Fullerton, A., Fischer, T., Lahti, A., Wilhem, KP., Takiwaki, H. and Serup, J. (1996) "Guidelines for measurement of skin colour and erythema." *Contact Dermatitis*, **35** (1) 1 – 10.

Gabay, C. (2006) "Interleukin-6 and chronic inflammation" *Arthritis Res. Ther.* **8** (suppl. 2) S3.

Gaga, M., Ong, YE., Benyahia, F., Aizen, M., Barkans, J. and Kay, AB. (2008) "Skin reactivity and local cell recruitment in human atopic and nonatopic subjects by CCL2/MCP-1 and CCL3/MIP-1α." *Allergy*, **63** (6) 703 – 711.

Gallin, J. (1985) "Neutrophil Specific Granule Deficiency." *Ann. Rev. Med.*, **36** 263 – 274.

Gangahharan, B., Antrobus, R., Dwek, RA. and Zitzmann, N. (2007) "Novel serum biomarker candidates for liver fibrosis in hepatitis C patients." *Clin. Chem.*, **53** (10) 1792 – 1799.

Gao, WM., Chadha, MS., Berger, RP, Omenn, GS., Allen, DL, Pisano, M., Adelson, PD., Clark, RS., Jenkins, LW. and Kochanek, PM. (2007) "A gel-based proteomic comparison of human cerebrospinal fluid between inflicted and non-inflicted pediatric traumatic brain injury." *J. Neurotrauma*, **24** (1) 43 – 53.

Garvin, S. and Dabrosin, C. (2008) "*In vivo* measurement of tumor estradiol and Vascular Endothelial Growth Factor in breast cancer patients." *BMC Cancer*, **8** article 73.

Gavard, J. and Gutkind, S. (2006) "VEGF controls endothelial-cell permeability by promoting the β-arrestin-dependent endocytosis of VE-cadherin." *Nat. Cell. Biol.*, **8** (11) 1223 – 1234.

Gear, AR. and Camerini, D. (2003) "Platelet chemokines and chemokine receptors: linking hemostasis, inflammation, and host defense." *Microcirculation*, **10** (3 – 4) 335 – 350.

Gerritsen, ME. and Bloor, CM. (1993) "Endothelial cell gene expression in response to injury." *FASEB J.*, **7** (6) 523 – 532.

Gibran, NS., Ferguson, M., Heimbach, DM. and Isik, FF. (1997) "Monocyte Chemoattractant Protein-1 mRNA Expression in the Human Burn Wound." *J. Surg. Res.*, **70** (1) 1 – 6.

Gillitzer, R. and Goebeler, M. (2001) "Chemokines in cutaneous wound healing." *J. Leukoc. Biol.*, **69** (4) 513 – 521.

Goebeler, M., Yoshimura, T., Toksoy, A., Ritter, U., Bröcker, EB. and Gillizer, R. (1997) "The Chemokine Repertoire of Human Dermal Microvascular Endothelial Cells and Its Regulation by Inflammatory Cells." *J. Invest. Dermatol.*, **108** (4) 445 – 451.

Goldman, M., Marchant, A. and Schandené, L. (1996) "Endogenous Interleukin-10 in Inflammatory Disorders: Regulatory Roles and Pharmacological Modulation." *Ann. N. Y. Acad. Sci.*, **796** 282 – 293.

Goldsmith, PC., Leslie, TA., Hayes, NA., Levell, NJ., Dowd, PM. and Foreman, JC. (1996) "Inhibitors of nitric oxide synthase in human skin." *J. Invest. Dermatol.*, **106** (1) 113 – 118.

Gordon, S. (2003) "Alternative activation of macrophages." *Nat. Rev. Immunol.*, **3** (1) 23 – 25.

Goren, I., Kämpfer, H., Müller, E., Schiefelbein, D., Pfeilschifter, J. and Frank, S. (2006) "Oncostatin M Expression is Functionally Connected to Neutrophils in the Early Inflammatory Phase of Skin Repair: Implications for Normal and Diabetes-Impaired Wounds." *J. Invest. Dermatol.*, **126** (3) 628 – 637.

Gorg, A., Weiss, W. and Dunn, MJ. (2004) "Current two-dimensional electrophoresis technology for proteomics." *Proteomics*, **4** (12) 3665 – 3685.

Grabb, MC., Sciotti, VM., Gidday, JM., Cohen, SA. and van Wylen, DG. (1998) "Neurochemical and morphological responses to acutely and chronically implanted brain microdialysis probes." *J. Neurosci. Methods*, **82** (1) 25 – 34.

Graham, MM. and Evans, ML. (1991) "A simple, dual tracer method for the measurement of transvascular flux of albumin into the lung." *Microvasc. Res.*, **42** (3) 266 – 279.

Graves, PR. and Haystead, TAJ. (2002) "Molecular Biologist's Guide to Proteomics." *Microbiol. Mol. Biol. Rev.*, **66** (1) 39 – 63.

Gray, H. (1918) Plates 941 and 944, in *Anatomy of the Human Body*, accessed via http://bartleby.com/107/illus941.html and http://bartleby.com/107/illus944.html.

Grenier, A., Dehoux, M., Boutten, A., Arce-Vicioso, M., Durand, G., Gougerot-Pocidalo, M. and Chollet-Martin, S. (1999) "Oncostatin M Production and Regulation by Human Polymorphonuclear Neutrophils." *Blood*, **93** (4) 1413 – 1421.

Grinnell, F. (1992) "Wound repair, keratinocyte activation and integrin modulation." *J. Cell Sci.*, **101** (1) 1 – 5.

Gronborg, M., Kristiansen, TZ., Stensballe, A., Andersen, JS., Ohara, O., Mann, M., Jensen, ON. and Pandey, A. (2002) "A mass spectrometrybased proteomic approach for identification of serine/threoninephosphorylated proteins by enrichment with phospho-specific antibodies." *Mol. Cell. Proteomics*, **1** (7) 517 – 527.

Grose, R., Hutter, C., Bloch, W., Thorey, I., Watt, FM., Fässler, R., Brakebusch, C. and Werner, S. (2002) "A crucial role of β1 integrins for keratinocyte migration in vitro and during cutaneous wound repair." *Development*, **129** (9) 2303 – 2315.

Groth, L., Jørgensen, A. and Serup, J. (1998) "Cutaneous Microdialysis in the Rat: Insertion Trauma and Effect of Anaesthesia Studied by Laser Doppler Perfusion Imaging and Histamine Release." *Skin Pharmacol. Appl. Skin Physiol.*, **11** (3) 125 – 132.

Groth, L. and Serup, J. (1998) "Cutaneous Microdialysis in Man: Effects of Needle Insertion Trauma and Anaesthesia on Skin Perfusion, Erythema and Skin Thickness." *Acta Derm. Venereol.*, **78** (1) 5 – 9.

Groth, L., Ortiz, PG. and Benfeldt, E. (2006) "Microdialysis Methodology for Sampling in the Skin." in J. Serup, GBE. Jemec and GL. Grove (ed.) *Handbook of Non-Invasive Methods and the Skin.* 2nd edn., Taylor & Francis Group, Boca Raton, FL. pp. 443 – 454.

Guillet, C., Fourcin, M., Chevalier, S., Pouplard, A. and Gascan, H. (1995) "ELISA detection of circulating levels of LIF, OSM and CNTF in septic shock." *Ann. NY Acad. Sci.* **762** 407 – 409.

Guo, M., Galan, J. and Tao, WA. (2007) "Soluble nanopolymer-based phosphoproteomics for studying protein phosphorylation." *Methods*, **42** 289-297.

Haaverstad, R., Romslo, I. and Myhre, HO. (1997) "The concentration of high molecular weight compounds in interstitial tissue fluid: A study in patients with post-reconstructive leg oedema." *Eur. J. Vasc. Endovasc. Surg.*, **13** (4) 355 – 360.

Hack, CE. and Zeerleder, S. (2001) "The endothelium in sepsis: Source of and a target for inflammation." *Crit. Care Med.*, **29** (7) (Suppl.) S21 – S27.

Haskins, WE., Watson, CJ., Cellar, NA., Powell, DH. and Kennedy, RT. (2004) "Discovery and Neurochemical Screening of Peptides in Brain Extracellular Fluid by Chemical Analysis of in Vivo Microdialysis Samples." *Anal. Chem.*, **76** (18) 5523 – 5533.

Henrich, PC., Castell, JV. and Andus, T. (1990) "Interleukin-6 and the acute phase response." *Biochem. J.*, **265** (3) 621 – 636.

Hoffman, M. and Monroe, DM. (2007) "Coagulation 2006: a modern view of hemostasis." *Hematol. Oncol. Clin. North Am.*, **21** (1) 1 – 11.

Höffner, L., Nielsen, JJ., Langberg, H. and Hellsten, Y. (2003) "Exercise but not prostanoids enhance levels of vascular endothelial growth factor and other proliferative agents in human skeletal muscle interstitium." *J. Physiol.*, **550** (1) 217 – 225.

Hom, DB., Linzie, BM. and Huang TC. (2007) "The Healing Effects of Autologous Platelet Gel on Acute Human Skin Wounds." *Arch. Facial Plast. Surg.*, **9** (3) 174 – 183.

Hu, S., Loo, JA. and Wong, DT. (2006) "Human body fluid proteome analysis." *Proteomics*, **6** (23) 6326 – 6353.

Huang, CM., Foster, KW., DeSilva, T., Zhang, J., Shi, Z., Yusuf, N., Van Kampen, KR., Elmets, CA. and Tang, DC. (2003) "Comparative proteomic profiling of murine skin." *J. Invest. Dermatol.*, **121** (1) 51 – 64.

Hulstein, JJJ., Lenting, PJ., de Laat, B., Derksen, RHWM., Fijnheer, R. and de Groot, PG. (2007) "β_2-Glycoprotein I inhibits von Willebrand factor-dependent platelet adhesion and aggregation." *Blood*, **110** (5) 1483 – 1491.

Human Soluble Protein Master Buffer Kit Instruction Manual (2007) *BD Biosciences* Available from http://www.bdbiosciences.com/ptProduct.jsp?prodId=571001.

Hunt, TK., Knighton, DR., Thakral, KK., Goodson, WH. and Andrews, WS. (1984) "Studies on inflammation and wound healing: Angiogenesis and collagen synthesis is stimulated in vivo by resident and activated wound macrophages." *Surgery*, **96** (1) 48 – 54.

Hunter, T. (1998) "The Croonian lecture 1997. The phosphorylation of proteins on tyrosine: its role in cell growth and disease." *Philos. Trans. R. Soc. Lond. B Biol. Sci.*, **353** 583–605 b.

Hunter, T. (2000) "Signaling – 2000 and Beyond." *Cell*, **100** (1) 113 – 127.

Iba, Y., Shibata, A., Kato, M. and Masukawa, T. (2004) "Possible involvement of mast cells in collagen remodeling in in the late phase of cutaneous wound healing in mice." *Int. Immunopharmacol.*, **4** (14) 1873 – 1880.

Imanishi, SY., Kochin, V. and Eriksson, JE. (2007) "Optimization of phosphopeptide elution conditions in immobilized Fe(III) affinity chromatography." *Proteomics*, **7** (1) 174 – 176.

Iversen, VV., Bronstad, A., Gjerde, EA. and Reede RK. (2003) "Continuous measurements of plasma protein extravasation with microdialysis after various inflammatory challenges in rat and mouse skin." *Am. J. Physiol. Heart Circ. Physiol.*, **286** (1) H108 – H112.

Jacobs, JM., Adkins, JN., Qian, WJ., Liu, T., Shen, Y., Camp, DG 2nd. and Smith, RD. (2005) "Utilizing Human Blood Plasma for Proteomic Biomarker Discovery." *J. Proteome Res.*, **4** (4) 1073 – 1085.

Jaskolla, TW., Lehmann, WD. and Karas, M. (2008) "4-Chloro-α-cyanocinnamic acid in advanced, rationally designed MALDI matrix." *Proc. Natl. Acad. Sci. USA*, **105** (34) 12200 – 12205.

Jiang, Y., Beller, DL., Frendl, G. and Graves, DT. (1992) "Monocyte Chemoattractant Protein-1 Regulates Adhesion Molecule Expression and Cytokine Production in Human Monocytes." *J. Immunol.*, **148** (8) 2423 – 2428.

Johnston, JJ., Boxer, LA. and Berliner, N. (1992) "Correlation of Messanger RNA Levels With Protein Defects in Specific Granule Deficiency." *Blood*, **80** (8) 2088 – 2091.

Juhasz, I., Murphy, GF., Yan, HC., Herlyn, M. and Albelda, SM. (1993) "Regulation of extracellular matrix proteins and integrin cell substratum adhesion receptors on epithelium during cutaneous human wound healing *in vivo*." *Am. J. Pathol.*, **143** (5) 1458 – 1469.

Kanitakis, J. (2002) "Anatomy, histology and immunohistochemistry of normal human skin." *Eur. J. Dermatol.*, **12** (4) 390 – 401.

Kauffman, H., Bailey, J. and Fussenegger, M. (2001) "Use of antibodies for detection of phosphorylated proteins separated by two-dimensional gel electrophoresis." *Proteomics*, **1** (2) 194 – 199.

Kerfoot, SM., Raharjo, E., Ho, M., Kaur, J., Serirom, S., McCafferty, D., Burns, AR., Patel, KD. and Kubes, P. (2001) "Exclusive Neutrophil Recruitment with Oncostatin M in a Human System." *Am. J. Pathol.*, **159** (4) 1531 – 1539.

Kilpatrick, L., Johnson, JL., Nickbarg, EB., Wang, ZM., Clifford, TF., Banach, M., Cooperman, BS., Douglas, SD. and Rubin, H. (1991) "Inhibition of human neutrophil

superoxide generation by α_1-antichymotrypsin." *J. Immunol.*, **146** (7) 2388 – 2393.

Kjellström, S. and Jensen, ON. (2004) "Phosphoric acid as a matrix additive for MALDI MS analysis of phosphopeptides and phosphoproteins." *Anal. Chem.*, **76** (17) 5109 – 5117.

Klede, M., Hendwerker, HO. and Schmelz, M. (2003) "Central Origin of Secondary Mechanical Hyperalgesia." *J. Neurophysiol.*, **90** (1) 353 – 359.

Klein, J., Permana, PA., Owecki, M., Chaldakov, GN., Böhm, M., Hausman, G., Lapiére, CM., Atanassova, P., Sowiński, J., Fasshauer, M., Hausman, DB., Maquoi, E., Tonchev, AB., Peneva, VN., Vlanchanov, KP., Fiore, M., Aloe, L., Slominski, A., Reardon, CL., Ryan, TJ., Pond, CM. and Ryan, TJ. (2007) "What are subcutaneous adipocytes really good for?" *Exp. Dermatol.*, **16** (1) 45 – 70.

Klemm, C., Otto, S., Wolf, C., Haseloff, RF., Beyermann, M. and Krause, E. (2006) "Evaluation of the titanium dioxide approach for MS analysis of phosphopeptides." *J. Mass Spectrom.*, **41** (12) 1623 – 1632.

Klinger, MH., Wilhelm, D., Bubel, S,. Sticherling, M., Shröder, JM. andKühnel, W. (1995) "Immunocytochemical localization of the chemokines RANTES and MIP-1 alpha within human platelets and their release during storage." *Int. Arch. Allergy Immunol.*, **107** (4) 541 – 546.

Kool, J., Reubsaet, L., Wesseldijk, F., Maravilha, RT., Pinkse, MW., D'Santos, CS., van Hilten, JJ., Zijlstra, FJ. and Heck, AJR. (2007) "Suction blister fluid as potential body fluid for biomarker proteins." *Proteomics*, **7** (20) 3638 – 3650.

Kralovich, KR., Li, L., Hembrough, TA., Webb, DJ., Karns, LR. and Gonias, SL. (1998) "Characterization of the Binding Sites for Plasminogen and Tissue-Type Plas-

minogen Activator in Cytokeratin 8 and Cytokeratin 18." *J. Protein Chem.*, **17** (8) 845 – 854.

Krogstad, AL., Lönnroth, P., Larson, G. and Wallin. BG. (1997) "Increased interstitial histamine concentration in the psoriatic plaque." *J. Invest. Dermatol.*, **109** (5) 632 – 635.

Kubes, P., Suzuki, M. and Granger, DN. (1991) "Nitric oxide: an endogenous modulator of leukocyte adhesion." *Proc. Natl. Acad. Sci. USA*, **88** (11) 4651 – 4655.

Kuhn, M., Wolber, R., Kolbe, L., Schnorr, O. and Sies, H. (2006) "Solar-simulated radiation induces secretion of IL-6 and production of isoprostanes in human skin *in vivo*." *Arch. Dermatol. Res.*, **297** (10) 477 – 479.

Lambrecht, A., Verbruggen, G., Verdonk, PCM., Elewaut, D. and Deforce, D. (2007) "Differential proteome analysis of normal and osteoarthritic chondrocytes reveals distortion of vimentin network in osteoarthritis." *Osteoarthritis Cartilage*, **16** (2) 163 – 173.

Larsen, MR., Thingholm, TE., Jensen, ON., Roepstorff, P. and Jørgensen, TJD. (2005) "Highly Selective Enrichment of Phosphorylated Peptides from Peptide Mixtures Using Titanium Dioxide Microcolumns." *Mol. Cell. Proteomics*, **4** (7) 873 – 886.

Laurens, N., Koolwijk, P. and de Maat, MPM. (2006) "Fibrin structure and wound healing." *J. Thromb. Haemost.*, **4** (5) 932 – 939.

Le, GT., Abbenante, G. and Fairlie, DP. (2007) "Profiling the Enzymatic Properties and Inhibition of Human Complement Factor B." *J. Biol. Chem.*, **282** (48) 34809 – 34816.

Leatherbarrow, RJ. and Dean, PDG. (1980) "Studies on the Mechanism of Binding of Serum Albumins to Immobilised Cibacron Blue F3G A." *Biochem. J.*, **189** (1) 27 – 34.

Leibovich, SJ. and Ross, R. (1975) "The role of macrophages in wound repair. A study with hydrocortisone and antimacrophage serum. *Am. J. Path.*, **78** (1) 71 – 100.

Levy, O. (1996) "Antibiotic proteins of polymorphonuclear leukocytes." *Eur. J. Haematol.*, **56** (5) 263 – 277.

Ley, K. (1996) "Molecular mechanisms of leukocyte recruitment in the inflammatory process." *Cardiovasc. Res.*, **32** (4) 733 – 742.

Ley, K., Laudanna, C., Cybulsky, MI. and Nourshargh, S. (2007) "Getting to the site of inflammation: the leukocyte adhesion cascade updated." *Nat. Rev. Immunol.*, **7** (9) 678 – 689.

Liao, F., Huynh, HK., Eiroa, A., Greene, T., Polizzi, E. and Muller, WA. (1995) "Migration of monocytes across endothelium and passage through extracellular matrix involve separate molecular domains of PECAM-1." *J. Exp. Med.*, **182** (5) 337 – 1343.

Lima, A. and Bakker, J. (2005) "Noninvasive monitoring of peripheral perfusion." *Intensive Care Med.*, **31** (10) 1316 – 1326.

Lindberg, RA., Juan, TSC., Welcher, AA., Sun, Y., Cupples, R., Guthrie, B and Fletcher, FA. (1998) "Cloning and Characterization of a Specific Receptor for Mouse Oncostatin M." *Mol. Cell Biol.*, **18** (6) 3357 – 3367.

Ling, Q., Jacovina, AT., Deora, A., Febbraio, M., Simantov, R., Silverstein, RL., Hempstead, B., Mark, WH. and Hajjar, KA. (2004) "Annexin II regulates fibrin homeostasis and neoangiogenesis in vivo." *J. Clin. Invest.*, **113** (1) 38 – 48.

Liu, T., Qian, WJ., Gritsenko, MA., Xiao, W., Moldawer, LL., Kaushal, A., Monroe, ME., Varnum, SM, Moor, RJ., Purvine, SO., Maier, RV., Davis, RW., Tompkins, RG., Camp, DG 2nd, Smith, RD, Inflammation and the Host Response to Injury Large Scale Collaborative Research Programm. (2006) "High dynamic range characterization of the trauma patient plasma proteome." *Mol. Cell Proteomics.*, **5** (10) 1899 – 1913.

Lorenz, HP. and Adzick, NS. (1993) "Scarless skin wound repair in the fetus." *West. J. Med.*, **159** (3) 350 – 355.

Low, QEH., Drugea, IA., Duffner, LA., Quinn, DG., Cook, DN., Rollins, BJ., Kovacs, EJ. and DiPietro, LA. (2001) "Wound Healing in MIP-1$\alpha^{-/-}$ and MCP-1$^{-/-}$ Mice." *Am. J. Pathol.*, **159** (2) 457 – 463.

Macdonald, N., Cumberbatch, M,. Singh, M., Moggs, JG., Orphanides, G., Dearman, RJ., Griffiths, CE. and Kimber, I. (2006) "Proteomic analysis of suction blister fluid isolated from human skin." *Clin. Exp. Dermatol.*, **31** (3) 445 – 448.

Madore, N., Camborieux, L., Bertrand, N. and Swerts, JP. (1999) "Regulation of Hemopexin Synthesis in Degenerating and Regenerating Rat Sciatic Nerve." *J. Neurochem.*, **72** (2) 708 – 715.

Maik-Rachline, G. and Seger, R. (2006) "Variable phosphorylation states of pigment-epithelium-derived factor differentially regulate its function." *Blood*, **107** (7) 2745 – 2752.

Mancone, C., Amicone, L., Fimia, GM., Bravo, E., Piacentini, M., Tripodi, M. and Alonzi, T. (2007) "Proteomic analysis of human very low-density lipoprotein by two-dimensional gel electrophoresis and MALDI-TOF/TOF." *Proteomics*, **7** (1) 143 – 154.

Mandinov, L., Mandinova, A., Kyurkchiev, S., Kyurkchiev, D., Kehayov, I., Kolev, V., Soldi, R., Bagala, C., de Muinck, ED., Lindner, V., Post, MJ., Simons, M., Bellum, S., Prudovsky, I. and Maciag, T. (2003) "Copper chelation repressed the vascular response to injury." *P. Natl. Acad. Sci. USA*, **100** (11) 6700 – 6705.

Marro, D., Guy, RH. and Delgado-Charro, MB. (2001) "Characterization of the iontophoretic permselectivity properties of human and pig skin." *J. Control. Release.*, **70** (1 – 2) 213 – 217.

Martin, P., D'Souza, D., Martin, J., Grose, R., Cooper, L., Maki, R. and McKercher, SR. (2003) "Wound Healing in the PU.1 Null Mouse - Tissue Repair is Not Dependent on Inflammatory Cells." *Curr. Biol.*, **13** (13) 1122 – 1126.

Mathy, FX., Denet, AR., Vroman, B., Clarys, P., Barel, A., Verbeeck, RK. and Préat, V. (2003) "In vivo Tolerance Assessment of Skin after Insertion of Subcutaneous and Cutaneous Microdialysis Probes in the Rat." *Skin Pharmacol. Appl. Skin Physiol.*, **16** (1) 18 – 27.

Matsumoto, K., Nishi, K., Kikuchi, M., Kadowaki, D., Tokutomi, Y., Tokutomi, N., Nisihi, K., Suenaga, A. and Otagiri, M. (2007) "α_1-Acid Glycoprotein Suppresses Rat Acute Inflammatory Paw Edema through the Inhibition of Neutrophils Activation and Prostaglandin E_2 Generation." *Bio. Pharm. Bull.*, **30** (7) 1226 – 1230.

Maurer, MH., Berger, C., Wolf, M, Fütterer, CD., Feldmann, RE. Jr., Schwab, S. and Kuschinsky, W. (2003) "The proteome of human brain microdialysate." *Proteome Sci.*, **14** (1) 7 – 15.

Maurer, MH., Haux, D., Sakowitz, OW., Unterberg, AW. and Kushinsky, W. (2007) "Identification of early markers for symptomatic vasospasm in human cerebral microdialysate after subarachnoid hemorrhage: Preliminary results of a proteome-wide

screening." *J. Cerebr. Blood F. Met.*, **27** (10) 1675 – 1683.

Mazzucco, L., Medici, D., Serra, M., Panizza, R., Rivara, G., Orecchia, S., Libener, R., Cattana, E., Levis, A., Betta, PG. and Borzini, P. (2004) "The use of autologous platelet gel to treat difficult-to-heal wounds: a pilot study." *Transfusion*, **44** (7) 1013 – 1018.

McDonald, WH. and Yates, JR 3rd. (2002) "Shotgun proteomics and biomarker discovery." *Dis. Markers*, **18** (2) 99 – 105.

McDowall, A., Leitinger, B., Stanley, P., Bates, PA., Randi, AM. and Hogg, N. (1998) "The I Domain of Integrin Leukocyte Function-associated Antigen-1 is Involved in a Conformational Change leading to High-Affinity Binding to Ligand Intercellular Adhesion Molecule-1 (ICAM-1)." *J. Biol. Chem.*, **273** (42) 27196 – 27403.

McKenzie, RC. and Sauder, DN. (1990) "The Role of Keratinocyte Cytokines in Inflammation and Immunity." *J. Invest. Dermatol.*, **95** (6) (Suppl.) 105S – 107S.

Meier, U., Gressner, O., Lammert, F. and Gressner, AM. (2006) "Gc-Globulin: Roles in Response to Injury." *Clin. Chem.*, **52** (7) 1247 – 1253.

Menke, NB., Ward, KR., Witten, TM., Bonchev, DG. and Diegelmann, RF. (2007) "Impaired wound healing." *Clin. Dermatol.*, **25** (1) 19 – 25.

Menten, P., Wuyts, A. and Van Damme, J. (2002) "Macrophage inflammatory protein-1." *Cytokine Growth F. R.*, **13** (6) 455 – 481.

Michiels, C. (2003) "Endothelial Cell Functions." *J. Cell. Physiol.*, **196** (3) 430 – 443.

Midwood, KS., Williams, LV. and Schwarzbauer, JE. (2004) "Tissue repair and the dynamics of the extracellular matrix." *Int. J. Biochem. Cell B.*, **36** (6) 1031 – 1037.

Miller, MD. and Krangel, MS. (1992) "The human cytokine I-309 is a monocyte chemoattractant." *Proc. Natl. Acad. Sci. USA*, **89** (7) 2950 – 2954.

Modur, V., Feldhaus, MJ., Weyrich, AS., Jicha, DL. and Prescott, SM. (1997) "Oncostatin M is a Proinflammatory Mediator." *Ann. NY Acad. Sci.* **100** (1) 158 – 168.

Moitra, J., Sammani, S. and Garcia, JGN. (2007) "Re-evaluation of Evans Blue dye as a marker of albumin clearance in murine models of acute lung injury." *Transl. Res.*, **150** (4) 253 – 265.

Moraes, TJ., Zurawska, JH. and Downey, GP. (2006) "Neutrophil granule contents in the pathogenesis of lung injury." *Curr. Opin. Hematol.*, **13** (1) 21 – 27.

Muller, WA. and Randolph, GJ. (1999) "Migration of leukocytes across endothelium and beyond: molecules involved in the transmigration and fate of monocytes." *J. Leukoc. Biol.*, **66** (5) 698 – 704.

Murdolo, G., Hammarstedt, A., Sandqvist, M., Schmelz, M., Herder, C., Smith, U. and Jansson, P. (2007) "Monocyte Chemoattractant Protein-1 in Subcutaneous Abdominal Adipose Tissue: Characterization of Interstitial Concentration and Regulation of Gene Expression by Insulin." *J. Clin. Endocrinolo. Metab.*, **92** (7) 2688 – 2695.

Murray, J., Marusich, MF., Capaldi, RA. and Aggeler, R. (2004) "Focused proteomics: Monoclonal antibody-based isolation of the oxidative phosphorylation machinery and detection of phosphoproteins using a fluorescent phosphoprotein gel stain." *Electrophoresis*, **25** (15) 2520 – 2525.

Nesvizhskii, AI. and Aebersold, R. (2005) "Interpretation of Shotgun Proteomics Data." *Mol. Cell. Proteomics*, **4** (10) 1419 – 1440.

Nicholas, B., Skipp, P., Mould, R,. Rennard, S., Davies, DE., O'Connor, CD. and Djukanovíc, R. (2006) "Shotgun proteomic analysis of human-induced sputum." *Proteomics*, **6** (15) 4390 – 4401.

Nogami, M., Hoshi, T., Kinoshita, M., Arai, T., Takama, M. and Takahashi, I. (2007) "Vascular endothelial growth factor expression in rat skin incision wounds." *Med. Mol. Morphol.*, **40** (2) 82 – 87.

Nuutinen, P., Harvima, IT. and Ackermann, L. (2007) "Histamine, but not leukotriene C4, is an essential mediator in cold urticaria wheals." *Acta. Derm. Venereol.*, **87** (1) 9 – 13.

Obreja, O., Rukwied, R., Steinhoff, M. and Schmelz, M. (2006) "Neurogenic components of trypsin- and thrombin-induced inflammation in rat skin, *in vivo*." *Exp. Dermatol.*, **15** (1) 58 – 65.

Oda, Y., Nagasu, T. and Chait, BT. (2001) "Enrichment analysis of phosphorylated proteins as a tool for probing the phosphoproteome." *Nat Biotechnol*, **19** (4) 379 – 382.

Okajima, K. and Uchiba, M. (1998) "The anti-inflammatory properties of antithrombin III: new therapeutic implications." *Semin. Thromb. Hemostat.*, **24** (1) 27 – 32.

Osaki, S., Johnson, DA. and Frieden, E. (1966) "The possible significance of the ferrous oxidase activity of ceruloplasmin in normal human serum." *J. Biol. Chem.*, **241** (12) 2746 – 2751.

Pachler, C., Ikoeka, D., Plank, J., Weinhandl, H., Suppan, M., Mader, JK., Bodenlenz,

M., Regittnig, W., Manggge, H, Pieber, TR. and Ellmerer, M. (2007) "Subcutaneous adipose tissue exerts proinflammatory cytokines after minimal trauma in humans." *Am. J. Physiol. Endocrinol. Metab.*, **293** (3) E690 – E696.

Paradela, A. and Albar, JP. (2008) "Advances in the Analysis of Protein Phosphorylation." *J. Proteome Res.*, **7** (5) 1809 – 1818.

Patchell, BJ., Wojcik, KR., Yang, TL., White, SR. and Dorscheid, DR. (2007) "Glycosylation and annexin II cell surface translocation mediate airway epithelial wound repair." *Am. J. Physiol. Lung Cell Mol. Physiol.*, **293** (2) L354 – L363.

Patel, BN., Dunn, RJ., Jeong, SY., Zhu, Q., Julien, JP. and David, S. (2002) "Ceruloplasmin Regulates Iron Levels in the CNS and Prevents Free Radical Injury." *J. Neurosci.*, **22** (15) 6578 – 6586.

Pawson, T. and Scott, JD. (2005) "Protein phosphorylation in signalling – 50 years and counting." *Trends Biochem. Sci.*, **30** (6) 286 – 290.

Perl, M., Gebhard, F., Knöferl, MW., Bachem, M., Gross, HJ., Kinzl, L. and Strecker, W. (2003) "The pattern of preformed cytokines in tissues frequently affected by blunt trauma." *Shock*, **19** (4) 299 – 304.

Petersen, LJ., Church, MK. and Skov, PS. (1997) "Histamine is released in the wheal but not the flare following challenge of human skin in vivo: a microdialysis study." *Clin. Exp. Allergy*, **27** (3) 284 – 295.

Petrache, I., Birukova, A., Ramirez, SI., Garcia, JGN. and Verin, AD. (2003) "The Role of the Microtubules in Tumor Necrosis Factor-α-Induced Endothelial Cell Permeability." *Am. J. Respir. Cell Mol. Biol.*, **28** (5) 574 – 581.

Petrak, J., Ivanek, R., Toman, O, Cmejla, R., Cmejlova, J., Vyoral, D., Zivny, J. and Vulpe, CD. (2008) "Dèjá vu in proteomics. A hit parade of repeatedly identified differentially expressed proteins." *Proteomics*, **8** (9) 1744 – 1749.

Pinkse, MWH., Uitto, PM., Hilhorst, MJ., Ooms, B. and Heck, AJR. (2004) "Selective Isolation at the Femtomole Level of Phosphopeptides from Proteolytic Digests Using 2D-NanoLC-ESI-MS/MS and Titanium Oxide Precolumns." *Anal. Chem.*, **76** (14) 3935 – 3943.

Planas, AM., Justicia, C., Solé, S., Friquis, B., Cervera, A., Adell, A. and Chamorro, A. (2002) "Certain Forms of Matrix Metalloproteinase-9 Accumulate in the Extracellular Space After Microdialysis Probe Implantation and Middle Cerebral Artery Occlusion/Reperfusion." *J. Cereb. Blood Flow Metab.*, **22** (8) 918 – 925.

Pollins, AC., Friedman, DB. and Nanney, LB. (2007) "Proteomic Investigation of Human Burn Wounds by 2D-Differential Electrophoresis and Mass Spectrometry." *J. Surg. Res.*, **142** (1) 143 – 152.

Raggiaschi, R., Gotta, S. and Terstappen, G. (2005) "Phosphoproteome Analysis." *Bioscience Rep.*, **25** (1) 33 – 44.

Rajan, V., Varghese, B., van Leeuwen, TG. and Steenbergen, W. (2007) "Review of methodological developments in laser Doppler flowmetry." *Lasers Med. Sci.*, **24** (2) 269 – 283.

Ramaha, A. and Patson, PA. (2002) "Release and Degradation of Angiotensin I and Angiotensin II from Angiotensinogen by Neutrophil Serine Proteinases." *Arch. Biochem. Biophys.*, **397** (1) 77 – 83.

Rathore, KI., Kerr, BJ., Redensek, A., López-Valez, R., Jeong, SY., Ponka, P. and

David, S. (2008) "Ceruloplasmin protects injured spinal cord from iron-mediated oxidative damage." *J. Neurosci.*, **28** (48) 12736 – 12747.

Redegeld, FA., Caldwell, CC. and Sitkovsky, MV. (1999) "Ecto-protein kinases: ectodomain phosphorylation as a novel target for pharmacological manipulation?" *Trends Pharmacol. Sci.*, **20** (11) 453 – 459.

Reilly, DM., Parslew, R., Sharpe, GR. and Green, MR. (2000) "Inflammatory Mediators in Normal, Sensitive and Diseased Skin Types." *Acta Derm. Venereol.*, **80** (3) 171 – 174.

Richards, CD., Brown, TJ., Shoyab, M., Baumann, H. and Gauldie, J. (1992) "Recombinant oncostatin M stimulates the production of acute phase proteins in HepG2 cells and rat primary hepatocytes *in vitro*." *J. Immunol.*, **148** (6) 1731 – 1736.

Riese, J., Boecker, S., Hohenberger, W., Klein, P. and Haupt, W. (2003) "Microdialysis: a new technique to monitor perioperative human peritoneal mediator production." *Surg. Infect. (Larchmt)*, **4** (1) 11 – 15.

Roemisch, J., Gray, E., Hoffman, JN. and Wiedermann, CJ. (2002) "Antithrombin: a new look at the actions of a serine protease inhibitor." *Blood Coagul. Fibrin.*, **13** (8) 657 – 670.

Rollins, BJ. (1997) "Chemokines." *Blood*, **90** (3) 909 – 928.

Romano, M., Sironi, M., Toniatti, C., Polentarutti, N., Fruscella, P., Ghezzi, P., Faggioni, R., Luini, W., van Hinsbergh, V., Sozzani, S., Bussolino, F., Poli, V., Ciliberto, G. and Mantovani, A. (1997) "Role of IL-6 and Its Soluble Receptor in Induction of Chemokines and Leukocyte Recruitment" *Immunity*, **6** (6) 315 – 325.

Rosdahl, H., Ungerstedt, U., Jorfeldt, L. and Henriksson, J. (1993) "Interstitial glucose and lactate balance in human skeletal muscle and adipose tissue studied by microdialysis." *J. Physiol.*, **471** (1) 637 – 657.

Rosenbloom, AJ., Sipe, DM. and Weedn, VW. (2005) "Microdialysis of Proteins: Performance of the CMA/20 probe." *J. Neurosci. Meth.*, **148** (2) 147 – 153.

Rožman, P. and Bolta, Z. (2003) "Use of platelet growth factors in treating wounds and soft-tissue injuries." *Acta Dermatoven APA*, **16** (4) 156 – 165.

Sako, D., Chang, XJ., Barone, KM., Vachino, G., White, HM., Shaw, G., Veldman, GM., Bean, KM., Ahern, TJ., Furie, B., Cumming, DA. and Larsen, GR. (1993) "Expression cloning of a functional glycoprotein for P-selectin." *Cell*, **75** (6) 1179 – 1186.

Santos, RAS., Campagnole-Santos, MJ. and Andrade, SP. (2000) "Angiotensin-(1-7): an update." *Regul. Peptides*, **91** (1 – 3) 45 – 62.

Sataranatarajan, K., Lee, MJ., Mariappan, M. and Feliers, D. (2008) "PKCδ regulates the stimulation of vascular endothelial factor mRNA translation by angiontensin II through hnRNP K." *Cell Signal.*, **20** (5) 969 – 977.

Sauerstein, K., Klede, M., Hilliges, M. and Schmelz, M. (2000) "Electrically evoked neuropeptide release and neurogenic inflammation differ between rat and human skin." *J. Physiol.*, **529** (3) 803 – 810.

Schäfer, M. and Werner, S. (2007) "Transcriptional control of wound repair." *Annu. Rev. Cell. Dev. Biol.*, **23** 69 – 92.

Schmelz, M., Luz, O., Averbeck, B. and Bickel, A. (1997) "Plasma extravasation and neuropeptide release in human skin as measured by intradermal microdialysis." *Neu-*

rosci. Lett., **230** (2) 117 – 120.

Schmidt, SR., Schweikart, F. and Andersson, ME. (2007) "Current methods for phosphoprotein isolation and enrichment." *J. Chromatogr. B Analyt. Technol. Biomed. Life Sci.*, **849** (1 – 2) 154 – 162.

Schroder, K., Hertzog, PJ., Ravasi, T. and Hume, DA. (2004) "Interferon-γ: an overview of signals, mechanisms and functions." *J. Leukoc. Biol.*, **75** (2) 163 – 189.

Senger, DR., Galli, SJ., Dvorak, AM., Peruzzi, CA., Harvey, VS. and Dvorak, HF. (1983) "Tumor cells secrete a vascular permeability factor that promotes accumulation of ascites fluid." *Science*, **219** (4587) 983 – 985.

Serhan, CN. and Savill, J. (2005) "Resolution of inflammation: the beginning programs the end." *Nat. Immunol.*, **6** (12) 1191 – 1197.

Shäfer, BM., Maier, K., Eickhoff, U., Todd, RF. and Kramer, MD. (1994) "Plasminogen Activation in Healing Human Wounds." *Am. J. Pathol.*, **144** (6) 1269 – 1280.

Shariat-Madar, Z., Mahdi, F. and Schmaier, AH. (2002) "Assembly and regulation of the plasma kallikrein/kinin system: a new interpretation." *Int. Immunopharmacol.*, **2** (13 – 14) 1841 – 1849.

Shevchenko, A., Wilm, M., Vorm, O. and Mann, M. (1996) "Mass Spectrometric Sequencing of Proteins from Silver-Stained Polyacrylamide Gels." *Anal. Chem.*, **68** (5) 850 – 858.

Shippenberg, TS. and Thompson, AC. (1997) "Overview of Microdialysis." in *Curr. Protoc. Neurosci.* (eds. Crawley, JN., Gerfen, CR., McKay, R., Rogawski, MA., Sibley, DR. and Skolnick, P.) Vol 1. Wiley, New York. pp. 7.1.1 – 7.1.22.

Sickmann, A. and Meyer, HE. (2007) "Phosphoamino acid analysis." *Proteomics*, **1** (2) 200 – 206.

Singer, AJ. and Clark, RA. (1999) "Cutaneous wound healing." *N. Engl. J. Med.*, **341** (10) 738 – 746.

Sjögren, F., Svensson, C. and Anderson, C. (2002) "Technical prerequisites for *in vivo* microdialysis determination of interleukin-6 in human dermis." *Br. J. Dermatol.*, **146** (3) 375 – 382.

Spiekstra, SW., Breetveld, M., Rustemeyer, T., Scheper, RJ. and Gibbs, S. (2007) "Wound-healing factors secreted by epidermal keratinocytes and dermal fibroblasts in skin substitutes." *Wound Repair Regen.*, **15** (5) 708 – 717.

Sriramarao, P. and DiScipio, RG. (1998) "Deposition of complement C3 and factor H in tissue traumatized by burn injury." *Immunopharmacology*, **42** 195 – 205.

Stenken, JA. (2006) "Microdialysis Sampling." in JG Webster (ed.) *Encyclopedia of Medical Devices and Instrumentation*, 2nd edn., Vol. 4. John Wiley & Sons, Inc. Hoboken, NJ. pp. 400 – 420.

Stern, MD. (1975) "*In vivo* evaluation of microcirculation by coherent light scattering." *Nature*, **254** (5495) 56 – 58.

Stoeckli, M., Chaurand, P., Hallahan, DE. and Capioli, RM. (2001) "Imaging mass spectrometry: A new technology for the analysis of protein expression in mammalian tissues." *Nat. Med.*, **7** (4) 493 – 496.

Stock, JB., Ninfa, AJ. and Stock, AM. (1989) "Protein Phosphorylation and Regu-

lation of Adaptive Responses in Bacteria." *Microbio. Rev.*, **53** (4) 450 – 490.

Stramer, BM., Mori, R. and Martin, P. (2007) "The Inflammation – Fibrosis Link? A Jekyll and Hyde Role for Blood Cells during Wound Repair." *J. Invest. Dermatol.*, **127** (5) 1009 – 1017.

Suffredini, AF., Fantuzzi, G., Badolato, R., Oppenheim, JJ. and O'Grady, NP. (1999) "New Insights into the Biology of the Acute Phase Response." *J. Clin. Immunol.*, **19** (4) 203 – 214.

Sugawara, T., Gallucci, RM., Simeonova, PP. and Luster, MI. (2001) "Regulation and role of interleukin 6 in wounded human epithelial keratinocytes." *Cytokine*, **15** (6) 328 – 336.

Sun, L. and Stenken, JA. (2003) "Improving microdialysis extraction efficiency of lipophilic eicosanoids." *J. Pharm. Biomed. Anal.*, **33** (5) 1059 – 1071.

Swain, ID. and Grant, LJ. (1989) "Methods of measuring skin blood flow." *Phys. Med. Biol.*, **34** (2) 151 – 175.

Swisher, JFA., Khatri, U. and Feldman, GM. (2007) "Annexin A2 is a soluble mediator of macrophage activation." *J. Leukoc. Biol.*, **82** (5) 1174 – 1184.

Szpaderska, AM., Zuckerman, JD. and DiPietro, LA. (2003) "Differential Injury Responses in Oral Mucosal and Cutaneous Wounds." *J. Dent. Res.*, **82** (8) 621 – 626.

Takada, A., Takada, Y. and Urano, T. (1994) "The physiological aspects of fibrinolysis." *Thromb. Res.*, **76** (1) 1 – 31.

Tan, NS., Michalik, L., Noy, N., Yasmin, R., Pacot, C., Heim, M., Flühmann, B.,

Desvergne, B. and Wahli, W. (2001) "Critical roles of PPARβ/δ in keratinocyte response to inflammation." *Genes Dev.*, **15** (24) 3263 – 3277.

Tao, WA., Wollscheid, B., O'Brien, R., Eng, JK., Li, XJ., Bodenmiller, B., Watts, JD., Hood, L. and Aebersold, R. (2005) "Quantitative phosphoproteome analysis using a dendrimer conjugation chemistry and tandem mass spectrometry." *Nat. Methods*, **2** (8) 591 – 598.

Thingholm, TE., Jensen, ON., Robinson, PJ. and Larsen, MR. (2008) "SIMAC (Sequential Elution from IMAC), a Phosphoproteomics Strategy for the Rapid Separation of Monophosphorylated from Multiply Phosphorylated Peptides." *Mol. Cell. Proteomics*, **7** (4) 661 – 671.

Timár, KK., Junnikkala, S., Dallos, A., Jarva, H., Bhuiyan, ZA., Meri, S., Bos, JD. and Asghar, SS. (2007) "Human keratinocytes produce the complement inhibitor factor I: Synthesis is regulated by interferon-γ." *Mol. Immunol.*, **44** (11) 2943 – 2949.

Toriyabe, M., Omote, K., Kawamata, T. and Namika, A. (2004) "Contribution of interaction between nitric oxide and cyclooxygenases to the production of prostaglandins in carrageenan-induced inflammation." *Anesthesiology*, **101** (4) 983 – 990.

Ungerstedt, U. (1991) "Microdialysis – principles and applications for studies in animals and man." *J. Intern. Med.*, **230** (4) 365 – 373.

Utgaard, JO., Jahnsen, FL., Bakka, A., Brandtzaeg, P and Haraldsen, G. (1998) "Rapid secretion of prestored Interleukin-8 from Weibel-Palade bodies of microvascular endothelial cells." *J. Exp. Med.*, **188** (9) 1751 – 1756.

Vaughan, DE. (2001) "Angiotensin, Fibrinolysis and Vascular Homeostasis." *Am. J. Cardiol.*, **87** (8A) 18C – 24C.

van Bruggen, N., Thibodeaux, H., Palmer, JT., Lee, WP., Fu, L., Cairns, B., Tumas, D., Gerlai, R., Williams, SP., van Lookeren Campagne, M. and Ferrara, N. (1999) "VEGF antagonism reduces edema formation and tissue damage after ischemia/reperfusion injury in the mouse brain." *J. Clin. Invest.*, **104** (11) 1613 – 1620.

Van Der Laan, N., de Leij, LF. and ten Duis, HJ. (2001) "Immunohistopathological appearance of three different types of injury in human skin." *Inflamm. Res.*, **50** (7) 350 – 356.

van Hinsbergh, VWM. and van Nieuw Amerongen, GP. (2002) "Intracellular signalling involved in modulating human endothelial barrier function." *J. Anat.*, **200** (6) 549 – 560.

Vennemann, P., Lindken, R. and Westerweel, J. (2007) "In vivo whole-field blood velocity measurement techniques" *Exp. Fluids*, **42** 495 – 511.

Vivers, S., Dransfield, I. and Hart, SP. (2002) "Role of macrophage CD44 in the disposal of inflammatory cell corpses." *Clin. Sci.*, **103** (5) 441 – 449.

Vogel, SM., Gao, X., Mehta, D., Ye, RD., John, TA., Andrade-Gordon, P., Tiruppathi, C. and Malik, AB. (2000) "Abrogation of thrombin-induced increase in pulmonary microvascular permeability in PAR-1 knockout mice." *Physiol. Genomics*, **4** (2) 137 – 145.

Vongsavan, N. and Matthews, B. (1993) "Some aspects of the use of laser doppler flow meters for recording tissue blood flow." *Exp. Physiol.*, **78** (1) 1 – 14.

Wahl, AF. and Wallace, PM. (2001) "Oncostatin M in the anti-inflammatory response." *Ann. Rheum. Dis.*, **60** (Suppl. iii) 75 – 80.

Wallez, Y. and Huber, P. (2008) "Endothelial adherens and tight junctions in vascular homeostasis, inflammation and angiogenesis." *Biochim. Biophys. Acta*, **1778** (3) 794 – 809.

Wang, X., Lennartz, MR., Loegering, DJ. and Stenken, JA. (2007) "Interleukin-6 Collection through Long-Term Implanted Microdialysis Sampling Probes in Rat Subcutaneous Space" *Anal. Chem.*, **79** (5) 1816 – 1824.

Wei, G., Ding, PT., Zheng, JM. and Lu, WY. (2006) "Pharmacokinetics of timolol in aqueous humor sampled by microdialysis after topical administration of thermosetting gels." *Biomed. Chromatogr.*, **20** (1) 67 – 71.

Weiss, SJ. (1989) "Tissue Destruction by Neutrophils." *New Engl. J. Med.*, **320** (6) 365 – 376.

Weller, K., Foitzik, K., Paus, R., Syska, W. and Maurer, M. (2006) "Mast cells are required for normal healing of skin wounds in mice." *FASEB J.*, **20** (13) 1628 – 1635.

Werner, S. and Grose, R. (2003) "Regulation of Wound Healing by Growth Factors and Cytokines." *Physiol. Rev.*, **83** (3) 835 – 870.

Werner, S., Krieg, T. and Smola, H. (2007) "Keratinocyte–Fibroblast Interactions in Wound Healing." *J. Invest. Dermatol.*, **127** (5) 998 – 1008.

Wetzler, C., Kämpfer, H., Pfeilschifter, J. and Frank, S. (2000) "Keratinocyte-Derived Chemotactic Cytokines: Expressional Modulation by Nitric Oxide *in Vitro* and during Cutaneous Wound Repair *in Vivo*." *Biochem. Biophys. Res. Com.*, **274** (3) 689 – 696.

Wiig, H., Aukland, K. and Tenstad, O. (2003) "Isolation of interstitial fluid from rat

mammary tumors by a centrifugation method." *Am. J. Physiol. Heart Circ. Physiol.*, **284** (1) H416 – H424.

Wiig, H., Sibley, L., DeCarlo, M. and Renkin, EM. (1991) "Sampling interstitial fluid from rat skeletal muscles by intramuscular wicks." *Am. J. Physiol.*, **261** (1 part 2) H155 – H165.

Williams, B., Baker, AQ., Gallacher, B. and Lodwick, D. (1995) "Angiotensin II Increases Vascular Permeability Factor Gene Expression by Human Vascular Smooth Muscle Cells." *Hypertension*, **25** (5) 913 – 917.

Williams, TJ. and Peck, MJ. (1977) "Role of prostaglandin-mediated vasodilatation in inflammation." *Nature*, **270** (5637) 530 – 532.

Winter, CD., Iannotti, F., Pringle, AK., Trikkas, C., Clough, GF. and Church, MK. (2002) "A microdialysis method for the recovery of IL-1β, IL-6 and nerve growth factor from human brain in vivo." *J. Neurosci. Meth.*, **119** (1) 45 – 50.

Witko-Sarsat, V., Rieu, P., Deschamps-Latscha, B., Lesavre, P and Halbwachs-Mecarelli, L. (2000) "Neutrophils: Molecules, Functions and Pathophysiological Aspects." *Lab. Invest.*, **80** (5) 617 – 653.

Wu, CC. and MacCoss, MJ. (2002) "Shotgun proteomics: tools for the analysis of complex biological systems." *Curr. Opin. Mol. Ther.*, **4** (3) 242 – 250.

Wu, NZ. and Baldwin, AL. (1992) "Transient venular permeability increase and endothelial gap formation induced by histamine." *Am. J. Physiol. Heart Circ. Physiol.*, **262** (4) 1238 – 1247.

Wu, SM., Patel, DD. and Pizzo, SV. (1998) "Oxidized α-2-Macroglobulin (α-2-M)

Differentially Regulates Receptor Binding by Cytokines/Growth Factors: Implications for Tissue Injury and Repair Mechanisms in Inflammation." *J. Immunol.*, **161** (8) 4356 – 4365.

Wynn, TA. (2008) "Cellular and molecular mechanisms of fibrosis." *J. Pathol.*, **214** (2) 199 – 210.

Yang, CS., Tsai, PJ., Chen, WY., Liu, L. and Kuo, JS. (1995) "Determination of extracellular glutathione in livers of anaesthetized rats by microdialysis with on-line high-performance liquid chromatography." *J. Chromatogr. B Biomed. Appl.*, **667** (1) 41 – 48.

Yano, S., Banno, T., Walsh, R. and Blumenberg, M. (2008) "Transcriptional Responses of Human Epidermal Keratinocytes to Cytokine Interleukin-1." *J. Cell Physiol.*, **214** (1) 1 – 13.

Yeoh-Ellerton, S. and Stacey, MC. (2003) "Iron and 8–Isoprostane Levels in Acute and Chronic Wounds." *J. Invest. Dermatol.*, **121** (4) 918 – 925.

Zamiri, P., Masli, S., Streilein, JW. and Taylor, AW. (2006) "Pigment Epithelial Growth Factor Suppresses Inflammation by Modulating Macrophage Activation." *Invest. Opth. Vis. Sci.*, **47** (9) 3912 – 3918.

Zhang, SX., Wang, JJ., Gao, G., Shao, C., Mott, R. and Ma, J. (2006) "Pigment epithelium-derived factor (PEDF) is an endogenous antiinflammatory factor." *FASEB J.*, **20** (2) 323 – 325.

Zhao, J., Lui, H, McLean, DI. and Zeng, H. (2008) "Integrated real-time Raman system for clinical *in vivo* skin analysis." *Skin Res. Technol.*, **14** (4) 484 – 492.

Zhaoritegu, S., Wan, G., Kaini, R., Jiang, Z. and Hu, CA. (2008) "ApoL1, a BH3-only lipid-binding protein, induces autophagic cell death." *Autophagy*, **4** (8) 1079 – 1082.

Zhou, Q. and Gallo, JM. (2005) "*In vivo* microdialysis for PK and PD studies of anticancer drugs." *AAPS J.*, **7** (3) E659 – E667.

Zimmerman, GA., Prescott, SM. and McIntyre, TM. (1992) "Endothelial cell interactions with granulocytes: tethering and signalling molecules." *Immuno. Today*, **13** (3) 93 – 100.

Zurovsky, Y., Mitchell, G. and Hattingh, J. (1994) "Composition and viscosity of interstitial fluid of rabbits." *Exp. Physiol.*, **80** (2) 203 – 207.